EROSION SURFACES AND GRAVEL SHOREFACE DEPOSITS: THE INFLUENCE OF TECTONICS ON THE SEDIMENTOLOGY OF THE CARROT CREEK MEMBER, CARDIUM FORMATION (TURONIAN, UPPER CRETACEOUS), ALBERTA, CANADA

BY

KATHERINE MARY BERGMAN,
B.Sc., M.Sc.

ERODSION SURFACES AND SEDIMENTOLOGY OF THE
CARROT CREEK MEMBER, CARDIUM FORMATION

EROSION SURFACES AND GRAVEL SHOREFACE DEPOSITS: THE INFLUENCE OF TECTONICS ON THE SEDIMENTOLOGY OF THE CARROT CREEK MEMBER, CARDIUM FORMATION (TURONIAN, UPPER CRETACEOUS), ALBERTA, CANADA.

By

Katherine Mary Bergman, M.Sc.

A thesis

Submitted to the School of Graduate Studies

in Partial Fulfillment of the Requirements

for the Degree

Doctor of Philosophy

McMaster University

(April) 1987

Doctor of Philosophy (1987) McMaster University
(Geology) Hamilton, Ontario

Title Erosion surfaces and gravel shoreface deposits: The influence of tectonics on the sedimentology of the Carrot Creek Member, Cardium Formation (Turonian, Upper Cretaceous), Alberta, Canada.

Author Katherine Mary Bergman, B.Sc. (University of Waterloo)
M.Sc. (McMaster University)

Supervisor Dr. R.G. Walker

Number of Pages xxii, 404 pp.

ABSTRACT

The Raven River Member of the Cardium Formation (Turonian, Upper Cretaceous) in the Carrot Creek -- Cyn-Pem area of Central Alberta, contains two coarsening upward sequences of marine mudstones into sandstones, separated by a gritty siderite. The gritty siderite is believed to represent a pause in deposition in the basin. The sandstones of the upper sequence contain hummocky cross stratification suggesting deposition below fair weather wave base in a storm-dominated setting. The two sequences are scoured to a variable depth by a major erosion surface with a relative relief of about 20 m.

Structure maps and 3-D mesh diagrams suggest that the erosion surface can be divided into four topographic areas: a relatively high, flat TERRACE, a BEVEL where underlying sediments are truncated, and an erosional remnant topography of BUMPS and HOLLOWS, which gradually fades basinwards into a relatively flat BASIN PLAIN. The erosion surface is covered by conglomerates with localized thicknesses of up to 20 m. These conglomerates are assigned to the Carrot Creek Member of the Cardium Formation. The thick conglomerates occur in relatively elongate northwest-southeast trending pools. They are overlain by the transgressive marine mudstones of the Dismal Rat Member of the Cardium Formation.

At first sight the coarsening upward sequence capped by conglomerates (Carrot Creek Member) appears to be similar to

other coarsening upward sequences encased in marine mudstones described from the Western Interior Seaway. These deposits have "traditionally" been interpreted as "offshore ridges", forming many tens of kilometres from the time equivalent shoreline. The Carrot Creek conglomerates, however, are separated from the Raven River Member coarsening upward sequence by an erosion surface, and thus are not genetically part of it. The erosion surface is believed to have formed during a rapid relative lowering of sea level. During maximum lowstand a new shoreface profile (the bevel) was established in the basin. Also during this lowstand, gravel was supplied to the shoreface by incised rivers, and reworked along the shelf by marine processes. Both upper and lower shoreface deposits can be recognized in the conglomerate pools. Subsequent transgression reworked gravel southwestwards across the terrace, while storms transported gravel stringers northeastwards into the transgressive muds accumulating in the hollows.

Similar erosion surfaces of this type have been described from Alberta at the Cardium, Viking, and Badheart horizons. The Gallup-Tocito Formation in New Mexico also invoke a similar erosion surface. The presence of these surfaces may be more widespread than presently documented. The results of this thesis suggest that sea level changes and shoreface incision should be considered as a possible alternative for other long, narrow, "offshore ridges", particularly when the offshore deposits are coarser than the proposed time equivalent shoreline deposits.

REVISION OF CARDIUM STRATIGRAPHY

The stratigraphy used throughout the thesis is that of Plint et al. (1986). Recent detailed correlation of the upper markers revealed inconsistencies in the identification of the E6/T6 and the E7/T7 horizons (A.G. Plint, pers. comm. Jan., 1987). The corrections do not affect any of the interpretations in the thesis, only the names given to the upper markers. For reference the old stratigraphy (Plint et al., 1986) is compared with the revised stratigraphy (Plint et al., 1987) below for well 3-14-52-14. The changes shown are consistent throughout the thesis.

3-14-52-14

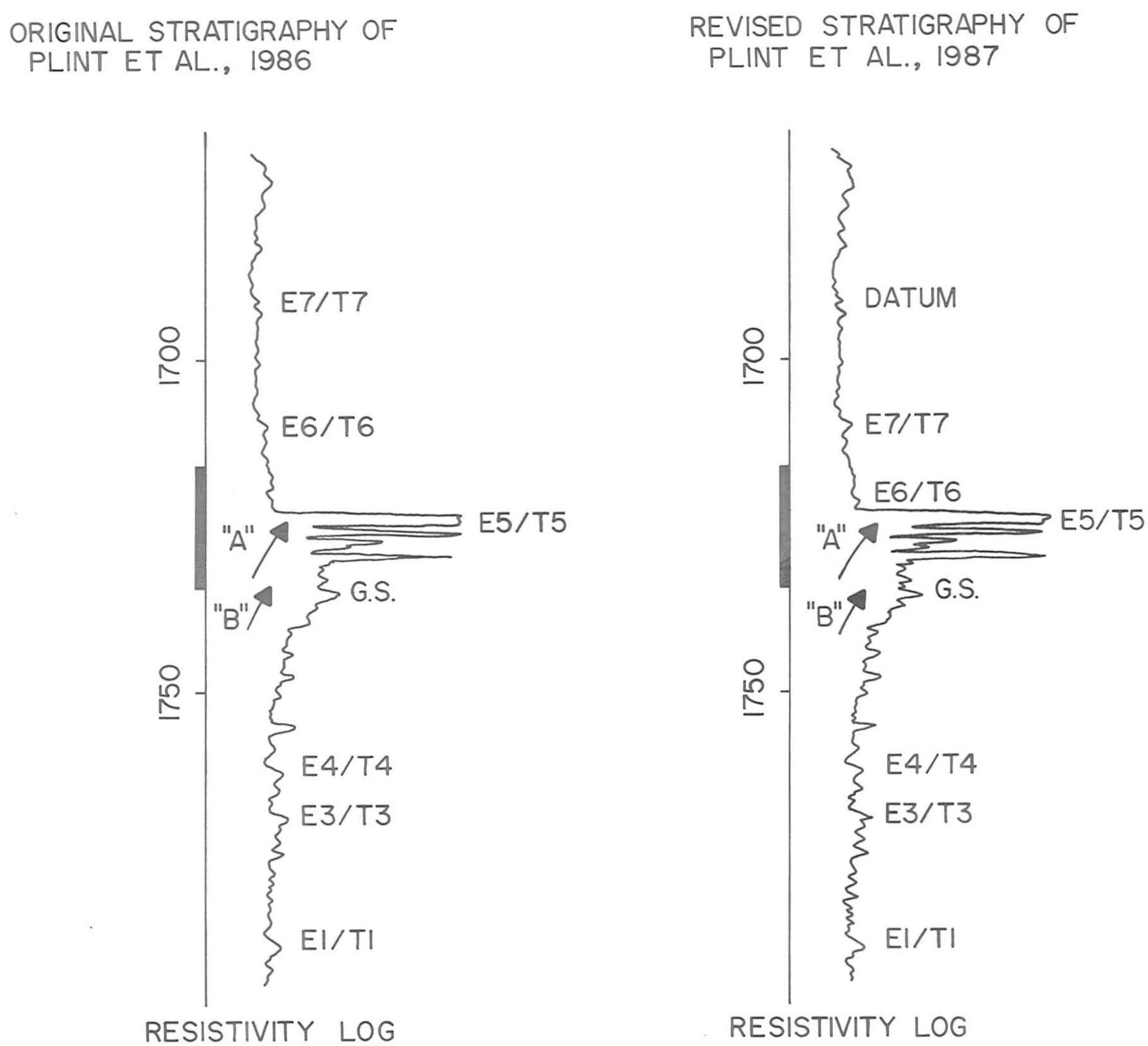
ORIGINAL STRATIGRAPHY OF PLINT ET AL., 1986
1700
1750
E7/T7
E6/T6
E5/T5
"A"
"B"
G.S.
E4/T4
E3/T3
E1/T1
RESISTIVITY LOG
REVISED STRATIGRAPHY OF PLINT ET AL., 1987
1700
1750
DATUM
E7/T7
E6/T6
E5/T5
"A"
"B"
G.S.
E4/T4
E3/T3
E1/T1
RESISTIVITY LOG

ACKNOWLEDGEMENTS

I would like to thank Dr. R.G. Walker. His continuous support and encouragement over the last four years is greatly appreciated. I would also like to thank Dr. A.G. (Guy) Plint who taught all of us, what the effects of varying sea level had on sedimentation. If it was not for Guy, the Cardium might still be interpreted as a turbidite deposit. To both Roger and Guy my heartfelt thanks for you both taught me Sedimentology.

Home Oil Company provided technical support. Access to well logs, maps, and computer analysis were necessary for this study. I would particularly like to thank George Fong, Gordon Stewart, Sid Leggett, and Hilary Stuart-Williams for their time and assistance. Various other oil companies provided support for this thesis. Coenerco allowed me to view confidential core within the study area. Canadian Hunter paid for the cutting of the conglomerate thin sections. C.I.F.E. gave me the pressure and reservoir data for the Carrot Creek -- Cyn-Pem Oil Fields.

All of the field work for the thesis was done out of the Energy Resources Conservation Board Core Research Centre. I would like to thank Mr. Shephard and his staff for making the three summers I spent in Calgary both enjoyable and productive.

During the three years spent in the field various McMaster students provided field assistance. To these students I express my thanks. I would like to thank my friends at McMaster for numerous stimulating discussions, as these discussions often generated new ideas. Jack Whorwood provided photographic assistance. Anne-Marie Plint shaded the 3-D mesh diagrams, and Jeremy Bartlett drew the block diagram shown in Figure 8.9.

To my parents I would like to extend my gratitude. They provided not only financial support, but continuous encouragement during the last four years.

Finally I would like to acknowledge the support of the Natural Sciences and Engineering Research Council. Strategic and Operating Grants to Dr. R.G. Walker and a graduate scholarship to myself provided the funding necessary for this thesis.

TABLE OF CONTENTS

LIST OF FIGURES

LIST OF TABLES

LIST OF FOLDOUTS

CHAPTER 1 -- INTRODUCTION

1.1 PURPOSE OF THIS CHAPTER

This chapter is intended to review, in broad outline only, some of the major ideas and problems, with respect to shallow marine sedimentation, particularly the interaction of depositional processes and environments with sea level fluctuations. The focus of the discussion will be on the storm dominated setting. It is not intended as a full review of the topics covered. For a more detailed review of the shallow marine environment, particularly the shelf environment, the reader is referred to Tillman et al. (1985). Some readers may wish to proceed directly to page 38 (preview of the results of the thesis); to page 43 (Chapter 2, background information of the Cardium Formation); or to page 68 (beginning of the presentation of new results).

1.2 PURPOSE OF THIS THESIS

This thesis was begun in May, 1983. At that time, one of the major controversies in clastic sedimentology was the mechanism by which coarse sediment could be transported across a storm dominated shelf, to depositional sites many tens of kilometres from a contemporaneous shoreline. This coarse material was then believed to be reworked by shelf processes to form long, narrow, en echelon, linear, offshore "ridges" or "bars" (one of the best examples is the Shannon

Sandstone, Tillman and Martinsen, 1984). For brevity, these will be referred to as ridges throughout the rest of the thesis. These ridges were believed to coarsen upward gradationally from the underlying bioturbated shelf deposits. After deposition, these ridges were then overlain by marine mudstones. The interpretation of long narrow sand bodies as offshore ridges still poses two main problems:

1) How was the sand transported across a storm dominated shelf ?

2) What processes focussed this sand on the shelf into long, narrow, coarsening upward ridges gradationally rooted in shelf deposits ?

In an attempt to address the first problem answers were sought by workers in both the modern environment and the ancient rock record. Two different hypotheses of sediment transport across storm dominated shelves evolved. Researchers working primarily in modern environments proposed that sediment was incrementally transported offshore during storms by geostrophic flows (summary in Swift and Niedoroda, 1985). Controversy arose as to whether geostrophic flows could wholly account for those deposits observed in the ancient rock record which were believed to be formed on a storm dominated shelf. Evidence from deposits in the ancient rock record (eg., Jurassic Fernie-Kootenay transition, Hamblin and Walker, 1979), coupled with data presented by Hayes (1967) on the aftermath of hurricane Carla, led to the hypothesis that transport of sediment offshore was by storm generated turbidity currents (summary in Walker, 1985a). The deposits of these two processes (geostrophic flows and turbidity currents) are not easily separated in the shelf environment, as both are characteristic of unidirectional waning flows that may have been subsequently reworked by storm wave processes or other fairweather processes operating on the shelf. These ideas will be discussed in detail below.

The second problem of focussing sediment into long narrow ridges is independent of the mechanism of transporting sediment across the shelf. There is no convincing model of how this coarse material is subsequently reworked on the outer shelf into long, narrow, coarsening upward ridges, gradationally rooted in marine shales. There are no known modern places where this is occurring.

The original problem addressed by the thesis was to examine shelf deposits in an attempt to separate geostrophic flows from turbidity currents as the primary transporters of sediment across a storm dominated shelf, and to examine the geometry of the resulting sand and/or conglomerate bodies. For brevity, these sand and conglomerate bodies will be collectively referred to as sandbodies throughout the rest of the thesis. The separation of the deposits of these two processes in fine grained sandstones is difficult. In both cases the sand is transported in suspension across the shelf by a waning unidirectional flow. The sands are then subject to subsequent reworking by storm waves. These two factors produce similar deposits by two completely different and unrelated driving mechanisms. Geostrophic flows are driven by pressure differences whereas turbidity currents are driven by gravity. The flow mechanisms within the moving fluid are probably similar, hence the deposits of the two flows are similar. In order to separate the two processes a coarser unit is required where some of the transport, particularly in the case of geostrophic flows, would be by bedload. A coarser sandbody was needed, encased in marine shales and apparently deposited many tens of kilometres from the shoreline. From this, a detailed study of the preserved facies might more readily distinguish between the two processes (i.e., geostrophic flows or turbidity currents). For this reason, the Turonian Cardium Formation conglomerate deposits at Carrot Creek oil field, Alberta, were selected. These deposits were interpreted by Swagor et al. (1976) to have formed on the shelf, many tens of kilometres from the nearest shoreline, as a "terrace bar". They suggested that the sediment was transported offshore during storms.

The Carrot Creek area was also chosen because the coarse grain size (1-2 cm long axis average diameter) made the problems of sediment transport across the shelf more acute. It was hoped that a detailed analysis of the preserved conglomerate fabric(s) would separate the two hypotheses of sediment transport across the shelf. The hypothesis to test was that if the preserved preferred fabric was "a" axis parallel, "a" axis imbricate (Walker, 1975a), then the gravel was moving dispersed above the bed, probably as a result of clast collisions at the base of a turbidity current. If however, the fabric was "a" transverse, "b" imbricate, then the gravel was rolling as bedload. This could be the result of either geostrophic flows or turbidity currents. A mixed orientation of the clasts would suggest that the sediment had been transported dispersed above the bed (i.e., turbidity currents) and then moved a little further as bedload. The reverse condition does not hold.

Detailed analysis of the conglomerate fabric and texture should yield information on the types of processes operating on the gravel (specifically) and on the shelf in general. A study of the conglomerates at Carrot Creek showed little in the way of preferred imbrication. In general the pebbles were found to lie in the plane of regional bedding or else no discernable preferred pebble fabric was observed. These initial results made it difficult to define the depositional environment of the gravel.

Initial correlation of well logs and core in the Carrot Creek area supported the conclusion of Swagor et al. (1976) that the base of the conglomerate was clearly erosive, scouring down to various depths, and not gradationally rooted in the underlying shelf deposits. The geometry of the conglomerates suggested a channel morphology, rather than the ridge morphology suggested by Swagor et al. (1976). I interpreted these initial sections (Bergman 1984 and supplement) as channels cut and filled by turbidity currents, similar to another Cardium channel described by Walker (1985b) at Ricinus. The difference between the two channels was the conglomeratic nature of the fill in the Carrot Creek area. More detailed correlation of well logs and cores from the field, however, revealed a "one-sided" geometry of the conglomerate bodies, rather than a channel-like morphology. The "one sided geometry" implies that the conglomerates are banked up against a more steeply dipping erosion surface on one side and pass laterally into basinal shelf muds on the other, without an erosional margin.

Instead of being transported many tens of kilometres across the shelf, the conglomerate deposits are interpreted in this thesis as shoreface deposits, formed as a result of a rapid relative lowering of sea level (Bergman and Walker, 1986; and in press). This interpretation is based primarily on the conglomerate geometry, preserved facies sequences, morphology of the lower erosion surface, and the regional stratigraphy as described by Plint et al. (1986).

The geometry of the deposits and their lower erosion surface has led to the environmental interpretation presented here. Consequently, the texture and fabric of the conglomerates will provide information on the variety of facies present in a gravelly shoreface, rather than defining the depositional environment of the conglomerates as was the original hypothesis of this thesis.

The problems in this thesis are now no longer associated with the transport of coarse material out onto the shelf, and the subsequent reworking into ridges. Rather, the problems are concerned with the effects of rapid sea level variation and the nature of the deposits which are preserved as a result of varying sea level.

1.3 SHELF PROCESSES

The modern shallow marine environment (< 200m) comprises about 5.3% of the earth's surface, and is one of the most complicated depositional environments. This is due to the number of processes interacting to transport and rework sediment, and the interaction of these processes with Coriolis force. The shallow marine environment may be sub-divided into three major types based on the dominant process operating on the shelf:

1) <u>storm-dominated</u> shelves which comprise 80% of the modern shelves (Swift et al., 1981), eg., North Atlantic Shelf,

2) <u>tide-dominated</u> shelves which comprise 15% of the

modern shelves (McCave, 1971), eg., North Sea, and

3) shelves dominated by <u>intruding ocean currents</u> which comprise 5% of the modern shelves (Flemming, 1980), eg., Southwest African Shelf.

It is generally agreed that the Cardium was deposited on a storm dominated shelf (Swagor et al., 1976; Wright and Walker, 1981; Krause, 1983; Krause and Nelson, 1984; Duke, 1985a; Walker, 1985c). Only the dominant processes of sediment transport operating in this environment will be discussed in this thesis. In order to understand the distribution of facies preserved on this type of shelf, an understanding of the dominant processes operating on the shelf sediments is necessary. Most of the data for modern storm dominated shelves comes from the Atlantic Continental Shelf. A detailed discussion of storm circulation patterns is given by Swift and Niedoroda (1985).

Tidal processes will not be discussed, but are reviewed by Swift and Niedoroda (1985). Good technical discussions of tidal current generation may be found in Fox (1983) and Howarth (1982).

The following sections are very brief reviews designed only to direct the reader into the literature.

A. GEOSTROPHIC FLOWS

In its simplest form (Fig. 1.1) a geostrophic flow will develop as the result of an onshore wind piling water up on the shore causing a coastal set up, and hence a seaward

Figure 1.1. Coastal set-up (storm surge) creates a seaward pressure gradient. Bottom water flows seaward as a result, but is deflected to the right (northern hemisphere) by Coriolis force to evolve into a geostrophic flow parallel to the isobaths (from Walker, 1984a, after Swift and Niedoroda, 1985).

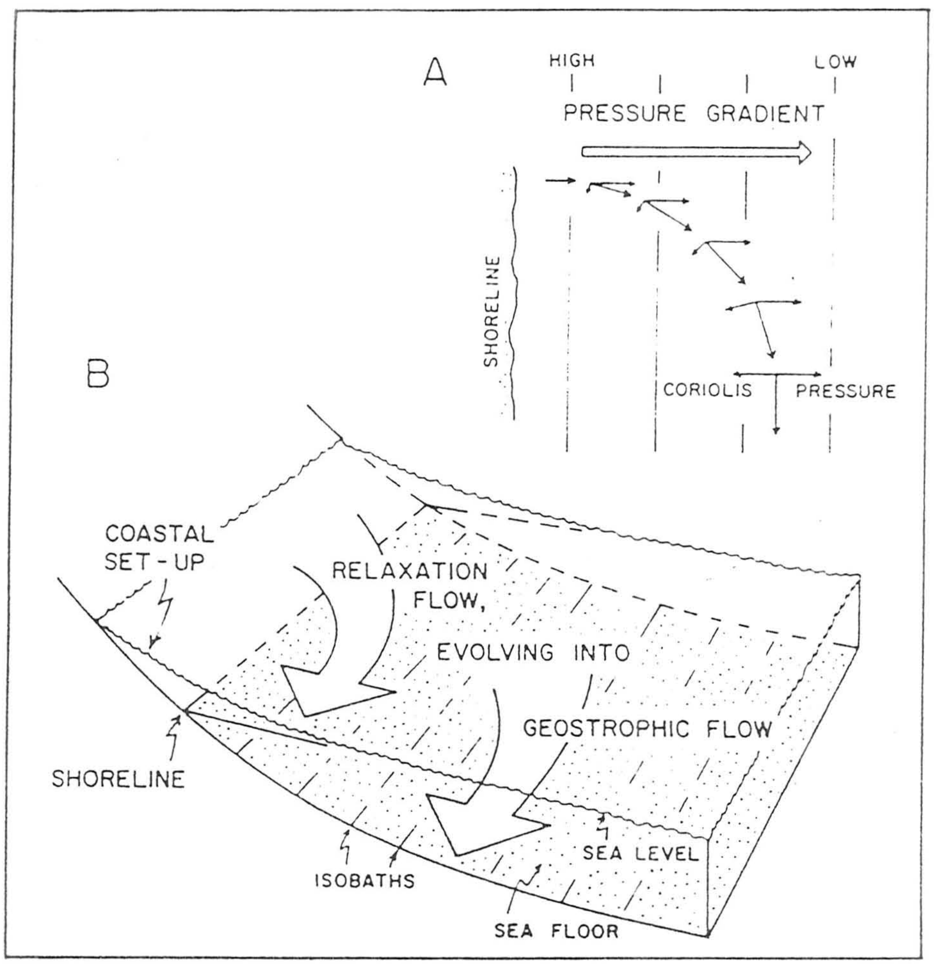
A
HIGH
LOW
PRESSURE GRADIENT
SHORELINE
CORIOLIS
PRESSURE
B
COASTAL SET - UP
RELAXATION FLOW,
EVOLVING INTO
GEOSTROPHIC FLOW
SHORELINE
ISOBATHS
SEA LEVEL
SEA FLOOR

pressure gradient. The relaxation bottom current flows seaward down the pressure gradient, and is gradually deflected to the right (Northern Hemisphere) due to Coriolis force, evolving into a geostrophic flow moving parallel to the isobaths. Storm surge ebb flows, in the sense of gravity driven seaward return flows (as envisaged by Hayes, 1967), are trivial when compared to the longshore discharge of a geostrophic flow of shelf width and depth, which may be prolonged for several days (Swift and Niedoroda, 1985). Swift (pers. comm.) has suggested that the geostrophic discharge may be 2000 to 3000 times as great as the storm surge ebb discharge for a two day storm.

Geostrophic flows will disperse sediment sub-parallel to the isobaths (i.e., along the strike of the palaeoslope). With each storm the sand will move incrementally across the shelf either as bedload or suspended load, or some combination of the two. Most catastrophic storm flows have been documented from the Gulf of Mexico. Forristall et al. (1977) monitored tropical storm Delia (Sept. 3-5, 1973) from a drilling platform located 50 km offshore in about 21 m of water. Alongshore flows of 2 m sec.$^{-1}$ were recorded, and seaward directed flows were between 50 to 75 cm sec.$^{-1}$. Murray (1970) measured wind and current velocities of Hurricane Camille (Aug. 16 - 18, 1969), 360 m offshore of the Florida coast in 6.3 m of water.

these storm events, suggests effective sand transport, and the creation of ripples, sinuous crested dunes and possibly upper plane bed (according to the stability fields given in Harms et al. 1982) during peak flow. These bedforms are subject to reworking by waning flows as the storm intensity decreases. The net result would be an increment of sand transport, but no preservation of sedimentary structures other than ripple cross lamination (Walker, 1984a).

B. STORM WAVES

Wind blowing across the water surface generates storm waves which entrain deeper and deeper water layers until flow at the bed may be capable of moving sediment as bedload, in suspension, or both.

A detailed discussion of wave properties and wave-formed structures was presented by Duke (1985a), and interested readers are referred to this reference. A brief discussion will be presented here outlining the basic ideas necessary in understanding facies distribution on the shelf. The wave orbital component of a storm flow is critical in sediment entrainment and transport (Fig. 1.2). Wave orbital diameter decreases exponentially with depth, until at a depth equal to 1/4 of the surface wavelength (Komar, 1976; Vincent et al., 1982), wave induced motion is negligible. In water sufficiently shallow for wave motion to impinge on the bottom, the orbits become flatter as the bottom is approached, and just above the bottom, exist as

Figure 1.2. Diagrammatic relationship between fluid motion characteristics under progressive surface waves and the interaction with the bed (after Komar, 1976; Vincent et al., 1982).

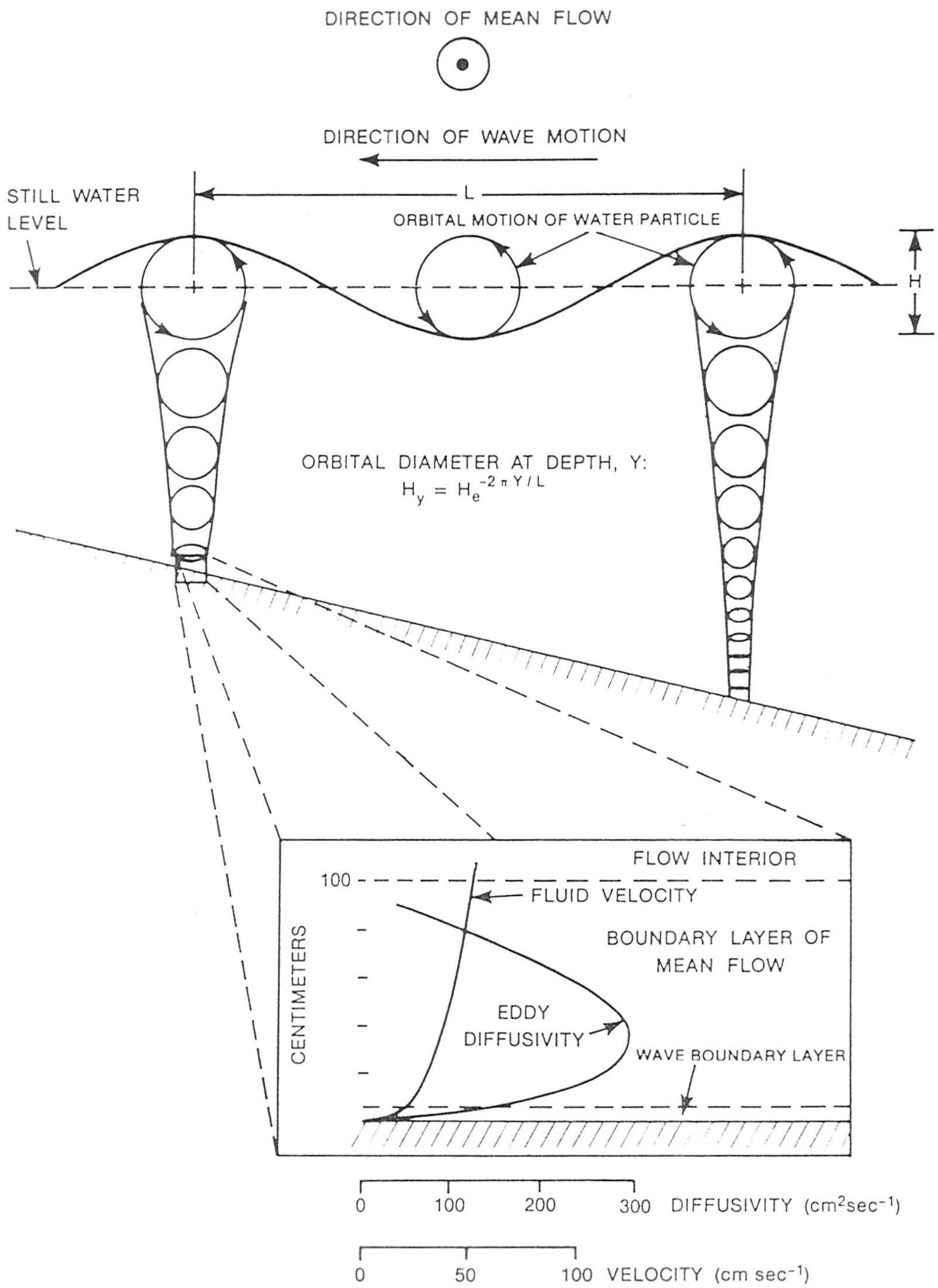
DIRECTION OF MEAN FLOW
DIRECTION OF WAVE MOTION
STILL WATER LEVEL
L
ORBITAL MOTION OF WATER PARTICLE
H
ORBITAL DIAMETER AT DEPTH, Y:
$H_y = H_e^{-2\pi Y/L}$
FLOW INTERIOR
100
FLUID VELOCITY
BOUNDARY LAYER OF MEAN FLOW
CENTIMETERS
EDDY DIFFUSIVITY
WAVE BOUNDARY LAYER
0 100 200 300 DIFFUSIVITY ($cm^2 sec^{-1}$)
0 50 100 VELOCITY ($cm\ sec^{-1}$)

a simple back and forth motion. The thin (on the order of several cm), transient boundary layer associated with the wave orbital current is more effective in entraining sediment compared with the mature, thick (on the order of 1m) boundary layer associated with the mean flow (Komar, 1976; Vincent et al., 1982). The vertical velocity gradient and hence the vertical shear stress gradient, is gentle in such a thick boundary layer.

During a storm the wave orbital current velocity gradient, confined to a boundary layer several centimeters thick, is very steep, hence the shear stresses associated with wave orbital currents are greater than those induced by the mean flow component. When a wave orbital current component and a mean flow component coexist near the bottom, they interact in a nonlinear fashion because of the nature of the turbulence generated by the combined flow. The resulting boundary shear stresses are greater than the sum of the stresses that would be developed by either the wave orbital component or the mean flow component (Grant and Madsen, 1979). The mean flow boundary layer experiences the thinner wave boundary layer as an additional degree of turbulence-generating bottom roughness. These highly turbulent bottom flows may be able to support a higher ratio of suspended load to bedload, and consequently sediment transport by combined wave orbital and storm wind driven flow components is therefore a highly efficient process.

The sedimentary structures produced from these storm waves have not been adequately documented from the modern environment, and only a limited amount of experimental work (Southard 1984) has been done. Duke (1985b) compiled a list of all known occurrences of hummocky cross stratification from a variety of environments. Hummocky cross stratification has been recognized and described in more than 100 stratigraphic units.

Harms (in Harms et al. 1975, p. 87-88) first proposed the term hummocky cross stratification and suggested that it was formed by "...strong surges of varying direction that are generated by relatively large storm waves...". This interpretation is supported in the geologic record by the facies found associated with hummocky cross stratified sandstones. The bioturbated mudstones found interbedded with the sharp based hummocky cross stratified beds suggest deposition in "quiet" environment. The sharp bases of the hummocky beds suggest rapid emplacement of the beds into this quiet environment. The absence of medium scale angle of repose cross bedding further suggests that deposition was below fairweather wave base. It is broadly agreed that hummocky cross stratification is formed by storm waves acting below fairweather wave base (Walker, 1984a, 1985a). Much controversy still exists however, as to the mechanism of emplacement of the sand into an originally quiet environment (i.e., geostrophic flow versus turbidity current). Detailed descriptions of the geometry of hummocky cross stratification (Fig. 1.3) have been given by Hunter and Clifton (1982), Dott and Bourgeois (1982), Walker (1982), and Walker et al., (1983). Greenwood (1984) described a similar feature from modern lake sediments.

C. TURBIDITY CURRENTS

Turbidity currents have never been observed on a modern shelf, but the geologic record seems to suggest that turbidity currents were operating on the shelf. Swift et al. (1971) suggested that density currents operate on the shelf. The turbidity current is a special case of the density current, where the density difference between the flow and the surrounding seawater is due to suspended sediment. A number of mechanisms might be capable of generating turbidity currents in the shelf environment:

1) major rivers supplying large amounts of sediment (Heezen et al. 1964; Shepard and Emery, 1973; for the Congo River).

2) slumping on delta slopes (Moore, 1961; Heezen 1956, in Kolla et al.,1984; Lindsay et al., 1984; Dengler et al., 1984).

3) earthquakes (as in the Grand Banks, Newfoundland, 1929 earthquake; Uchupi and Austin, 1979).

There are examples (Fernie-Kootenay Transition, Banff Traffic Circle, Hamblin and Walker, 1979) in the geologic record where deposition appears to be by turbidity currents

Figure 1.3. A) Diagrammatic representation of the idealized hummocky cross stratified sequence proposed by Dott and Bourgeois (1982). B) Idealized hummocky cross stratification sequence proposed by Walker et al. (1983). In this model it is suggested that the bedform can in places grow upward from a flat bed. This sequence contrasts with the sequence proposed by Dott and Bourgeois (1982) model, where the hummocky and swaley laminae are shown to drape a previously scoured bed.

A

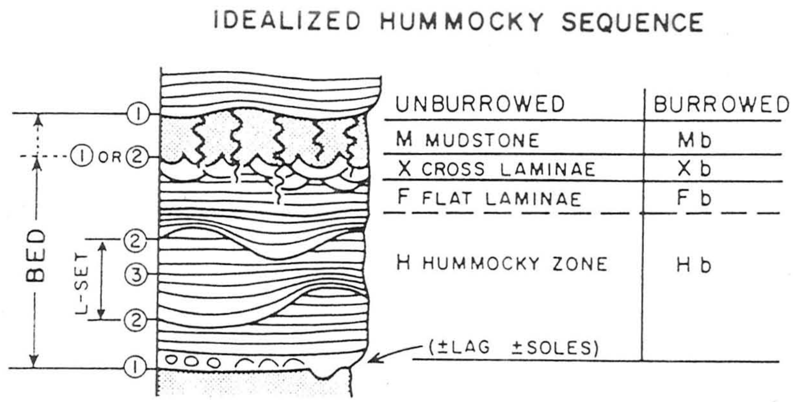
IDEALIZED HUMMOCKY SEQUENCE
UNBURROWED
BURROWED
M MUDSTONE
Mb
X CROSS LAMINAE
Xb
F FLAT LAMINAE
Fb
H HUMMOCKY ZONE
Hb
(±LAG ±SOLES)
BED
L-SET
1 OR 2

B

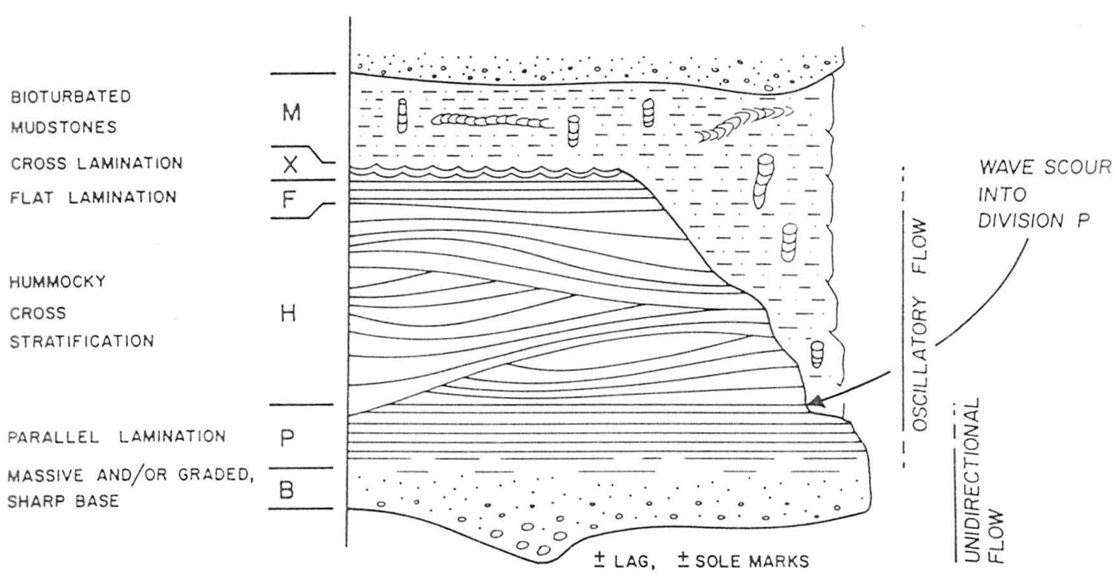
BIOTURBATED MUDSTONES
M
CROSS LAMINATION
X
FLAT LAMINATION
F
HUMMOCKY CROSS STRATIFICATION
H
PARALLEL LAMINATION
P
MASSIVE AND/OR GRADED, SHARP BASE
B
± LAG, ± SOLE MARKS
WAVE SCOUR INTO DIVISION P
OSCILLATORY FLOW
UNIDIRECTIONAL FLOW

(preservation of Bouma BC sequences and the absence of wave formed features of any scale). These turbidites are directly overlain by interbedded muds and hummocky cross stratified and wave rippled sands. The orientation of tool marks on the bases of the hummocky cross stratified beds are consistent with the underlying turbidites, suggesting that the hummocky cross stratified beds were emplaced down the same palaeoslope by turbidity currents, but deposition occurred above storm wave base. These beds, deposited above storm wave base, are subject to reworking by storm waves to form hummocky cross stratification and wave ripples. This association of turbidites grading up into hummocky cross stratified and wave rippled sand beds with consistent palaeoflow directions between both units, as seen at the Banff Traffic Circle, suggests storm generation of turbidity currents. Hamblin and Walker (1979) initially proposed that the storm would suspend enough sediment at the shoreline to generate a turbidity current. Swift (pers. comm.) rejected this mechanism of generating turbidity currents, because he felt that storms could not suspend sufficient volumes of sediment at the shoreline, to meet the autosuspension criteria (Pantin, 1979). Both Pantin (1979; 1983) and Parker (1982) in separate studies suggested that the autosuspension criteria was unlikely to be achieved in the shelf environment.

Sterling and Strohbeck (1975) concluded that cyclic wave loading during major hurricanes, occurring about once in a hundred years, could cause sufficient bottom pressures to create instability, and subsequent failure of the substrate. Walker (1984a) extended this idea as a method of storm generation of turbidity currents on the shelf (Fig. 1.4). Cyclic wave loading of rapidly deposited fine sediment may cause liquefaction of the substrate. The downslope flow and combination of flow acceleration and expulsion of pore fluids could keep fine and very fine sediments in suspension and generate a turbidity current.

Studies on modern shelves however, have revealed no evidence for the existence high velocity spasmodic turbidity currents. Hayes (1967) originally interpreted an inner shelf sand deposit on the east Texas shelf in the aftermath of hurricane Carla as a turbidite. More recent analysis by Morton (1981) suggests that the Carla bed was deposited by longshore geostrophic flows.

As discussed in section 1.2, neither of these processes (geostrophic flows or turbidity currents) accounted for the accumulation of gravels in the Carrot Creek study area. Analysis of the conglomerate body geometry and the morphology of the erosion surface led to interpretation of these conglomerate bodies as shoreface deposits.

1.4 SHOREFACE MORPHOLOGY

The previous section has discussed fluid and sediment dynamics on storm dominated shelves. This section will

Figure 1.4. Storm winds create coastal set up, and cyclic wave loading of the substrate by storm waves may liquefy the substrate. The liquefied sediment may flow and accelerate basinward, transforming into a turbidity current with all of the sediment in suspension. Deposition from this flow below storm wave base would result in turbidites with Bouma sequences. Above storm wave base waves feeling the bottom would rework the turbidity current deposits into hummocky cross stratification (after Walker, 1984a, 1985a).

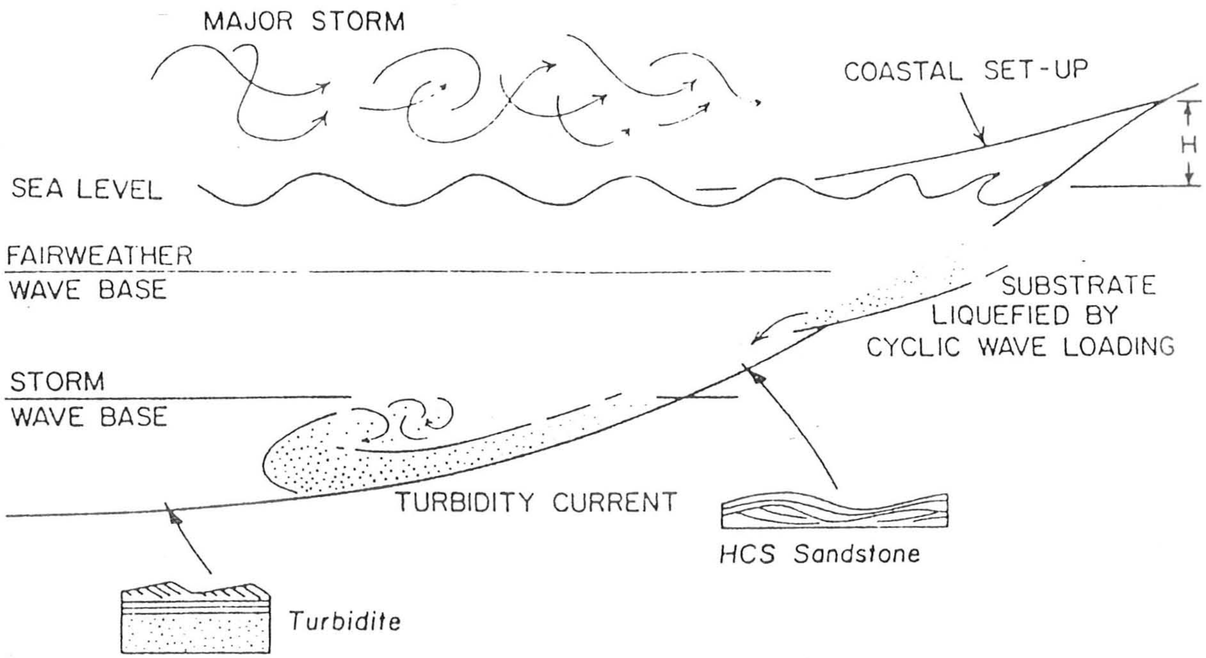
MAJOR STORM
COASTAL SET-UP
H
SEA LEVEL
FAIRWEATHER
WAVE BASE
SUBSTRATE
LIQUEFIED BY
CYCLIC WAVE LOADING
STORM
WAVE BASE
TURBIDITY CURRENT
HCS Sandstone
Turbidite

consider the morphology of storm dominated shorefaces. Flow in this inner shelf area is complex and highly structured.

Barrell (1912) defined the shoreface as the relatively steeply dipping, innermost portion of the continental shelf. The break in slope where the shoreface merges with the inner shelf floor may take place in depths of 15 to 20 m (see review by Walker, 1985a, on the depth of the base of the shoreface) the depth being greater with increased rigour of the wave and current climate. On unconsolidated coasts exposed to marine processes, shorefaces are surfaces curved about an axis parallel to the shoreline, and exhibit little change in the alongshore direction (Fig. 1.5). On rocky coasts however, the time required for the profile to be incised into the substrate is long relative to the rate of sea-level change, hence rocky shorefaces are poorly developed. Local sand accumulations on rocky coasts develop well defined shorefaces, but these shoreface fragments are irregularly distributed in plan view (Swift and Niedoroda, 1985).

In general the slope of the shoreface increases with;

a) increasing grain size (Langford-Smith and Thom, 1969; Wright and Coleman, 1972),

b) decreasing sediment input (Wright and Coleman, 1972), and

c) decreasing fluid power (Wright and Coleman, 1972).

The shoreface may be sub-divided into two major regimes, the

Figure 1.5. The geomorphology of a straight two-dimensional shoreface formed on unconsolidated coasts exposed to marine processes (Swift and Niedoroda, 1985, after Barrell, 1912).

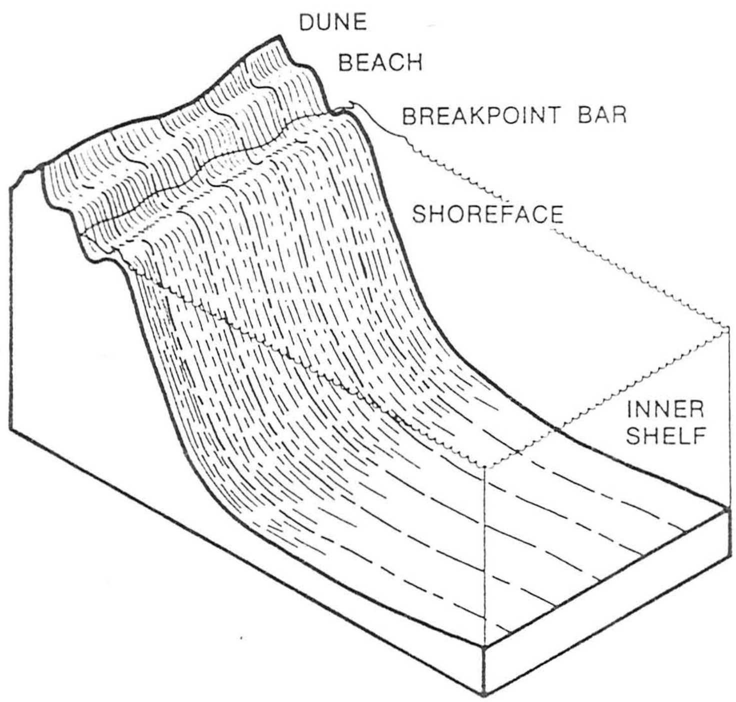
DUNE
BEACH
BREAKPOINT BAR
SHOREFACE
INNER
SHELF

lower shoreface and the upper shoreface. The upper shoreface is dominated by shoaling and breaking waves. Marine currents tend to be less intense over the upper shoreface where they are inhibited by greater bottom friction. The reverse is true of the lower shoreface. The boundary between these two zones is transitional and is a function of the wave intensity and the current climate. In terms of effect on the bottom, depths of 10 to 15 m seem to mark a valid generalized division between the upper and lower shoreface (Swift and Niedoroda, 1985). The problem is to relate the upper and lower shoreface regimes to each other and to the larger scale coastal flow system.

Some authors (eg., Clifton et al., 1971; Hunter et al., 1979; Dupre et al., 1980) have chosen to use dynamic zone terminology rather than geomorphic terminology in describing modern coastal processes and their deposits. Although their usage has advantages in that the term shoreface may suggest a narrow topographically restricted zone, shoreface type deposits in the geologic record will typically represent a mixture of several dynamic zones and processes and hence dynamic names may be misleading. Figure 1.6 modified from Bourgeois and Leithold (1984) and Walker (1984a) shows diagrammatically the correlation of the dynamic and geomorphic terminology for the nearshore environment.

Figure 1.6. Cartoon relating the geomorphic terminology used by researchers in ancient sediments to the dynamic terminology of the shoreface used by researchers working in the modern environment (after Bourgeois and Leithold, 1984; Walker, 1984a).

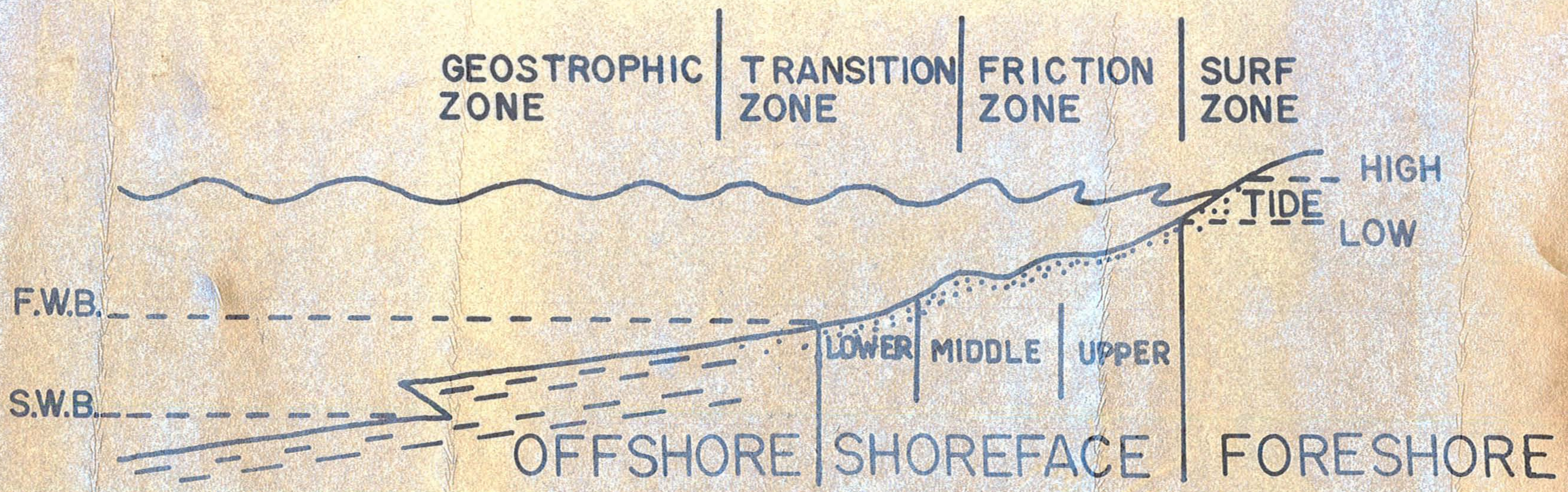
GEOSTROPHIC ZONE
TRANSITION ZONE
FRICTION ZONE
SURF ZONE
HIGH
TIDE
LOW
F.W.B.
S.W.B.
LOWER
MIDDLE
UPPER
OFFSHORE
SHOREFACE
FORESHORE

1.5 LINEAR OFFSHORE RIDGES

Many Cretaceous formations in the Western Interior Seaway, such as the Shannon, Frontier, Ferron, Gallup, Viking, and Cardium, are characterized by a series of linear sandstone and conglomerate bodies. These sandstone and conglomerate bodies have commonly been regarded as long, narrow, en echelon ridges, trending parallel to sub-parallel to the regional strandline. They were apparently deposited in an open marine setting, many tens of kilometres from the nearest contemporaneous shoreline. In general these ridges are overlain and underlain by marine shales, and may pass laterally into marine siltstones and muddy sandstones. Internally, the ridges have been described as containing coarsening upward sequences, suggesting that the sandstones and/or conglomerates at the tops of the ridges are gradationally rooted in marine shales. Tillman (1985, p.35) suggested that "... if a coarsening upward sequence can be identified as being on the outer shelf on the basis of palaeontology and regional geology, it will almost always be a sand ridge" .

The morphology of the long, narrow ridges has been tabulated by Walker (1984a, p. 164) and Slatt (1984, p. 1109). One of the best examples of presumed deposition in an offshore setting, some "70 to 100 miles [112 to 160km] east of the contemporaneous shoreline" (Tillman and Martinsen, 1984, p. 122) is the Lower Campanian Shannon

Sandstone of Montana and Wyoming (Shurr, 1984; Tillman and Martinsen, 1984; Tye et al., 1986).

Tillman and Martinsen (1984) developed a summary block diagram for the Upper Cretaceous Shannon Sandstone, Wyoming, which implies geostrophic transport of sand. The summary (Fig. 1.7) consists of five main facies:

A) Shelf facies -- bioturbated siltstones

B) Interbar facies -- interbedded sharp based, wave rippled sands and muds

C) High Energy Bar Margin facies -- glauconitic, coarse grained, medium, scale trough cross bedded sands, with no mud, very few ripples and siderite clasts

D) Low Energy Bar Margin facies -- fine grained interbedded trough cross bedded sand with wave ripples and muds

E) Bar Crest facies -- fine grained trough cross bedded sands with no mud.

These facies are complexly intertongued due to lateral shifting of the bar crest. Many shelf sandstones show a coarsening upward sequence and "...generally are coarser grained than their time equivalent shoreline deposits" (Tillman, 1985, p. 5). The Shannon sandstone has a very sharp upper contact with the overlying marine shales. This lateral shifting of facies results in sequences which are difficult to explain, especially when the Low energy Bar

Figure 1.7. A) Relatively closely spaced sections on the southwest part of the Salt Creek Anticline, Shannon outcrop. Lateral changes from Central Bar Facies to lower energy facies and doubling of thickness of the upper Shannon sandstone between sections are shown. B) Model of facies deistribution of mid-shelf Shannon Sandstone shelf-ridge complex. The diagram has extreme vertical exaggeration, but the abrupt lateral changes indicated are substantiated by outcrop (after Tillman and Martinsen, 1984).

a

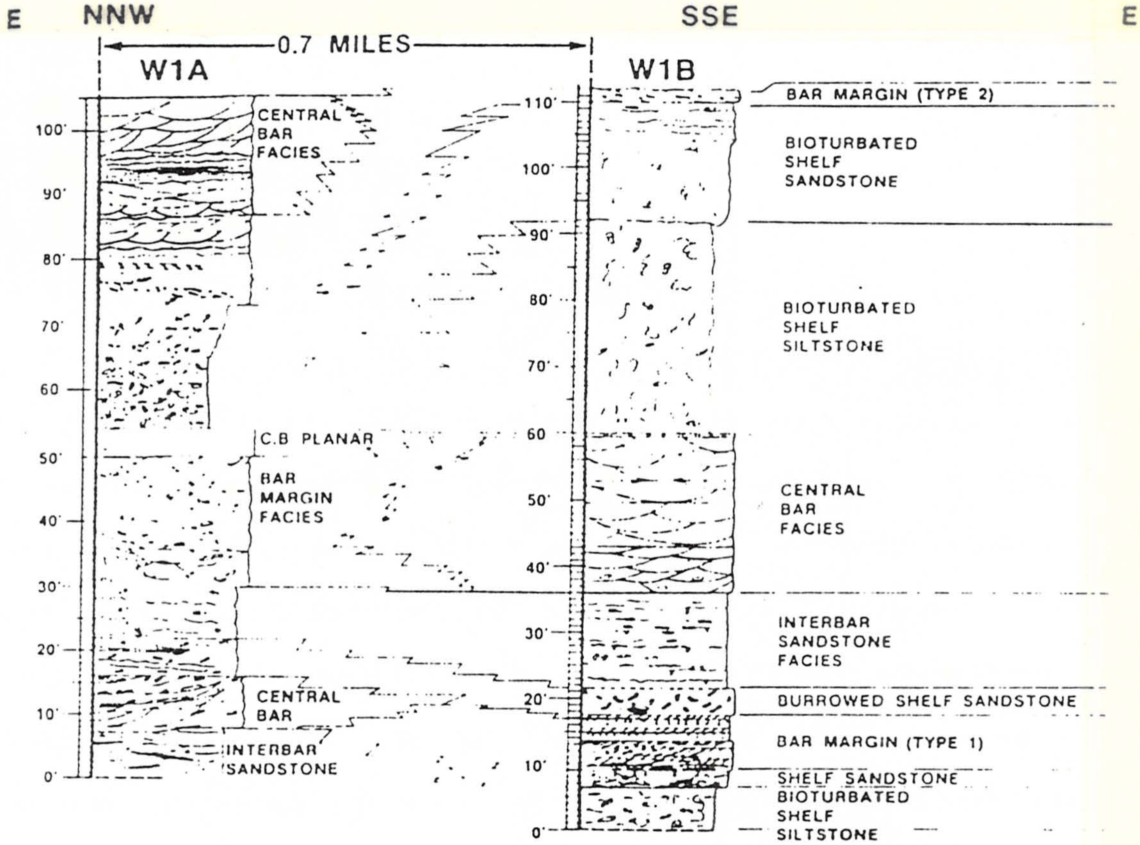
E
NNW
SSE
E'
0.7 MILES
W1A
W1B
CENTRAL BAR FACIES
C.B PLANAR
BAR MARGIN FACIES
CENTRAL BAR
INTERBAR SANDSTONE
BAR MARGIN (TYPE 2)
BIOTURBATED SHELF SANDSTONE
BIOTURBATED SHELF SILTSTONE
CENTRAL BAR FACIES
INTERBAR SANDSTONE FACIES
BURROWED SHELF SANDSTONE
BAR MARGIN (TYPE 1)
SHELF SANDSTONE
BIOTURBATED SHELF SILTSTONE

b

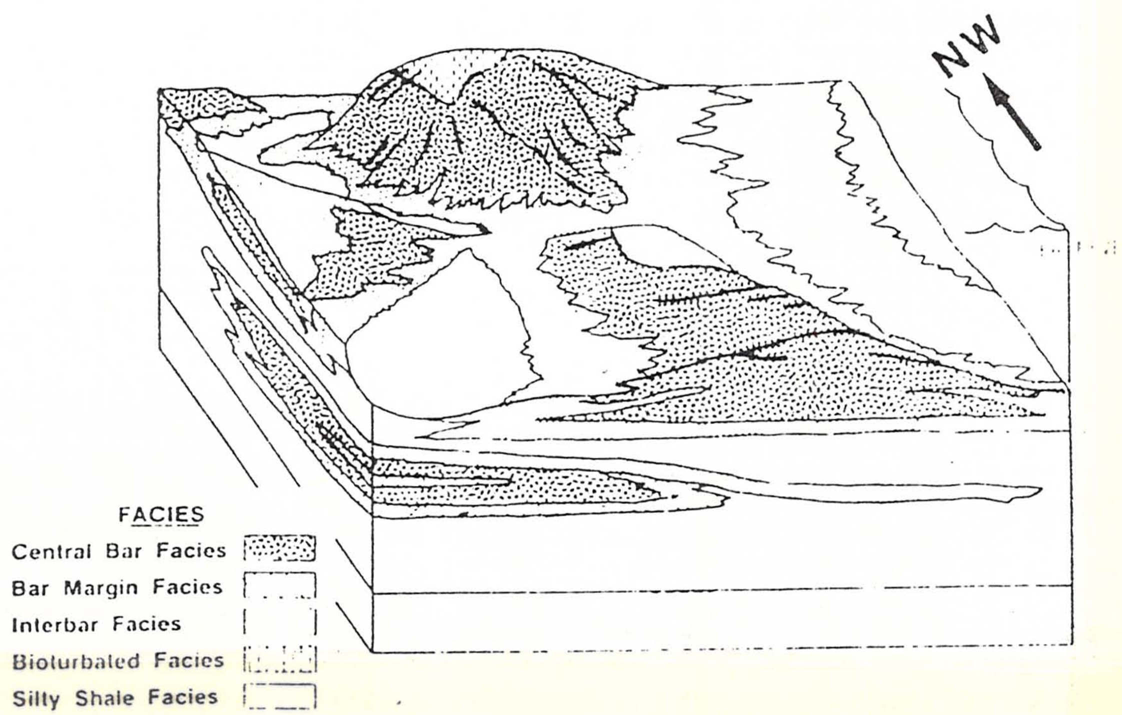
NW
FACIES
Central Bar Facies
Bar Margin Facies
Interbar Facies
Bioturbated Facies
Silty Shale Facies

Margin facies rests directly on the High Energy Bar Margin facies (Tye et al., 1986; fig. 7), with no preservation of the thick (up to 10 m) Central Bar facies. This transition from high energy bar margin to low energy bar margin occurs in less than a metre.

The primary objections to the sand ridge model, however, are more fundamental than lateral shifting of facies. The first problem concerns the mechanism by which coarse material is transported from the shoreline to depositional sites many tens of kilometres offshore. Spearing (1976, p. 76) envisaged transport of the Shannon sandstone 100 km offshore by a "...storm system, superimposed on oceanic or tidal currents." Seeling (1978) gave an equally illuminating interpretation of the Shannon sandstone. He suggested an "...ancient hydraulic environment...analogous in some important respects to those present day environments with prominent currents off the east coast of the United States and in the southern part of the North Sea". Similar interpretations were presented for the Sussex (Berg, 1975; Brenner, 1978). The study by Hobson et al. (1982) is one of the few to propose a transgressive origin for the sandbodies. From the interpretations presented by these authors, it is apparent that there is no clear consensus of how the sand was transported across the shelf. These interpretations do not even attempt to address the second problem of focussing the sediment into long, narrow, coarsening upward ridges.

In later studies of linear shelf ridges, storm generated geostrophic flows have generally been invoked as the process by which sediment is transported offshore (Winn et al., 1983, Frontier Formation; Berven, 1966, Cardium Formation at Crossfield; Swagor et al., 1976, Cardium Formation at Carrot Creek). There is also some suggestion that turbidity current transport of sediment offshore occurred; particularly in the geologic record (Hamblin and Walker, 1979; Walker, 1983 a, b, 1985 a, b).

The second problem concerns the molding of this sediment on the shelf into long, narrow, en echelon, coarsening upward ridges. To date, no clear suggestion as to how this molding took place has been given. It is not clear from the interpretations presented by the various authors cited above why these ridges should preserve coarsening upward sequences, with coarse material (sand and/or gravel) preferentially transported to the tops of these ridges. The third problem concerns the observation that these shelf ridges are generally coarser than their apparent time equivalent shoreline deposits.

Several ridges, at first sight similar to those discussed above, have been documented in the Cardium Formation. Their depositional environment has been regarded as "offshore", with storm-influenced deposition below fair weather wave base, but above storm wave base (Berven, 1966; Swagor et al., 1976; Almon, 1979; Walker, 1983a; Krause and Nelson, 1984; Keith, 1985). In the Cardium the conglomeratic nature of the ridges makes the problems of linear ridge development even more acute. The Carrot Creek Member (Plint et al., 1986) contains elongate en echelon conglomerate bodies up to 20 m thick with no connection to any known shoreline (Plint et al., 1986). Swagor et al. (1976) suggested storm transport of thse conglomerates across the shelf, with deposition as "terrace bars" (after Campbell, 1971) in the lee of pre-existing topographic features.

At Carrot Creek the nature of the coarsening upward sequences, the morphology of the conglomerate bodies and their associated erosion surfaces, and the problems of sediment transport and focussing, have forced a re-evaluation of the hypothesis of deposition tens of kilometres from the shoreline. In this thesis, I will demonstrate that the conglomerates are <u>not</u> genetically part to the coarsening upward sequence, but overlie an erosion surface with about 20 m of relief. The erosion surface appears to represent an incised shoreface (Bergman and Walker, 1986; in press), and the gravels may have been transported to this shoreface by longshore drift during a low stand of sea level. The problems now appear to concern sea level fluctuations, rather than sediment transport and focussing in open marine settings.

1.4 SEA LEVEL CHANGES AND SEDIMENTATION

The idea that sea level fluctuation can affect sedimentation is not new to sedimentology. Lyell (1832) first proposed tectonic control of sea level. Suess (1906) suggested that sea level fluctuations were eustatic. The relative roles played by eustatic movements of sea level and tectonic movements, in determing ancient transgressions and regressions within orogenic and cratonic basins, remain to be determined.

Modern stratigraphic thinking has been influenced by the ideas of Vail et al. (1977 a, b) on global eustatic controls of unconformity bounded sequences (refer to Vail et al., 1977 a, b; Hancock and Kauffman, 1979; for historical discussion and modern concepts of sea level variation). There are at least four, possibly five, scales of sequence development in the stratigraphic record related to sea level fluctuations in the Phanerozoic. Vail et al. (1977b) defined the four cycles, in terms of their regional and inter-regional extent and the length their of duration (Fig. 1.8; Table 1.1). The first order cycles include two extended periods of maximum marine transgression, and a period of maximum marine regression. The second order cycles (supercycles) correspond roughly to the cratonic sequences defined by Sloss (1963), and range in length from 10 Ma - 100 Ma. Third order cycles vary in length from less than 1 Ma to about 10 Ma. Fourth order cycles correspond to

Figure 1.8. Chart showing the first and second order cycles during the Phanerozoic (Vail et al., 1977b)

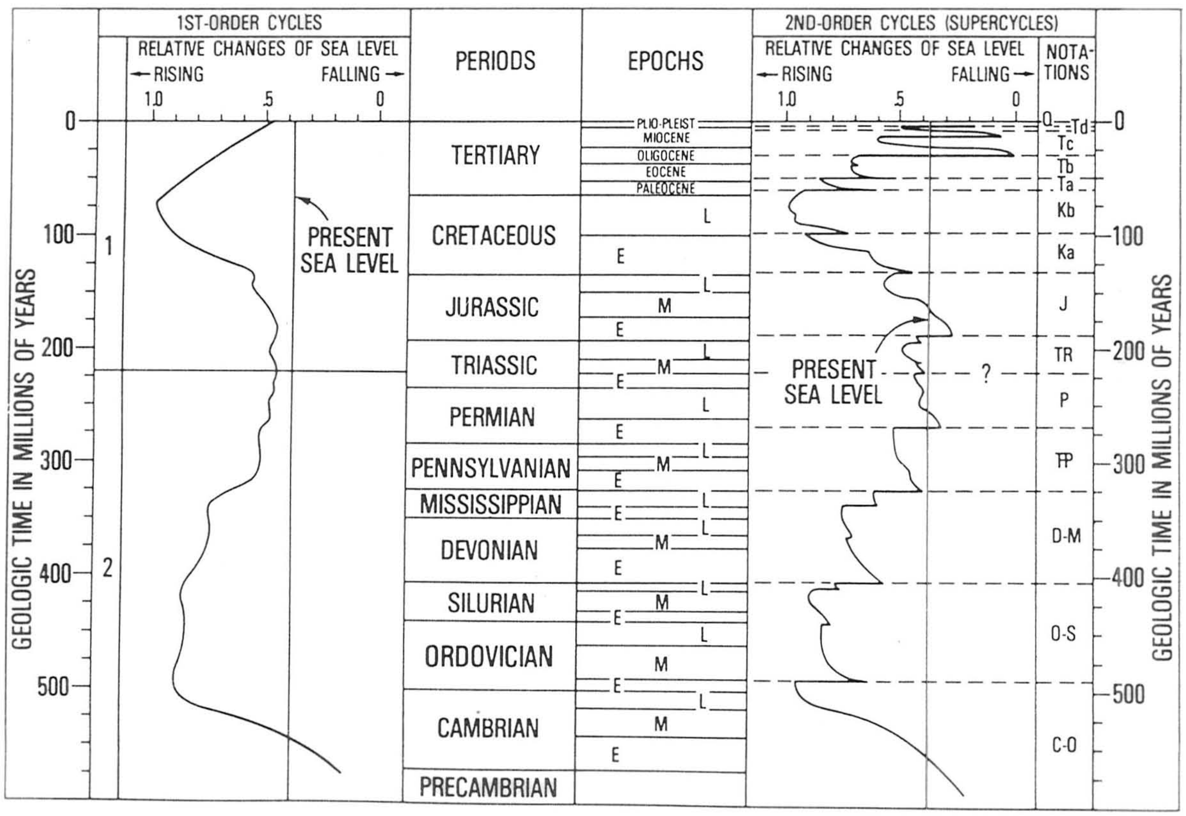
1ST-ORDER CYCLES
RELATIVE CHANGES OF SEA LEVEL
← RISING
FALLING →
1.0
.5
0
PERIODS
EPOCHS
2ND-ORDER CYCLES (SUPERCYCLES)
NOTA-TIONS
GEOLOGIC TIME IN MILLIONS OF YEARS
0
100
200
300
400
500
1
2
PRESENT SEA LEVEL
TERTIARY
CRETACEOUS
JURASSIC
TRIASSIC
PERMIAN
PENNSYLVANIAN
MISSISSIPPIAN
DEVONIAN
SILURIAN
ORDOVICIAN
CAMBRIAN
PRECAMBRIAN
PLIO-PLEIST
MIOCENE
OLIGOCENE
EOCENE
PALEOCENE
E
M
L
?
Q
Td
Tc
Tb
Ta
Kb
Ka
J
TR
P
ℙ
D-M
O-S
C-O

Table 1.1. Stratigraphic cycles and their causes (after Vail et al., 1977b).

Type (Vail et al., 1977b)	Other terms	Duration Ma	Probable cause
First order	—	200–400	major eustatic cycles caused by formation and breakup of supercontinents
Second order	supercycles (Vail et al., 1977b) sequence (Sloss, 1963) synthem (Ramsbottom, 1979)	10–100	eustatic cycles induced by volume changes in global mid-oceanic spreading ridge system
Third order	mesothem (Ramsbottom, 1979)	1–10	possibly produced by ridge changes and/or continental ice growth and decay
Fourth order	cyclothem (Wanless and Weller, 1932)	0.2–0.5	rapid eustatic fluctuations induced by growth and decay of continental ice sheets, growth and abandonment of deltas

the relatively very rapid changes of sea level. These cycles range in length from 10^4 to 10^6 years. A discussion of examples of third and fourth order cycles is given by Miall (1984).

The broad conclusions of Vail and his coworkers have been widely accepted. There is a large body of evidence for continuous sea level changes throughout the Phanerozoic (see discussions Hallam, 1984; Miall 1984). The Phanerozoic cycles appear to be global in extent (Soares et al., 1978), and these cycles have been interpreted, for the Late Cretaceous and Cenozoic, as a response to volume changes of oceanic spreading centers (Hallam, 1963). Volume changes in oceanic spreading ridges are caused by variations in the sea floor spreading rate and probably account for second and possibly third order cycles. Changes in the volume of land ice can account for fourth order cycles and possibly third order cycles. The probable causes for global changes in sea level are presented in Table 1.1 (Vail et al., 1977b). Changes in sea level are due to a change in the total volume of sea water, or a change in the the total volume of the oceans basins, or some combination of the two. A discussion of controls on sea level fluctuations is given by Kauffman (1985). The major problems associated with eustacy are in determining a mechanism for the short term changes in sea level, when growth and decay of ice sheets (eg., the Mesozoic) cannot account for the shifts in sea level (Miall, 1986).

Jeletzky (1978) summarized the detailed biostratigraphic documentation for sea level changes in 5 Cretaceous basins in Canada, and compared these changes to the Cretaceous sea level curves of Hancock and Kauffman (Fig. 1.9). He argued that the lack of interbasin correlation between periods of rising and falling events and the sea level curves does not support the eustatic control hypothesis. The lack of correlation in these diagrams is convincing, but certain events do seem to occur simultaneously in several basins (eg., early Turonian transgression, late Santonian transgression, mid-Campanian regression, late Maastrichtian regression). As noted by Miall (1984), Jeletzky (1978) selected all of his basins from marginal to mobile belts where tectonic overprinting would be expected to mask the passive type of sea level change.

The fundamental control on the accumulation and preservation of cratonic sediment is base level, the equilibrium surface separating erosional and depositional regimes. In general base level approximates sea level (Sloss, 1984). Depositional base level is commonly defined by wave base. Sediments must be carried below base level by a rise in sea level or by subsidence of the depositional site.

Vail, Mitchum and Thompson (1977b) illustrate typical

Figure 1.9. Correlation of sea level changes in 5 Cretaceous Basins in Canada, compared to the sea level curves of Hancock and Kauffman replotted to correspond to the equal stage time subdivisions. The lack of correlation between the basins and the sea level curve suggests that sea level control was tectonic rather than eustatic. Careful examination of the curves reveals some interbasin correspondance in the timing of some of the events (eg., early Turonian transgression, late Santonian transgression, mid-Campanian regression, late Maastrichtian regression). All 5 basins occur in marginal to mobile areas where tectonic overprinting of passive sea level change would be expected. (after Jeletzky, 1978).

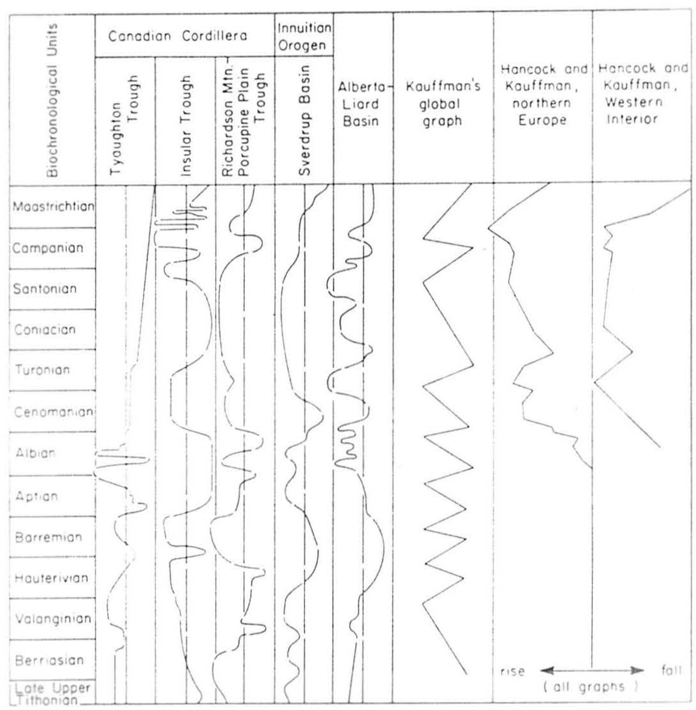
Biochronological Units
Canadian Cordillera
Tyaughton Trough
Insular Trough
Richardson Mtn.-Porcupine Plain Trough
Innuitian Orogen
Sverdrup Basin
Alberta-Liard Basin
Kauffman's global graph
Hancock and Kauffman, northern Europe
Hancock and Kauffman, Western Interior
Maastrichtian
Campanian
Santonian
Coniacian
Turonian
Cenomanian
Albian
Aptian
Barremian
Hauterivian
Valanginian
Berriasian
Late Upper Tithonian
rise
fall
(all graphs)

highstand and lowstand conditions and associated unconformities (Fig. 1.10). The highstand diagram represents a depositional system that might be observed in many coastal areas today or at times of highstand in the past. The four main components are:

1) coastal plain

2) shelf

3) slope

4) rise (deep water basin)

The unconformity related to coastal onlap during the rise in sea level is shown. If sea level drops to the edge of the continental shelf (lowstand), sediment bypasses the shelf and is deposited in deep water. The entire shelf is exposed to sub-aerial erosion with streams incising into the shelf sediments due to the lowered base level. The depocentre shifts from deltaic in the highstand to marine subsea fans in the lowstand. Unconformities are present within the marine strata and the coastal plain deposits. The most easily recognized breaks commonly occur within shelf sequences.

Sea level curves for the Cretaceous have been published by Hancock (1975), Kauffman (1977), Hancock and Kauffman (1979), and Weimer (1984). The ages of the stage boundaries are based on work done by Obradovich and Cobban (1975) for the Western Interior Cretaceous and modified by Lanphere and Jones (1978) and Fouch (1983). The positions of some

Figure 1.10. Depositional pattern expected to be preserved during A) highstand and B) lowstand. A) This type of depositional system might be observed in modern coastal settings. The four main components are: coastal plain, shelf, slope, and rise (deep water basin). The unconformity shown is related to coastal onlap during the rise in sea level.

B) During lowstand of sea level, sediment bypasses the shelf and is deposited in deep water. The entire shelf is exposed to sub-aerial erosion. The depocentre shifts from deltaic during highstand to marine subsea fans during lowstands. Unconformities are present in both the marine and coastal plain deposits (after Vail et al., 1977b).

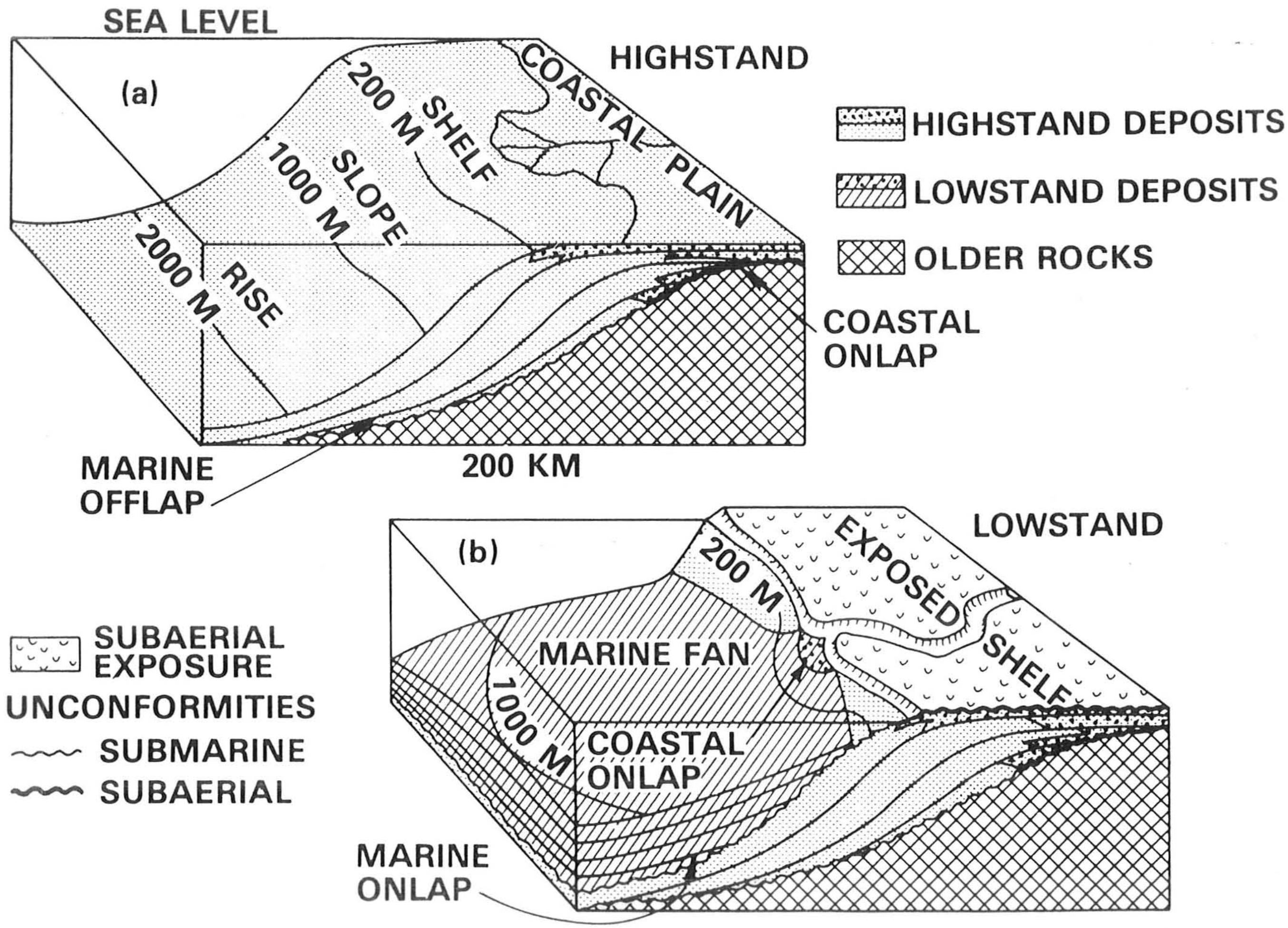
SEA LEVEL
(a)
HIGHSTAND
COASTAL PLAIN
SHELF
200 M
SLOPE
1000 M
2000 M
RISE
HIGHSTAND DEPOSITS
LOWSTAND DEPOSITS
OLDER ROCKS
COASTAL ONLAP
MARINE OFFLAP
200 KM
(b)
LOWSTAND
EXPOSED SHELF
200 M
MARINE FAN
1000 M
COASTAL ONLAP
MARINE ONLAP
SUBAERIAL EXPOSURE
UNCONFORMITIES
SUBMARINE
SUBAERIAL

of the stage boundaries relative to the radiometric time scale are not in agreement with those published by others workers (Van Hinte, 1976; Kauffman, 1977).

Changes in sea level have a direct influence on base level of erosion and deposition. The influence varies among the major environments, but the most noticable effects are in the non-marine and the shallow marine environment. McGookey (1972) found in the Western Interior that in general the amount of erosion of underlying strata associated with each break is less than 100 m. Kauffman (1984) noted that the smaller scale fluctuations, particularly those recorded for the Cretaceous Western Interior Seaway, profoundly affected the shape and size of epicontinental seas, because of their broad, shallow, relatively flat submarine topography, small changes in sea level, will produce widespread strandplain migrations, which stongly affect sedimentation patterns throughout the basin.

1.7 SCIENTIFIC CONTRIBUTION OF THIS THESIS: PREVIEW OF RESULTS

There are three major scientific contributions in this thesis.

FIRST, a major erosion surface is documented. It is believed to have formed as a result of a rapid relative lowering of sea level. The details of the morphology of this surface were established from approximately 1000 well logs and 400 cores. A surface of this detail could not have been documented in outcrop because there is no independent datum on which to hang the measured sections, and the data point control is limited. To the best of my knowledge the only other published map of an erosion surface is that of McCubbin (1969).

The erosion surface at Carrot Creek can be divided into four well developed, areally distinct topographic features. The TERRACE is a broad undulating area preserved in the southwest corner of the study area. The BEVEL is a narrow belt located along the edge of the terrace and marks the final preserved position of the shoreface in the study area. The BUMPS and HOLLOWS are located basinwards of the bevel and represent erosional remnants marking earlier positions of the shoreface. The BASIN PLAIN is a broad relatively flat area basinwards of the bumps and hollows. When the pre-erosion sediments are restored to their original basinward sedimentary dip, the erosion surface appears to consist of a series of stepped shoreface profiles, which are represented by the bump and hollow topography.

Many authors have suggested the existence of a series of stepped profiles from work on the Holocene transgression (eg., Swift et al., 1973), although they have never been able to document them. Other similar erosion surfaces from the ancient rock have been described by Weimer and Flexer (1985), Rosenthal and Walker (in press), Plint and Walker (in press).

SECOND, the conglomerates are interpreted in this thesis as shoreface deposits. The distribution of the conglomerates is directly related to the morphology of the underlying erosion surface. The conglomerates bodies are preserved as long narrow deposits completely encased in marine shales, and at first sight appear to have been deposited many tens of kilometers from a time-equivalent shoreline. They differ from other previously described offshore shelf ridges in two significant aspects, firstly they do not coarsen upward from the underlying shelf deposits. Rather, they are separated from these deposits by an erosional unconformity. Secondly they are overlain by transgressive mudstones associated with a relative sea level rise.

Our understanding of coarse shoreface deposits is limited only to a few examples. The sequence of conglomerates preserved at Carrot Creek shares both similarities and marked differences with other previously described sections (eg., Sandstone of Floras Lake, Leithold and Bourgeois, 1984). The shoreface, particularly the high energy shoreface, is extremely difficult to study in the modern environment, hence well documented examples in the ancient rock record serve to increase our understanding of the dominant processes operating in the shoreface, and the range of variability present.

THIRD, one of the questions proposed when this study began concerned the transport of coarse material across the shelf. This study strongly suggests that perhaps we have been asking the wrong questions. The hypothesis that coarsening upward long, linear, en echelon ridges may have formed many tens of kilometres from the nearest contemporaneous shoreline needs to be re-evaluated, particularly in sequences where the correlative shelf deposits are coarser than the supposed time equivalent shoreline deposits. The results of this thesis strongly suggest that all of these deposits be re-examined considering the effects of rapid relative sea level change and how these changes in sea level would effect the position of the shoreface.

1.6 ECONOMIC JUSTIFICATION

Oil was discovered in the Cardium Formation in 1953. In the search for other Cardium reservoirs interest in the Cardium depositional history increased rapidly. Since then, there has been much controversy about the depositional environment of the Cardium. In order to locate more efficiently any future reservoirs, it is necessary to document the controls on gravel depositional localities. The conglomerates in the Carrot Creek study are recognizable on high resolution seismic if thicker than about 5 m, due to the high velocity differential between the conglomerates and the encasing shales. The anomaly formed by the presence of a conglomerate cannot be distinguished from sandstones on seismic profiles. If, however, the structure map of the erosion surface is used in conjunction with seismic it should be possible to separate these two types of deposits more accurately. For example, if a good seismic anomaly is developed in an area where the erosion surface shows the development of a topographic high, then the rocks are most likely sandstones below the unconformity. This distinction is important in this area, because the sandstones are tight. The documentation of the nature, morphology, and extent of an erosion surface, particularly where it is the major control on sedimentation, is therefore, a powerful exploration tool.

CHAPTER 2 -- REGIONAL SETTING

2.1 STRATIGRAPHY

The Upper Cretaceous (Turonian) Cardium Formation crops out along the fold and thrust belt of the Western Canadian Rockies, and continues eastward, in the subsurface, into the Central Plains of Alberta (Fig. 2.1). It is composed of mudstones, sandstones, and conglomerates. The Cardium Formation (Fig. 2.2) is encased in 750 m of marine shales of the Alberta Group (equivalent to the Colorado Group in the U.S.); about 250 m of Blackstone Formation shales below and about 500 m of Wapiabi Formation shales above (Stott, 1963). The Cardium is an approximate time equivalent of the Frontier, Ferron, and Gallup sandstones located in the south central portion of the Western Interior Seaway.

A brief discussion of Cardium stratigraphy is presented below. More detailed discussions may be found in the references cited in the text.

A. CORRELATION OF OUTCROP AND SUBSURFACE

In independent studies Plint et al. (1986) and Duke (1985a) established a stratigraphy for the subsurface and outcrop respectively based on the recognition and correlation of sharply bounded coaresening upward sequences. Correlation of the outcrop to the subsurface (Fig. 2.3) was recently attempted by W.L. Duke, A.G. Plint, and R.G. Walker (pers. comm.) based on the recognition and

Figure 2.1. Map of South Central Alberta showing the location of subsurface Cardium. Open dots indicate nearby outcrop exposure at Seebe and Clearwater River. Black dots give palinspastic reconstruction of these outcrop sections (Walker, 1986).

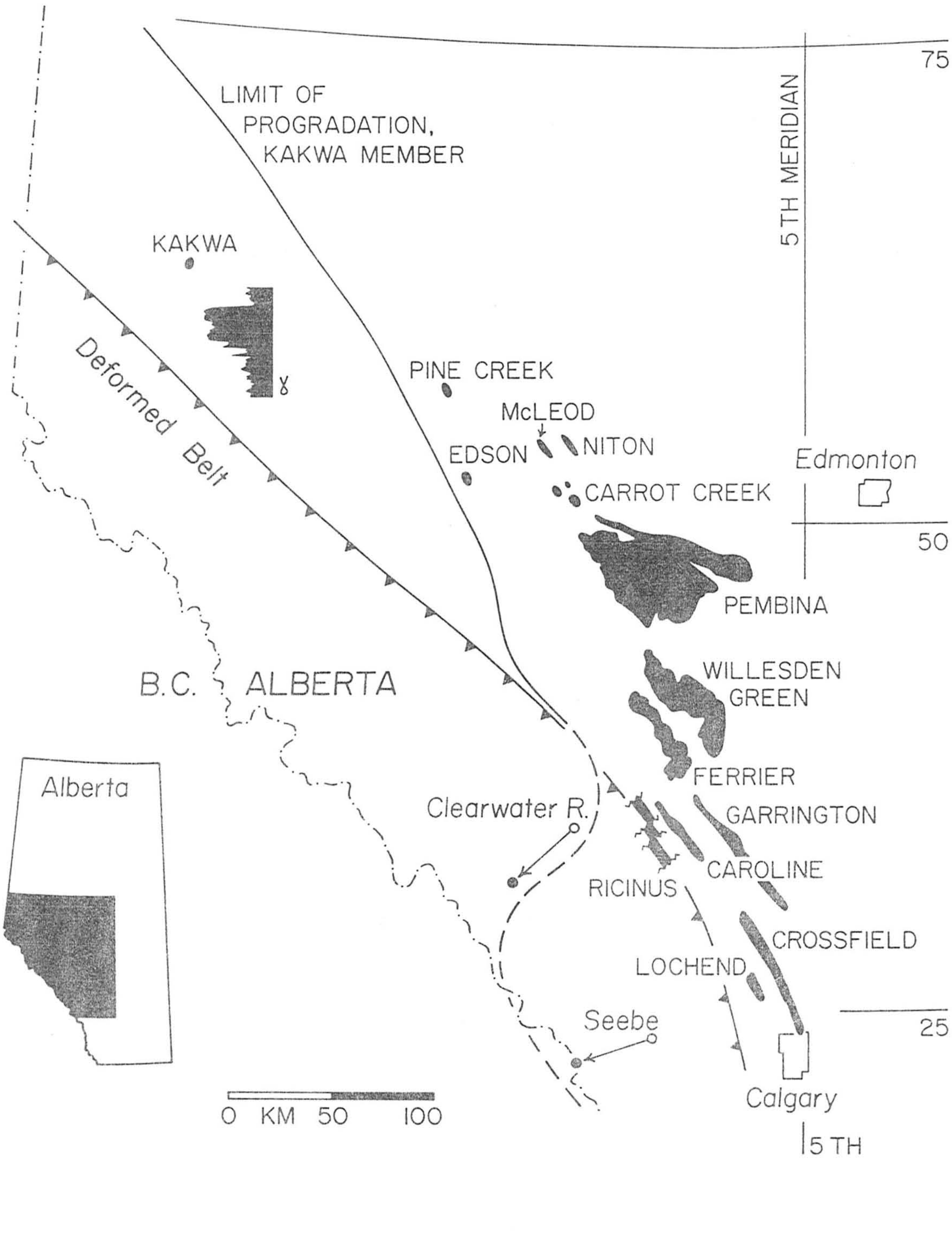
LIMIT OF
PROGRADATION,
KAKWA MEMBER
5TH MERIDIAN
75
KAKWA
Deformed Belt
PINE CREEK
McLEOD
NITON
EDSON
CARROT CREEK
Edmonton
50
PEMBINA
B.C.
ALBERTA
WILLESDEN
GREEN
FERRIER
Alberta
Clearwater R.
GARRINGTON
CAROLINE
RICINUS
CROSSFIELD
LOCHEND
Seebe
25
0 KM 50 100
Calgary
5 TH

Figure 2.2. Stratigraphy of the Alberta Group (Colorado Group) in the Alberta Foothills. Absolute ages (Palmer, 1983) are given at left (after Walker, 1985c).

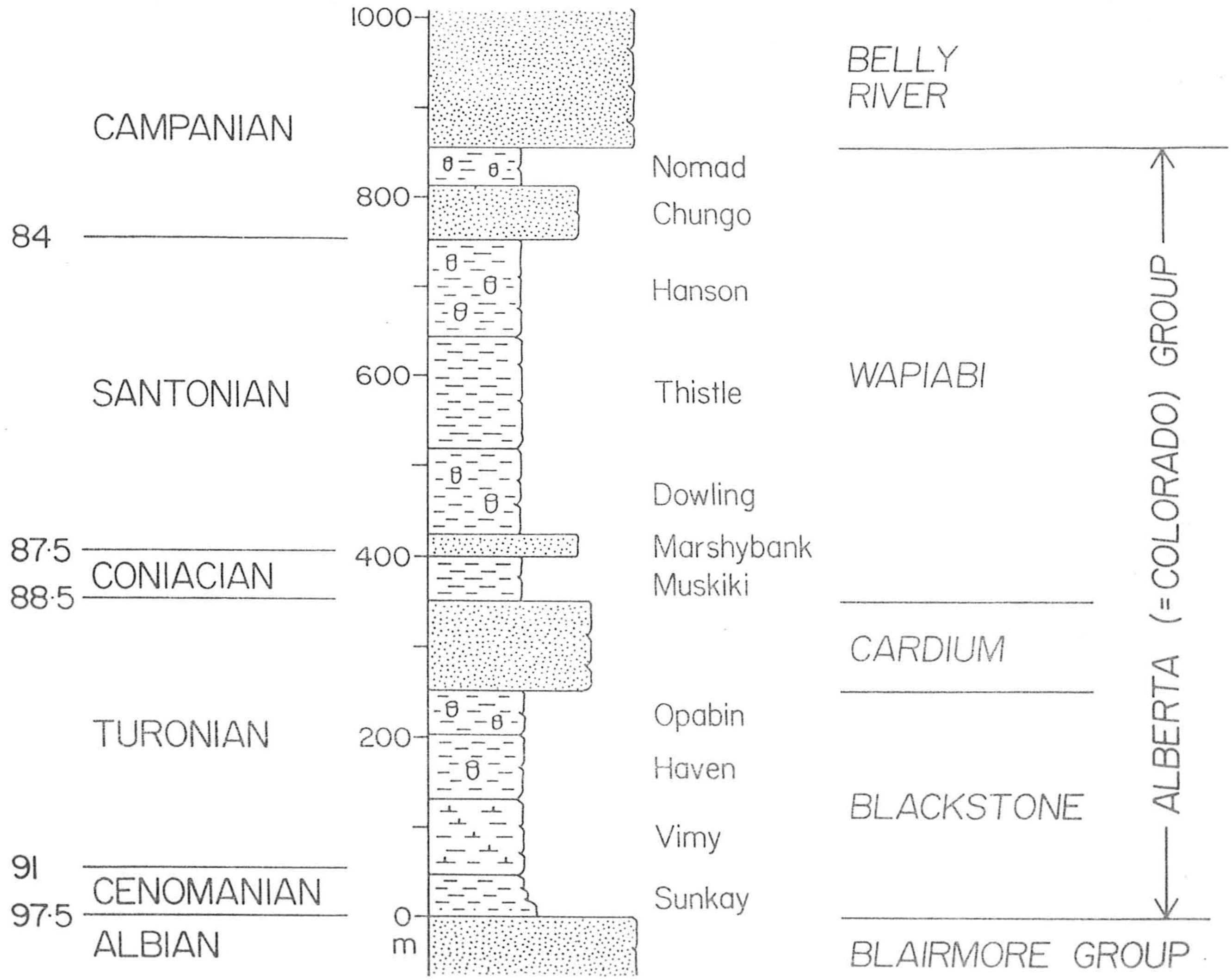

CAMPANIAN
84
SANTONIAN
87·5
CONIACIAN
88·5
TURONIAN
91
CENOMANIAN
97·5
ALBIAN
1000
800
600
400
200
0
m
Nomad
Chungo
Hanson
Thistle
Dowling
Marshybank
Muskiki
Opabin
Haven
Vimy
Sunkay
BELLY RIVER
WAPIABI
CARDIUM
BLACKSTONE
BLAIRMORE GROUP
ALBERTA (=COLORADO) GROUP

correlation of these sharply bounded coarsening upward sequences (a detailed discussion of this correlation is presented by Walker, 1986). The bounding surfaces were found to be erosional, and covered by conglomerate that varied from a veneer to 20 m in thickness. The proposed stratigraphic nomenclature for outcrop and subsurface is outlined in Fig. 2.3. The corresponding terminology of Wright and Walker (1981) and Stott (1963) to the proposed stratigraphy by Duke (1985a) is shown for the outcrop. The corresponding terminology of industry to the proposed stratigraphy by Plint et al. (1986) is shown for the subsurface.

In general (Fig. 2.3), Duke's non-marine Cutpick Member is equivalent to Stott's non-marine Moosehound Member. This non-marine tongue is correlative with, but not laterally continuous with the non-marine tongue in the subsurface (Musreau Member). The Seebe Member of Duke (Ram Member of Stott) is equivalent to but not laterally continuous with the Kakwa Member in the subsurface. In both the outcrop and subsurface stratigraphies the sequence-bounding conglomerates have been given member names and the proposed correlation is shown in Fig. 2.3.

The top of the Cardium in the proposed correlation (Fig. 2.3) is taken as the top of the last sequence-bounding conglomerate (Mackenzie Creek Member in outcrop and Amundson Member in the subsurface). This differs from the definition

Figure 2.3. Proposed outcrop nomenclature (Duke, 1985a) and subsurface nomenclature (Plint et al., 1986), with suggested correlations. The stratigraphy is based on the recognition and correlation of sharply bounded coarsening upward sequences. Previous stratigraphic nomenclature is shown in relative position to the proposed stratigraphy. In general the non-marine Cutpick Member in outcrop is correlative with the non-marine Musreau Member in the subsurface, and the Seebe Member in outcrop is correlative with the Kakwa Member in the subsurface. The suggested correlation of the sequence bounding conglomerates is also shown. (after Walker, 1986).

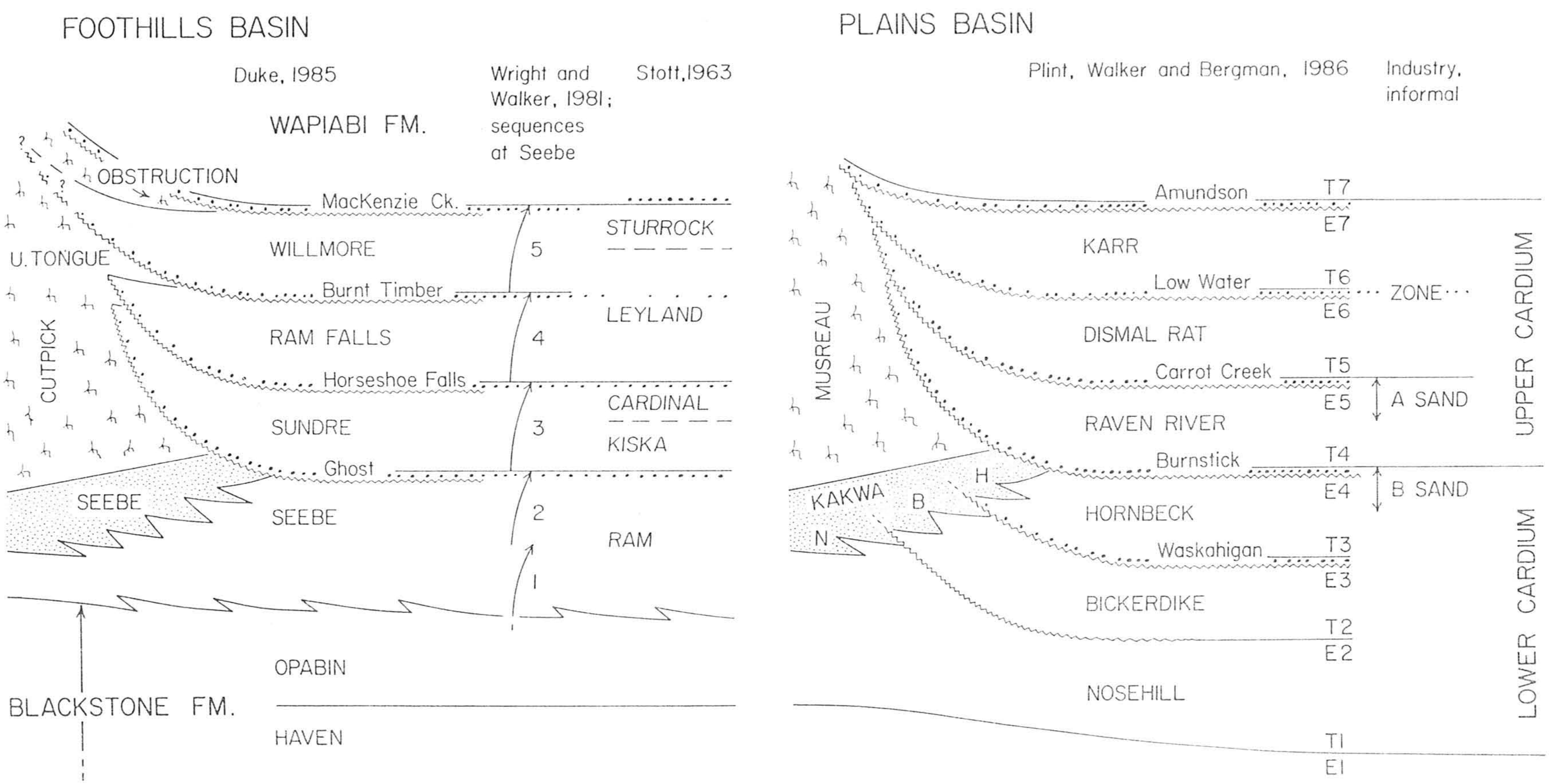
FOOTHILLS BASIN
Duke, 1985
Wright and Walker, 1981; sequences at Seebe
Stott, 1963
WAPIABI FM.
OBSTRUCTION
MacKenzie Ck.
STURROCK
U. TONGUE
WILLMORE
5
Burnt Timber
LEYLAND
CUTPICK
RAM FALLS
4
Horseshoe Falls
CARDINAL
SUNDRE
3
KISKA
Ghost
SEEBE
SEEBE
2
RAM
1
OPABIN
BLACKSTONE FM.
HAVEN
PLAINS BASIN
Plint, Walker and Bergman, 1986
Industry, informal
Amundson
T7
E7
KARR
Low Water
T6
ZONE
E6
MUSREAU
DISMAL RAT
Carrot Creek
T5
E5
A SAND
RAVEN RIVER
UPPER CARDIUM
Burnstick
T4
E4
B SAND
KAKWA
H
B
HORNBECK
N
Waskahigan
T3
E3
BICKERDIKE
T2
E2
NOSEHILL
LOWER CARDIUM
T1
E1

of the top of the Cardium as defined by Stott (1956) who placed the top of the Cardium at the base of the uppermost pebble beds. In outcrop the base of the Cardium was drawn at the base of the thick sands of the Seebe Member (Duke, 1985a). Harding (1955) and Stott (1963) defined the base of the Cardium in the same way. The base of the Cardium in the subsurface as defined by Plint et al. (1986) correlates with the contact between the Haven and Opabin Members of the Blackstone Formation in outcrop (Fig. 2.3). The correlation of outcrop and subsurface presented by Walker (1986) is similar to that first proposed by Michaelis (1957). Michaelis (1957; Fig. 2.4 of this thesis) recognized and correlated 5 coarsening upward sequences in the subsurface and outcrop. In this correlation the lower bounding surfaces of the seqences were overlain by conglomerates, as subsequently recognized by Duke (1985a) for the Cardium in outcrop. Michaelis (1957) correctly suggested that the main sand at Pembina (Raven River Member; "A" sand of industry) was correlative with the third coarsening upward sequence in outcrop (Sundre Member; Kiska- Cardinal Members of Stott). Both Stott (1963) and Swagor et al. (1976) tentatively correlated the Low Water Member ("Cardium Zone") with the MacKenzie Creek Member (Sturrock Member; Stott, 1963). This correlation is now believed to be incorrect (Walker, 1986).

Figure 2.4. Original correlation of outcrop to subsurface proposed by Michaelis (1957). Note that the conglomerates are shown as separate from the underlying coarsening upward sequences. The position of the E5 surface (Plint et al., 1986) in the subsurface is shown on the right hand side of the diagram (after Michaelis, 1957).

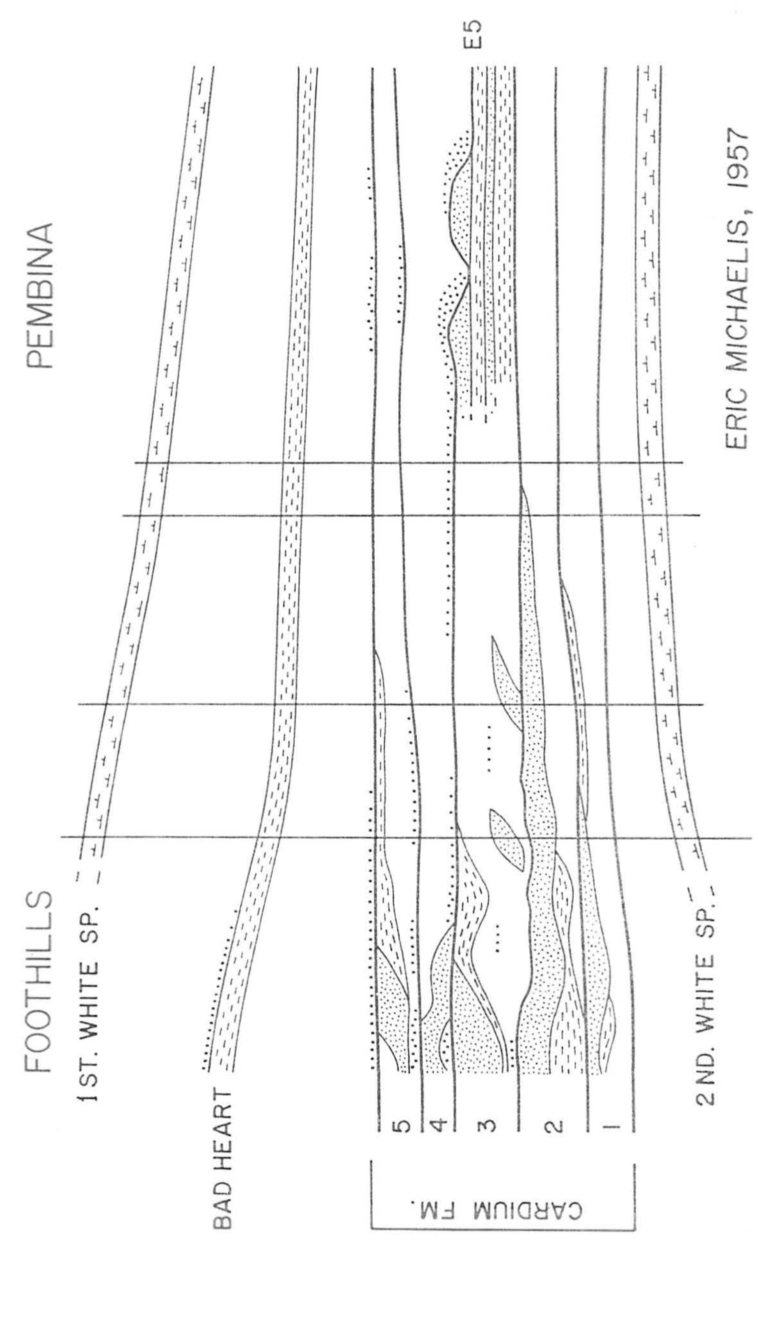
FOOTHILLS
PEMBINA
1 ST. WHITE SP.
BAD HEART
CARDIUM FM.
5
4
3
2
1
E5
2 ND. WHITE SP.
ERIC MICHAELIS, 1957

B. SRATIGRAPHY OF THE CARDIUM FORMATION IN OUTCROP

In outcrop the Cardium Formation is approximately 100 m thick. Outcrop locations are given by Duke (1985a). Stott (1963) recognized and described six distinct members within the Cardium Formation. From oldest to youngest they are: the Ram, Moosehound, Kiska, Cardinal, Leyland, and Sturrock. Of these six members, five are marine; the Moosehound is a non-marine tongue. Stott (1963) interpreted a cyclic depositional environment for the Cardium Formation and suggested that these cycles were important for correlation within individual members. These cycles present within the members, were not named in Stott's stratigraphy. Subsequently, it was recognized that cycle boundaries crossed Stott's member boundaries, as discussed by Wright and Walker (1981) and Duke (1985a). Stott's terminology implies a "layer-cake stratigraphy", compared with the proposed "event" stratigraphy of Duke (1985a).

Wright and Walker (1981) and Duke (1985a) emphasized a series of sharply bounded coarsening upward sequences. The sharp bounding surfaces are typically erosional or non-depositional, and are punctuated by conglomerate beds (Duke, 1985a). Duke (1985a) proposed that the old stratigraphy of Stott (1963) be abandoned and that a new member system be defined for the Cardium Formation in the Alberta Foothills, based upon these lithologically correlative Cardium seqences. Each coarsening upward sequence was believed to represent deposition in one overall regressive event.

Duke (1985a) proposed a six member stratigraphy similar to Stott's original stratigraphy but based on the recognition and correlation of coarsening upward sequences, punctuated by non-marine tongues. From oldest to youngest they are: the Seebe, Cutpick, Sundre, Willmore, and Obstruction. The stratigraphic position of the Baytree Member was not adressed by Duke (1985a). The Seebe, Sundre and Willmore Members are exclusively marine, whereas the Cutpick and Obstruction Members contain non-marine deposits. The depositional environment of the Baytree Member was not known. For a detailed discussion of the members, their sequences and associated facies, the reader is referred to Duke (1985a). This proposed stratigraphy emphasizes the intertonguing nature of the sediments, rather than the "layer-cake" stratigraphy emphasized by Stott (1963).

In the stratigraphy proposed by Duke (1985a) the conglomerates overlie the lower bounding surface and are <u>not</u> part of the coarsening upward sequence. This is apparent in his member sub-division where none of the marine conglomerates is designated as having member status. Duke (1985a) does not emphasize the stratigraphic significance of the conglomerates which truncate the coarsening upward sequences. Recent terminology in the subsurface (Plint et al., 1986) suggests that Duke's stratigraphy be slightly modified, so that the conglomerates resting at the top of coarsening upward sequences, even where there is only a thin veneer preserved, be given member status.

C. STRATIGRAPHY OF THE CARDIUM FORMATION IN THE SUBSURFACE

In the subsurface, the Cardium varies from about 50 to 100 m in thickness and is composed of 6 coarsening upward sequences. Industry developed an informal terminology of "A" sand, "B" sand, and "Cardium Zone". This system is inadequate because the stratigraphy adopted may not be correlative from field to field. Walker (1983 b,c) proposed Member names for the Cardium Formation at Ricinus-Caroline-Garrington; the names, with some modifications have been incorporated into the formal Cardium stratigraphy proposed by Plint et al. (1986). Krause and Nelson (1984) proposed two formal lithostratographic units for the Cardium Formation at Pembina oil field. These names were both found to be unsuitable according to the rules of the American Commission on Stratigraphic Nomenclature. A detailed discussion of the reasons for the rejection of the proposed nomenclature is given in Plint et al., (1986).

The formal stratigraphy proposed by Plint et al. (1986) (Fig. 2.5) for the Cardium in subsurface is based on the recognition and correlation of a series of erosional surfaces E1 through E7. These surfaces truncate progressively coarsening upward sequences and are overlain

Figure 2.5. Proposed event stratigraphy and Member terminology for the Cardium Formation in the subsurface. The stratigraphy is based on the recognition and correlation of erosional surfaces labelled E1 through E7. These surfaces truncate progressive coarsening upward sequences and are overlain by conglomerates varying in thickness from a thin veneer to about 20 m. The conglomerates are subsequently overlain by transgressive surfaces T1 through T7. Where the conglomerate is reduced to a thin veneer the E7/T7 surfaces are essentially coincident (after Plint et al., 1986).

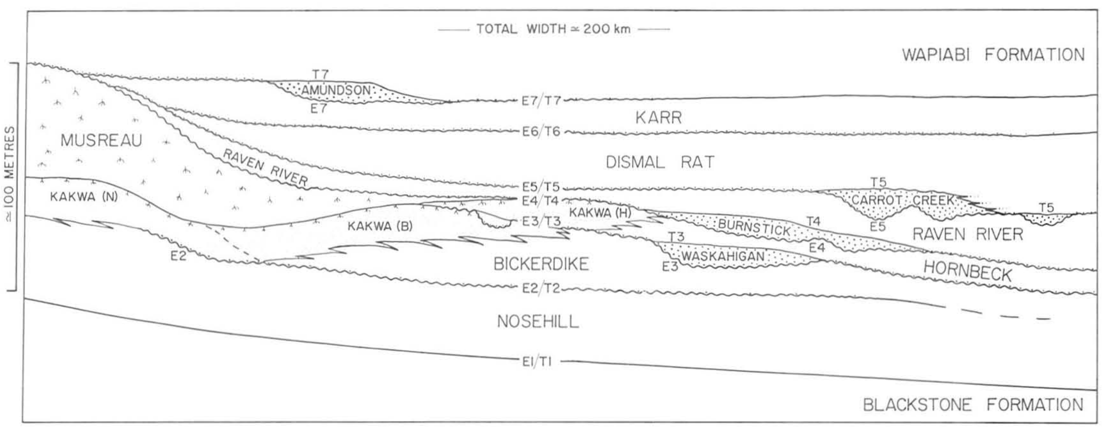

TOTAL WIDTH ≃ 200 km
WAPIABI FORMATION
≃100 METRES
T7
AMUNDSON
E7
E7/T7
KARR
E6/T6
MUSREAU
RAVEN RIVER
DISMAL RAT
E5/T5
T5
CARROT CREEK
T5
KAKWA (N)
E4/T4
KAKWA (H)
E3/T3
KAKWA (B)
BURNSTICK
T4
E5
RAVEN RIVER
T3
E4
E2
BICKERDIKE
WASKAHIGAN
E3
HORNBECK
E2/T2
CARDIUM FORMATION
NOSEHILL
E1/T1
BLACKSTONE FORMATION

by conglomerates, varying in thickness from a thin veneer to about 20 m in thickness. The conglomerates are subsequently overlain by transgressive surfaces numbered T1 through T7. Where the conglomerate is reduced to a thin veneer, the E and T surfaces are essentially coincident, and are referred to (for example) as E4/T4. The base of the Cardium is formally drawn at the E1/T1 surface and the top at the E7/T7 surface (Plint et al., 1986). The members defined by these erosional and transgressive surfaces are shown in Figure 2.5.

Four members defined by these erosional and transgressive surfaces (Plint et al., 1986) have been cored in the Carrot Creek area. The Raven River Member (first defined by Walker, 1983 b, c) includes all of the coarsening upward sequence between the T4 and E5 surfaces. The Carrot Creek Member (named after the Carrot Creek Oil Field) includes the conglomerates deposited on the E5 surface. The Dismal Rat Member (named after the confluence of Dismal Creek and Rat Creek) includes the pebbly mudstones (facies 3P, 4P, and 5P) and other mudstone facies that overlie T5, up to the log marker known to industry as the "Cardium Zone". The Low Water Member is the name now given to the conglomerate veneer at the E6/T6 horizon; it does not always have a sharp erosive base..

2.2 HISTORY OF IDEAS ON CARDIUM DEPOSITIONAL HISTORY

Oil was discovered in the Cardium Formation at Pembina, Alberta in 1953. This discovery sparked an interest in the depositional environment of the Cardium. Since this time much controversy has arisen concerning the Cardium depositional environment, and the mechanisms of sediment transport in the shelf environment. Much of this controversy has resulted from an unsatisfactory or non-existent stratigraphic frameworks within which to develop depositional models. The recognition and correlation of the sedimentologic sequences described above, serves to establish a regional framework from which a better understanding of the "sand body" geometry and basin morphology may be developed.

A comprehensive review of early (pre-1955) ideas concerning the Cardium depositional history was presented by Stott (1963, p. 3-9 and 53-81). A more recent (post-1955) comprehensive review of ideas concerning Cardium depositional environments, with emphasis on modern sedimentological problems, was presented by Walker (1983a) and Duke (1985a). A brief discussion of the major ideas will be presented here; for details see Walker (1983a) or Duke (1985a). In this discussion I will be concerned primarily with the changes in ideas concerning the depositional environment, and process of sediment transport across the shelf, which have led to the present interpretation.

Beach (1955) first proposed the idea that the pebbles at the top of the main Cardium sandstones were deposited by turbidity currents. De Wiel (1956) disagreed strongly, on the grounds of the shallow water depth and the extremely low slope of the basin floor, and suggested that the low slope would prevent the generation of turbidity currents. The problem of flow generation has not yet been resolved. Some suggestions of generating mechanisms have been tsunamis (Beach, 1957), storms (Hamblin and Walker, 1979; Wright and Walker, 1981), cyclic wave loading (Walker, 1984a), and fluvial discharge (Walker, 1985b). As an alternative explanation, De Wiel (1956) suggested that the thick sandstones and conglomerates were regressive deposits associated with a prograding shoreline resulting from sea level fluctuations. This idea is developed in this thesis.

Nielsen (1957) proposed that the Cardium at Pembina was a shallow marine offshore sandbody. Like De Wiel (1956), he argued against the turbidity current hypothesis, suggesting instead that the Cardium represented a regressive deposit "exposed to the erosive effects of normal marine currents". The regressive units are then overlain by transgressive mudstones. Nielsen (1957) was the first to recognize the erosive nature of the conglomerate deposits.

The ubiquitous coarsening upward sequences preserved in the Cardium were first interpreted as regressive shoreline deposits by Michaelis (1957). He believed that these coarsening upward sequences were separated vertically by periods of erosional transgression. Michaelis (1957) interpreted the conglomerates in outcrop as being deposited during these erosional transgressions. This is evident from his correlation diagram, where the conglomerates overlie the lower bounding surface rather than forming an integral part of the coarsening upward sequence (Fig. 2.4). Michaelis (1957) agreed with the shallow water origin proposed by Nielsen (1957) and suggested different environments for correlative sequences in different parts of the basin. He interpreted the deposits at Pembina as a regressive offshore shoal sandstone capped with conglomeratic beach deposits.

The next major contribution to our understanding of the Cardium Formation was the stratigraphic synthesis of the outcrop by Stott (1963). He tentatively suggested a beach environment for the thicker sand bodies and interpreted the conglomerates as transgressive "beach concentrates".

Off (1963) and Michaelis and Dixon (1969) invoked tidal currents and storm enhancement of tidal currents respectively in their interpretation of the Cardium deposits. The study of Michaelis and Dixon (1969) is the first to invoke storm enhancement of processes occurring in the basin. The tidal interpretation however, is incompatible with the preserved sedimentary structures and lithologies and has largely been forgotten. Bridges (in Stride, 1982) cited these studies on the Cardium in a table of examples of tidal ridges. More recent work in the

Cardium has shown this interpretation to be unlikely.

Beginning with Berven (1966), the next major interpretation of the Cardium depositional setting was as offshore bars. Berven (1966) was the first person to publish a correlation between Cardium fields. His ideas were supported by Sinha (1970) who interpreted the Cardium deposits in the Edson field as NW-SE trending offshore bars locally capped with conglomerate "deposited on the partly scoured and semi-consolidated upper surface of the sandstones". Sinha supported Neilson's (1957) observation that there was erosion at the base of the conglomerates. This erosion surface was further documented by Swagor et al. (1976), who recognized that the conglomerates rested unconformably on the underlying bioturbated mudstones in the Carrot Creek field. They inferred, in the absence of any evidence for emergence and development of subaerial topographic relief, that "the erosion surface beneath the conglomerate is submarine in origin, not subaerial" (p. 92), but gave no interpretation of its possible origin.

Swagor et al. (1976) suggested that the conglomerates were transported offshore, by storm-generated bottom flows. This mechanism of transport was supported by Krause and Nelson (1984), and Krause (1983, 1984) for deposits in the Pembina field. Swagor et al. (1976) suggested that the gravels accumulated in the lee of an original topographic break in slope as a "terrace bar" (a term introduced by

Campbell, 1971).

Walker (1986) has published a summary of all the Cardium research both completed and ongoing by the McMaster group. The first published study of the Cardium Formation by the McMaster group was that of Wright and Walker (1981) from outcrop exposures at Seebe and Horseshoe dams. Wright and Walker (1981) suggested that emplacement of gravels into the basin as bedload, by a single storm driven bottom flow, would require an unreasonably long period of time. In order to circumvent the perceived problem of time required to accumulate the thick gravel deposits preserved in the Cardium, they suggested transport of the gravels by turbidity currents. The turbidity current hypothesis for <u>sand</u> transport was further developed in a series of publications by Walker (1983 a,b,c; 1985a, b) concerning deposition in the Ricinus-Caroline-Garrington Fields in the southeast, and by Bergman (1984, 1986) for the Carrot Creek area. In these studies, the problems of flow generation, and sand-body geometry and occurence of the linear en echelon deposits still existed. These papers served to re-establish the controversy concerning the Cardium depositional history, and mechanisms of transporting sediment across the shelf (i.e., geostrophic flows versus turbidity currents).

The study of the Cardium Formation by the McMaster group has gained increased momentum over the last four years. In the Winter of 1983, Dr. Walker suggested to me that an interesting thesis might be the examination of the preserved fabrics in the conglomerates at Carrot Creek. It was suggested that these conglomerates might be channelized turbidite deposits. Initial compilation of the data (Bergman, Tech. Memo 84-1) alluded to the erosive nature of the conglomerates and the possibility that these conglomerates were associated with channels. In a search for higher markers on which to hang the Cardium, Plint (pers. comm., Sept. 1984; Plint and Walker, in press) demonstrated significant erosion on the Badheart Formation. The erosion surface did not suggest channelization, but cut down progressively to the northeast before becoming unrecognizable on well logs. The Badheart Formation is a sand body in the overlying Wapiabi shales, very similar in setting to the Cardium Formation. In December, 1984, Bergman (Supplement to Tech. Memo 84-1) documented conclusively the erosional nature of the base of the conglomerates and alluded to the presence of a remnant erosional topography (later termed Bumps and Hollows), and the absence of channels in the Carrot Creek area (see cross-section EE-EE', p.30 of the Supplement).

In the early winter of 1984, Plint and Bergman recognized the one-sided geometry of the sand-bodies in the Cardium. Regional correlations were done to try to establish the correlative stratigraphy from field to field.

In April 1985, Bergman produced the first mesh diagram which illustrated the topography of the erosion in the Carrot Creek area. The surface illustrated for the first time the presence of distinct topographic features prior to the deposition of the gravels.

Simultaneously, Duke (1985a) was finishing his Ph.D. thesis on the Cardium Formation in outcrop in Central Alberta. His regional study showed similar features to those observed in the subsurface. Duke viewed the conglomerates capping the underlying mudstones as lag deposits reworked from the underlying sandstones during a subsequent transgression. In outcrop however, there is never more than about 3 m of conglomerate preserved, which is a perhaps reasonable maximum thickness for lag deposits. Plint and Bergman, from regional work in the subsurface, viewed the conglomerate as forming during a rapid drop in relative sea level, with new input of gravel into the basin during lowstand. In the subsurface, the deposition of gravel entirely as transgressive lags is not a reasonable solution because in some areas gravel thickness is up to about 20 m.

In April 1985, Plint, Walker and Bergman submitted a formal stratigraphy for the Cardium in subsurface to Bulletin of Canadian Petroleum Geology. This stratigraphy was based on the recognition and correlation of regionally extensive erosion surfaces. Further study revealed that this proposed stratigraphy was wrong and the article was withdrawn for modification. The corrected version was resubmitted for publication in December, 1985 and appeared for publication in the June, 1986 issue of Bulletin of Canandian Petroleum Geology (Plint et al., 1986).

The details of the morphology of the erosion surfaces are illustrated for the Cardium (Carrot Creek area; Bergman and Walker 1986, in press) and the Badheart (Plint and Walker, in press) Formations. Both of the erosion surfaces are documented with mesh diagrams.

The major break through in our understanding of the Cardium depositional history has come with the recognition of the major Carrot Creek erosion surface. This led to the recognition and correlation of basin wide erosion surfaces, whose formation we believe to be the result of relative sea level changes. This concept has been put forward for the Cardium Formation by Duke (1985a), Rine (1986), Smith (1986), Plint et al. (1986), Bergman and Walker (1986, in press) and Walker (1986). The major difference in the ideas of the these workers is the definition of the major factors controlling the facies relationships. Duke (1985a), Rine (1986), and Smith (1986) recognize transgressions as being the major control on the facies variations. Duke (1985a), after an extensive study of the Cardium in outcrop concluded that "coarsening upward sequences are best interpreted as partial or complete prograding shelf to shoreline sequences...non-marine deposits are inferred to have been removed by transgression...the thick capping conglomerates represent eroded transgressive lag deposits... resedimented over the drowned shoreface" (p. 36-37). In his member classification none of the marine conglomerate deposits are recognized as having member status. In outcrop it would be virtually impossible to recognize these erosion surfaces, due to the lack of control between outcrops, and the lack of markers on which to hang the stratigraphy. Plint et al. (1986), and Bergman and Walker (1986, in press), now suggest that the major controls on sedimentation in the Cardium are drops in relative sea level resulting in regionally extensive erosion surfaces.

2.3 FORMER INTERPRETATIONS OF CARROT CREEK

Studies of Carrot Creek include those of Swagor (1975), Swagor et al. (1976), and Bergman (1984, 1986). The study by Swagor (1975) and Swagor et al. (1976) was based on fewer than 20 wells, all of the available data at the time. Swagor (1975) and Swagor et al. (1976) recognized that although the conglomerates rested on marine mudstones, they were separated from them by an unconformity surface. They proposed that the conglomerate was deposited in the lee of an original shelf topographic feature, as a "terrace bar", with the pebbles driven dominantly by storms across a shallow shelf. They suggested that the erosion surface beneath the conglomerate was submarine in origin.

At the beginning of this study, I tentatively suggested (Bergman, 1984 and 1984 Supplement) that the conglomerates rested in channels. It was proposed that the channels were cut by turbidity currents and that the conglomerates were channel fill sediments deposited by turbidity currents. This idea was later rejected due primarily to the morphology of the erosion surface, which will be discussed later.

2.4 STUDY AREA

The thesis area is located in the Plains of South Central Alberta well east of the edge of the disturbed belt of the Canadian Cordillera. In the plains the strike of the Cardium Formation is in a general northwest direction with a southwest dip of 0.36° to 0.50°. Jones (1980) suggested that numerous and widespread vertical faults (isostatic adjustment faults) characterized by a comparatively long straight strike have effectively controlled the position of a large number of stratigraphic, structural and diagenetic traps in the Alberta basin. The faults associated by Jones (1981), with the Viking and Cardium are believed to have formed after deposition of the productucting sands, and are presumably the result of late Tertiary isostatic adjustment. The presence of these faults do not appear to be a significant feature controlling sedimentation or the geometry of the deposits in the area of study in this thesis.

The study area includes townships 50 to 56, ranges 9 to

14 west of the Fifth Meridian (Fig. 2.1), and includes the oil and gas fields of Carrot Creek, Bigoray, Cyn-Pem, Niton, McLeod, and the north-eastern corner of Pembina. These fields all contain localized areas of long, linear, en echelon, thick (up to 20 m) conglomerate bodies. The reserves estimated by the Energy Resources Conservation Board (ERCB) of conventional crude oil as of December 31, 1984 are presented in Table 2.1. The field land boundaries, for each of the fields present within the study area, are shown in Fig. 2.6.

The data base for this thesis consists of 963 wells of which full core was cut for 438 wells (refer to data list in Appendix 1). This comprises all of the publically available wells as of September, 1985. Of these cored wells, 378 were logged. Many of the other cores, particularly in the Pembina area (T50, R9-11) were not viewed, mostly because the cores are no longer available. Prior to 1962 it was not mandatory to save the cores, and hence many of the early cores were thrown out.

This study is based on gamma ray and induction log signatures and core. The gamma ray mirrors the induction log signature and is of limited availability, hence only the induction log signatures are shown on the cross-sections. Facies and facies sequences were measured in all 378 cores.

Figure 2.6. Location map showing the land boundaries of the fields studied in this thesis.

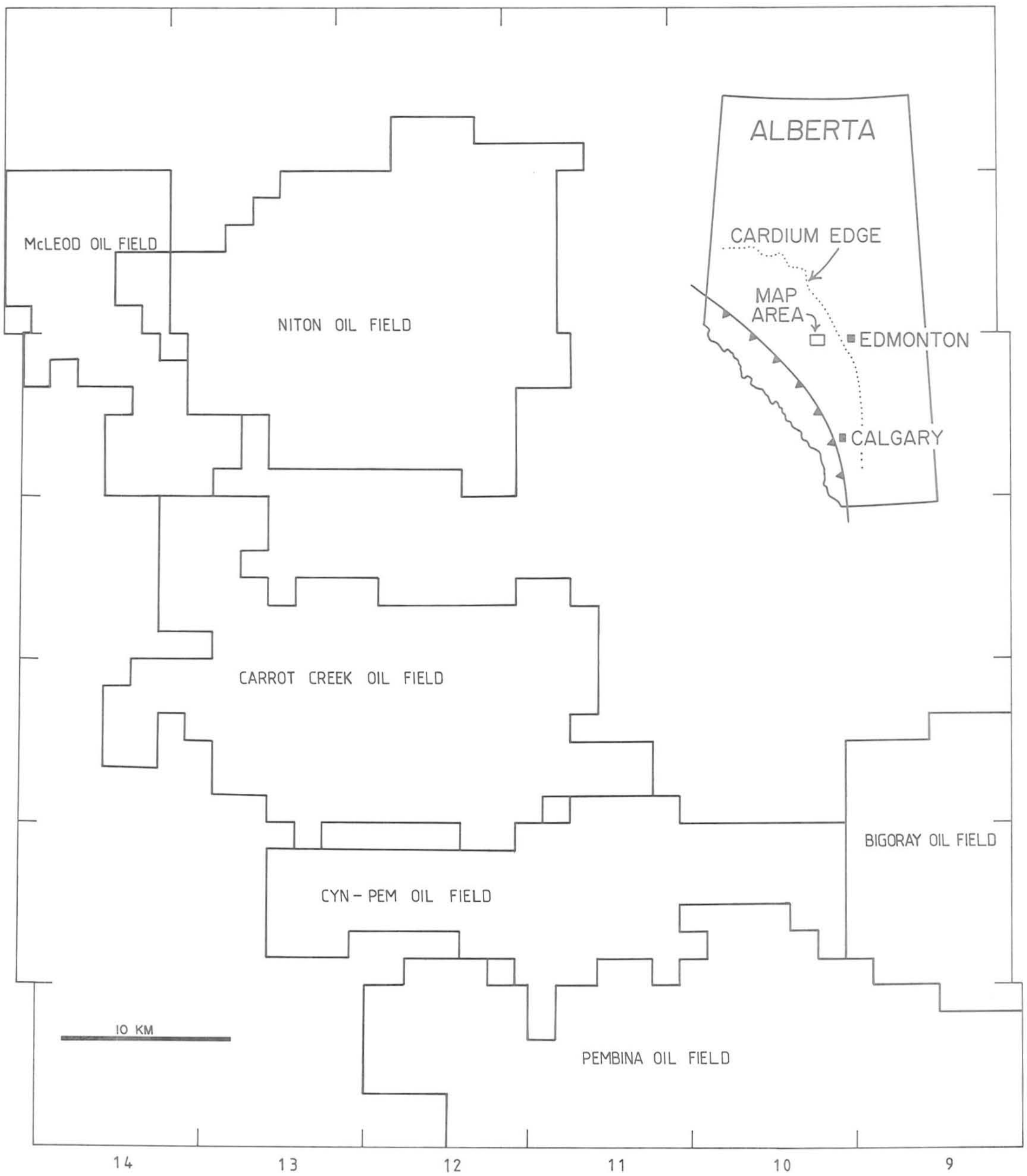

ALBERTA
CARDIUM EDGE
MAP AREA
EDMONTON
CALGARY
McLEOD OIL FIELD
NITON OIL FIELD
CARROT CREEK OIL FIELD
CYN - PEM OIL FIELD
BIGORAY OIL FIELD
PEMBINA OIL FIELD
10 KM
56
55
54
53
52
51
50
14
13
12
11
10
9

Table 2.1. Estimated in place reserves of conventional crude oil, as of December 31, 1984.

OIL FIELD NAME	DISCOVERY YEAR	DISCOVERY WELL	ESTIMATED IN PLACE RESERVES X 10^3 M	ENHANCED RECOVERY X 10^3 M	ENHANCED RECOVERY ERCB POOLS
CARROT CREEK FIG. 2.5	1963	PAN AM A-1 CARROT CREEK A16-7-52-12W5	1124.4	322.0	CARDIUM A and F
BIGORAY FIG. 2.6	1978	HUBER-PEMBINA 8-8 A8-8-51-9W5	270.0	675.0	CARDIUM B
CYN-PEM FIG. 2.7	1962	CHAMPLIN ET AL. CYN PEM A6-14-51-11W5	1730.3	1470.0	CARDIUM A
NITON FIG. 2.8	1970	DUNCAN HB ZD NITON A6-3-55-13W5	8.1		
McLEOD FIG. 2.9	1976	ATKINSON W NITON A10-7-54-13W5	32.0		
PEMBINA FIG. 2.10	1953	SOCONY SEABOARD'S PEMBINA NO. 1 A4-16-48-8W5	130777.3	108000.0	

PART A: MORPHOLOGY OF THE E5 SURFACE

CHAPTER 3 -- FACIES DESCRIPTIONS AND FACIES RELATIONSHIPS

3.1 INTRODUCTION

The facies and facies sequences found in the Carrot Creek study area will be described in this chapter. An extended discussion of the concept implied by the term facies is given by both Middleton (1973) and Walker (1984b). The term facies, as used in this text, describes the complete assemblage of primary characteristics, both physical (lithology, texture, fabric) and biological (body and trace fauna), of the rock. The facies are <u>not</u> stratigraphically confined. In some cases the facies have been divided into sub-facies in order to preserve the affinity with the parent facies.

The facies and overall facies sequence found in the Carrot Creek study area are shown in an idealized stratigraphic section (Fig. 3.1) and are essentially the same as those described by Walker (1983c, 1985c) for the Raven River "sequence" (Walker, 1983c; now the Raven River Member of Plint et al., 1986) in the Caroline - Garrington area farther south. The Raven River "sequence" has now been divided into two members (Plint et al., 1986) -- the Raven River and Carrot Creek Members, and is transgressively overlain by the Dismal Rat Member. These members are based

Figure 3.1. Idealized vertical sequence showing facies relationships. The sequence is drawn roughly to scale, but absolute values will vary. Member names are shown on the left hand side, and facies numbers are shown on the right beside each facies.

IDEALIZED VERTICAL FACIES SEQUENCE

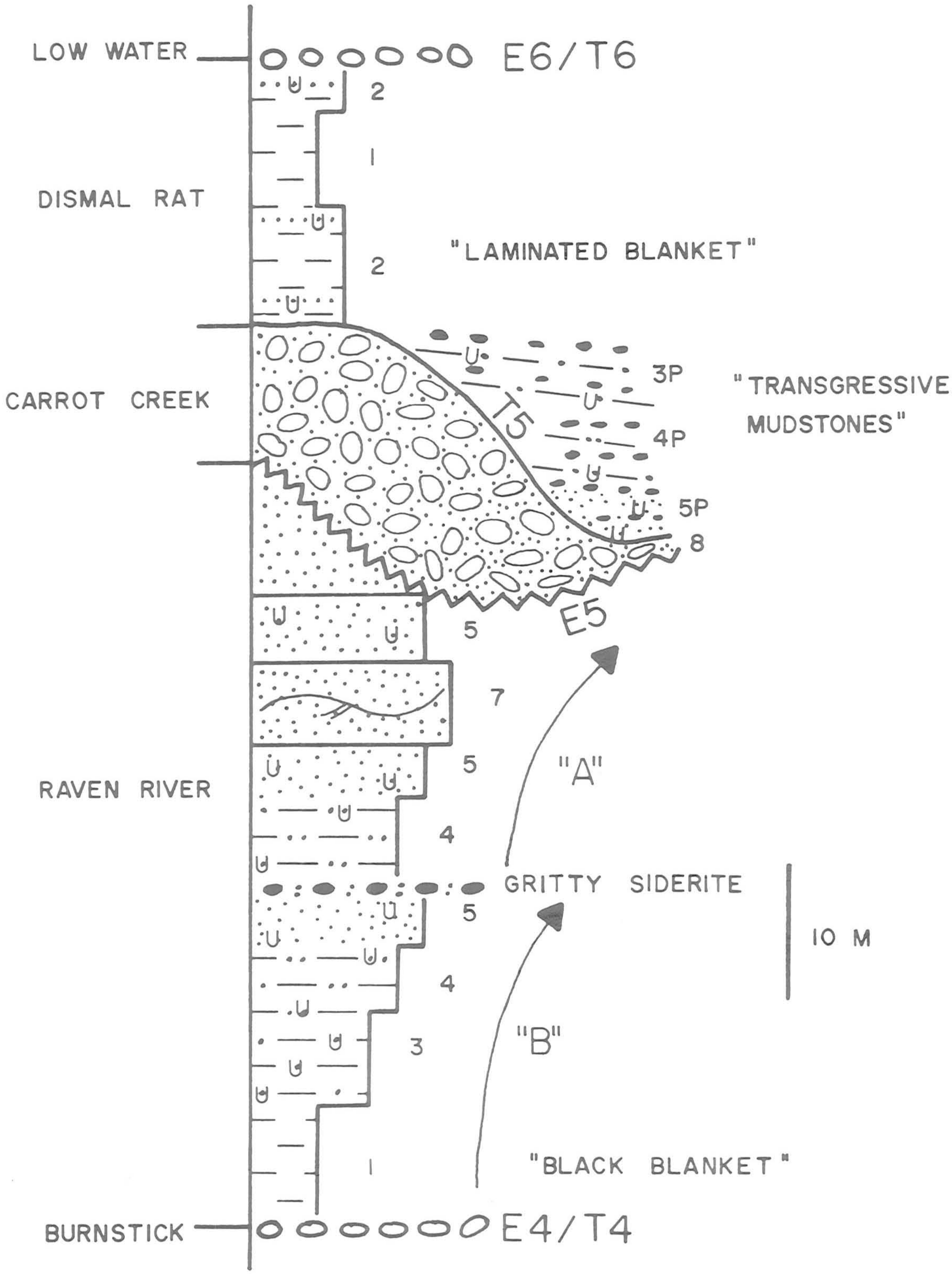

on the recognition of erosion and transgressive surfaces.

The facies found in the Carrot Creek area have been described and illustrated by Bergman and Walker (1986, in press). They presented both core box photos and detailed photos of individual facies from the Carrot Creek area. The major difference between Walker's (1983c, 1985c) study area and the Carrot Creek area is the thickness of conglomerate (Carrot Creek Member) preserved at Carrot Creek.

Only brief descriptions of the various facies associated with the Raven River and the Dismal Rat Members (Plint et al., 1986) are presented, as descriptions and illustrations of these facies have been previously published (Walker, 1983c, 1985c; Bergman and Walker, 1986). With each description a brief interpretation of the environment of deposition will be given. For a more detailed description of these facies the reader is referred to the papers cited above. The textural variations of the conglomerates (facies 8) of the Carrot Creek Member will be described in Chapter 7. Only those facies in the Raven River and the Dismal Rat Members not discussed by Walker (1983c, 1985c) will be described in detail below.

3.2 FACIES DESCRIPTIONS

Facies 1 -- Massive Dark Mudstone (Fig. 3.2)

These are very black structureless muds, with less than 5% silt. There are no recognizable burrow forms (Gordia may be present), but there is an overall "stirred aspect" to the

Figure 3.2. Facies 1 -- Massive Dark Mudstones

A) Photo is taken from well 16-7-52-12, 5512 ft. B) Photo is taken from well 9-1-52-12, 1630.5 m. C) Photo is taken from well 16-21-52-11, 4998 ft. D) Photo is taken from well 4-12-52-12, 5382 ft. Photos are taken from 3 in. drill core.

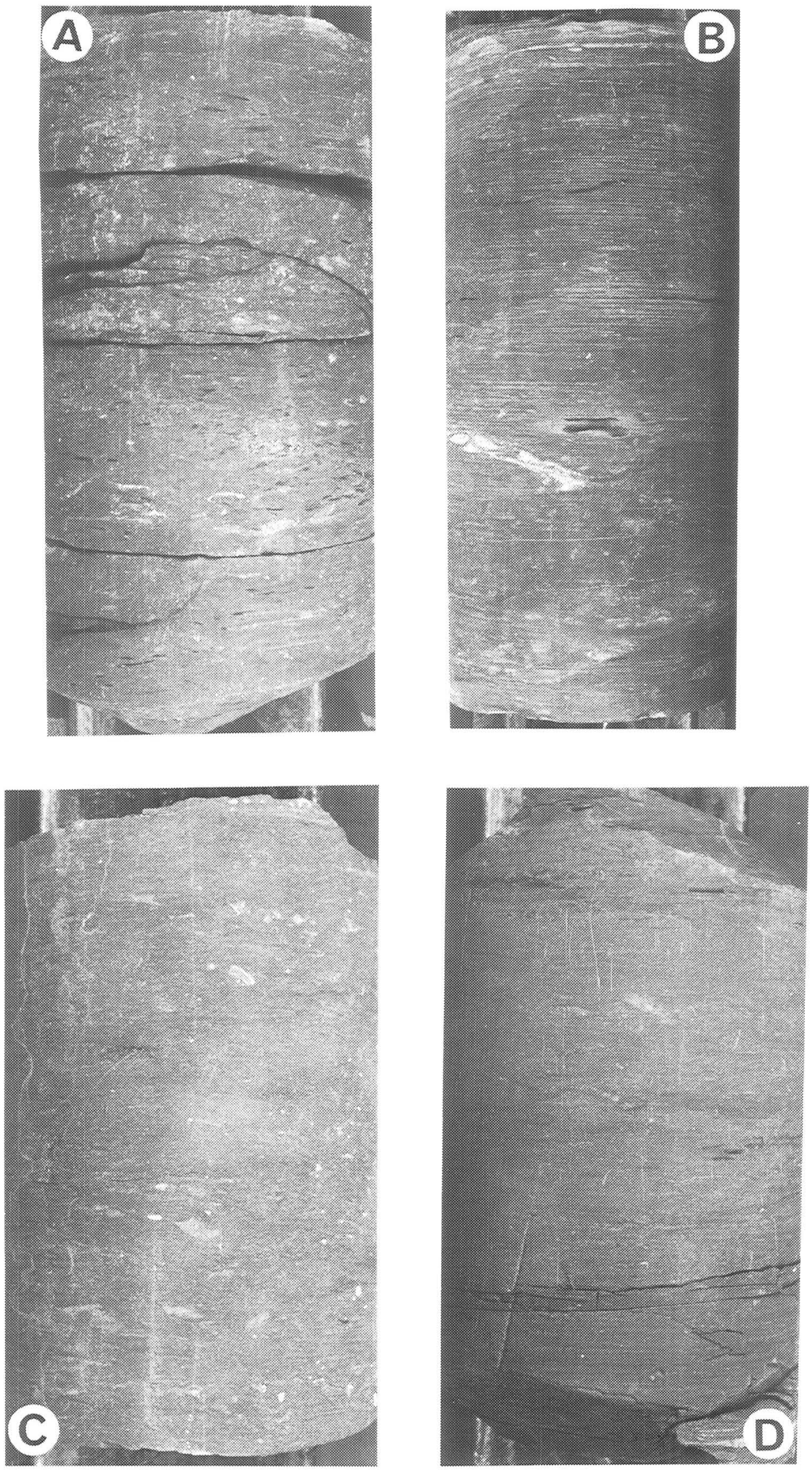
A
B
C
D

mud. One or two very thin (less than 1 cm) sharp based silty laminae may be preserved. This facies was found in two particular associations by Walker (1983c), first blanketing the Burnstick Member and second, overlying the laminated blanket of the Dismal Rat Member. These associations were also observed in the Carrot Creek area (Fig. 3.1). These mudstones are interpreted to have been deposited in a deep, quiet, shelf environment.

Facies 2 -- Laminated Dark Mudstones (Fig. 3.3)

This facies contains dark mudstones with preserved silty laminae up to 1 cm thick. These laminae commonly have sharp bases and bioturbated tops, may be parallel laminated, ripple cross laminated (usually starved ripples), and/or graded (fining upwards). There are no recognizable burrow forms, although the facies has an overall "stirred aspect". This facies blankets the Carrot Creek Member and the pebbly facies in the Dismal Rat Member (Fig. 3.1), and is identical to the "laminated blanket" of Walker (1983c, 1985c,) in the Caroline-Garrington-Ricinus area. Facies 2 is interpreted as a deep water shelf mudstone, although it may be shallower than facies 1 mudstones.

Facies 3 -- Dark Bioturbated Muddy Siltstones (Fig. 3.4)

There is an increase in the silt content from that in Facies 2. Bioturbation increases, so that preservation of silty laminae is rare; predominantly sand and mud are bioturbated together. Where preserved, the laminae are 1-2

Figure 3.3. Facies 2 -- Laminated Dark Mudstones

A) Photo is taken from well 15-7-52-11, 1599 m. B) Photo is taken from well 16-21-52-11, 4989 ft. C) Photo is taken from well 9-1-52-12, 1632 m. D) Photo is taken from well 4-17-52-12, 5388 ft. Photos are taken from 3 in. drill core.

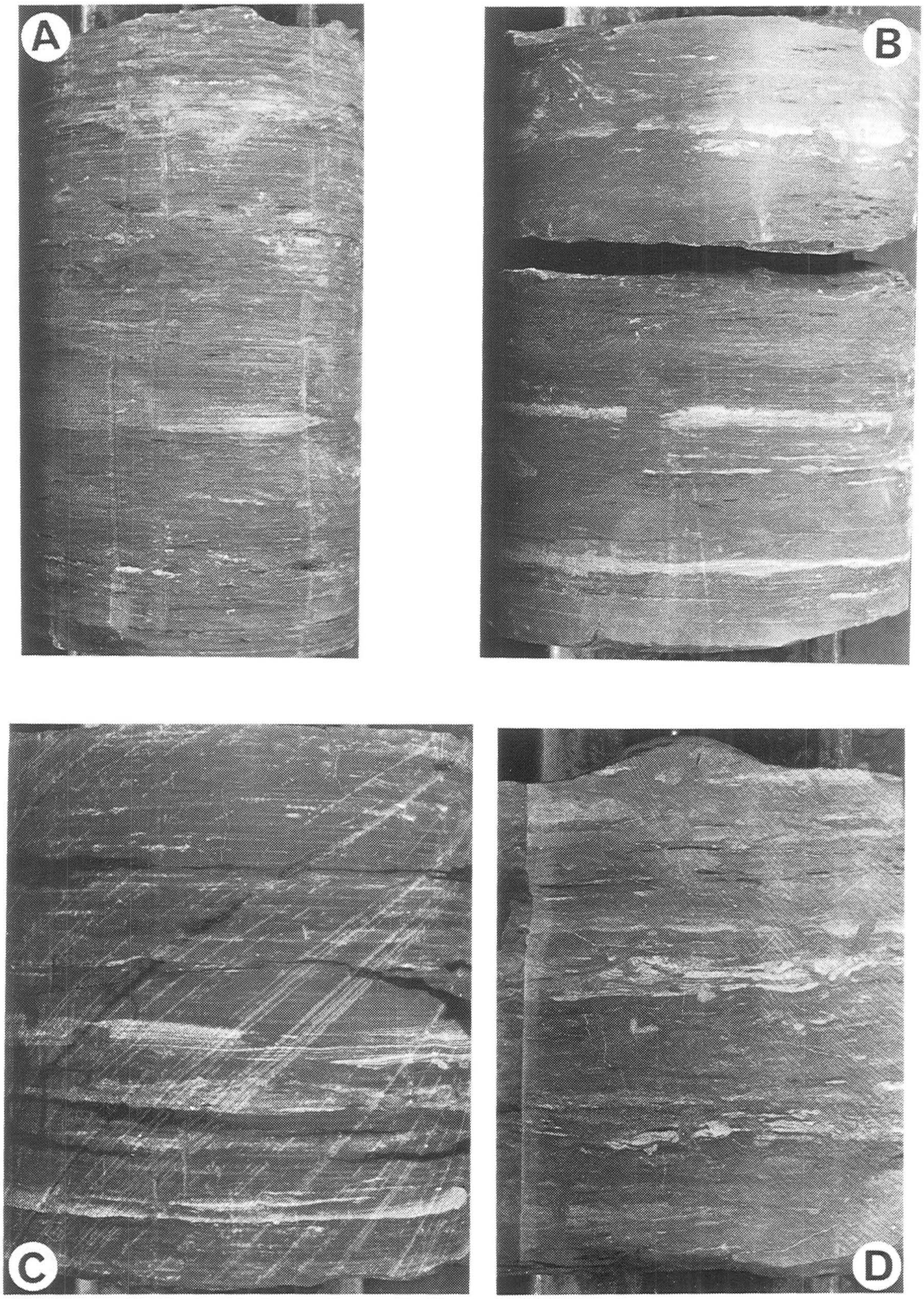
A
B
C
D

Figure 3.4. Facies 3 -- Dark Bioturbated Muddy Siltstones A) Photo is taken from well 12-17-52-12, 5405 ft. B) Photo is taken from 4-12-52-12, 5468 ft. C) Photo is taken from well 5-22-52-12, 5382 ft. D) Photo is taken from well 15-23-52-12, 5263 ft. Photos are taken from 3 in. drill core.

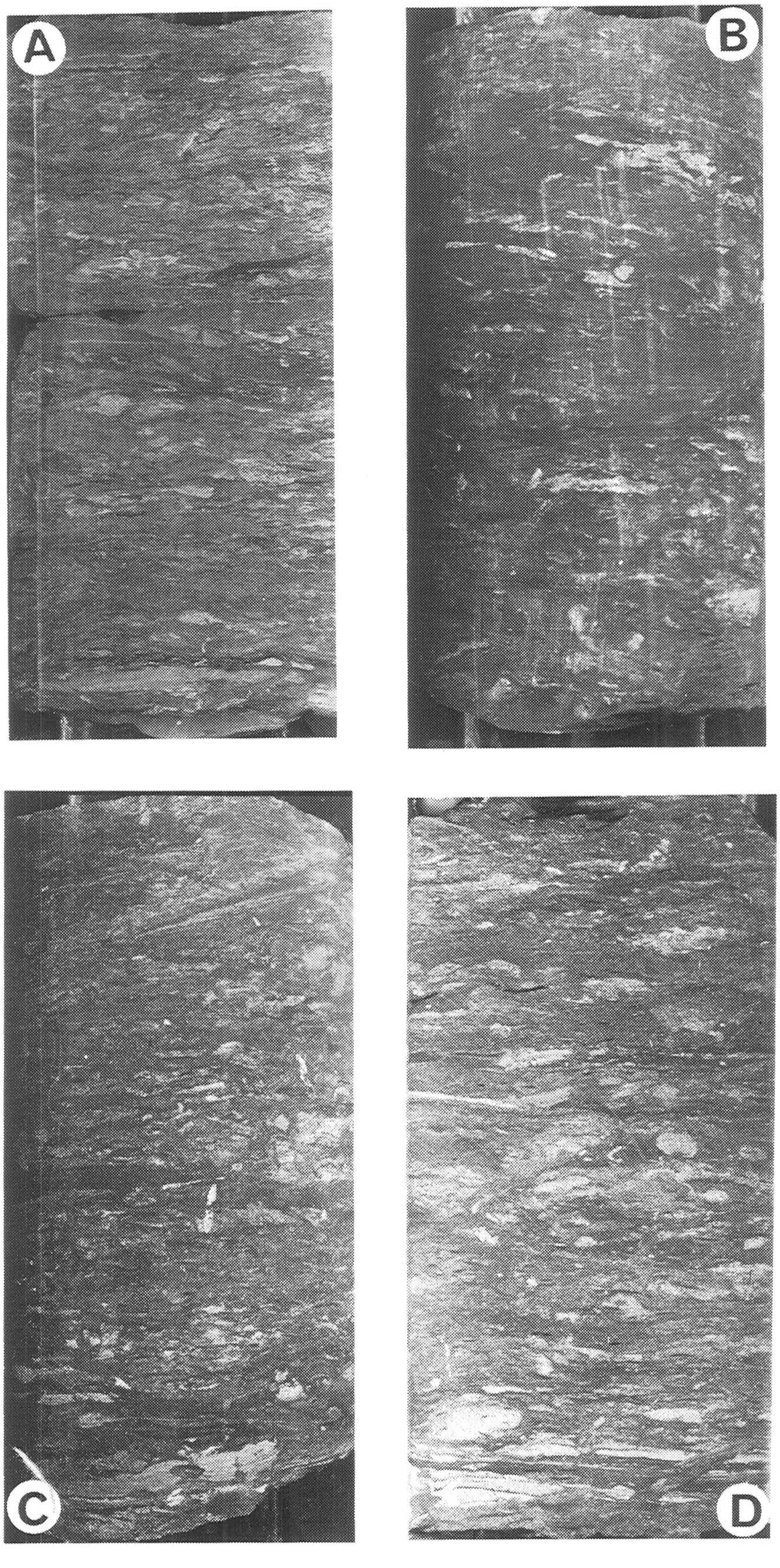
A
B
C
D

cm thick, sharp based, and may show parallel laminations, and/or wave ripple cross laminations and/or a colour grading (reflecting a fining upwards). Very few distinct identifiable burrow forms are present. These mudstones are interpreted to have been deposited in a deep, quiet shelf environment. They are similar to facies 1 and 2, but generally more bioturbated.

Sub-Facies 3P (Fig. 3.5)

This facies is similar to facies 3, but is characterised by a decrease in the amount of bioturbation and the presence of a few thin (1 to 2 cm thick) sharp based, clast supported, chert pebble beds, and scattered chert pebbles within mudstone (hence the P designation in the facies number). The chert grains range in size from coarse sand to a long axis diameter of about 1 cm. This facies is always capped by a pebbly mudstone (sub-facies 8B, described in Chapter 6). It is only locally developed, but where present is always found underlying the laminated mudstones of facies 2 (Fig. 3.1) This facies was not recognized by Walker (1983c). These mudstones are interpreted to have been deposited on the shelf in an environment accessible to gravel input (will be discussed in detail later) during transgression.

Facies 4 -- Pervasively Bioturbated Muddy Siltstones (Fig. 3.6)

This facies comprises sand and mud bioturbated

Figure 3.5. Facies 3P -- Dark Bioturbated Muddy Siltstones with Pebbles

A) Photo is taken from well 10-21-51-11, 5357 ft. B) Photo is taken from well 10-22-51-10, 1556 m. C) Photo is taken from well 6-1-53-13, 5146 ft. Scale bar is 3 cm.

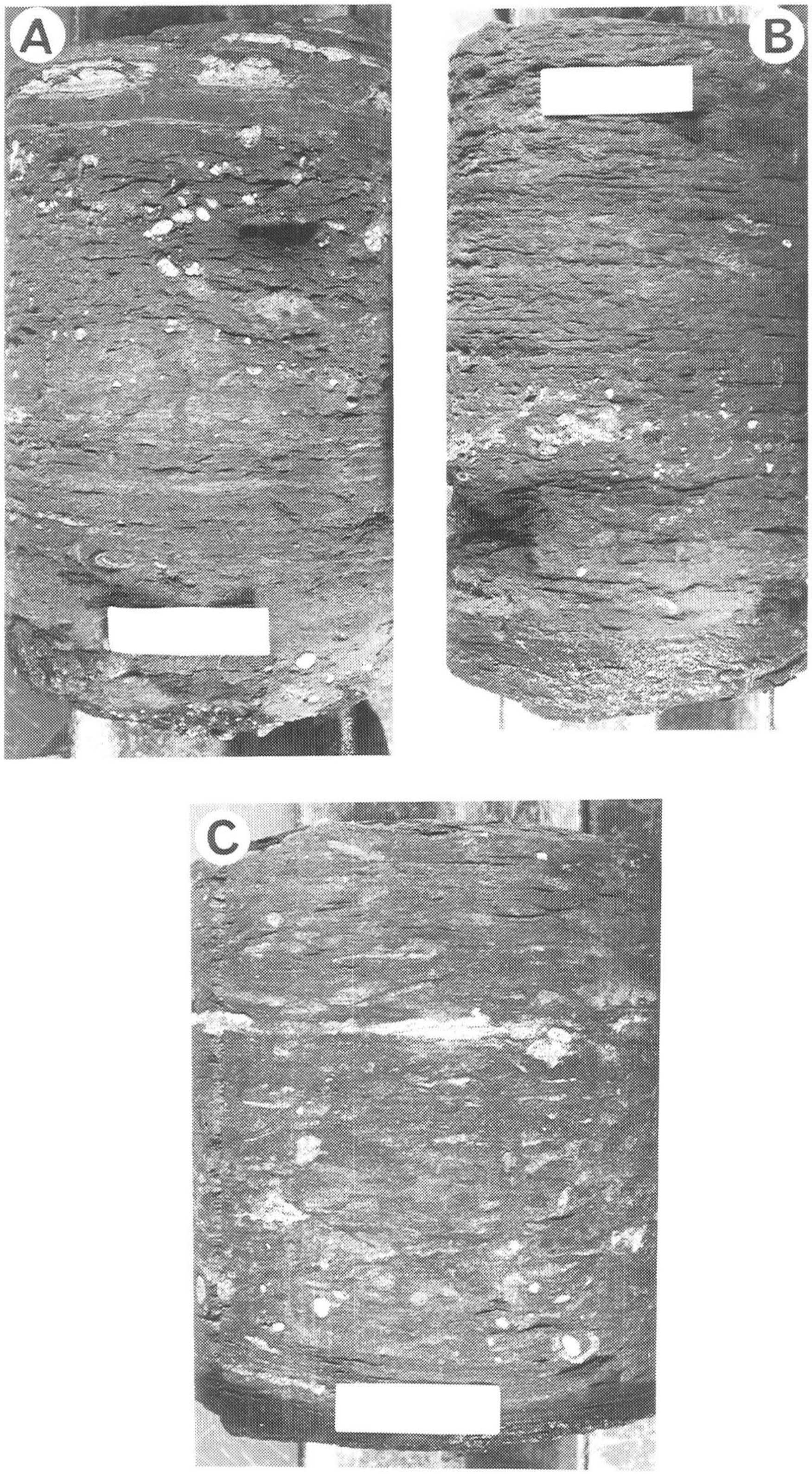
A
B
C

Figure 3.6. Facies 4 -- Pervasively Bioturbated Muddy Siltstones

A) Photo is taken from well 12-17-52-12, 5396 ft. B) Photo is taken from well 4-12-52-12, 5461. Note the Zoophycos burrow located in the middle of the core photo. C) Photo is taken from well 16-21-52-11, 5023 ft. D) Photo is taken from well 3-14-52-12, 1653 m. Photos are taken from 3 in. drill core.

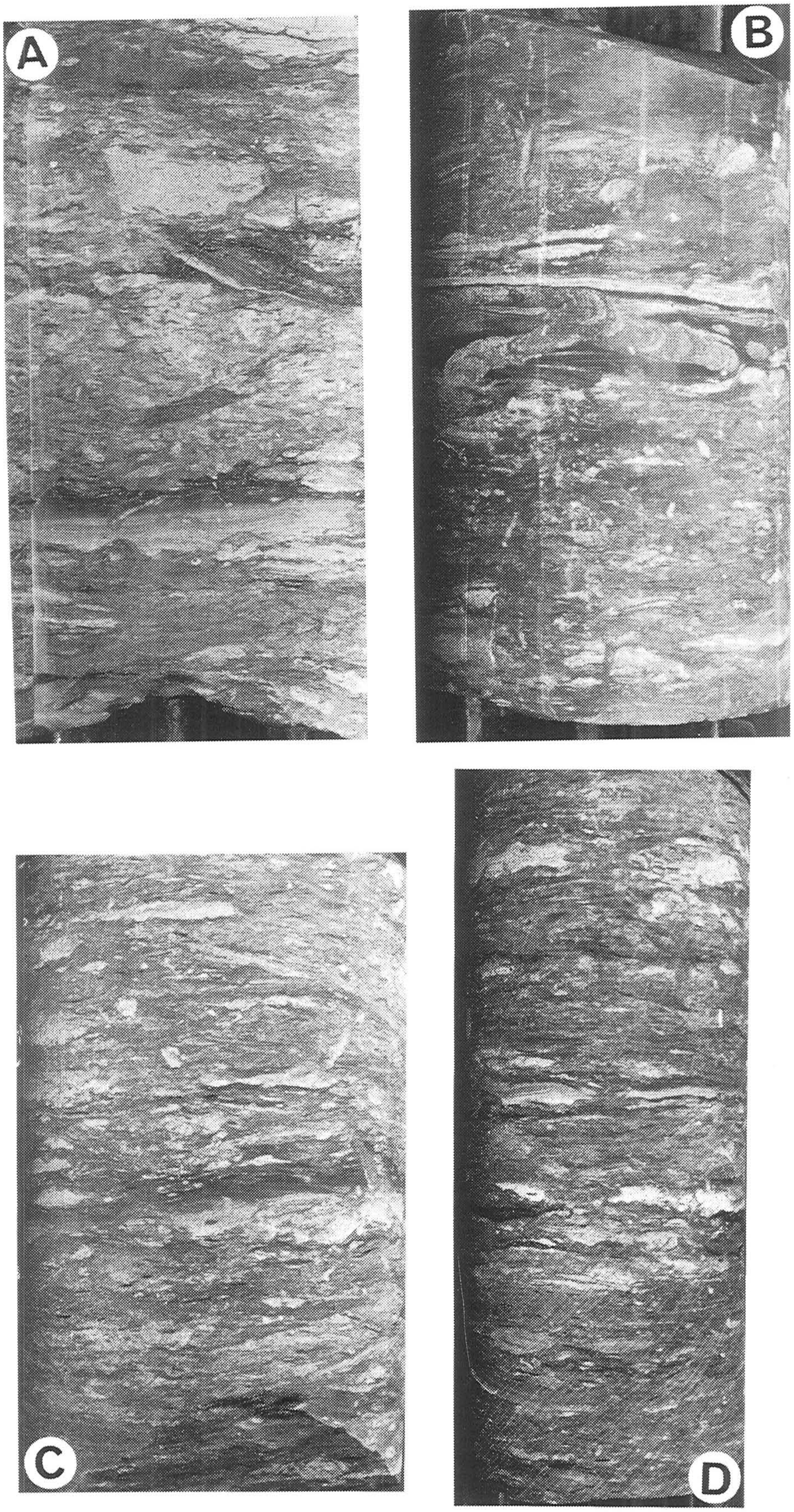
A
B
C
D

together, with a number of identifiable burrow forms. These include Teichichnus, Terebellina, Rhizocorallium, and Planolites. Generally, this facies shows an increase in sand upwards, and silty beds are preserved. The beds are usually 1-5 cm thick, sharp based and generally show parallel laminations, and/or wave ripple cross lamination, and/or grading. Both silt content and the degree of bioturbation have increased from that of facies 3. These siltstones are interpreted to have been deposited in the shelf environment. The presence of the thicker sharp based wave rippled and graded beds associated with bioturbated siltstones suggests sudden input of silt into quiet environment below fair weather wave base, but above storm wave base.

Sub-Facies 4P (Fig. 3.7)

This facies is similar to facies 4, but is characterized by a decrease in the amount of bioturbation and the presence of sharp based, clast supported chert pebble beds 1 to 2 cm thick and scattered chert pebbles within mudstones. The chert grains range in size from coarse sand to a long axis diameter of about 1 cm. The facies is always capped by a pebbly mudstone (sub-facies 8B described in Chapter 6). Sub-Facies 4P is only locally developed, but where present is always found underlying sub-facies 3P. This facies was not recognized by Walker (1983c). These siltstones are interpreted as having been

Figure 3.7. Facies 4P -- Pervasively Bioturbated Muddy Siltstones with Pebbles A) Photo is taken from well 16-31-53-11, 1388 m. B) Photo is taken from well 10-22-51-10, 1563 m. C) Photo is taken from same well as in A, in order to show the variety within the facies, 1387.5 m. D) Photo is taken from well 10-21-51-11, 5366 ft. Scale bar is 3 cm

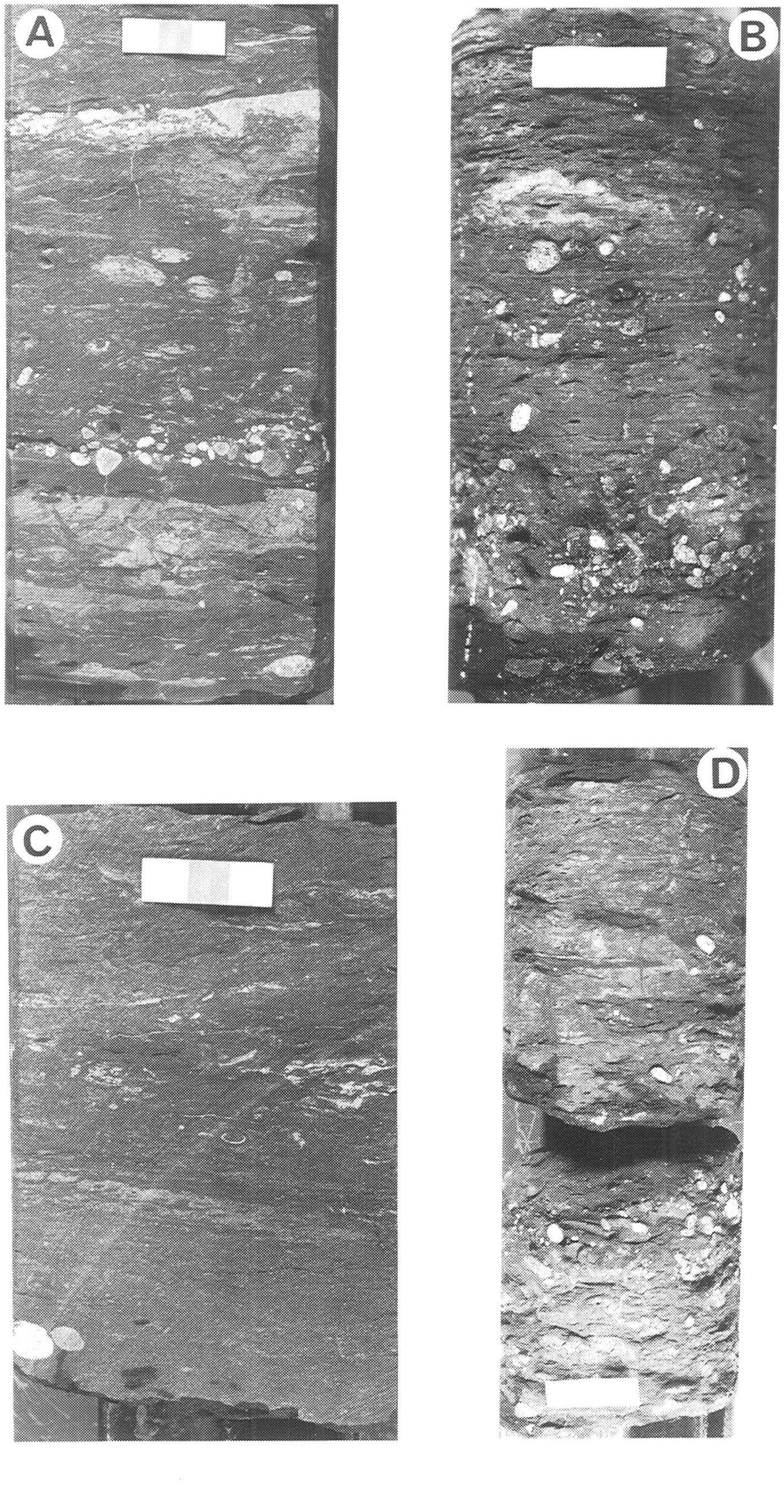
A
B
C
D

deposited on the shelf close to a gravel source, as will be discussed in detail later.

Facies 5 -- Bioturbated Sandstone (Fig. 3.8)

This facies consists predominantly of sand, although mud is still present. Beds up to 7 cm thick are preserved, with sharp bases, parallel laminations, wave ripple cross laminations (sometimes climbing), grading (fining upwards) and shale rip up clasts. The sand and mud are generally bioturbated together. There is a marked increase in bioturbation, with many identifiable burrow forms, including *Zoophycos*, *Rhizocorallium*, *Teichichnus*, and *Chondrites*. Compared with facies 3 and 4, there is an increase in the abundance of the vertical burrow form *Skolithos*. These sandstones are interpreted as having been deposited in a shelf environment similar to facies 4, possibly slightly shallower.

Sub-Facies 5P (Fig. 3.9)

This facies is found occasionally throughout the study area. It is similar to facies 5, but is characterised by a decrease in the amount of bioturbation and the presence of sharp based, clast supported, chert pebble beds (1 to 2 cm) thick, and scattered chert pebbles in mudstones and siltstones. The chert grains range in size from coarse sand to a long axis diameter of about 1 cm. The facies is always capped by about 10 cm of pebbly mudstone (sub-facies 8B, described in Chapter 6). Where present, this facies is

Figure 3.8. Facies 5 -- Bioturbated Sandstones

A) Photo is taken from well 5-22-52-12, 5369 ft. B) Photo is taken from well 15-23-52-12, 5246 ft. C) Photo is taken from well 3-14-52-12, 1646.4 m. D) Photo is taken from well 2-21-51-11, 5437 ft. Scale bar is 3 cm. Note the abundance of Skolithos burrows present in C and D; this is a common association in this facies. Photos are taken from 3 in. drill core.

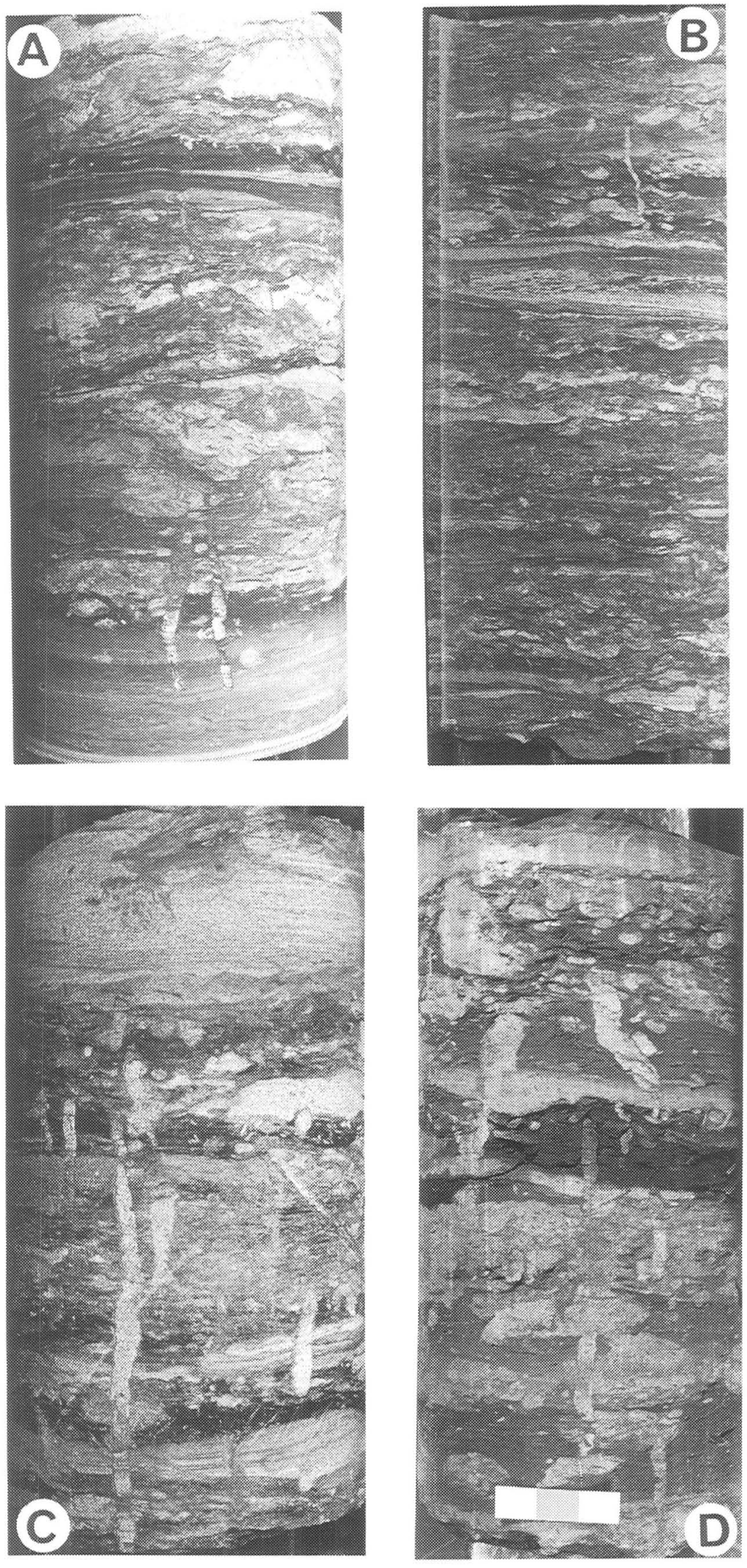
A
B
C
D

Figure 3.9. Facies 5P -- Bioturbated Sandstones with Pebbles

Both photos are taken from the same well, 16-31-53-11, in order to illustrate the variability within the facies.

A) Preservation of a 5 cm thick wave rippled sand bed; no pebbles present in this photo, 1390 m. B) Thinner sand beds are preserved in this photo as well scattered chert pebbles immediately below the sand bed, 1395.5 m. Scale bar is 3 cm.

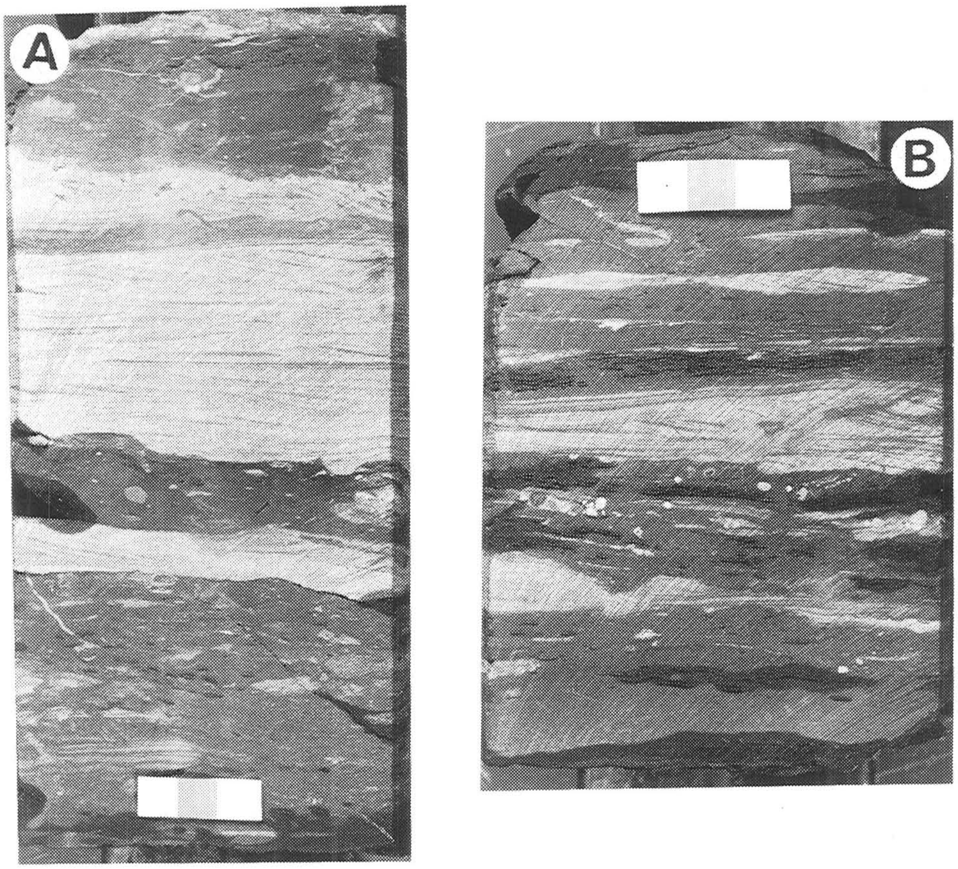
A
B

always found underlying sub-facies 4P, and overlying the Carrot Creek Member. These sandstone are interpreted to have been deposited in a shelf environmnent accessible to a gravel supply.

Facies 6 -- Speckled Gritty Mudstone

This facies was not found in the Carrot Creek area. In Walker's (1983c, 1985c) facies descriptions, it occurred "exclusively just below the sandstones and conglomerates of the Burnstick Member" (1983c, p. 220). In current terminology (Plint et al., 1986), it therefore occurs in the uppermost Hornbeck Member or (more likely) is the basal facies of the Burnstick Member.

Facies 7 -- Non-Bioturbated Sandstone (Fig. 3.10)

The sandstones associated with this facies consist of sharp based, very fine sands, showing a variety of sedimentary structures. These include massive sandstones, parallel stratification, low angle inclined stratification, and wave ripples. The tops of the sand beds may be either sharp or gradational. The sands often scour into each other and contain mud rip up clasts or sideritized mud clasts. The sand thickness varies from 10 cm to tens of cms. Very little bioturbation is associated with this facies. These are interpreted as shelf sands, located above storm wave base. The low angle inclined stratification is interpreted as hummocky cross stratification. This facies is interpreted as being shallower than facies 5.

Figure 3.10. Facies 7 -- Non-Bioturbated Sandstones

A) Photo is taken from well 2-29-52-13, 5483 ft. This photo shows a massive sand with a mud rip up clast in upper right corner. B) Photo is taken from well 2-29-52-13, 5482 ft. This photo shows preserved climbing wave ripples. C) Photo is taken from well 4-9-52-12, 5550 ft. D) Photo is taken from well 7-34-52-13, 5315 ft. The last two photos show low angle inclined stratification, which is interpreted in this study as hummocky cross stratification. Photos are taken from 3 in. drill core.

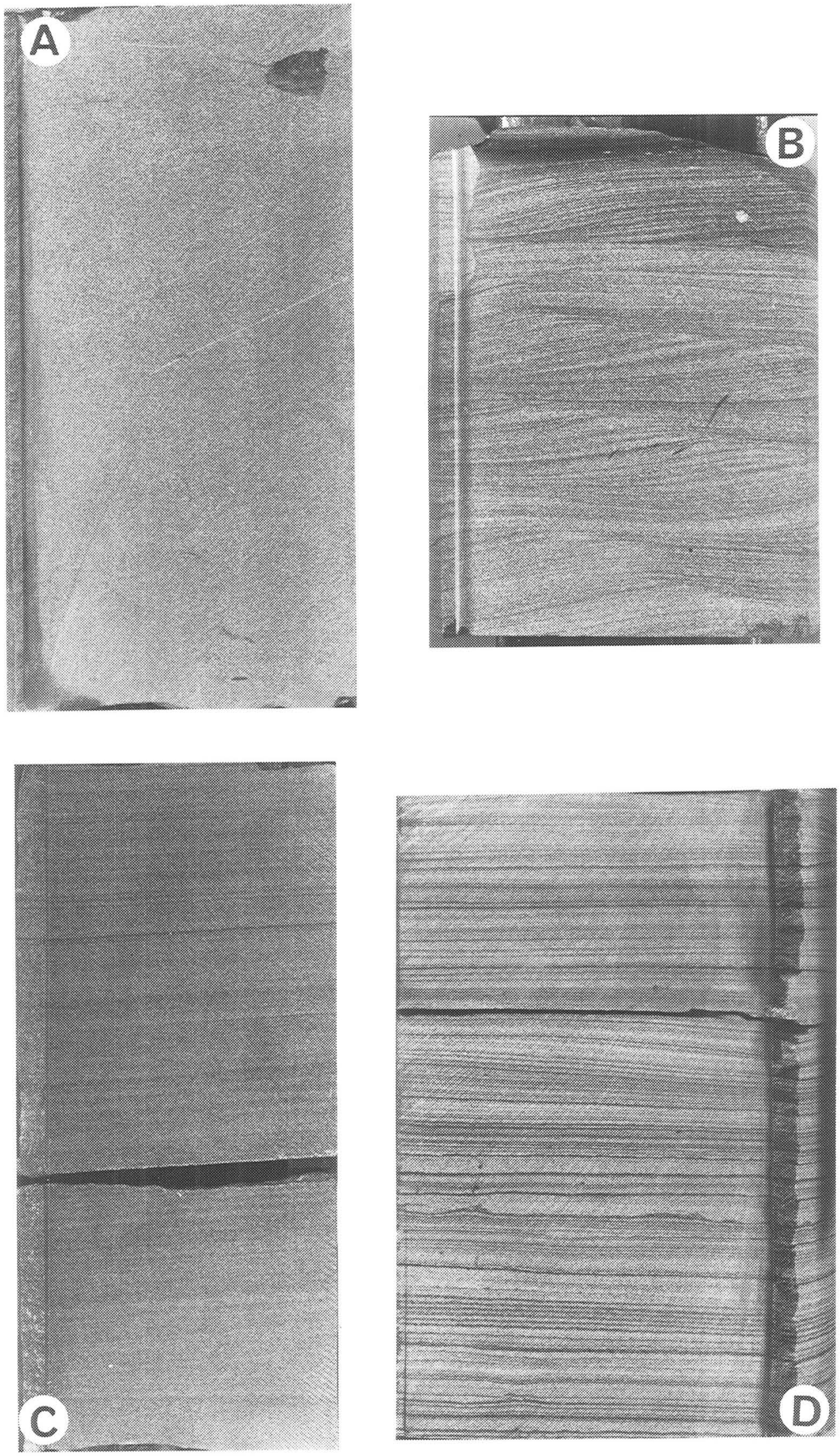
A
B
C
D

Sub-Facies 7A -- Interbedded Sand and Shale (Fig. 3.11)

The sands making up this facies are very fine grained. The beds are generally 3-5 cm thick, sharp based, wave rippled, and graded. They are separated by thinner beds (1-2 cm thick) of very black non-bioturbated mudstones. The overall thickness of the facies is highly variable. This facies occurs as a transitional facies between the Bioturbated Sandstone of facies 5 and the Non-Bioturbated Sandstone of facies 7. It is always found associated with the non-bioturbated sandstones of facies 7. This facies was not recognized by Walker (1983c). It is interpreted as a shelf sandstone deposited above storm wave base and below fairweather wave base. Facies 7A is believed to be intermediate between facies 5 and 7.

Facies 8 -- Conglomerates (Fig. 3.12)

The conglomerates vary in thickness from a thin veneer to about 19 m, and rest unconformably on the underlying sandstones and siltstones of the Raven River Member. The Carrot Creek Member is composed primarily of clast supported conglomerates. The average long axis diameter of the pebbles is 1 to 2 cm. Stratification is rare, but many textural varieties occur and are defined by grain size, sorting, and the presence or absence of matrix. The lower portion of the conglomerate tends to be bedded while the upper portion is massive. A detailed discussion of the textural variations is presented in Chapter 6.

Figure 3.11. Facies 7A -- Interbedded Sand and Shale

A) Photo is taken from well 7-20-51-11, 1675.2 m. Note the Chondrites burrows preserved in the muds interbeds, particularly by the scale bar, and the wave rippling preserved in the sand beds. Scale bar is 3 cm. B) Photo is taken from well 4-12-52-12, 5426 ft. C) Photo is taken from well 10-1-53-14, 5407 ft. Note the layer of mud rip up clasts, and the wave rippling at the top of the sand bed. D) Photo is taken from well 2-29-52-13, 5471 ft. Note the low angle inclined stratification, which is interpreted as hummocky cross stratification, passing vertically upwards into wave ripples. Photos are taken from 3 in. drill core.

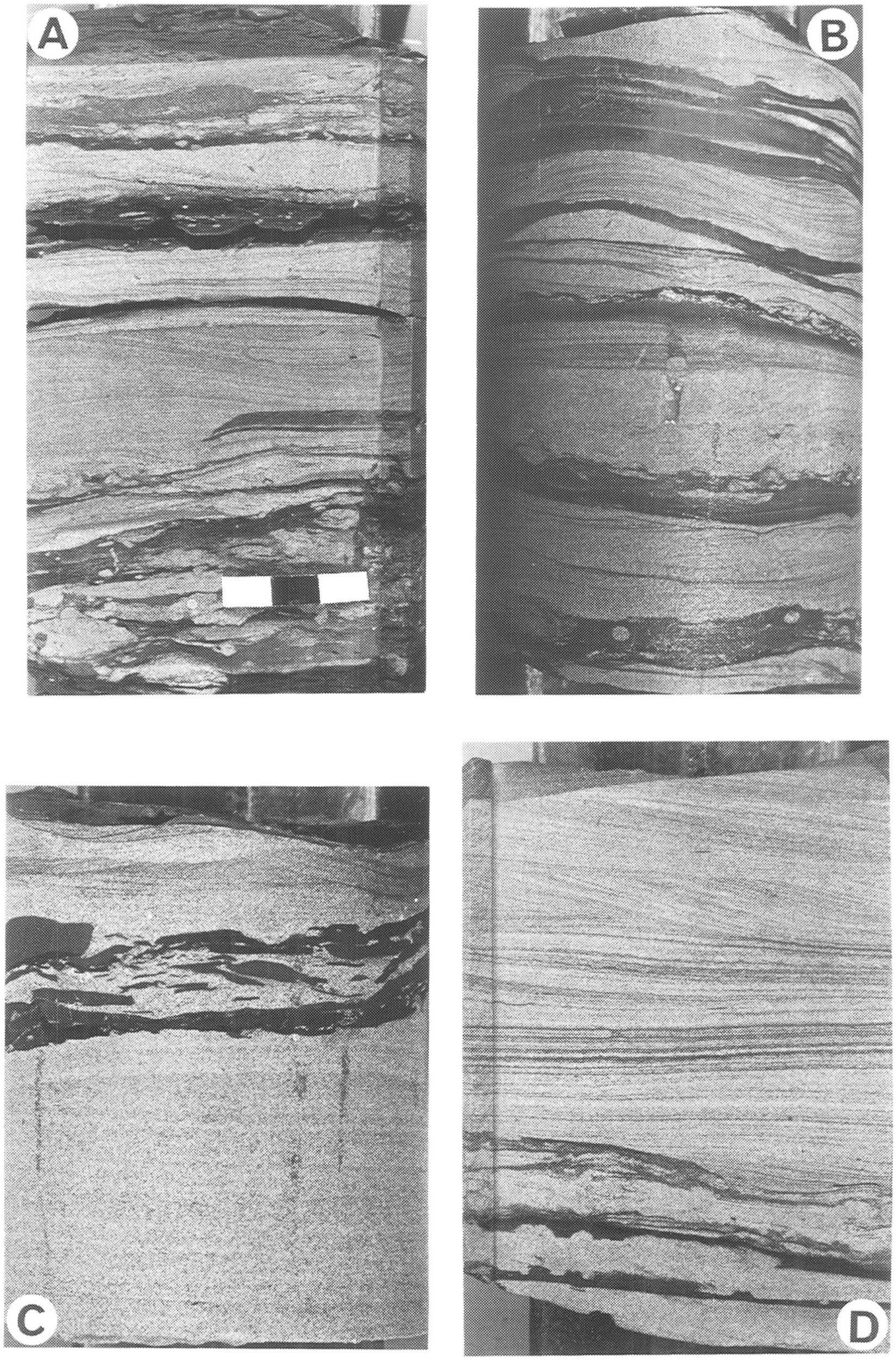
A
B
C
D

Fig. 3.12. Facies 8 -- Conglomerate

A) Photo is taken from well 12-19-52-12, 1624 m. Core is 3 in. wide. B) Photo is taken from well 10-30-51-10, 1550 m. Scale bar is 3 cm. C) Photo is taken from well 6-10-53-13, 1621 m. Scale bar is 3 cm. D) Photo is taken from well 6-36-50-10, 4929 ft. A Conichnus burrow is preserved in the centre of the core. Scale bar is 3 cm.

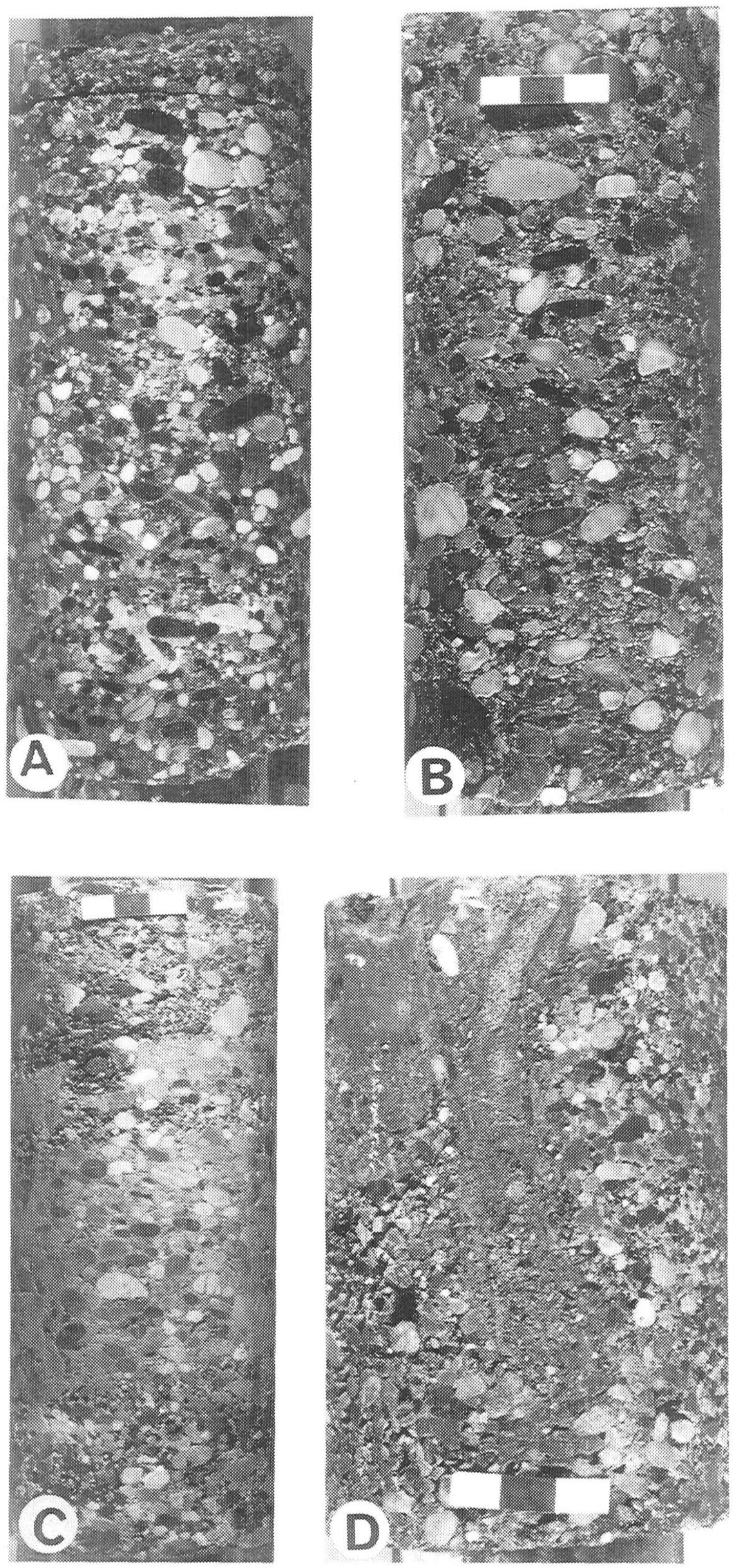
A
B
C
D

Sub-Facies 8 G.S. -- Gritty Siderite Facies (Fig. 3.13)

The Gritty Siderite Facies is a new facies not recognized by Walker (1983c, 1985c). It is found in the Raven River Member, where it is significant as a marker horizon (which will be discussed later).

This sub-facies is composed of bioturbated silts and muds, associated with coarser chert grains; it is pervasively sideritized. The upper and lower contacts are both gradational over 1-2 cm, and the overall facies thickness varies from 20-30 cm.

The facies is characterized by an abrupt change in grain size from the underlying and overlying very fine grained bioturbated sandstones. The coarse grains range in size from medium sand to several mm in diameter. Stratification consists only of vague remnants of sandy beds. The facies is thoroughly bioturbated, and often the coarser chert grains are found within the burrow forms. The siderite is patchy and contains numerous sideritized <u>Chondrites</u> burrows. Other burrow forms commonly associated with this facies are <u>Skolithos</u> and <u>Teichichnus</u>. Concentrations of carbonaceous (primarily wood fragments) debris are associated with this facies in some locations (eg., 16-33-50-10W5). Mud rip up clasts are commonly found.

The gritty siderite horizon makes an excellent core marker. Where present (i.e., not eroded by overlying conglomerates) it <u>always</u> occurs at the top of the "b"

Fig. 3.13. Facies 8 G.S. -- Gritty Siderite

Photos A and B are both taken from well 6-11-53-13, 1593 m. Scale bar is 3 cm. A) This photo shows an overview of the entire facies in core. B) This photo is a detail picture of the photo shown in A. C) Photo is taken from well 12-19-52-12, 1627 m. Scale bar is in cms. D) Photo is taken from well 10-20-51-11, 5490 ft. Scale bar is in cms.

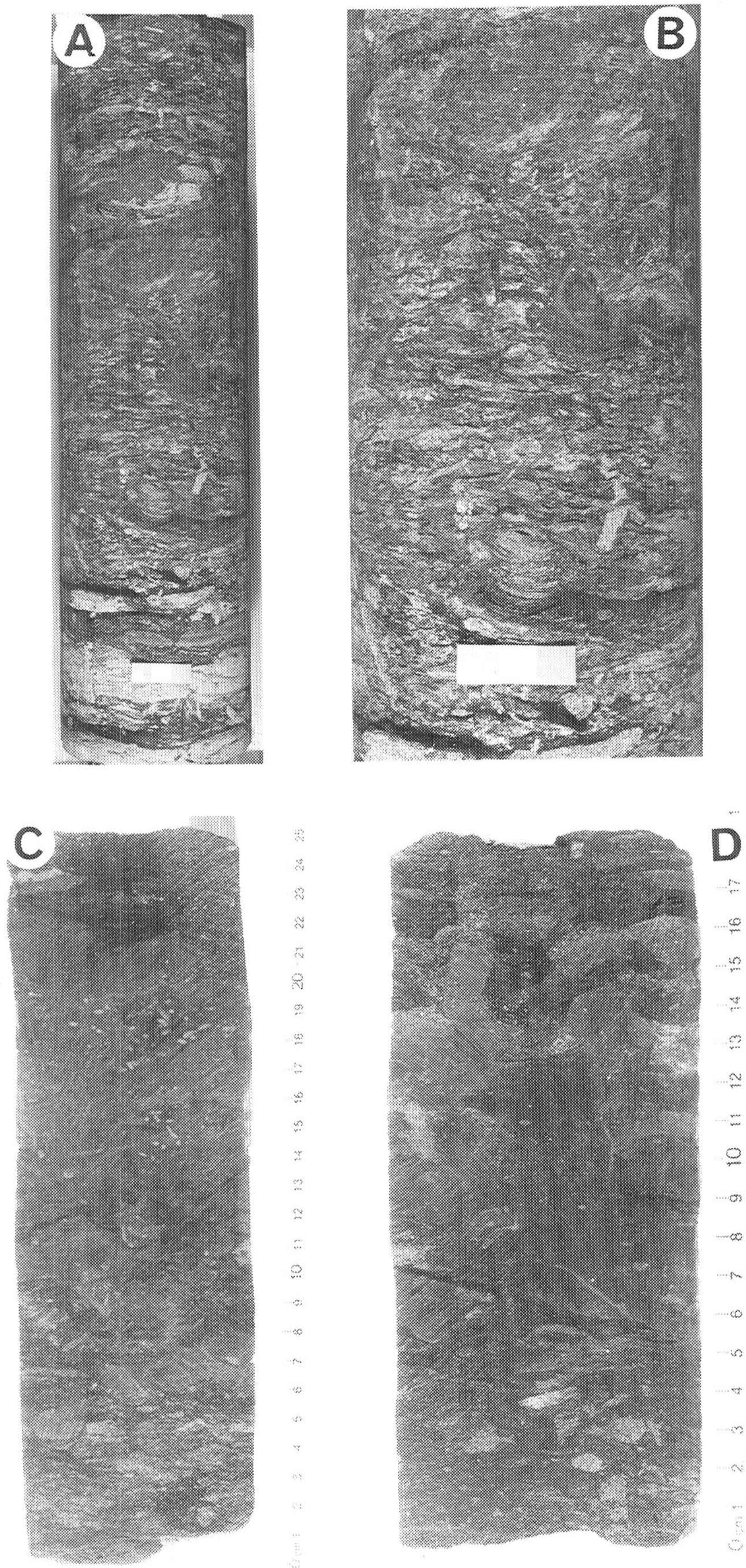
A
B
C
D

sequence (Fig. 3.1). It is not very variable in aspect, and is of a relatively constant thickness. This facies is believed to represent a period of non-deposition, presumably due to a rapid relative rise of sea level or a stillstand.

3.3 GENERAL FACIES SEQUENCE

The overall facies sequence (Fig. 3.1) is one of progressive coarsening upwards (Walker 1983c, 1985c; Plint et al., 1986). The Raven River Member consists of two coarsening upward sequences. The lower "b" sequence begins with the massive dark mudstones of facies 1 and coarsens upwards through facies 3 and 4 into the bioturbated sandstones of facies 5. These are overlain by the gritty siderite (facies 8 G.S.). The upper "a" sequence begins with facies 4 or 5 and coarsens upwards into the hummocky cross stratified (HCS) sandstones of facies 7. The "a" sequence has a maximum preserved thickness of 12 m (refer to wells 4-28-50-12 and 10-11-51-13 in APPENDIX 2). The thickness of the "b" sequence is about 26 m, of which about 11 m has been cored (refer to well 13-5-51-11 on cross section B, Foldout 2).

The conglomerates (facies 8) of the Carrot Creek Member rest unconformably, with a variable depth of scour, on different parts of the "a" and "b" sequences of the Raven River Member. The conglomerate contact may sharp or bioturbated.

Above the Carrot Creek Member facies 5P, 4P, and 3P of the Dismal Rat Member are locally developed. After deposition of all the pebbles (conglomerate and last pebble stringer), the "laminated blanket" (facies 2) spreads over the entire area. These mudstones in turn grade upward into the massive dark mudstones of facies 1. The two facies are separated by dispersed mm size chert grains.

The above facies sequence may be divided into three types based on 1) the nature of the well log response; 2) the core sequence; and 3) the depth of scour. Core box photos, lithologs and geophysical logs of these various sequence types are presented. More examples of each facies sequence type may be found in APPENDIX 2 and the cross sections (Foldouts 1 through 4).

TYPE I (Figs. 3.14 to 3.17): These facies sequences are characterized by a large negative deflection in both the gamma ray and induction log signatures. The Raven River Member coarsens upwards. The response is <u>not</u> blocky. The core shows the development of both the "a" and "b" facies sequences, separated by the gritty siderite horizon. Non-bioturbated sandstones (facies 7 and/or 7A) are always preserved. Depending on the depth of erosion into the sandstones, the Carrot Creek Member may be represented by a thin gravel veneer (TYPE 1A; Figs. 3.14 and 3.15) or a thicker (generally 1 to 2 m) clast supported and matrix supported conglomerate (TYPE 1B; Figs. 3.16 and 3.17).

Fig. 3.15. The core of well 10-16-51-11 is typical of the Type 1A sequence. The next four pages show core photographs of well 10-16-51-11. The corresponding litholog and resistivity log is shown in Fig. 3.15. Core depths are given in feet; the bottom of the core is in the lower left and the top in the upper right. Coarsening upward sequence "b" begins below 5487 ft. and continues to the gritty siderite. Sequence "a" begins with facies 4 above the gritty siderite and coarsens upward into the hummocky cross stratified and wave rippled sandstones (facies 7A). In this well two sand sequences separated by a bioturbated sandstone (facies 5) are preserved. The sandstones are abruptly overlain by conglomerate (facies 8). The conglomerates pass vertically upwards into the pebbly mudstones (facies 4P and 3P). The tops of both of these facies are marked by pebbles. The bioturbated mudstones are overlain by the "laminated blanket" (facies 2).

10-16-51-11

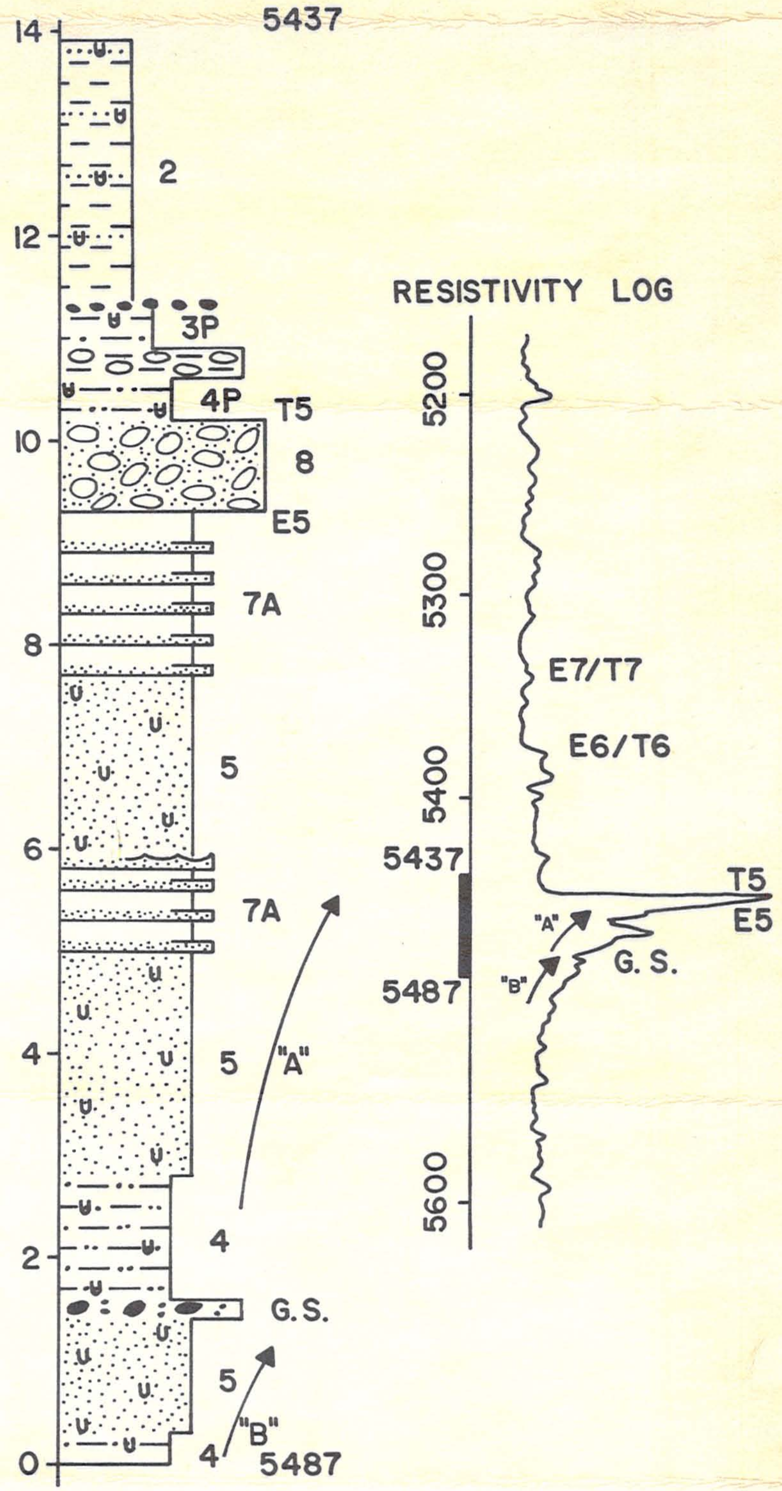

TYPE 1A

Fig. 3.14. Facies Sequence Type 1A -- Type Well 10-16-51-11. See descriptions in text. Vertical scale on the litholog is in metres. The facies numbers are given on the right hand side of the litholog, and the positions of the E5/T5 surfaces are shown. Vertical scale on the resistivity log is in feet. The cored interval is shown by solid black bar on the resisitivity log, and the depth of the cored interval is given. The positions of the E/T surfaces are shown on the right hand side of the resisitivity log. G.S. indicates the position of the Gritty Siderite horizon on both logs. The position of the "A" and "B" sequences of the Raven River Member are shown on both the litholog and resistivity log. Core box photos of this sequence type are shown in Fig. 3.15.


FACIES 4
GRITTY
SIDERITE
FACIES 5
FACIES 5
10-16-51-11
5487

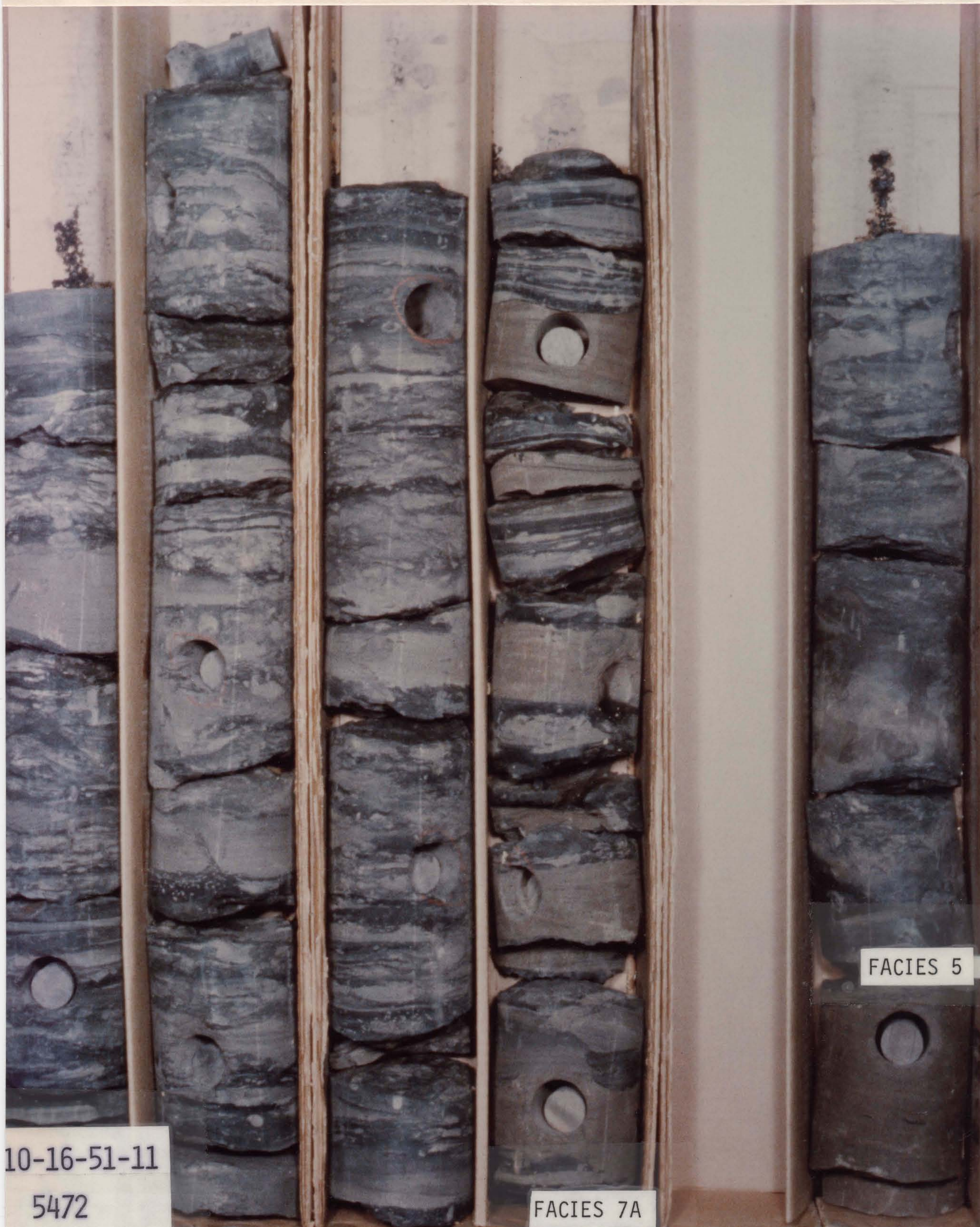
10-16-51-11
5472
FACIES 7A
FACIES 5


FACIES 7A
CONGLOMERATE
CONTACT
10-16-51-11
5457

12-16-51-11

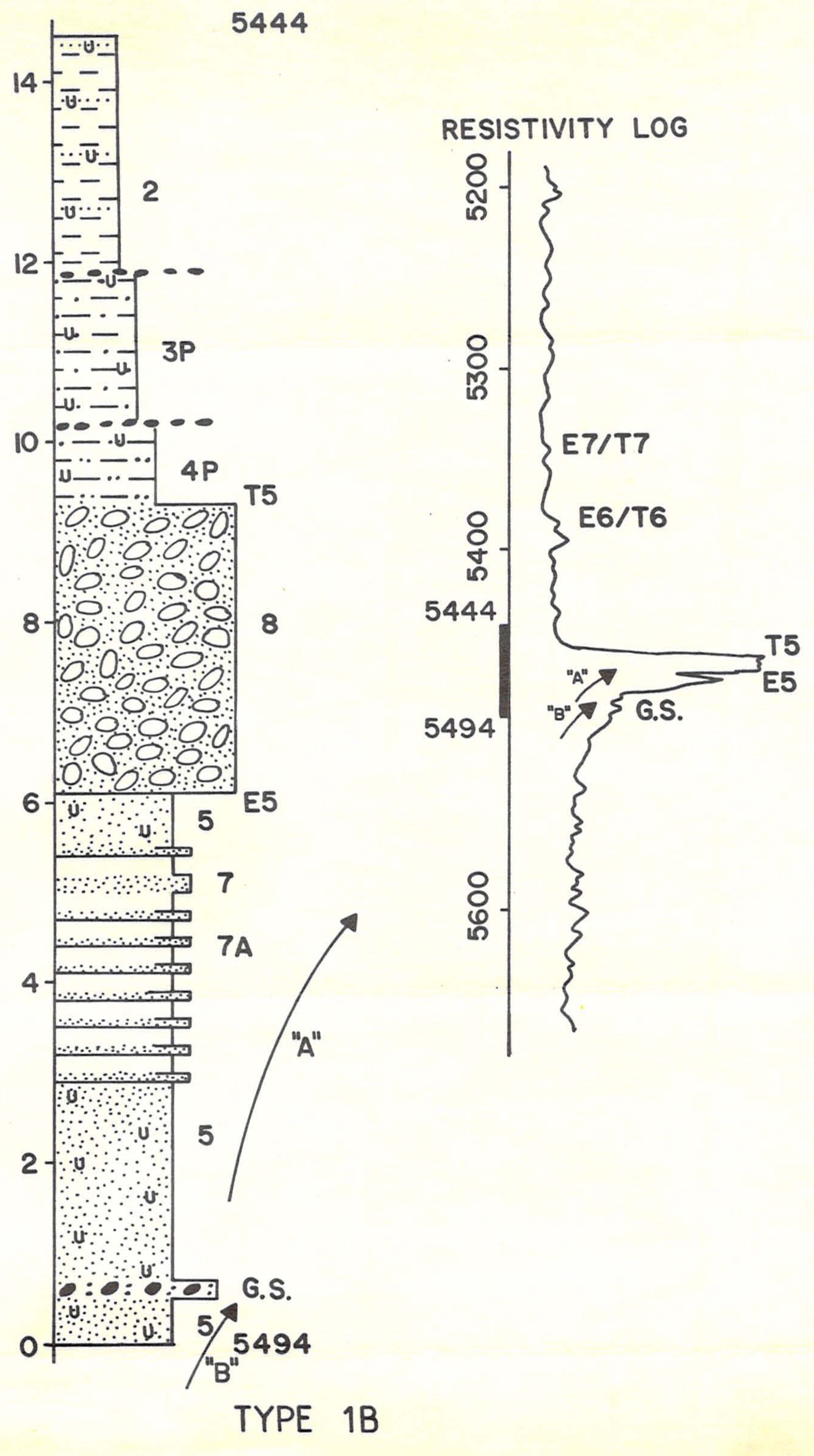

TYPE 1B

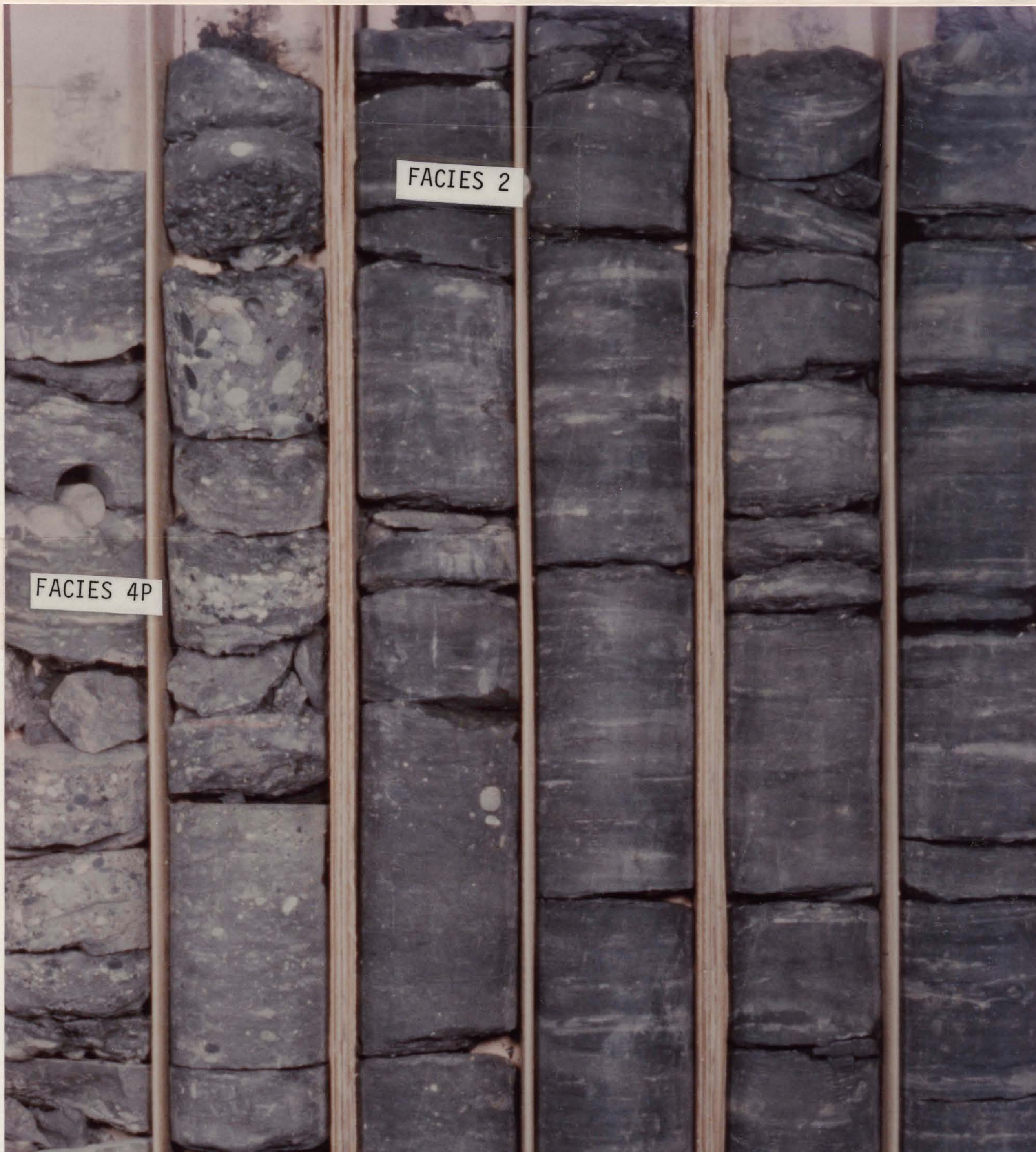
FACIES 2
FACIES 4P
FACIES 3P
10-16-51-11
5442

Fig. 3.16. Facies Sequence Type 1B -- Type well 12-16-51-11. See descriptions in text. Vertical scale on the litholog is in metres. The facies numbers are shown on the right hand side of the litholog. The position of the E5 and T5 surfaces in the core are shown. The vertical scale on the resistivity log is in feet. The positons of the the cored interval is shown by a solid balck on the resistivity log, and the depth of the cored interval is given. The positions of the E/T surfaces on the log are shown on the right hand side of the resistivity log. G.S. indicates the position of the Gritty Siderite on both logs. The "A" and "B" sequences of the Raven River Member are shown on both the litholog and resistivity log. Core box photos of this sequence type are shown in Fig. 3.17.

Fig. 3.17. The core of well 12-16-51-11 is representative of Type 1B sequence. The next four pages show core photographs of well 12-16-51-11. The corresponding litholog and resistivity log are shown in Fig. 3.16. Core depths are all given in feet; the bottom of the core is in the lower left and the top in the upper right. Coarsening upward sequence "b" begins below 5494 ft. and continues to the gritty siderite. The sequence begins with facies 5 above the gritty siderite and coarsens upwards into hummocky cross stratified and wave rippled sandstones of facies 7A. This well differs from Fig. 3.15 in that only one sand is developed. The conglomerates (facies 8) rest abruptly on bioturbated sandstones (facies 5), separating the two sand (facies 7 and 7A) sequences. The conglomerates pass vertically upwards into facies 4P and 3P. Each of these facies is capped by pebbles. The bioturbated mudstones are overlain by the "laminated blanket" (facies 2).

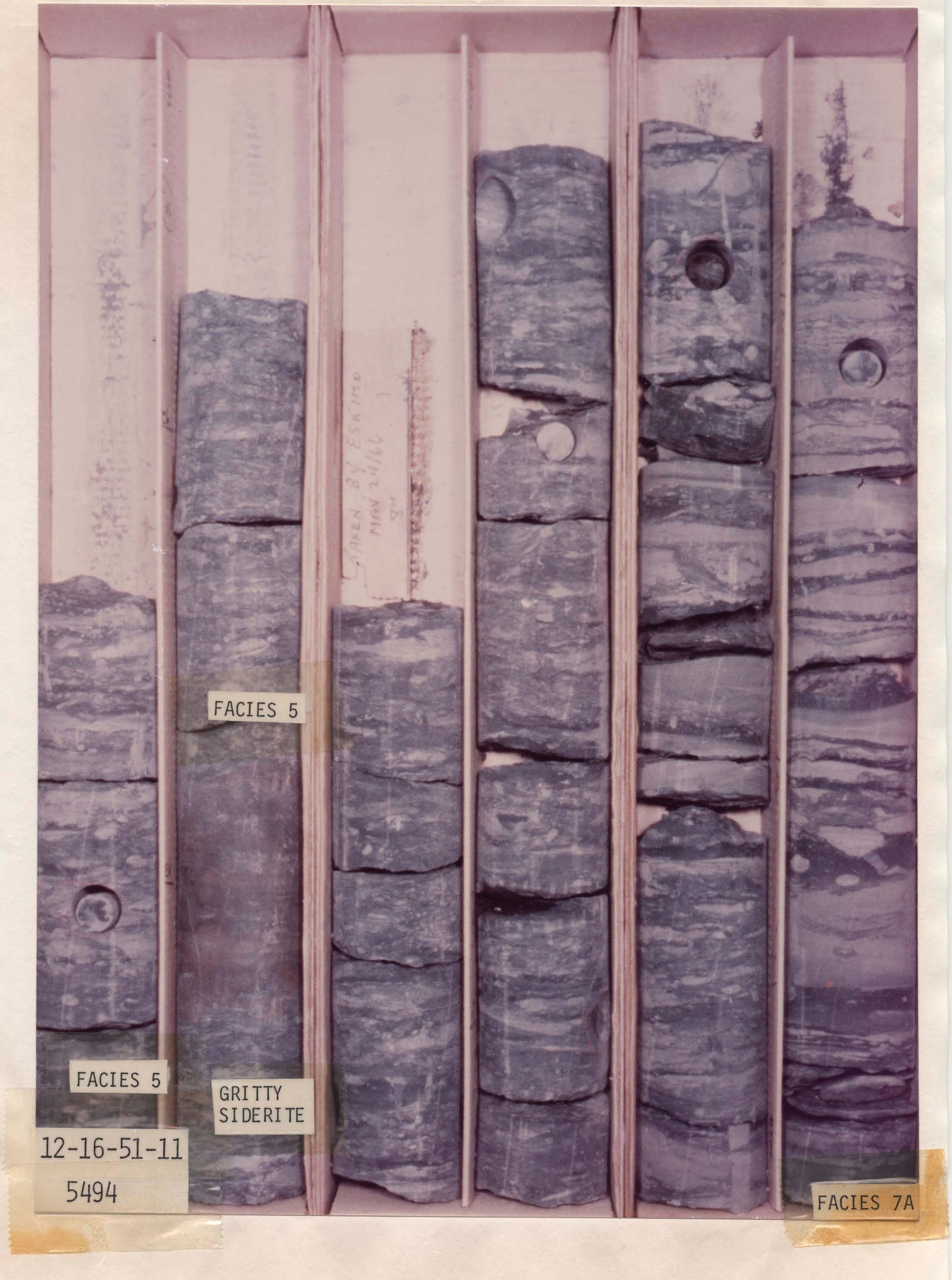
FACIES 5
FACIES 5
GRITTY SIDERITE
12-16-51-11
5494
FACIES 7A


CONGLOMERATE
CONTACT
12-16-51-11
5479

12-16-51-11

5464


FACIES 2
12-16-51-11
5449

TYPE 2 (Figs. 3.18 to 3.21): Facies sequences of this type are characterized by an abrupt truncation of the coarsening upward "a" and "b" sequences of the Raven River Member, by the erosion surface E5. The Carrot Creek Member in these wells has a characteristic blocky gamma ray and induction log signature. In core, these wells are characterized by thick (up to 19 m) clast supported conglomerates (facies 8). Above these thick gravels, facies 3P, 4P, and 5P may be locally developed. These wells may be subdivided into two types reflecting the depth of erosion of the E5 surface. TYPE 2A (Figs. 3.18 and 3.19) represents a thick conglomerate (blocky log response) resting on bioturbated sandstones and siltstones (facies 4 or 5) of the "a" sequence. TYPE 2B (Figs. 3.20 and 3.21) represents a thick conglomerate accumulation resting on the bioturbated sandstones and siltstone (facies 3, 4, or 5) of the "b" sequence.

TYPE 3 (Figs. 3.22 to 3.25): In these facies sequences, erosion surface E5 truncates the coarsening upward "a" and "b" sequences of the Raven River Member. These facies sequences differ from Type 2 facies sequences in the thickness of preservation of the Carrot Creek Member, which here is only a thin gravel veneer. The log response of the Carrot Creek Member is <u>not</u> blocky. Above this gravel veneer, facies 3P, 4P, and 5P are locally developed depending on the depth of erosion. They show a fining

Fig. 3.18. Facies Sequence Type 2A -- Type well 6-31-53-13. See descriptions in text. Vertical scale on the litholog is in metres. The facies numbers are shown on the right hand side of the litholog. The positions of the E5 and T5 surfaces in the core are shown. The vertical scale on the resistivity log is in metres. The positon of the the cored interval is shown by a solid balck on the resistivity log, and the depth of the cored interval is given. The positions of the E/T surfaces on the log are shown on the right hand side of the resistivity log. G.S. indicates the position of the Gritty Siderite on the resistivity log. The "A" sequence of the Raven River Member is shown for the litholog. The "A" and "B" sequences of the Raven River Member are shown on the resistivity log.

6-31-53-13

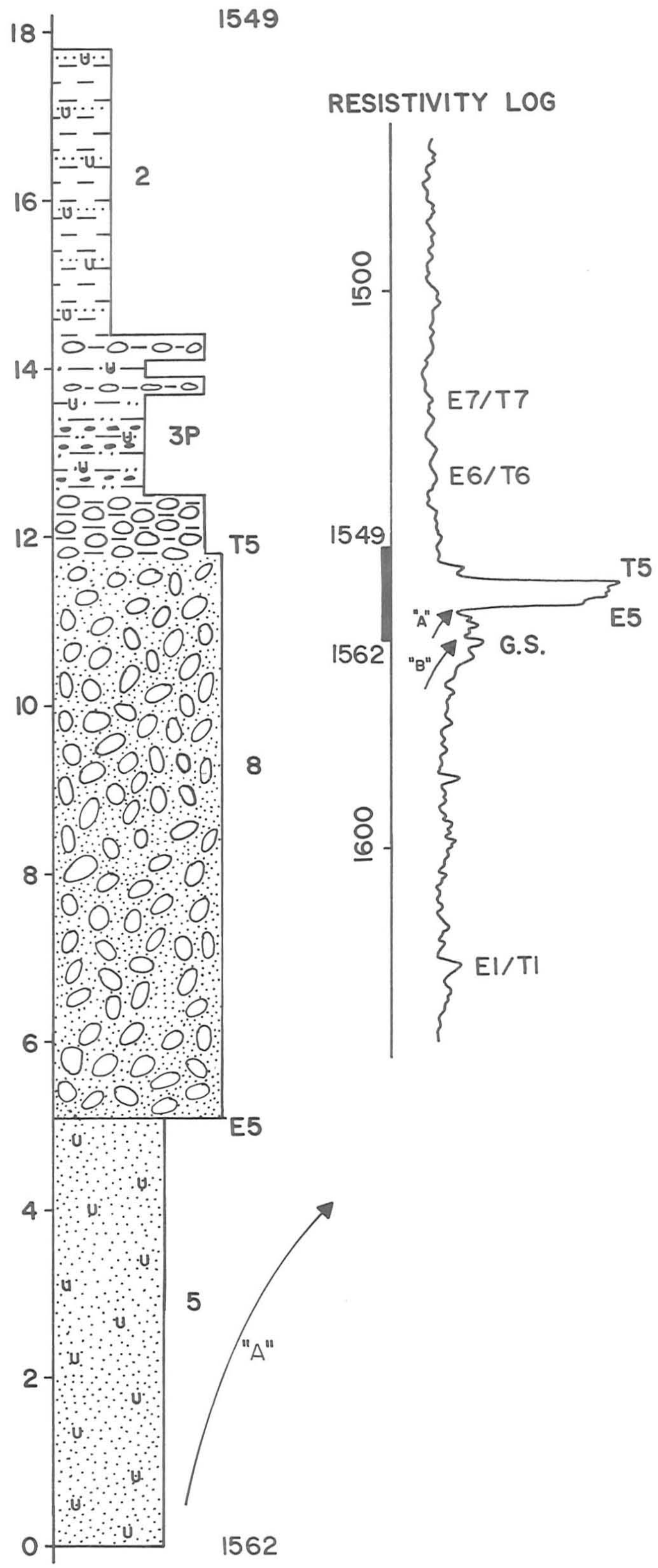

TYPE 2A

Fig. 3.19. The core of well 6-31-53-13 is representative of the Type 2A sequence. The next four pages show core photographs of well 6-31-53-13. The corresponding litholog and resistivity log are shown in Fig. 3.18. Core depths are all given in metres.; bottom of the core is in the lower left and the top in the upper right. Coarsening upward sequence "b" was not cored in this well. Its presence and the presence of the gritty siderite were recognized on the well logs and are labelled in Fig. 3.18. Coarsening upward sequence "a" begins below 1562 m. The conglomerate (facies 8) overlies facies 5 of the "a" sequence. There is no good development of facies 7 or 7A (hummocky cross stratified sandstones) in these sequence types. The conglomerate is about 7 m thick in this well and passes vertically upwards into bioturbated mudstones of facies 4P, capped by pebbles. The "laminated blanket" (facies 2) overlies the bioturbated mudstones.


FACIES 5
6-31-53-13
1562


CONGLOMERATE
CONTACT
6-31-53-13
1558


6-31-53-13
1554


FACIES 2
FACIES 4P
6-31-53-13
1551

Fig. 3.20. Facies Sequence Type 2B -- Type well 3-23-51-10. See descriptions in text. Vertical scale on the litholog is in metres. The facies numbers are shown on the right hand side of the litholog. The positions of the E5 and T5 surfaces in the core are shown. The vertical scale on the resistivity log is in metres. The position of the the cored interval is shown by a solid black on the resistivity log, and the depth of the cored interval is given. The positions of the E/T surfaces on the log are shown on the right hand side of the resistivity log. The "B" sequence of the Raven River Member is shown for both logs.

3-23-51-10

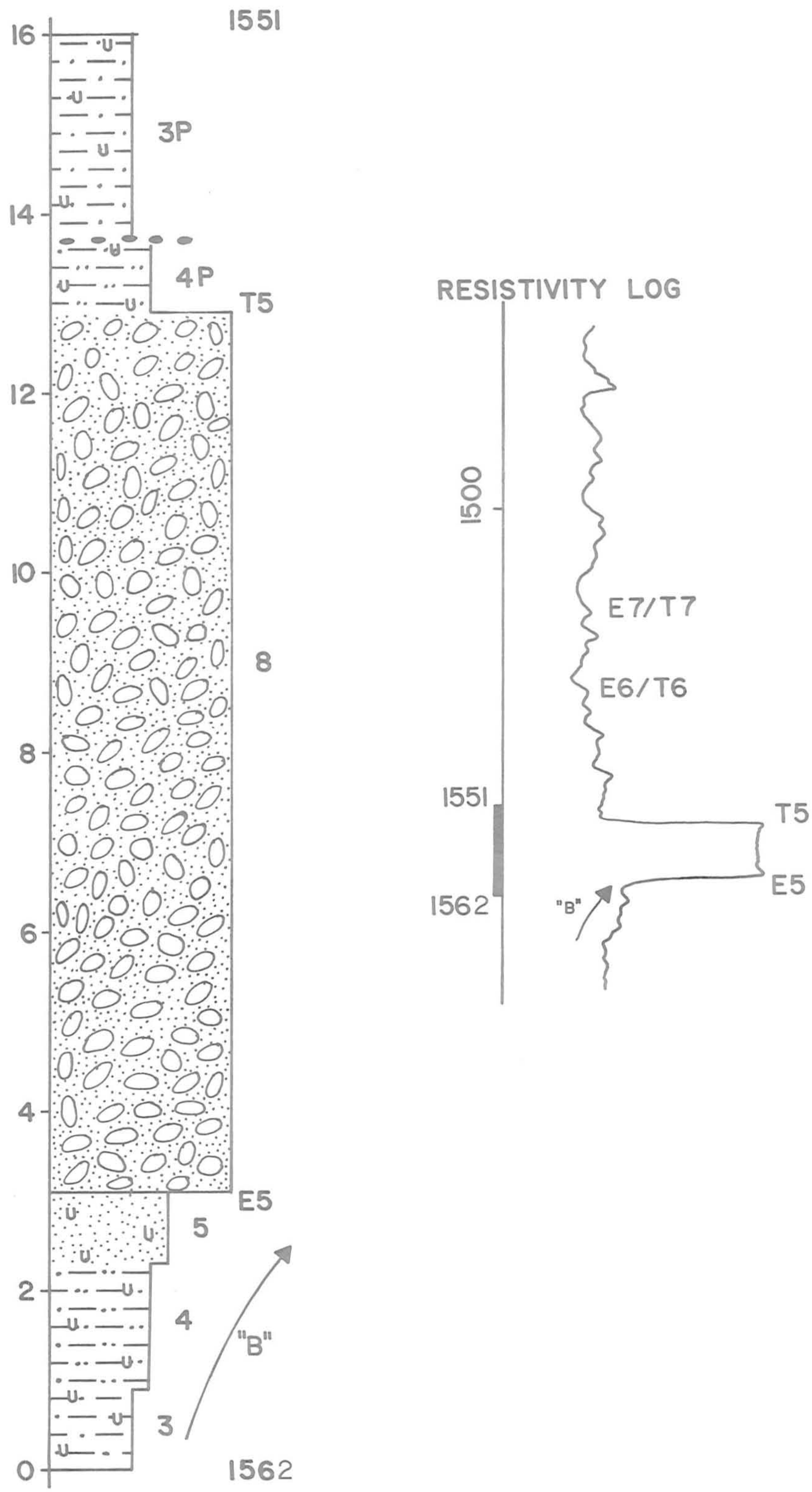

TYPE 2B

Fig. 3.21. The core of well 3-23-51-10 is representative of the Type 2B sequence. The next three pages show core photographs of well 3-23-51-10. The corresponding litholog and resistivity log are shown in Fig. 3.20. Core depths are all given in metres; the bottom of the core is in the lower left and the top in the upper right. Coarsening upward sequence begins below 1562 m with bioturbated dark mudstones of facies 3 and continues upward into the bioturbated sandstones of facies 5. The conglomerates (facies 8) rest abruptly on the bioturbated sandstones (facies 5) of the "b" sequence. There is no preservation of the gritty siderite and the overlying "a" sequence. The conglomerates in this well are about 10 m thick, and are overlain by the bioturbated mudstones of facies 4P and 3P. The "laminated blanket" (facies 2) was not cored in this well but is believed to overlie the bioturbated mudstones facies.


FACIES 4
CONGLOMERATE
CONTACT
FACIES 5
FACIES 3
3-23-51-10
1562


3-23-51-10
1557


FACIES 4P
3-23-51-10
1554
FACIES 3P

upward sequence from the bioturbated sandstones with pebbles (facies 5P) through to the dark bioturbated mudstone with pebbles (facies 3P). Each of these facies is capped by a pebbly mudstone (facies 8B, described in Chapter 6). TYPE 3 facies sequences may be subdivided on the basis of the depth of erosion on the E5 surface. TYPE 3A (Figs. 3.22 and 3.23) wells represent sequences where the E5 surface is contained in the bioturbated sandstones and siltstones (facies 4 or 5) of the "a" sequence. TYPE 3B (Figs. 3.24 and 3.25) wells are those where the erosion surface rests on the bioturbated sandstones, siltstones, and mudstones (facies 3, 4, and 5) of the "b" sequence.

3.4 CONGLOMERATE CONTACT

The lower contact of the Carrot Creek Member with the underlying Raven River may be sharp or bioturbated. The nature of the contact depends on the depth of erosion into the underlying Raven River Member. In all three types of facies sequences, the conglomerate contact, in any one well, does not necessarily suggest the presence of a major erosion surface. In many cases the contacts do not suggest erosion; they are often bioturbated. The erosion is determined from regional considerations, and the contacts have to be interpreted in this light, not vice versa. This will be illustrated in Chapter 4.

When the conglomerates rest on the non-bioturbated sandstones (facies 7), as in TYPE 1 (Fig. 3.26) facies

Fig. 3.22. Facies Sequence Type 3A -- Type well 14-10-53-13. See descriptions in text. Vertical scale on the litholog is in metres. The facies numbers are shown on the right hand side of the litholog. The positions of the E5 and T5 surfaces in the core are shown. The vertical scale on the resistivity log is in metres. The positon of the the cored interval is shown by a solid balck on the resistivity log, and the depth of the cored interval is given. The positions of the E/T surfaces on the log are shown on the right hand side of the resistivity log. G.S. on the resistivity log shows the inferred position of the Gritty Siderite horizon. This horizon was not found in the core. The position of the "A" and "B" sequences of the Raven River Member are shown on both logs.

14-10-53-13

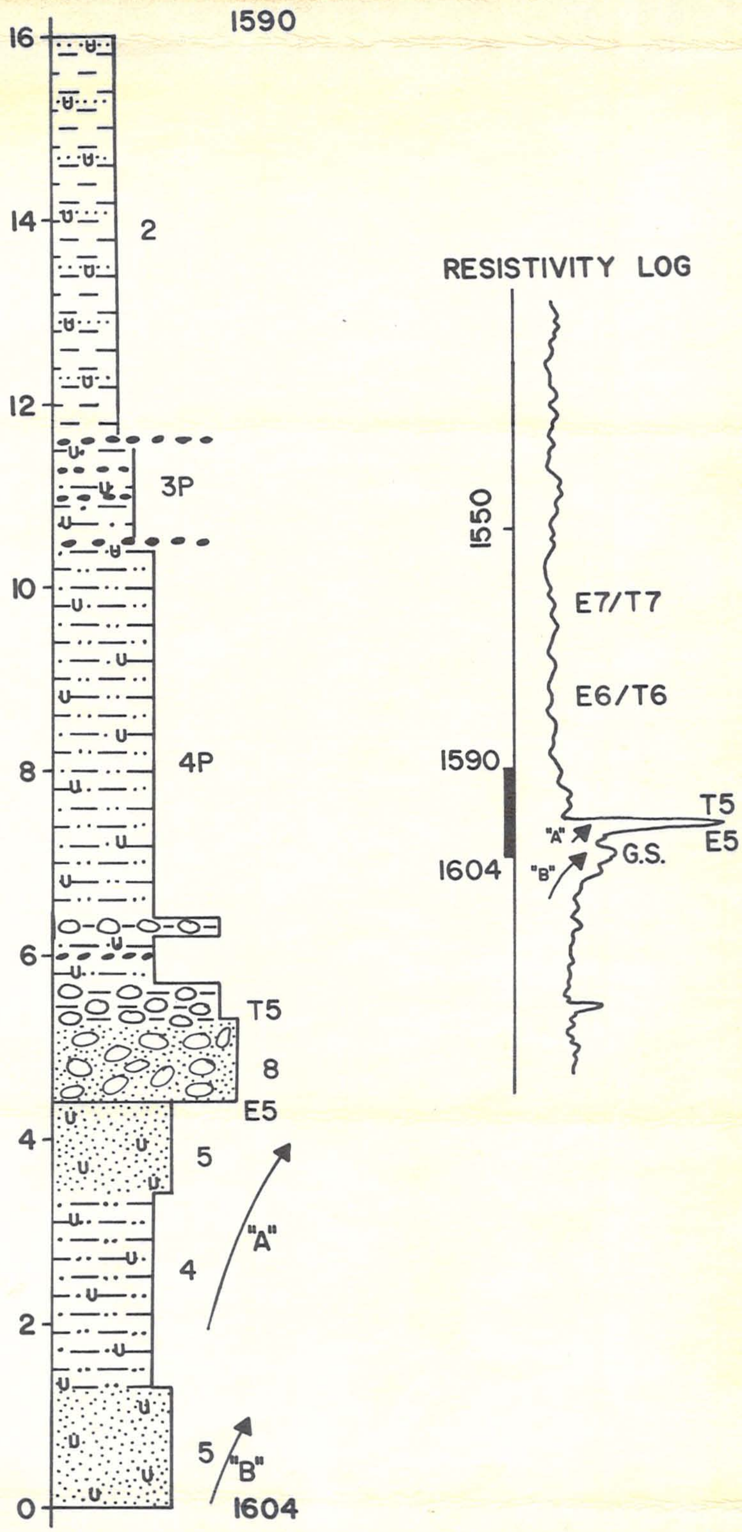

TYPE 3A

Fig. 3.23. The core of well 14-10-53-13 is representative of the sequence type 3A. The next four pages show core photographs of well 14-10-53-13. The corresponding litholog and resistivity log are shown in Fig. 3.22. Core depths are all given in metres; the bottom of the core is in the lower left and the top in the upper right. Coarsening upward sequence "b" begins below 1604 m, and ends in facies 5. The gritty siderite horizon was not observed at the top of the "b" sequence in this well. The "a" coarsening upward sequence begins with facies 4 and continues up to facies 5. The bioturbated mudstones (facies 5) of the "a" sequence are abruptly overlain by conglomerate (facies 8). There is no good development of hummocky cross stratified and wave rippled sandstones (facies 7 and 7A). The thickness of the conglomerate is less than 1 m. The conglomerates pass vertically upwards into bioturbated mudstones of facies 4P and 3P, both facies are capped by pebbles. The "laminated blanket" (facies 2) overlies the bioturbated mudstones.

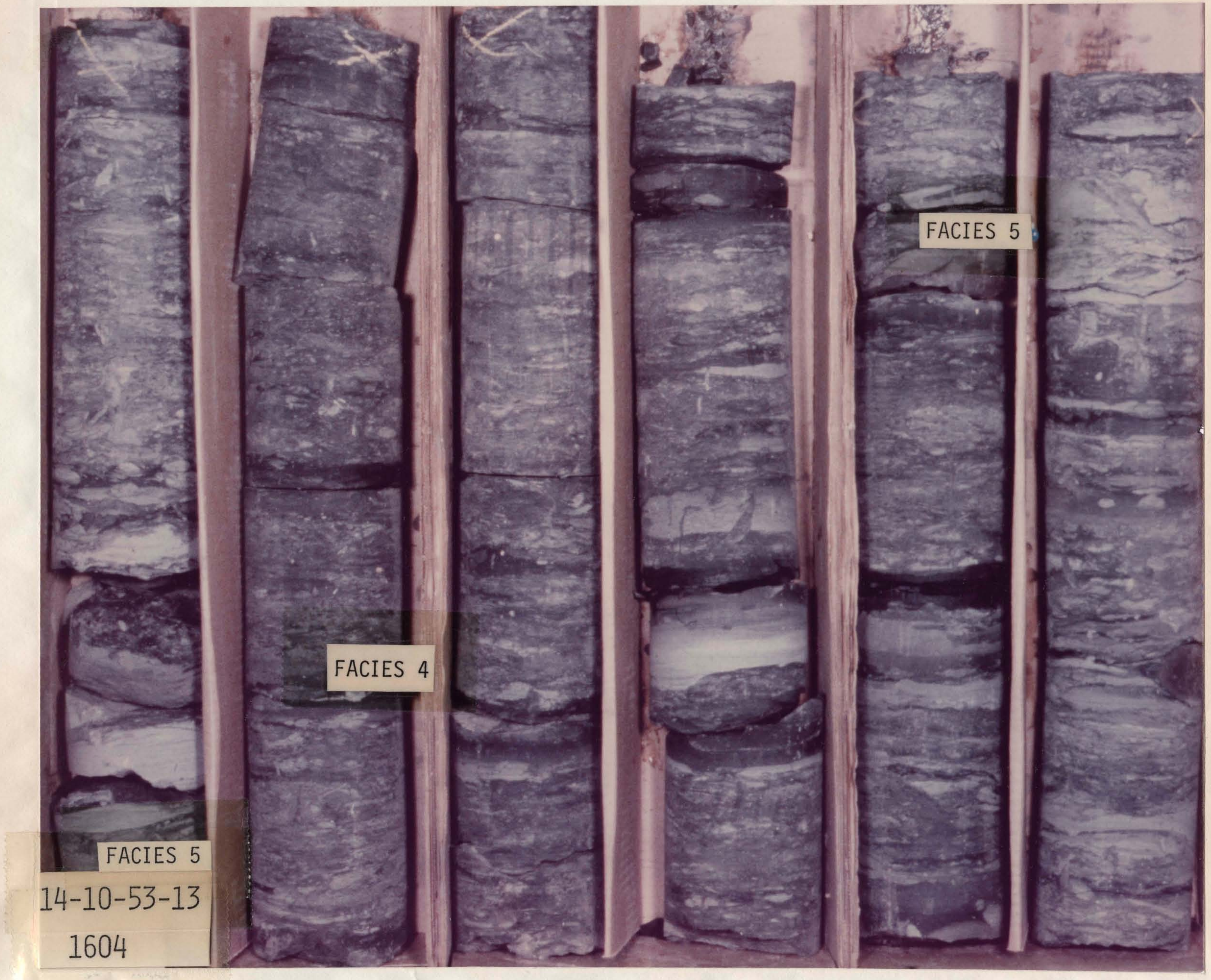
FACIES 5
FACIES 4
FACIES 5
14-10-53-13
1604

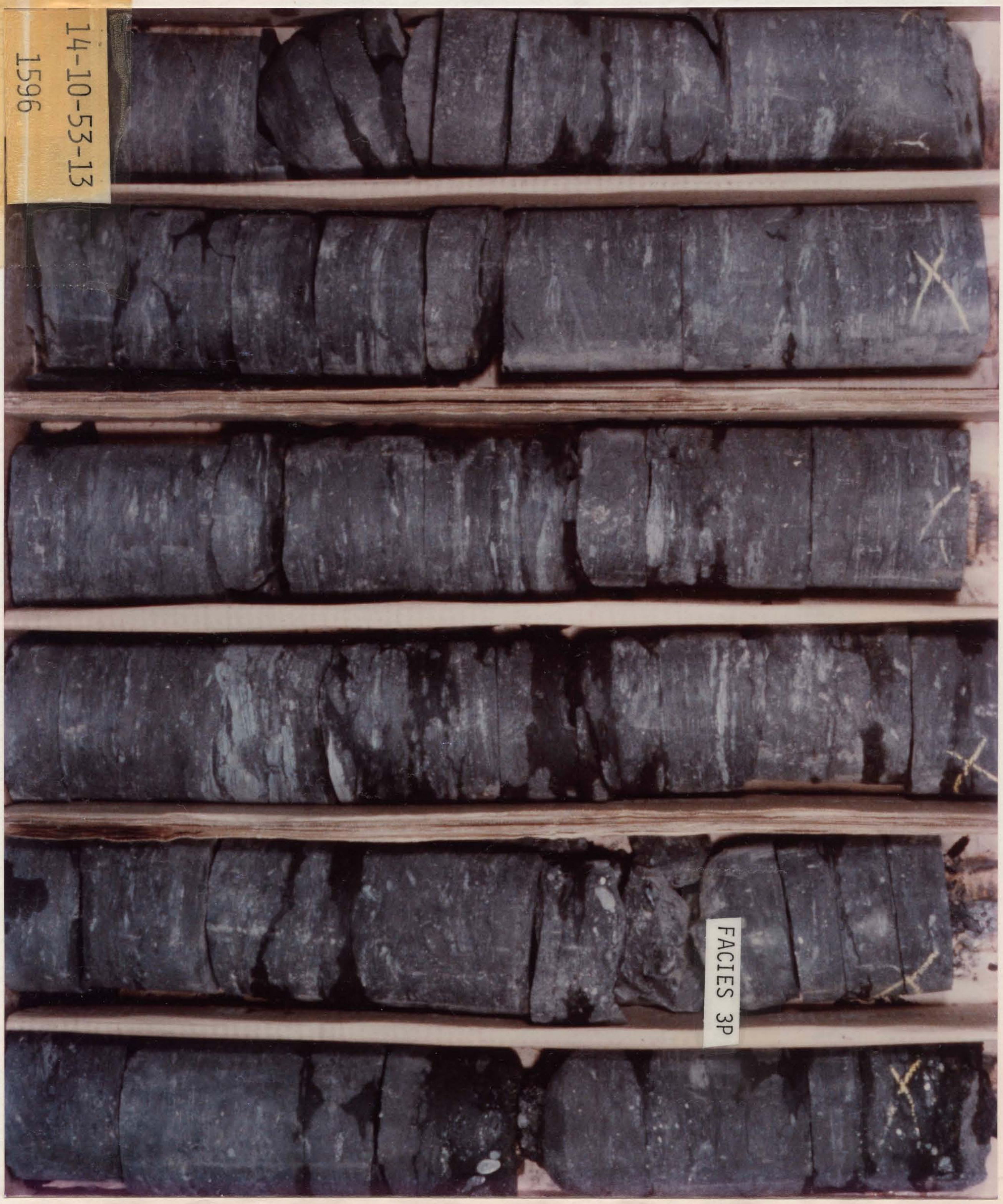
14-10-53-13
1596
FACIES 3P

14-10-53-13
1593
FACIES 2

Fig. 3.24. Facies Sequence Type 3B -- Type well 7-29-51-9. See descriptions in text. Vertical scale on the litholog is in metres. The facies numbers are shown on the right hand side of the litholog. The positions of the E5 and T5 surfaces in the core are shown. The vertical scale on the resistivity log is in feet. The positon of the the cored interval is shown by a solid balck on the resistivity log, and the depth of the cored interval is given. The positions of the E/T surfaces on the log are shown on the right hand side of the resistivity log. The position of the "B" sequence of the Raven River Member is shown on both logs.

7-29-51-9

4700

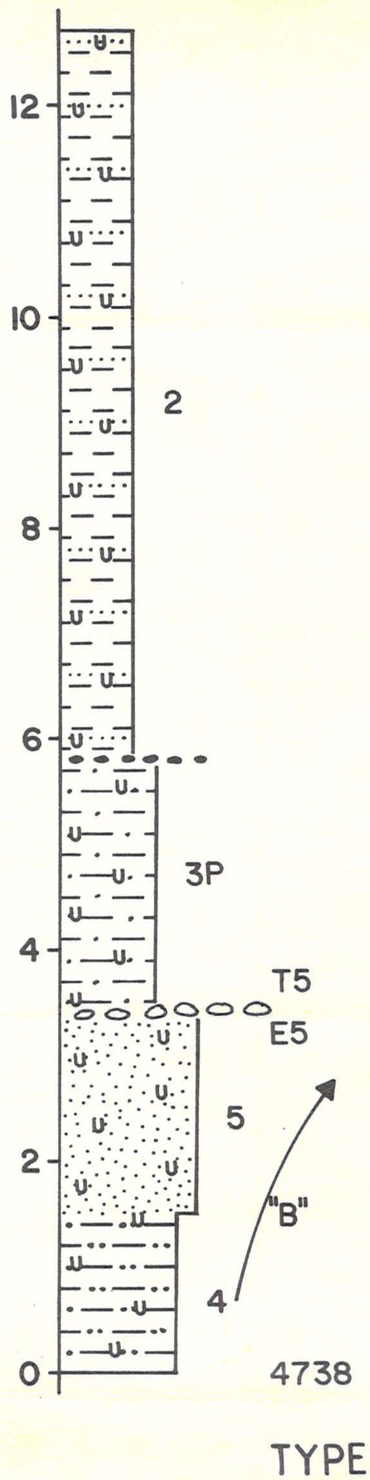

RESISTIVITY LOG

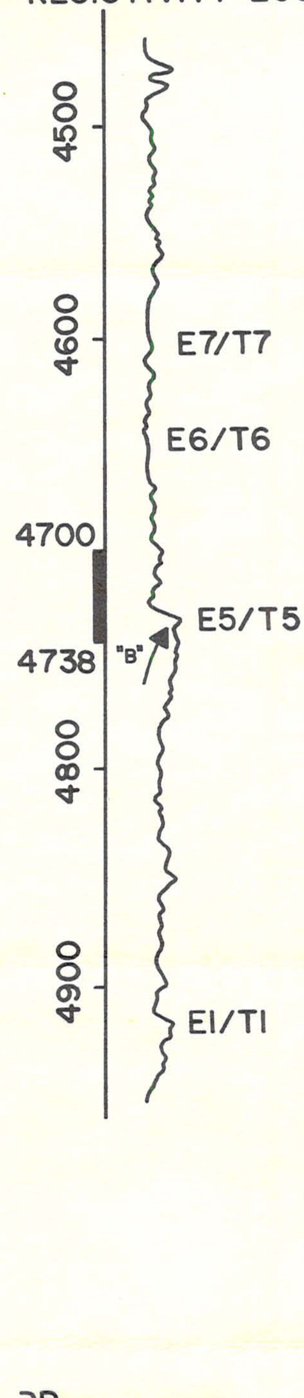

TYPE 3B

Fig. 3.25. The core of well 7-29-51-9 is representative of the sequence Type 3B. The next two pages show core photographs of well 7-29-51-9. The corresponding litholog and resistivity log are shown in Fig. 3.24. Core depths are all given in feet; the bottom of the core is in the lower left and thop in the upper right. Coarsening upward sequence "b" begins below 4738 ft and continues up through facies 4 and facies 5. The conglomerate (facies 8) is found on top of facies 5 of the "b" sequence. The conglomerate thickness in this well is a veneer overlain by the bioturbated mudstone facies 3P. The "laminated blanket" (facies 2) overlies the bioturbated mudstone facies.

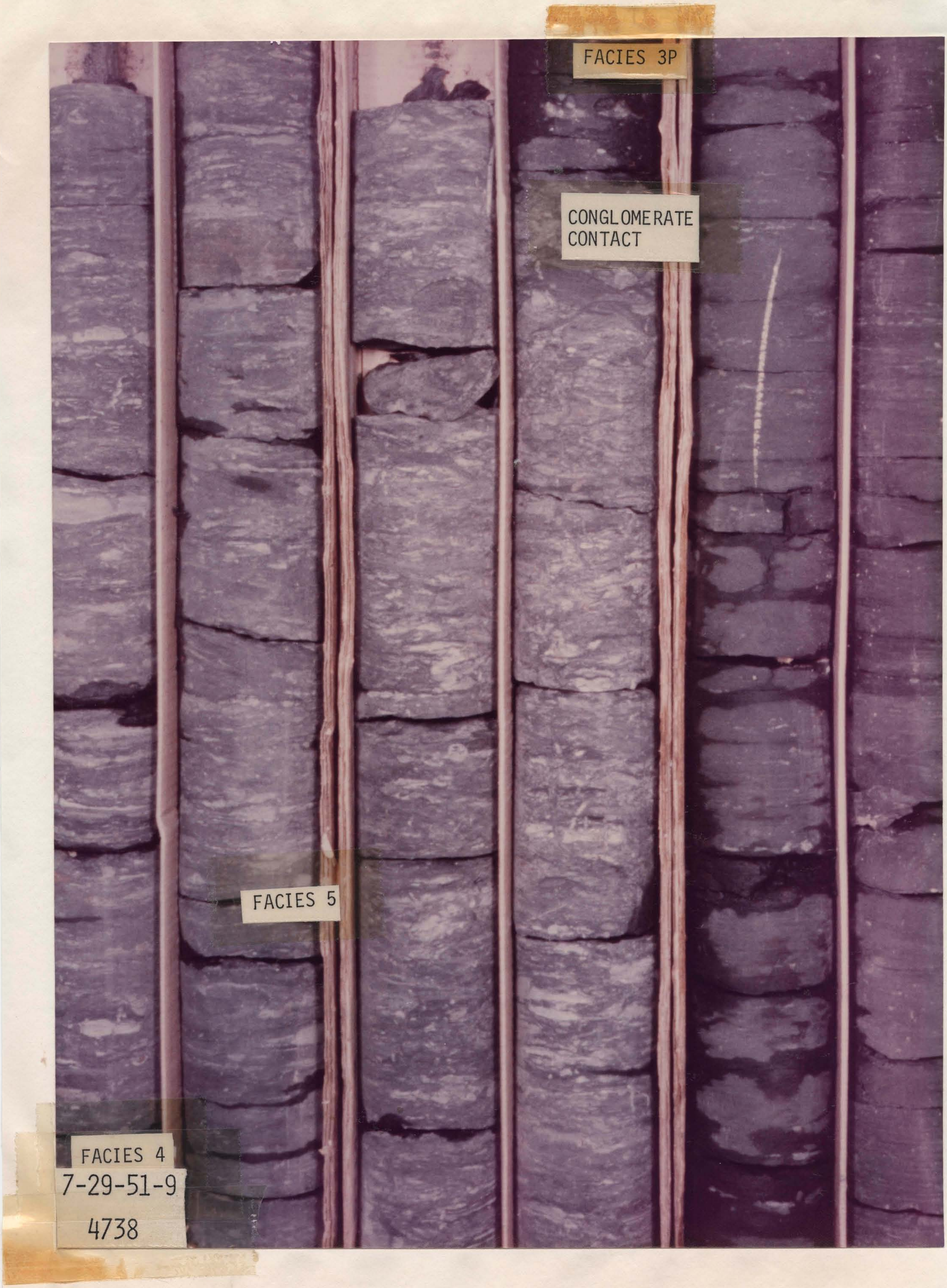
FACIES 3P
CONGLOMERATE CONTACT
FACIES 5
FACIES 4
7-29-51-9
4738

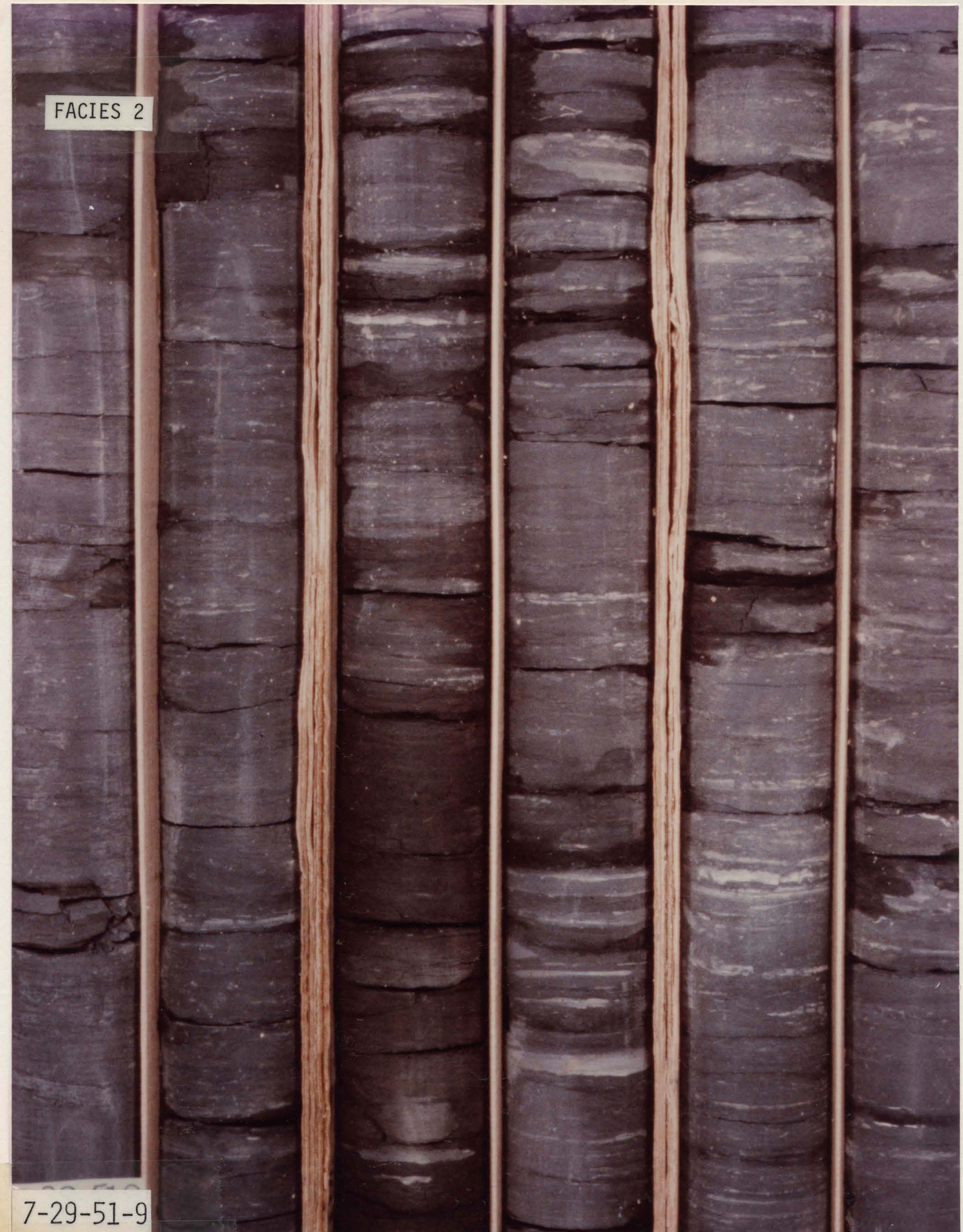
FACIES 2
7-29-51-9
4723
4723

sequences, the contact is generally sharp. In some wells the contact is loaded (eg., 2-29-52-13) with dewatering pipes between the loads.

In TYPE 2 (Fig. 3.27) facies sequences, where the conglomerate rests on the bioturbated facies of the Raven River Member, the contact is generally bioturbated. The contact appears to have been sharp initially, as in well 3-23-51-10, with the apparently diffuse nature of the contact being due to subsequent reworking of the pebbles downward by organisms. In many cases there are small chert grains found in the burrow forms. S. Vossler (M.Sc. thesis in progress, pers. comm.) suggested that the dominant burrow form was Thalassinoides, and that such burrows are associated with development of a Glossifungites ichnofacies, indicating a firm ground setting. This ichnofacies is indicative of burrowing in semiconsolidated but unlithified sediments, and is developed in marginal to open marine environments. Thalassinoides burrows have been documented along disconformities associated with erosion surfaces.

In other wells pebbles interbedded with mudstones (sub-facies 8A, described in Chapter 6) initiate the conglomerate sequence, and some of the pebbles may be bioturbated into the mud associated with this facies (eg., well 6-31-53-13). This would suggest that the E5 surface is below the first chert pebble, and that this is a mud on mud contact. If this were so, it makes picking the E5 surface

Fig. 3.26. Conglomerate Contact -- Type 1.

These photos show the nature of the conglomerate contact associated with Type 1 wells. A) Photo is taken from well 2-29-52-13, 5416 ft. Notice the loading and dewatering pipes associated with the conglomerate contact. Scale bar is 3 cm. B) Photo is taken from well 10-21-52-13, 5396 ft. Notice the sharp contact with the underlying sands (facies 7A). Core is 3 in. wide. C) Photo is taken from well 12-16-51-11, 5474 ft. Notice the sharp contact of the conglomerate on the underlying bioturbated sandstone (facies 5). Scale bar is 3 cm. D) Photo is taken from well 13-5-51-11, 5644 ft. The conglomerate contact with the underlying sediments is sharp. Scale bar is in cm.

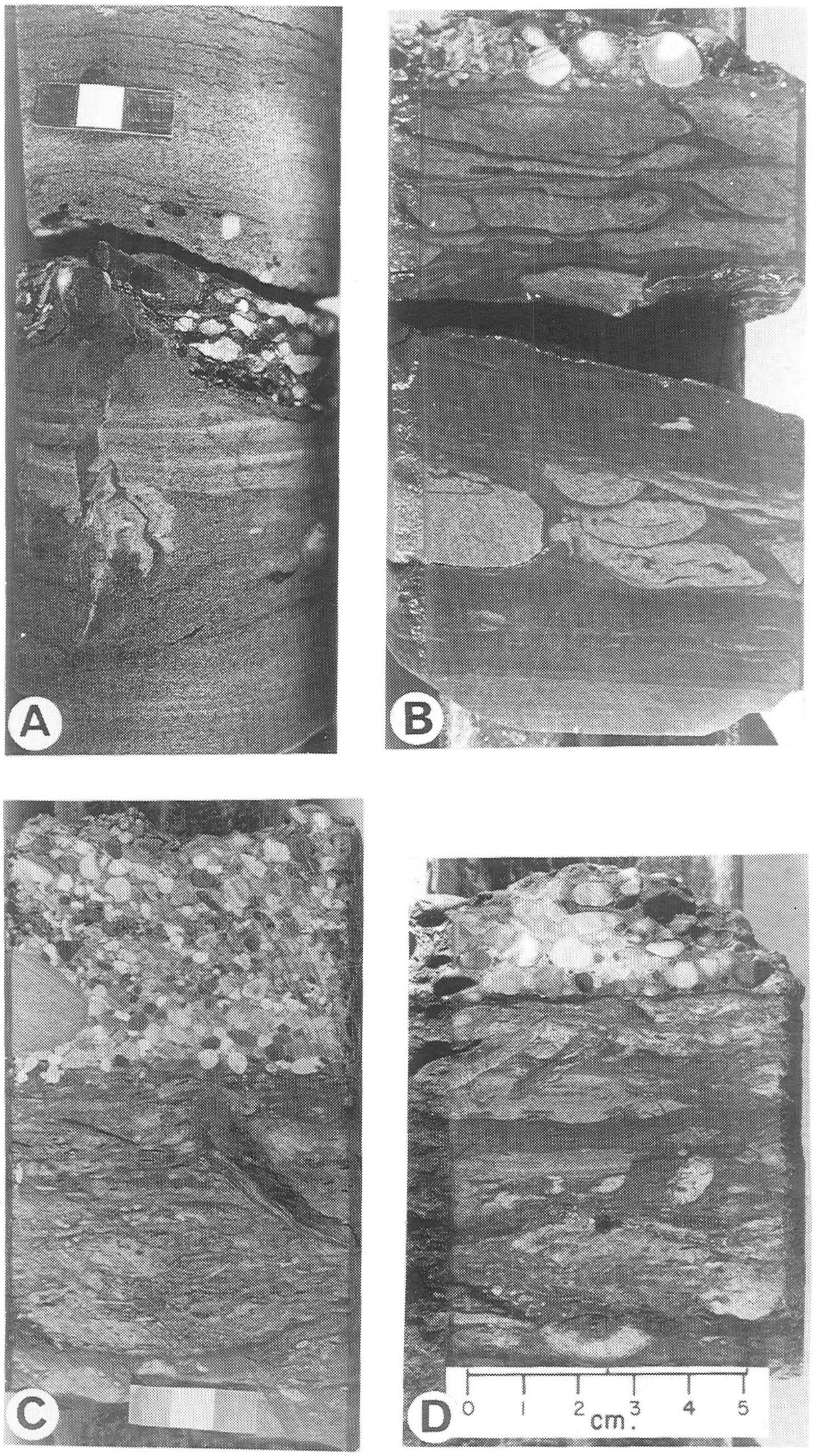
A
B
C
D
0 1 2 3 4 5
cm.

Fig. 3.27. Conglomerate Contact -- Type 2.

These photos show the nature of the conglomerate contact associated with Type 2 wells. Scale bar is 3 cm. A) Photo is taken from well 6-31-53-13, 1561 m. The contact of the conglomerate with the underlying mudstones appears gradational in this well. B) Photo is taken from well 4-13-51-11, 1638 m. Notice the pebble filled burrows underneath the sharp conglomerate contact. C) Photo is taken from well 3-23-51-10, 1561 m. Notice the circular cluster (presumably bioturbated down) underneath the sharp conglomerate contact. The mudstones directly below the contact are sideritized. D) Photo is taken from well 5-3-51-9, 1471 m. The conglomerate contact appears to be bioturbated in this well. Notice the pebble filled, diagonal burrow extending downwards from the conglomerate contact.

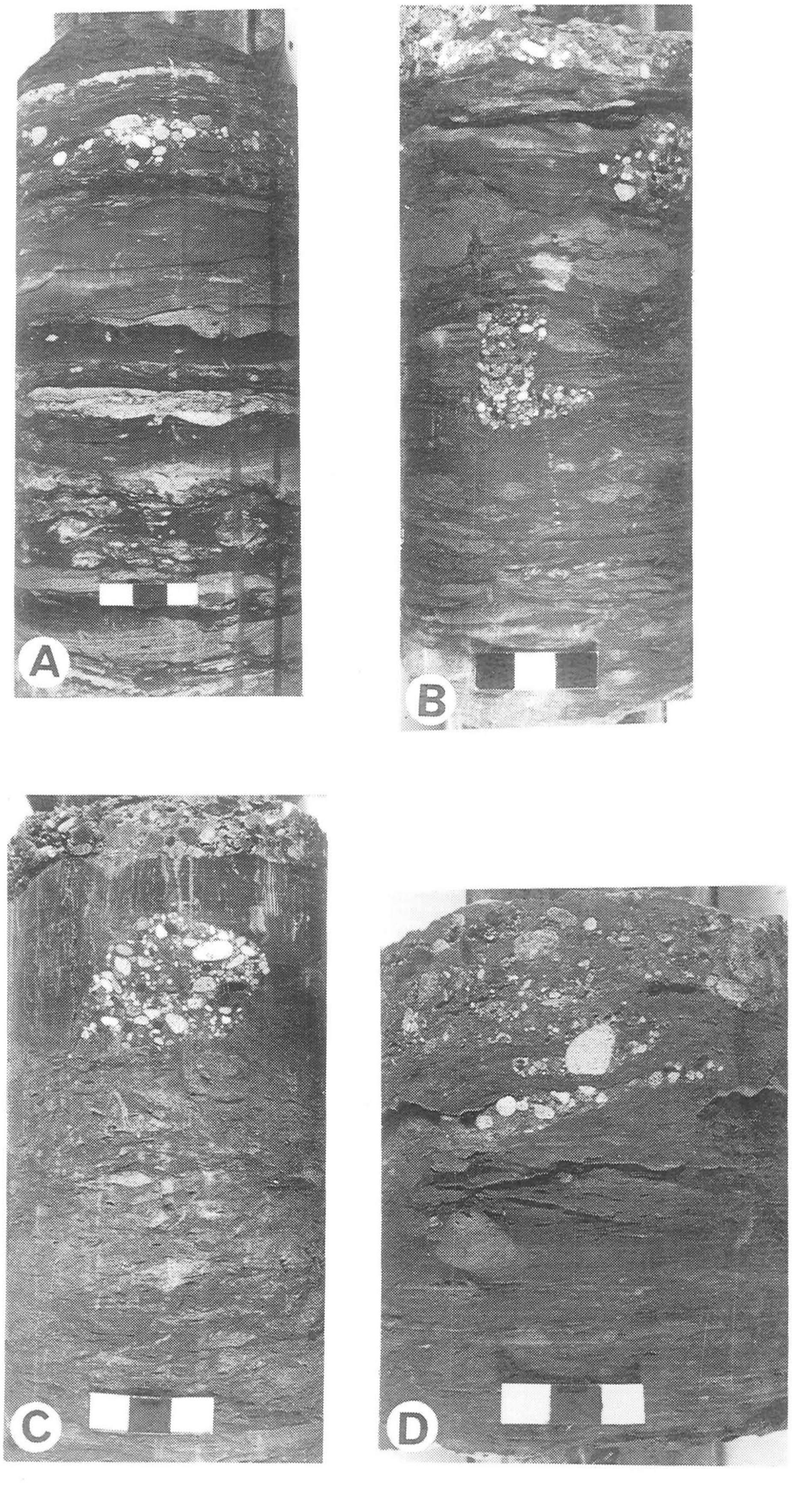
A
B
C
D

Fig. 3.28. Conglomerate Contact -- Type 3.

These photos show the nature of the conglomerate contact associated with Type 3 wells. Scale bar is 3 cm. A) Photo is taken from well 14-10-53-13, 1601 m. In this well the conglomerate contact with the underlying shelf mudstones is sharp. B) Photo is taken from well 2-36-53-13, 4915 ft. The conglomerate contact appears to be more gradational in appearance in this well. The Zoophycos burrow directly beneath the conglomerate is probably not responsible for the burrowing associated with the conglomerate contact, but was formed during previous deposition of the bioturbated sandstones. C) Photo is taken from well 7-29-51-9, 4729 ft. The conglomerate contact appears to be more gradational in this well. D) Photo is taken from well 10-23-51-10, 5011 ft. The conglomerate contact appears to be more gradational in this well.

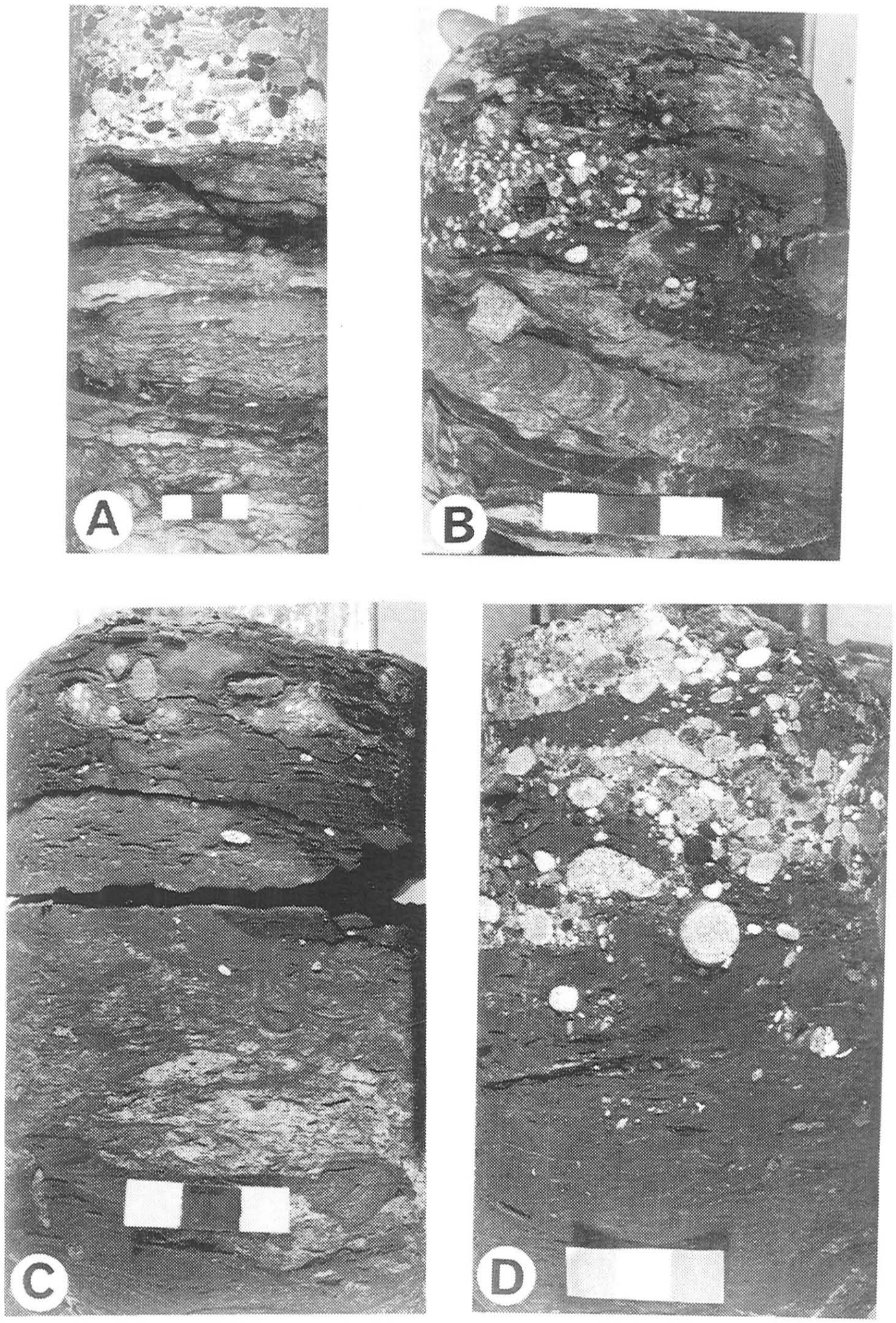
A
B
C
D

difficult. Generally, the mud associated with the conglomerates is very black and not as heavily bioturbated as the underlying bioturbated facies of the Raven River Member. In these cases the contact is picked at this change in mudstones associated with the incoming of the chert pebbles.

TYPE 3 (Fig. 3.28) wells preserve only a thin veneer of gravel on the E5 surface. The contact is similar to that of TYPE 2 wells. Generally, the E5 surface is marked by the incoming of pebbles truncating the top of the progressive coarsening upward sequence, and the decrease in the amount of sand and bioturbation present in the mudstones associated with the conglomerates.

CHAPTER 4 -- MORPHOLOGY OF THE E5 SURFACE

4.1 INTRODUCTION

The presence of a major erosion surface (E5 of Plint et al., 1986) will be established from cross sections, both log and core, in this chapter. The morphology of this surface will be illustrated using mesh diagrams generated from an isopach map of the E5 surface. It will be shown that the location and geometry of the conglomerate bodies are directly controlled by the morphology of the E5 surface.

The morphology of the E5 surface has been discussed by Bergman and Walker (1986) for the Carrot Creek field (T. 51-53, R. 11-14). The presence of the major erosion surface (E5 of Plint et al., 1986) was demonstrated, resulting in the recognition of three areally distinct regions within the study area. The TERRACE, located in the western area, is a broad, undulating, expanse characterized by Type 1A wells. The BEVEL is a narrow belt located along the edge of the terrace, where hummocky cross stratified sandstones of facies 7 are truncated. It is characterized primarily by Type 1B wells, although wells of Type 2A may be present depending on the depth of erosion. The BUMPS and HOLLOWS located basinwards (northeastwards) of the bevel represent a remnant erosional topography. They are long and narrow, and trend slightly obliquely to the bevel. The well type varies according to the depth of erosion. The maximum erosional relief on the bumps and hollows is about 20 m.

Expansion of the study area (Bergman, 1986; Bergman and Walker, in press) to include T.50-56, R.9-14, has revealed one more topographic area not recognized by Bergman and Walker (1986). Basinwards of the Bumps and Hollows the topography gradually fades away into a relatively "flat" surface, the BASIN PLAIN.

4.2 CORRELATIONS

Log and core cross-sections were constructed both parallel and normal to the trend of the conglomerate bodies. Four of these sections (located in Figs. 4.1, 4.6 and 4.10), incorporating as much core as possible, were chosen to illustrate the presence of a major erosion surface (E5), the two dimensional geomtry of the conglomerate bodies, and the vertical and lateral facies relationships.

Log markers above and below the Carrot Creek Member were easily recognized and correlated, particularly the upper datum (E7/T7), and the lower markers E4/T4, E3/T3, and E1/T1. The gritty siderite facies, recognized in core, gives the subtle log response labelled G.S. In some wells a prominent inflection point (IN) was recognized and correlated. The base of the conglomerate marks the erosion surface E5, and is represented on the cross sections as a jagged line. The E6/T6 surface ("Cardium Zone") which has traditionally been used as datum in Cardium studies was not used for two reasons; first it becomes a difficult marker to

Figure 4.1. Map showing the location of the Carrot Creek -- Cyn-Pem conglomerate pods. The location of the cross sections discussed in this Chapter are shown.

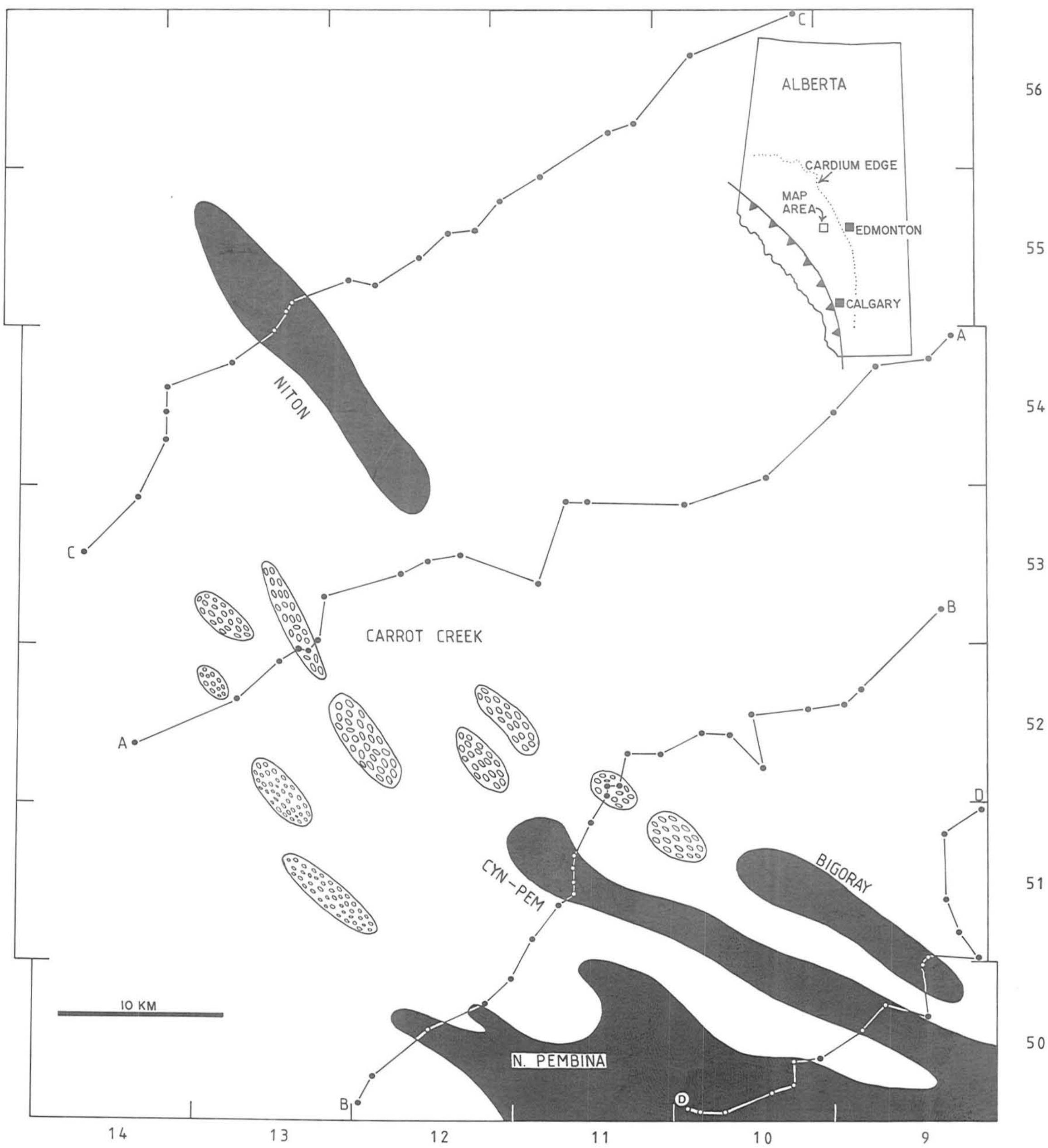
C
ALBERTA
CARDIUM EDGE
MAP AREA
EDMONTON
CALGARY
A
NITON
C
CARROT CREEK
B
A
D
BIGORAY
CYN-PEM
10 KM
N. PEMBINA
B
D
56
55
54
53
52
51
50
14
13
12
11
10
9

pick in the northeastern part of the basin and secondly, towards the northeast the surface can be shown to be erosional with about 10 m of relief (which will be discussed later).

The sections are all hung on a pair of induction peaks, the upper of which is the stratigraphic marker E7/T7, about 32 m above the top of the Carrot Creek Member. The lower stratigraphic markers E4/T4, E3/T3, and E1/T1 are sub-parallel to the upper marker (E7/T7). The E1/T1 surface is separated from the E7/T7 surface by 92 to 107 m over 4200 km^2, the entire area of study. The sand/conglomerate bodies are "boxed in" by these essentially flat and roughly parallel markers. The Cardium section thins northeastwards.

The cored interval in each well is indicated by a solid black bar. The placement of the core with respect to the various well logs was done by comparing an obvious core and log marker (eg., the top of the conglomerate). In this way the core depth was adjusted to the log depth. The core sections are presented on an expanded vertical scale compared with the well logs, in order to highlight the geometry of the sand-body and the lateral and vertical facies relationships in the sections. Detailed core cross sections may be found for each line as Foldouts 1 through 4 located in a pocket at the back of the thesis. In wells where core was not cut, but the well was essential to accurately reflect the erosional topography, the E5/T5 surfaces and gritty siderite (when present) were picked from the well logs. A hatched vertical line on the litholog indicates that the core was not cut for this part of the well and that the lithology was inferred from the well log signature.

A cartoon core section, using an expanded vertical scale is shown below the respective log cross section in order to illustrate the relative positions of the E5/T5 surfaces, the gritty siderite, and the position of the laminated blanket (facies 2). The cartoon is based on core data where available, and well logs. In wells which are not cored the markers are picked from the well logs. Both the full core sections, the cartoon core sections, and the log sections are hung on the same upper marker, the E7/T7 datum. The horizontal separation between the log traces and core sections in the cross sections does not represent true distance between the wells.

The downward curvature of the gritty siderite horizon under the thick conglomerate deposits (eg., 2-21-51-11, Cross Section B, Fig. 4.3) is believed to be the result of differential compaction. In some wells the top of the conglomerate (eg., 2-21-51-11) is higher than the projected top of the terrace and the preserved bumps. This is also believed to be the result of differential compaction of the mudstone facies relative to the thick gravel deposits.

<u>Cross</u> <u>Section</u> <u>A</u>: Fig. 4.2

This is an extension of cross section A presented by Bergman and Walker (1986, in press). The base of the conglomerate is clearly erosive, cutting out the hummocky cross stratified sandstones of the terrace and part of the "a" sequence between wells 13-21-52-13 and 10-35-52-13 (a distance of about 4.9 km). It continues to cut downward, removing all of the "a" sequence, the gritty siderite, and part of the "b" sequence between 10-35-52-13 and 6-1-53-13 (about 3 km). The bevel is well developed in this cross section (10-35-52-13 and 14-35-52-13) with thick conglomerate accumulating against it.

Northeastwards of the bevel a topography of bumps and hollows is preserved. The difference in amplitude between bumps and hollows decreases gradually basinwards, until the surface is essentially flat, characterising the basin plain. The topography (bumps and hollows) is believed to be erosional rather than depositional, because an almost identical facies sequence is preserved in both the terrace and bumps (compare facies sequences in 3-14-52-14 and 14-12-53-13 on Foldout 1). This is discussed in more detail in cross section B (Fig. 4.3 and Foldout 2).

Thick (up to 15 m) accumulations of conglomerate occur banked up against the bevel (13-21-52-13 to 10-35-52-13) and in some of the hollows (8-33-53-11). The top of the conglomerate is essentially flat across the terrace and bevel, but the conglomerate thins dramatically at the toe of the bevel. The conglomerate is only a thin veneer in core 6-1-53-13. Basinwards thick conglomerates may accumulate in the hollows as in 8-33-53-11, but generally in the basin the erosion surface E5 is marked by a thin veneer of conglomerate.

The thinner conglomerates and conglomerate veneers are overlain by bioturbated mudstones with pebble stringers of facies 5P, 4P and 3P, as in core 6-1-53-13. In well 8-33-53-11 the thick conglomerate is overlain by mudstones with pebbly stringers of facies 3P and 4P. The Laminated Dark Mudstones of facies 2 (Laminated Blanket, labelled L.B. on the cross sections) then blanket the entire sequence, and are overlain in turn by Massive Dark Mudstones of facies 1.

<u>Cross</u> <u>Section</u> <u>B</u>: Fig. 4.3

This is an extension of cross section B presented by Bergman and Walker (1986, in press). The section was initially constructed to investigate the nature of the bumps and hollows, specifically, to examine whether the bumps represented a remnant erosional topography, or whether they represented new sand bodies that have been deposited on top the erosion surface E5. The section has been extended to determine how the bumps and hollows are related to the bevel and the terrace, and to examine what happens basinwards of the bumps and hollows.

Figure 4.2. Cross section A as located in Fig. 4.1. The position of the wells, with respect to the topographic features present on the E5 surface, are given below the well log section. A cartoon core section is presented below the log section. A detailed core cross section is presented in Foldout 1, located in a pocket at the back of the thesis. Dark bars beside log section show the cored interval. The various E/T surfaces are shown. L.B. = Laminated Blanket, G.S. = Gritty Siderite, "A" and "B" refer to the two coarsening upward sequences preserved in the Raven River Member. Scale is in metres.

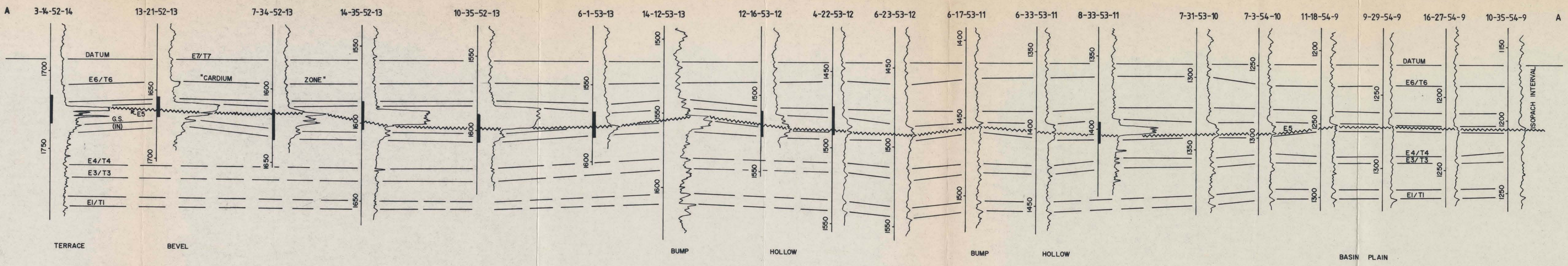

A
3-14-52-14
13-21-52-13
7-34-52-13
14-35-52-13
10-35-52-13
6-1-53-13
14-12-53-13
12-16-53-12
4-22-53-12
6-23-53-12
6-17-53-11
6-33-53-11
8-33-53-11
7-31-53-10
7-3-54-10
11-18-54-9
9-29-54-9
16-27-54-9
10-35-54-9
A
DATUM
E7/T7
"CARDIUM
ZONE"
E6/T6
E5
G.S.
(IN)
E4/T4
E3/T3
E1/T1
ISOPACH INTERVAL
TERRACE
BEVEL
BUMP
HOLLOW
BUMP
HOLLOW
BASIN PLAIN

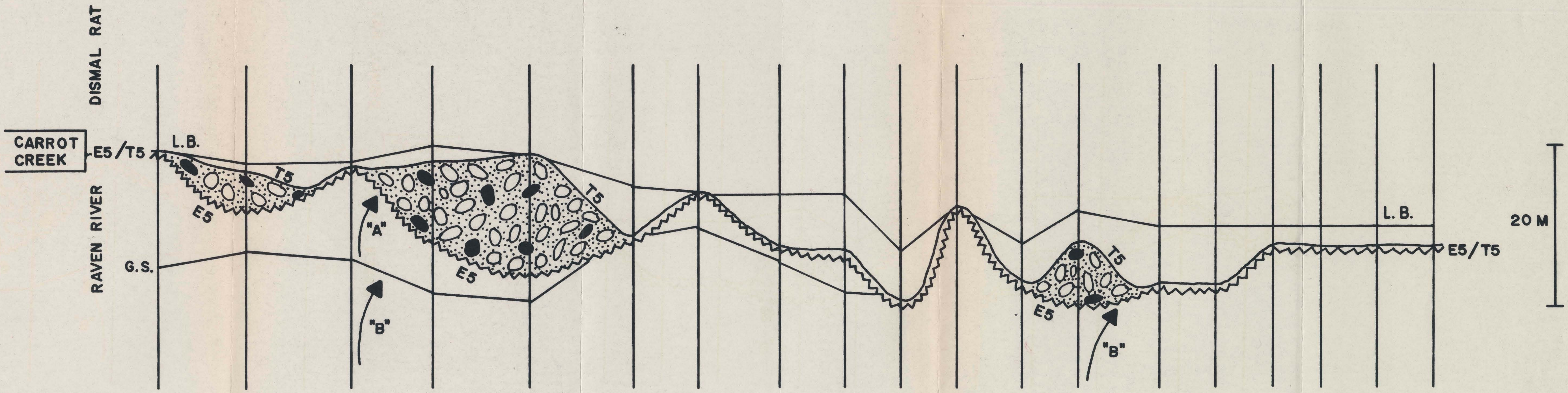

DISMAL RAT
CARROT CREEK
RAVEN RIVER
E5/T5
L.B.
G.S.
T5
E5
"A"
"B"
"B"
L.B.
E5/T5
20 M

In this section the bevel is not as well developed as it is in cross section A and is not covered by thick conglomerate. The erosion surface cuts progressively downward through the hummocky cross stratified sands, with only a thin veneer of gravel marking the surface. The toe of the bevel is in the area of well 13-5-51-11 (see Foldout 2). Basinwards of the bevel, the bump and hollow topography is well developed between wells 4-16-51-11 and 5-22-52-10. The bump and hollow topography fades away into an essentially flat surface, the basin plain.

Within the bumps (4-16-51-11/10-16-51-11, 2-28-51-11, 8-3-52-11, refer to Foldout 2), the stratigraphic section consists of the "b"sequence, the gritty siderite, and the "a" sequence, which may be capped by hummocky cross stratified sands. This vertical sequence is very similar to that underlying the terrace. It would be an extraordinary coincidence if this sequence, including the gritty siderite, had developed independently of that of the terrace, and after the formation of the erosion surface. This suggests that the bumps represent a remnant erosional topography.

In this section most of the hollows are filled with thick gravels banked up against the bumps (2-21, 9-3 to 15-11, 11-16, and 5-22). The conglomerate thins into the toe of the hollow and is overlain by facies 5P, 4P, and 3P (refer to wells 9-3-52-11, 11-2-52-11, 15-11-52-11 on Foldout 2). In well 4-34-51-11 only facies 5P, 4P, and 3P are preserved, suggesting that this well is located just basinward of a thick conglomerate accumulation. The morphology of the hollows in this area is similar to the morphology of the bevel shown in cross section A. After emplacement of all the pebbles, the "laminated blanket" (facies 2) was deposited over the entire area, and in turn was blanketed by massive dark mudstones of facies 1.

Cross Section C: Fig. 4.4

This section is outside the study area discussed by Bergman and Walker (1986, in press). It is located to the north of cross section A. The section shows a well developed terrace and bevel. The bumps and hollows are not well developed -- the surface is gently undulating with relief around 5 m. The undulations fade basinward leaving an essentially flat erosion surface, the basin plain, marked by a thin pebble veneer.

The erosion surface cuts progressively downwards through the hummocky cross stratified sands, the "a" sequence, and the gritty siderite. The bevel in this section has thick accumulations of conglomerates, as seen in wells 14-34-54-13 and 11-2-55-13 (Foldout 3). There are no thick conglomerate accumulations basinward of the bevel on this cross section (refer to Foldout 3).

Cross Section D: Fig. 4.5

This section is outside the study area discussed by Bergman and Walker (1986, in press). It is located to the

Figure 4.3. Cross section B as located in Fig. 4.1. The position of the wells, with respect to the topographic features present on the E5 surface, are given below the well log section. A cartoon core section is presented below the log section. A detailed core cross section is presented in Foldout 2, located in a pocket at the back of the thesis. Dark bars beside the log section show the cored interval. The various E/T surfaces are shown. L.B. = Laminated Blanket, G.S. = Gritty Siderite, "A" and "B" refer to the two coarsening upward sequences preserved in the Raven River Member. Scale is in metres.

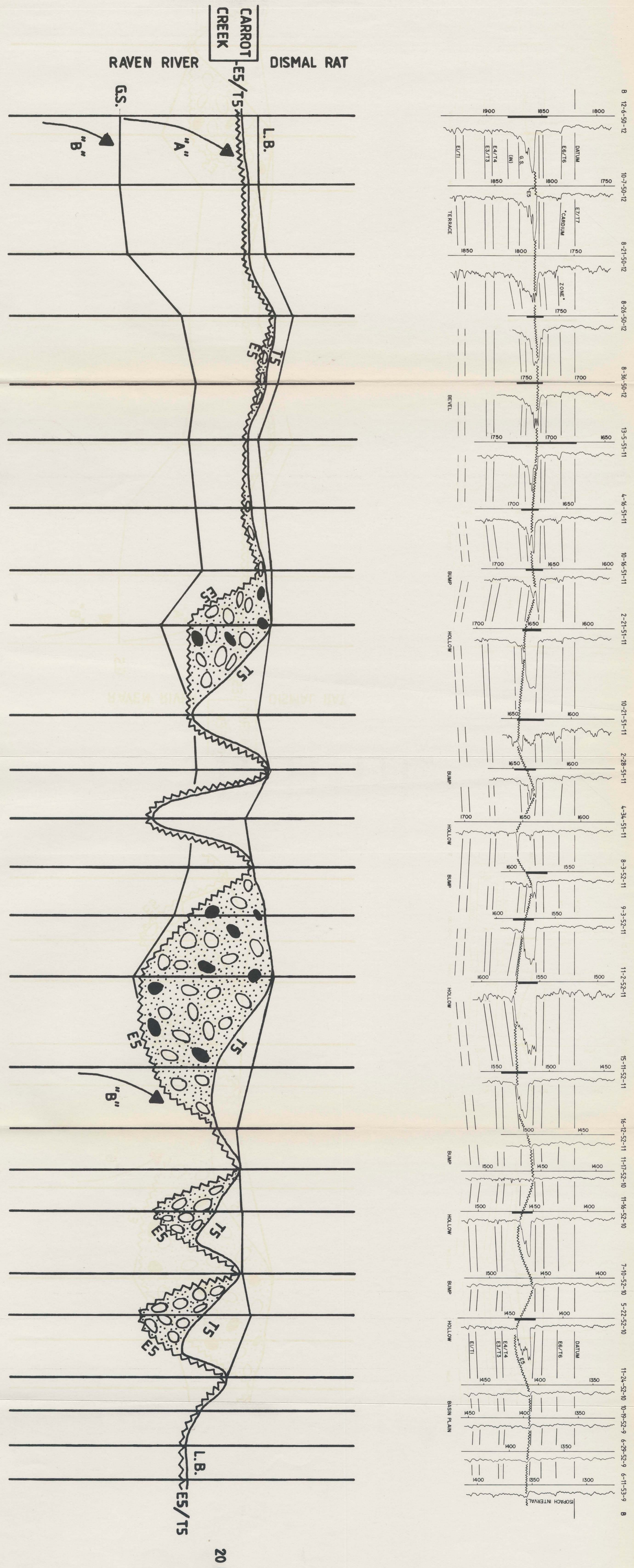

CARROT CREEK
RAVEN RIVER
DISMAL RAT
E5/T5
G.S.
L.B.
"A"
"B"
E5
T5
20 M
ISOPACH INTERVAL
DATUM
E6/T6
E7/T7
"CARDIUM ZONE"
TERRACE
BEVEL
BUMP
HOLLOW
BASIN PLAIN

Figure 4.4. Cross section C as located in Fig. 4.1. The position of the wells, with respect to the topographic features present on the E5 surface, are given below the well log section. A cartoon core section is presented below the log section. A detailed core cross section is presented in Foldout 3, located in a pocket at the back of the thesis. Dark bars beside the log section show the cored interval. The various E/T surfaces are shown. L.B. = Laminated Blanket, G.S. = Gritty Siderite, "A" and "B" refer to the two coarsening upward sequences preserved in the Raven River Member. Scale is in metres.

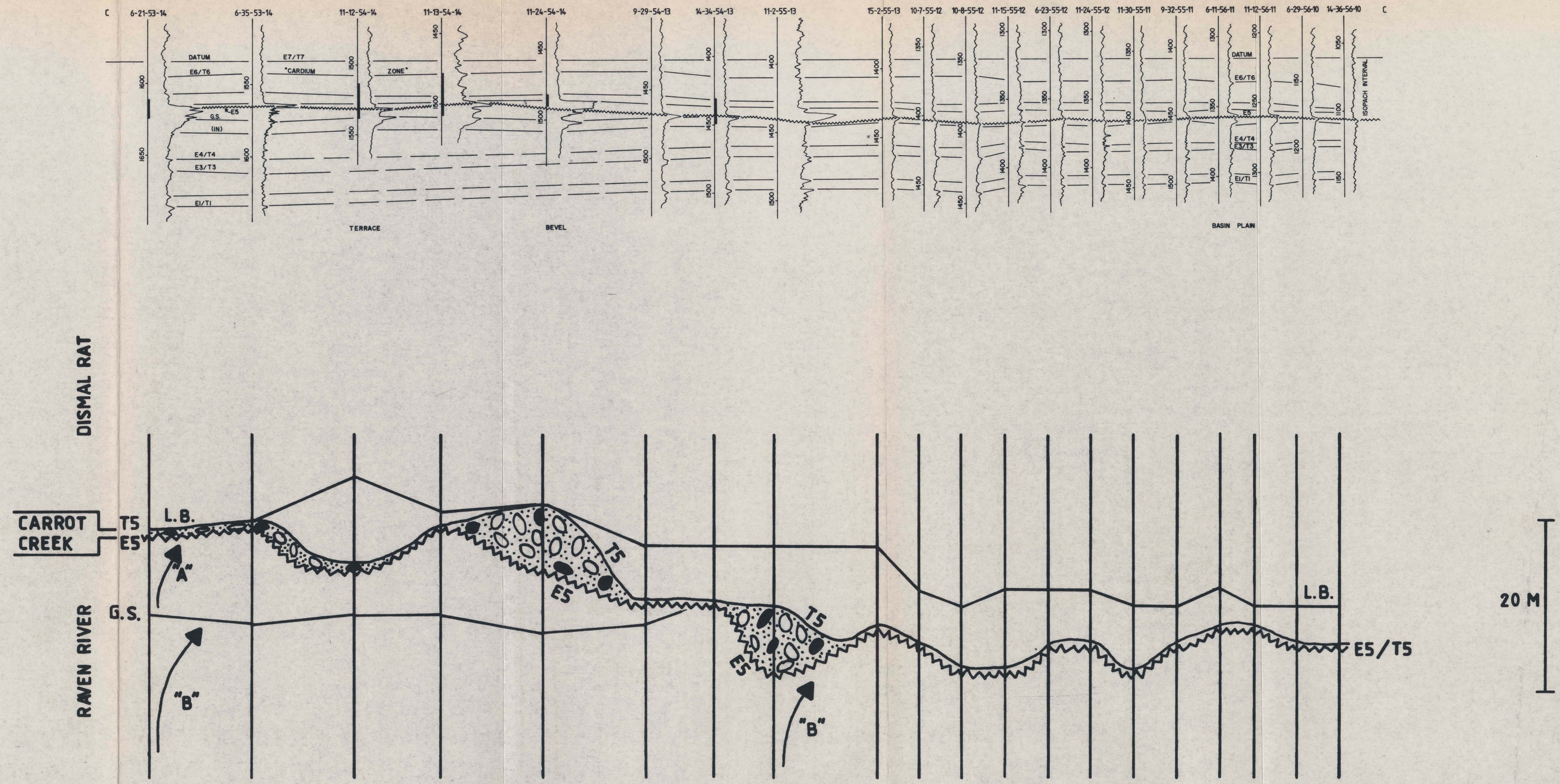

C
6-21-53-14
6-35-53-14
11-12-54-14
11-13-54-14
11-24-54-14
9-29-54-13
14-34-54-13
11-2-55-13
15-2-55-13
10-7-55-12
10-8-55-12
11-15-55-12
6-23-55-12
11-24-55-12
11-30-55-11
9-32-55-11
6-11-56-11
11-12-56-11
6-29-56-10
14-36-56-10
C
DATUM
E6/T6
E7/T7
"CARDIUM
ZONE"
E5
G.S.
(IN)
E4/T4
E3/T3
E1/T1
ISOPACH INTERVAL
TERRACE
BEVEL
BASIN PLAIN
DISMAL RAT
CARROT
CREEK
T5
E5
L.B.
"A"
G.S.
RAVEN RIVER
"B"
T5
E5
T5
E5
"B"
L.B.
E5/T5
20 M

south of cross section B. The section was drawn to try to establish the position of the bevel in the south, and to further examine the bump and hollow topography. As in cross section B, the bevel is not well developed and does not have thick conglomerates accumulating on it. Basinwards of the bevel is a well developed bump and hollow topography, with thick conglomerates occurring in some of the hollows. Basinwards of the bumps and hollows the erosion surface flattens out, (basin plain) and is marked by a thin veneer of conglomerate (refer to Foldout 4).

Why thick congl. in 2-3-51-9? - K6 basal erosion - ie no hollow.

4.3 EROSION SURFACE

The four cross sections (particularly the core sections Foldouts 1 through 4) document the presence of a major erosion surface. This surface is divided into four areally distinct topographic features (terrace, bevel, bumps and hollows, and basin plain). The similarity of the facies preserved in the Terrace and in the Bumps suggests that the Bumps represent a remnant erosional topography (refer to Fig. 4.3, and Foldout 2). The cross sections presented herein demonstrate that this surface extends throughout the study area, with a maximum erosional relief of about 20 m. The presence of this erosion surface E5 was established by Bergman (1984) and published by Bergman and Walker (1986, in press) in the Carrot Creek area.

The interval from the datum (E7/T7) to the base of the conglomerate (E5 surface), has been isopached in order to

Figure 4.5. Cross section D as located in Fig. 4.1. The position of the wells, with respect to the topographic features present on the E5 surface, are given below the well log section. A cartoon core section is presented below the log section. A detailed core section is presented in Foldout 4, located in a pocket at the back of the thesis. Dark bars beside the log section show the cored interval. The various E/T surfaces are shown. L.B. = Laminated Blanket, G.S. = Gritty Siderite, "A" and "B" refer to the two coarsenin upward sequences preserved in the Raven River Member. Scale is in metres.

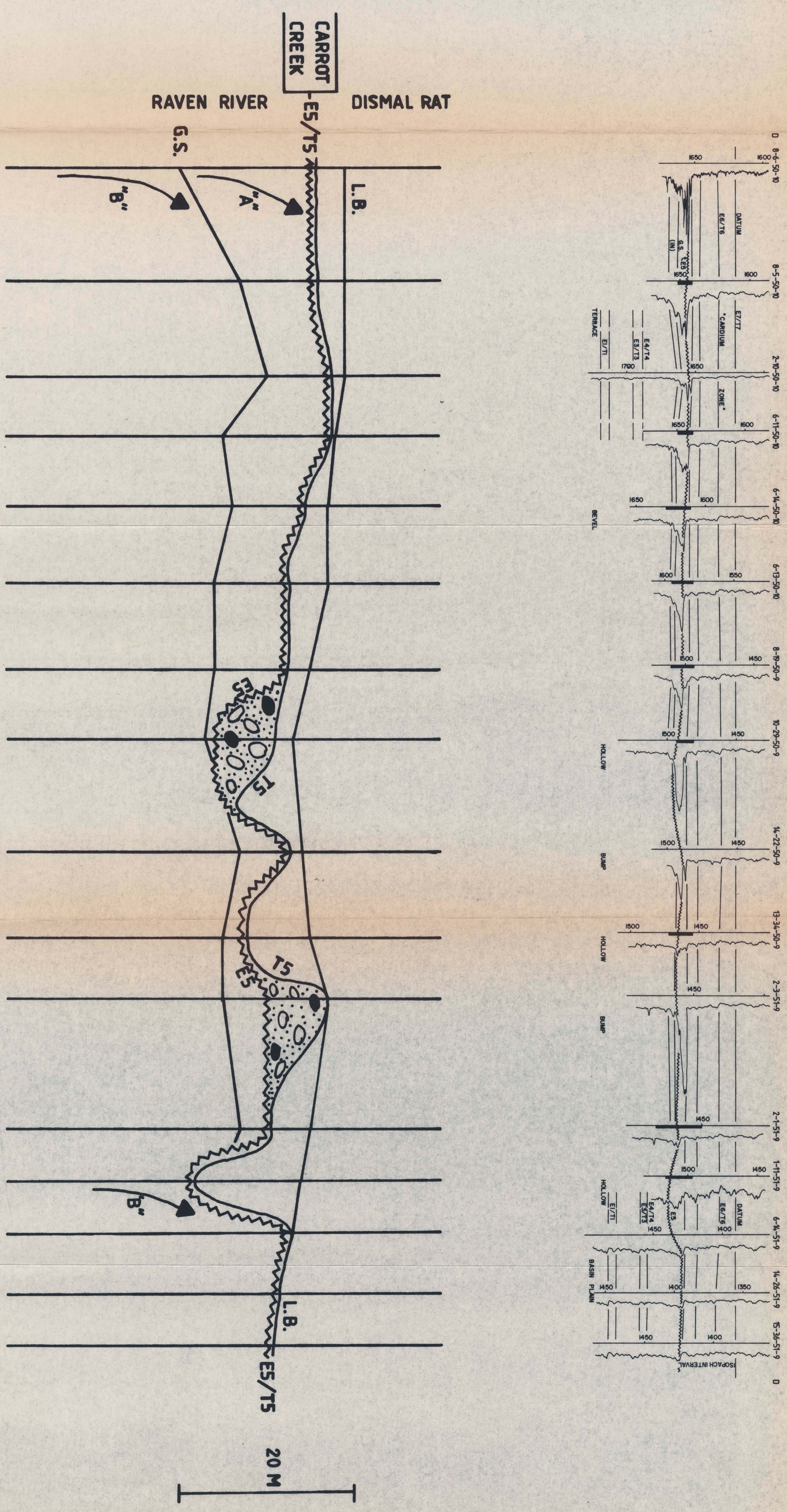

CARROT CREEK
RAVEN RIVER
DISMAL RAT
E5/T5
G.S.
L.B.
"A"
"B"
E5
T5
20 M
8-6-50-10
8-5-50-10
2-10-50-10
6-11-50-10
6-14-50-10
6-13-50-10
8-19-50-9
10-29-50-9
14-22-50-9
13-34-50-9
2-3-51-9
2-1-51-9
1-11-51-9
6-14-51-9
14-26-51-9
15-36-51-9
DATUM
E6/T6
E7/T7
"CARDIUM ZONE"
TERRACE
BEVEL
HOLLOW
BUMP
HOLLOW
BUMP
HOLLOW
BASIN PLAIN
ISOPACH INTERVAL

determine the morphology of the E5 surface using well logs and core. In most cases it was possible to pick the base of the conglomerate from logs alone, particularly if there was nearby core control. A contour map of the this surface is shown in Figure 4.6 (a map including data values is given as Foldout 5), where the contour values represent distances below the E7/T7 marker: the higher the contour value the deeper the scour.

The combination of cross sections and isopach map allows the recognition of four areas of distinct topography, based on the distance below the marker and the underlying facies preserved. These are the TERRACE is a broad undulating expanse, where the conglomerates rest on hummocky cross stratified sands, located in the south and southwestern parts of the map. The BEVEL is a narrow belt, crudely trending northwest-southeast, where the hummocky cross stratified sandstones (facies 7 and 7A) are truncated. The bevel is better developed in the northwestern portion of the map. South of Cyn-Pem the bevel trends almost east-west along the "drilling gap" in the Pembina oil field (McLaughlin, 1986). Basinwards (northeastwards) of the bevel, especially in the southern part of the map is the well developed BUMP and HOLLOW erosional remnant topography. This topography extends along the mortheastern edge of Pembina (McLaughlin, 1986). The bump and hollow topography is not as well developed in the

Figure 4.6. Isopach map of the E5 surface. Four topographically distinct areas have been recognized on the map. The broad undulating TERRACE, located in the southwest corner of the map, the narrow BEVEL trending roughly northwest-southeast, located immediately basinward of the terrace. Northeastwards of the bevel is remnant erosional topography of BUMPS and HOLLOWS trending roughly parallel to the bevel, which fades gradually basinwards in a relatively flat expanse, the BASIN PLAIN. The positions of the cross sections are shown.

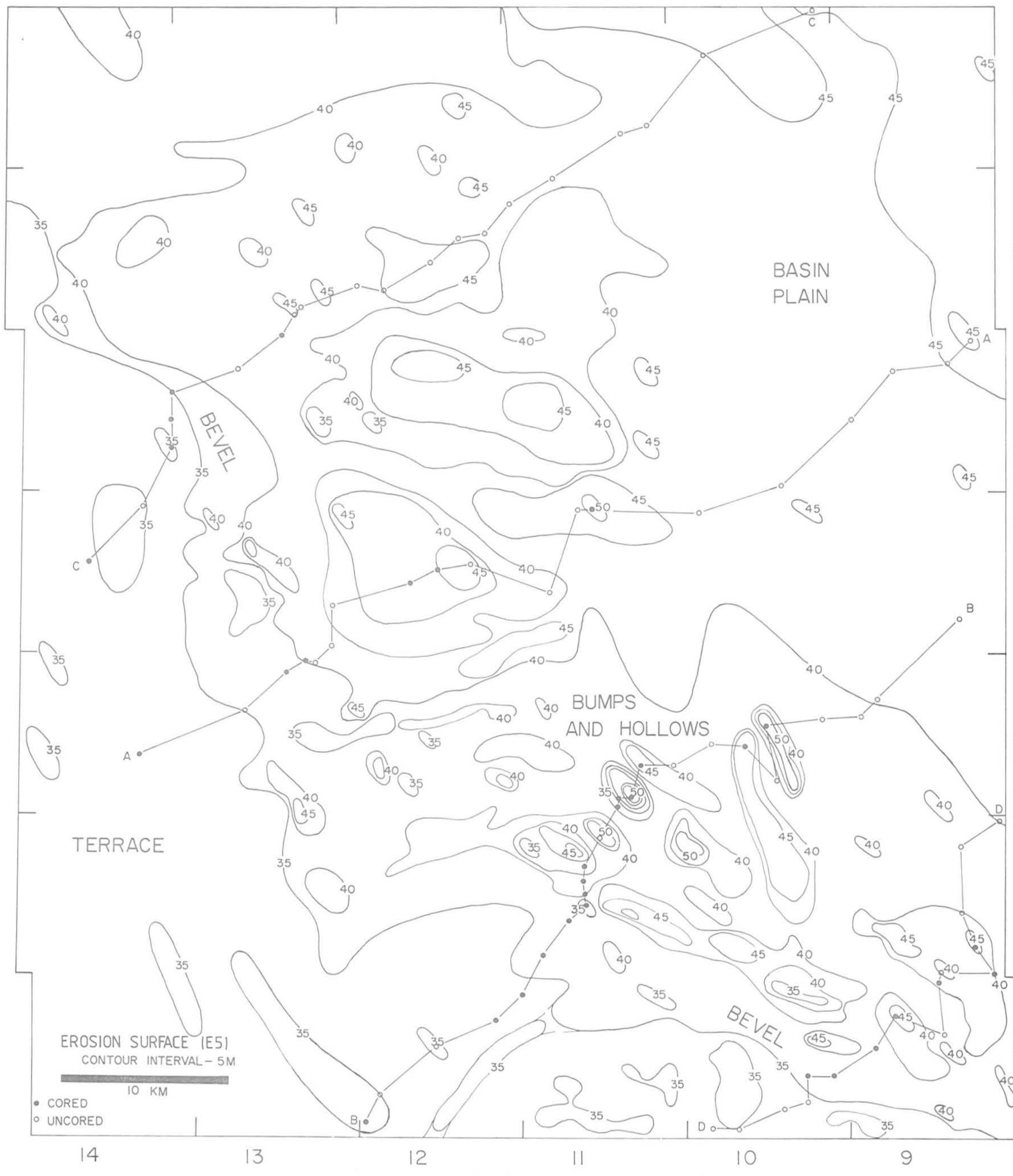
BASIN PLAIN
BEVEL
BUMPS AND HOLLOWS
TERRACE
BEVEL
EROSION SURFACE (E5)
CONTOUR INTERVAL - 5M
10 KM
CORED
UNCORED
14
13
12
11
10
9
56
55
54
53
52
51
50

northern part of the map. The BASIN PLAIN (not specifically named by Bergman and Walker, 1986) is an essentially flat area basinwards of the bumps and hollows. Apart from the surface documented by McCubbin (1969) for the Cretaceous strike-valley sandstone reservoirs in northwestern New Mexico, there is no similar published isopach map detailing the morphology of this type of erosion surface.

The facies sequence type (described in Chapter 3) was plotted on a map (Fig. 4.7), in order to establish the areal distribution of each type. From this map it can be seen that facies sequences are associated with the various morphologic features recognized on the erosion surface. Type IA wells are characteristic of the sequences found on the terrace and in the bumps. The bevel is characterized primarily by wells of Type IB; sometimes wells of Type 2A are found in the bevel. Well Type 2A and 2B are characteristic of the landward side of hollows. Type 3A and sometimes 3B are found on the basin side of the hollows basinwards of the Type 2 wells. The basin plain is characterized by wells of Type 3B.

4.4 MESH DIAGRAMS OF THE E5 SURFACE

In order to visualize the morphology of this surface a mesh diagram was constructed using the same data. The mesh diagrams were made using the commercially available software package published by ZYCOR Inc., of Austin Texas. The technical details are presented in more detail in Appendix

Figure 4.7. Facies sequence map. This map shows the areal distribution of the facies sequence types described in Chapter 3. The position of the bevel, the 40 and 45 m contour lines are drawn on for reference to the morphology of the E5 surface (Fig. 4.6).

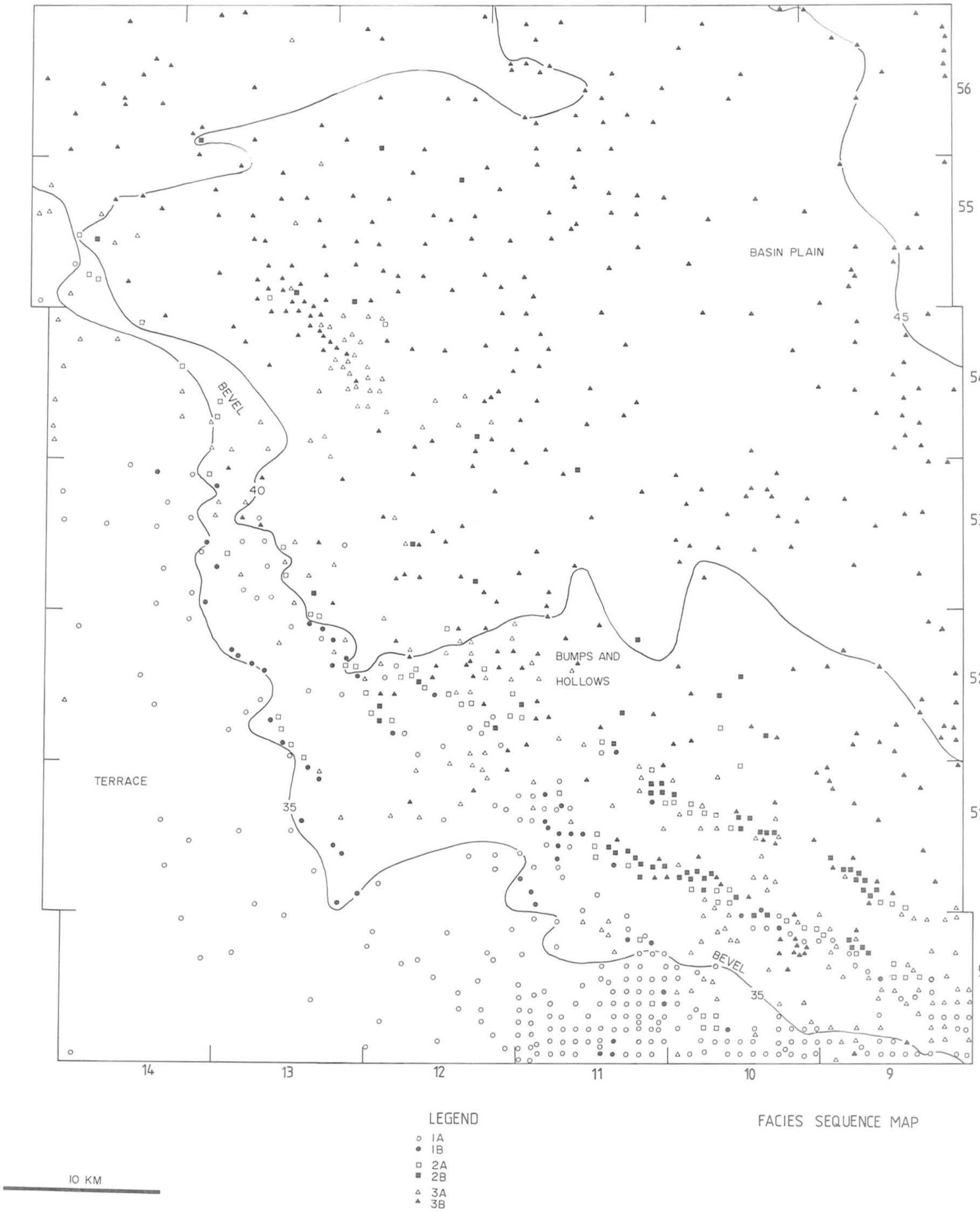

FACIES SEQUENCE MAP

3. Briefly, a regular grid of points was set up, using a weighted least squares procedure to calculate grid point values from surrounding real data points. The data grid was then smoothed to produce the mesh diagram, and shading applied to emphasize the topography of the surface. Differences between the mesh diagram and the hand-contoured isopach map are due to the smoothing procedures involved in making the mesh surface.

Two views of the mesh diagram are presented, one from the northeast (Fig. 4.8) and the other from the northwest (Fig. 4.9). The relief is highly exaggerated in the figures; the actual relief on the surface is about 20 m, and covers an area of 1512 mi^2 (4200 km^2). The cross sections, particularly the core sections, clearly demonstrate that the bumps are not gravel and sand ridges which have aggraded on top of an originally smooth surface.

The two mesh diagrams (Figs. 4.8, 4.9) illustrate the four areally distinct areas recognized on the isopach map. The two views show the morphology of the individual features recognized, and their lateral variation. The gradual transition from the bumps and hollows to the basin plain is more evident on the mesh surface than the isopach map. The mesh surface also shows the change in the development of the bevel from the north the south and the association with the bumps and hollows more clearly than the isopach map.

If the conglomerates were superimposed on this surface,

Figure 4.8. Mesh Diagram of the E5 surface when viewed from the northeast corner of the study area. The topographic features described from the isopach map (Fig. 4.6) are shown.

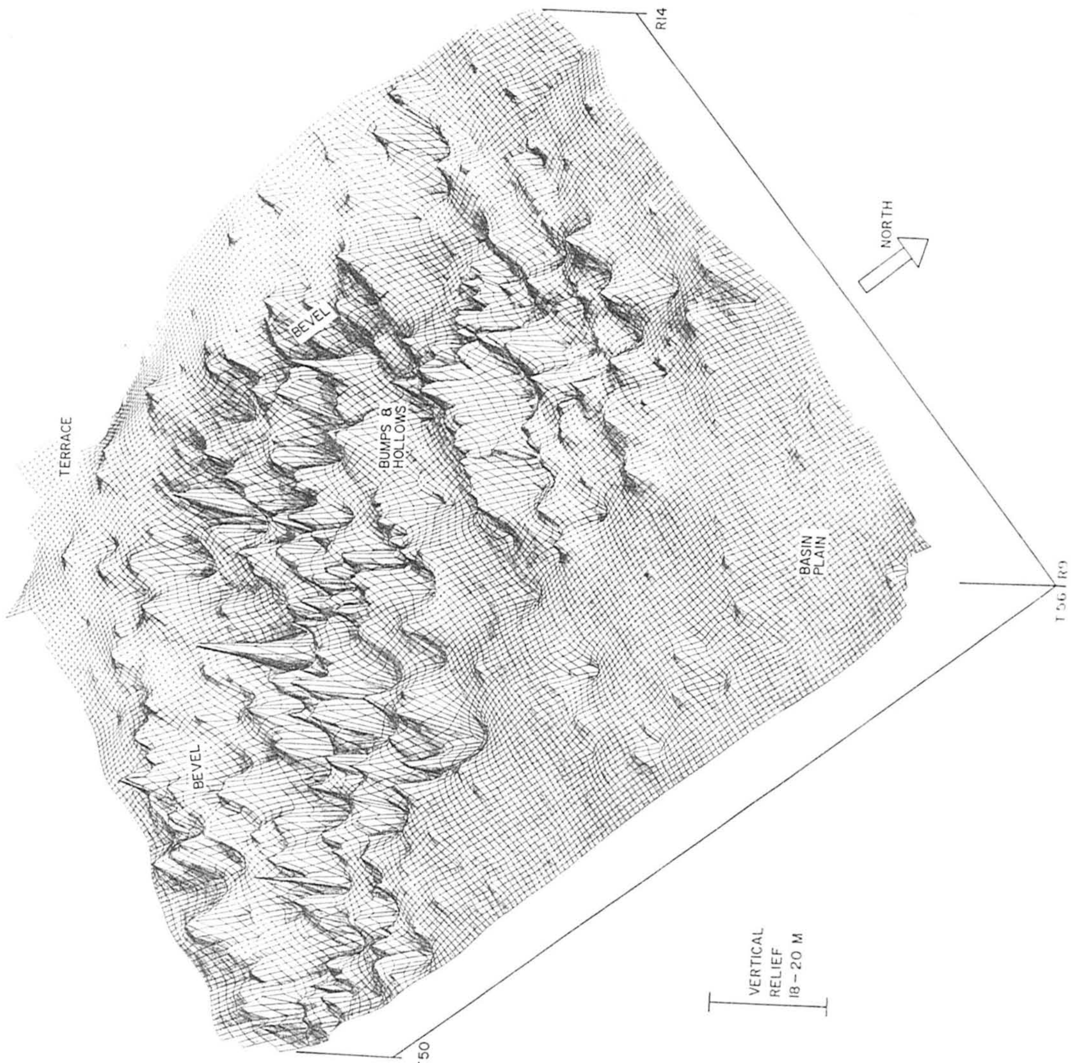
TERRACE
BEVEL
BEVEL
BUMPS & HOLLOWS
BASIN PLAIN
NORTH
R14
T56 R9
T50
VERTICAL RELIEF 18-20 M

Figure 4.9. Mesh Diagram of the E5 surface when viewed from the northwest corner of the study area. The bevel is evident as a prominent feature in this view. The topographic features are labelled.

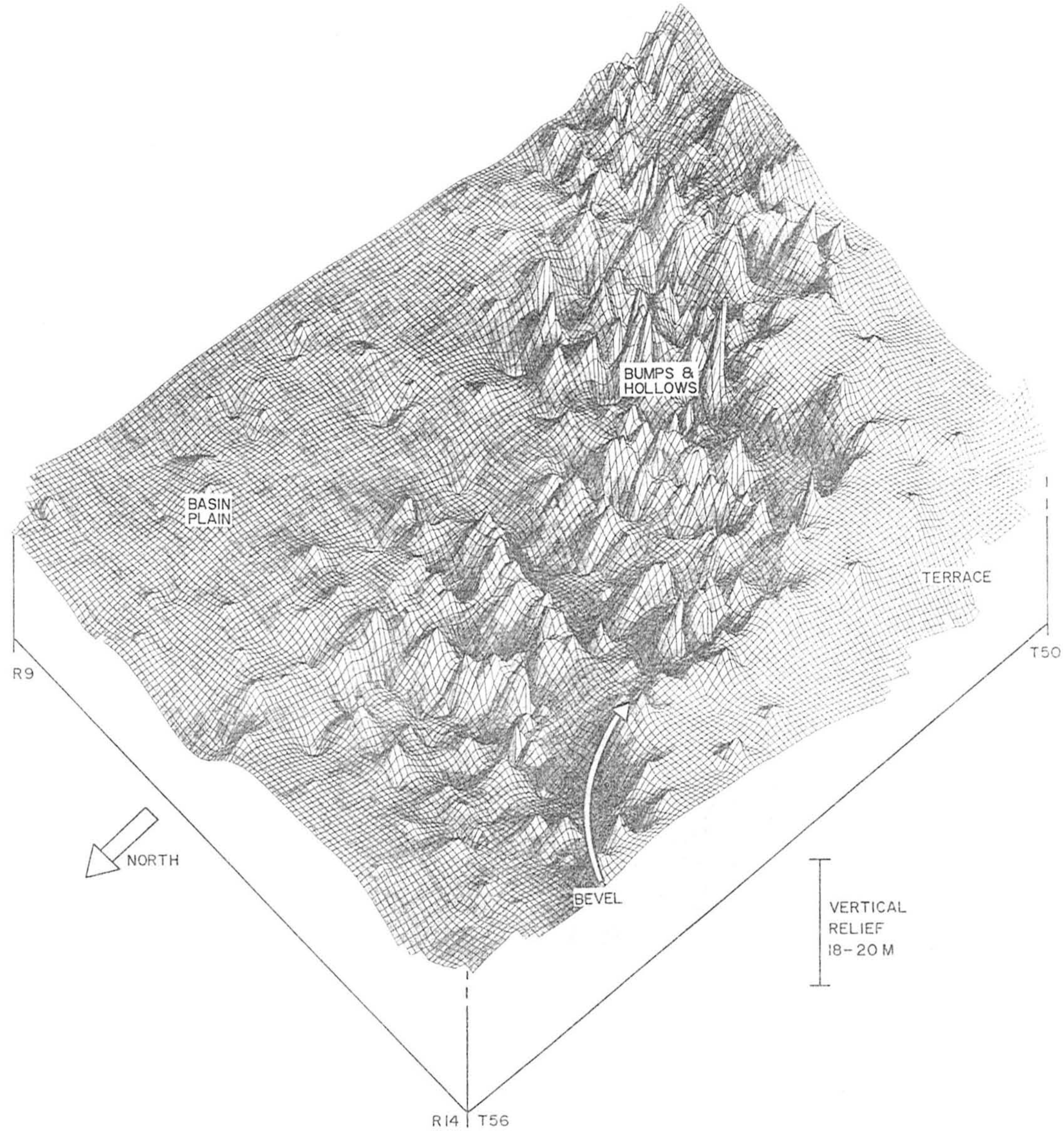
BUMPS & HOLLOWS
BASIN PLAIN
TERRACE
R9
T50
NORTH
BEVEL
VERTICAL RELIEF 18-20 M
R14
T56

they would be found associated with the deeper scours (refer to Fig. 4.3 and Foldout 2, wells 2-21-51-11, 11-2-52-11, 11-16-52-10, and 5-22-52-10). The thick conglomerates were found banked up against the bevel (Fig. 4.2 and Foldout 1, well 14-35-52-13 and 10-35-52-13) and the bumps (Fig. 4.3 and Foldout 2, refer to wells listed above). These thick conglomerates pass basinwards into mudstones with pebbly stringers and scattered chert pebbles (facies 3P, 4P, and 5P).

4.5 RELATIONSHIP OF CONGLOMERATE TO THE E5 SURFACE

The conglomerate thickness isopach map (Fig. 4.10) was constructed using both core and log data. A map including the thickness values of the conglomerates is given as Foldout 6. The cores were used to confirm the well log response. The thickness of the conglomerates was determined primarily from well logs. In many cases the core could not be used because more than a metre of conglomerate was missing from the core boxes. Conglomerate thickness was calculated from the induction log response and where possible compared with the thickness recorded by the gamma ray log signature. Thickness of the conglomerate was determined by measuring the thickness of the blocky log response at half the resistivity value (Fig. 4.11).

A series of linear en echelon bodies, with up to 19 m of conglomerate, were found. Those bodies of gravel adjacent to the bevel surface are parallel to the bevel.

Figure 4.10. Conglomerate Isopach Map showing the distribution of the thick conglomerate pools on the E5 surface. The positions of the cross sections are shown.

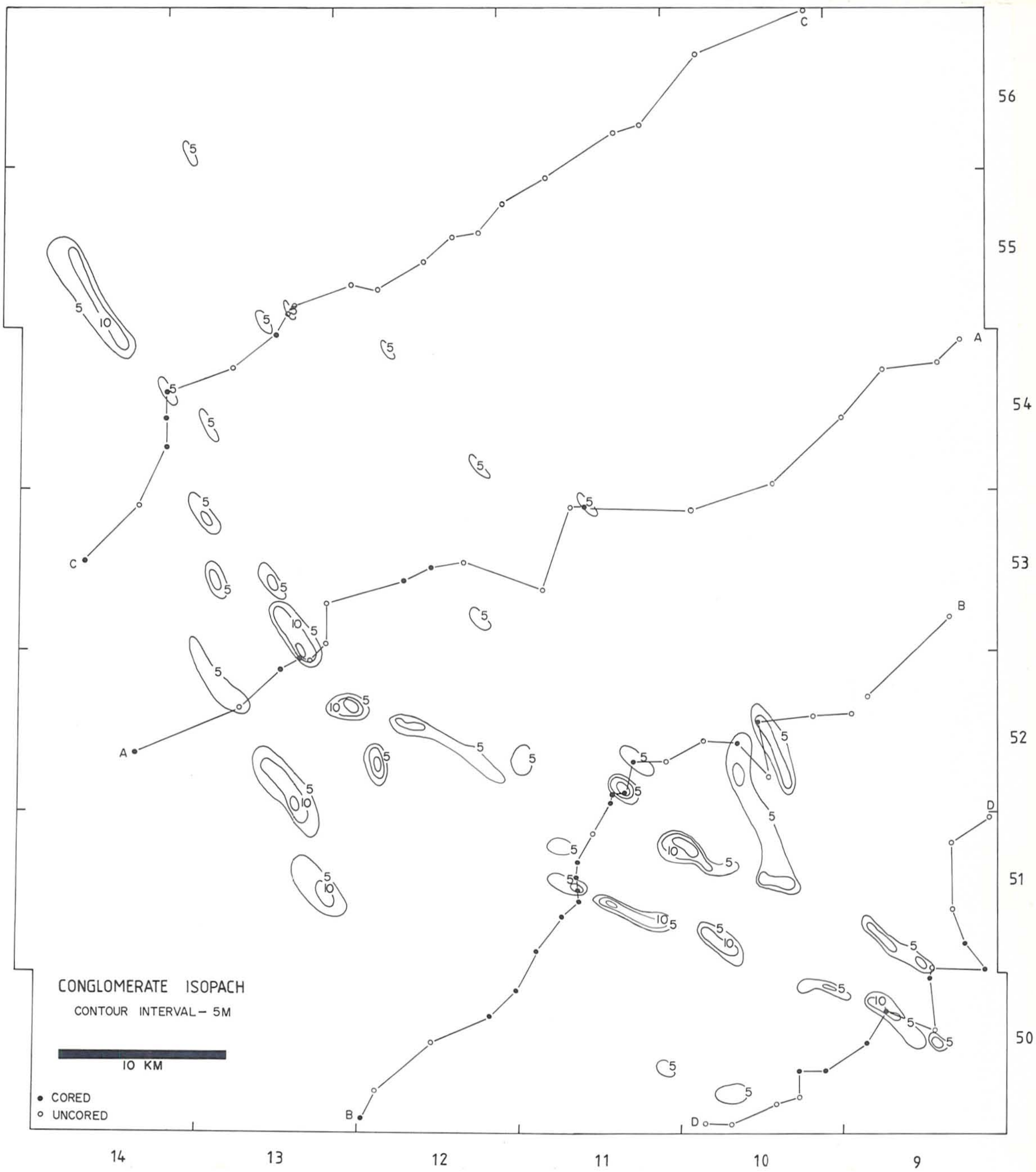
CONGLOMERATE ISOPACH
CONTOUR INTERVAL – 5M
10 KM
● CORED
○ UNCORED
A
B
C
D
56
55
54
53
52
51
50
14
13
12
11
10
9

Figure 4.11. Resistivity log illustrating how the conglomerate thickness was calculated from the resistivity log. The measurement of conglomerate thickness was made at a position equal to approximately half the resistivity value. The diagram also shows the log signature of the various E/T surfaces, as well as the gritty siderite. Below the conglomerate is a coarsening upward sequence associated with the Raven River Member; G.S. indicates the log response of the gritty siderite, sub-facies 8 G.S. This coarsening upward sequence has been truncated by the E5 surface. Above the conglomerate (T5) is a fining upward sequence associated with transgressive mudstones of the Dismal Rat Member. The black bar shows the position of the cored interval. Scale is in metres.

12-19-52-12

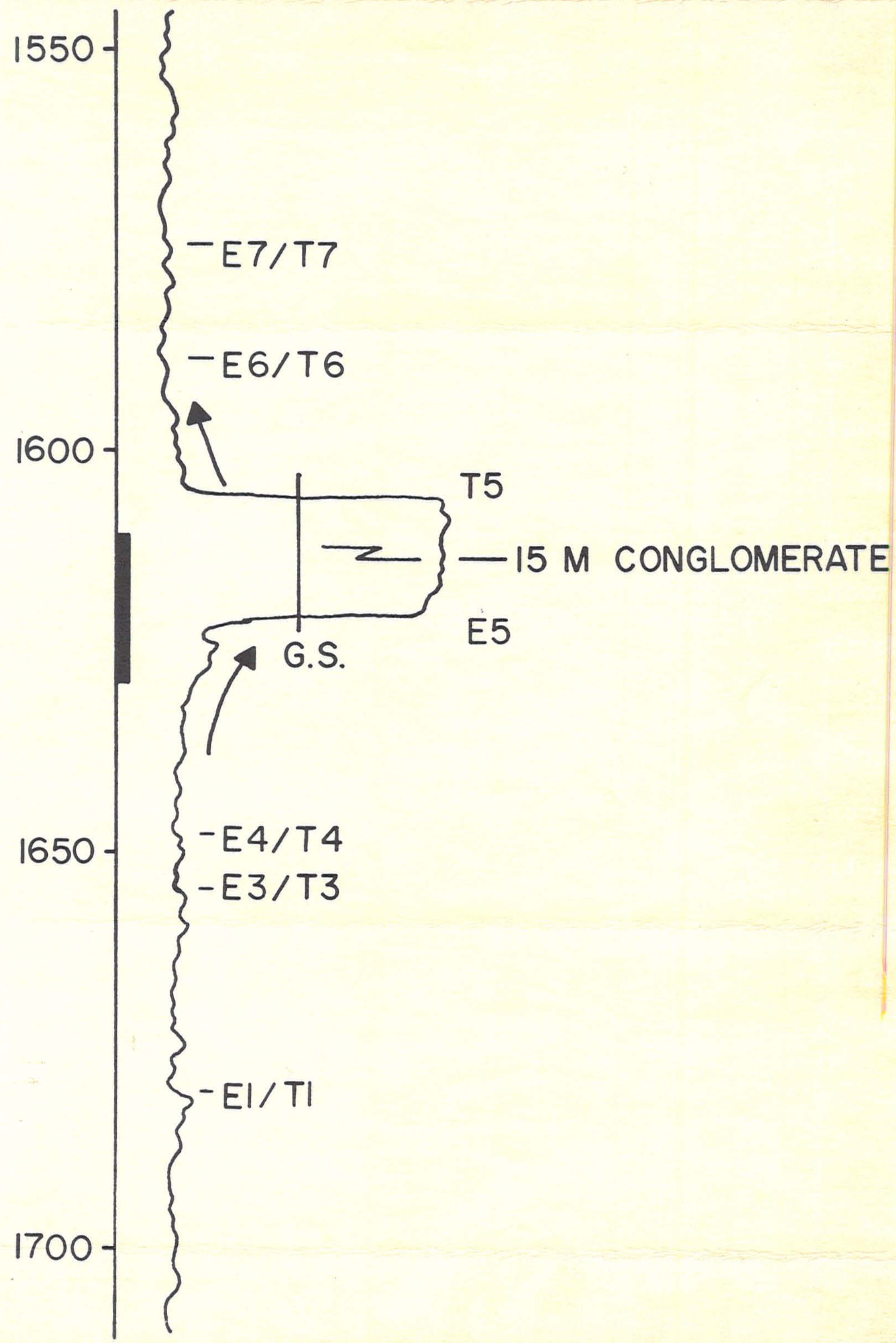
1550
1600
1650
1700
E7/T7
E6/T6
T5
15 M CONGLOMERATE
E5
G.S.
E4/T4
E3/T3
E1/T1

Basinwards of the bevel the pods trend slightly obliquely to the orientation of the bevel and are parallel to the hollows. Generally, the thickest gravels are found associated with the deepest hollows. Between the conglomerate bodies, a continuous veneer of conglomerate, usually less than a metre thick, is present in all wells. A more detailed discussion of the conglomerates is given in Chapter 7.

4.6 "CARDIUM ZONE" -- LOW WATER MEMBER

The Low Water Member (more commonly known as Cardium "zone") is contained between the E6/T6 surfaces. It is composed of pebbles in siderite (eg., 13-5-51-11; Fig. 4.12). This horizon has commonly been used as a regional datum in Cardium studies (Griffiths, 1981; Krause and Nelson, 1984; Krause, 1983; Keith, 1985). In many areas, the E6 surface can be demonstrated to be a reliable marker for correlation, trending parallel or sub-parallel to other regional markers. In other areas, however, there may be more than 20m of erosion on this surface (eg., in the area of Ricinus field; Plint, pers. comm.).

The E6 surface in the Carrot Creek area is mostly a "flat" horizon, trending parallel or sub-parallel to other regional markers. The major problem with using the E6/T6 surface in this area is that the marker becomes difficult to pick basinwards. In the northeast corner of the study area, approximately 10 m of erosion can be documented on the E6/T6

Figure 4.12. "Cardium Zone" -- Low Water Member.

The Low Water Member is characterized by chert pebbles and granules dipersed in siderite. A) Photo is taken from well 6-31-49-10, 5450 ft. B) Photo is taken from well 13-5-51-11, 5575 ft. Photos are taken from 3 in. drill core.

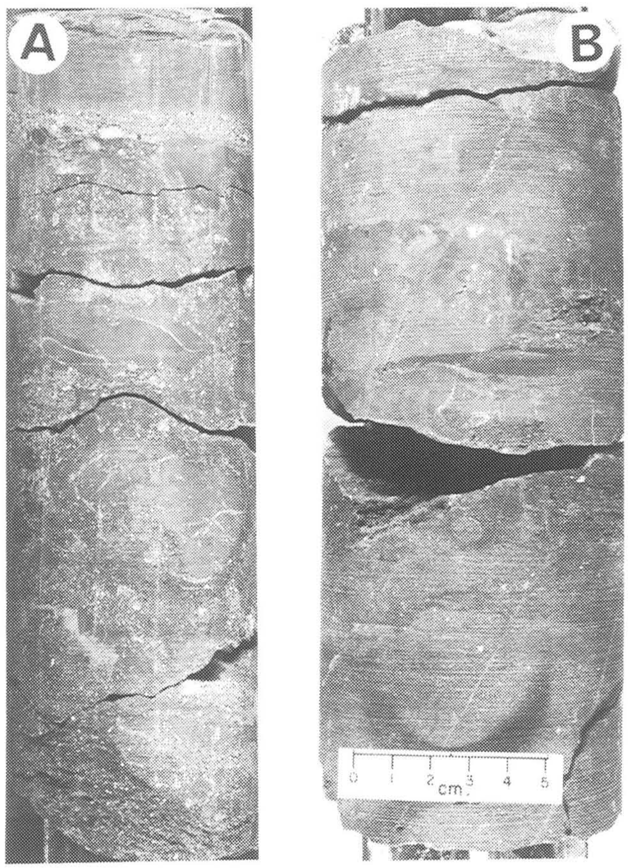
A
B
0
1
2
3
4
5
cm

surface with respect to the upper datum (E7/T7), as seen on cross sections A and C (Figs. 4.2 and 4.4 respectively). The area of interest on these lines is shown in more detail on cross sections A' and C' (Figures 4.13 and 4.14 respectively). These correlations are based entirely on well logs as there is no core available.

<u>Cross section A'</u>: Fig. 4.13

On this section there is approximately 8m of erosional downcutting on the E6 (Low Water Member) surface between wells 7-31-53-10 and 7-3-54-10. This surface truncates underlying marker horizons. Above this surface, overlying markers can be shown to onlap onto this surface (compare wells 7-31 and 7-3).

<u>Cross Section C'</u>: Fig. 4.14

On this section two stages of erosional downcutting are documented. The first downcutting occurs between wells 9-29-54-13 and 14-34-54-13, and has approximately 5m of relief. The second downcutting occurs between wells 10-8-55-12 and 11-15-55-12, and has approximately 5m of erosional relief. The surface truncates underlying markers, and overlying markers onlap onto this surface.

The E6 surface in the Carrot Creek area shows similar features to those documented in detail for the E5 surface. The main differences are in the scale of erosion (a maximum of 10m on the E6 surface compared with approximately 20 m of erosional downcutting on E5), and the lack of thick

Fig. 4.13. Detailed section of cross section A (Fig. 4.2) showing the morphology of the Low Water Member ("Cardium Zone"), E6/T6 surface. Scale in metres.

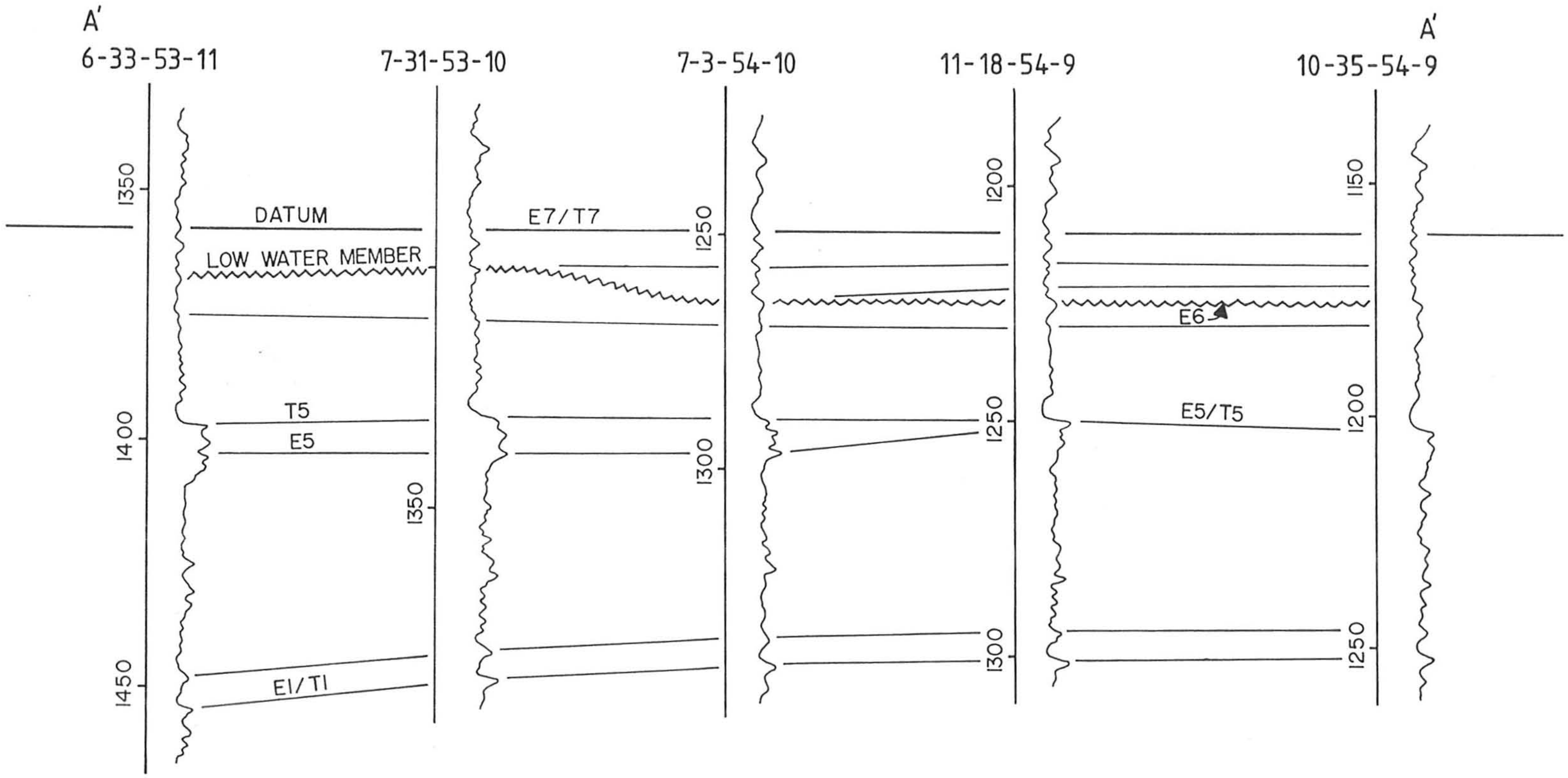
A'
6-33-53-11
7-31-53-10
7-3-54-10
11-18-54-9
A'
10-35-54-9
DATUM
LOW WATER MEMBER
E7/T7
E6
T5
E5
E5/T5
E1/T1
1350
1400
1450
1350
1250
1300
1200
1250
1300
1150
1200
1250

Fig. 4.14. Detailed section of cross section C (Fig. 4.4) showing the morphology of the Low Water Member ("Cardium Zone"), E6/T6 surface. Scale in metres.

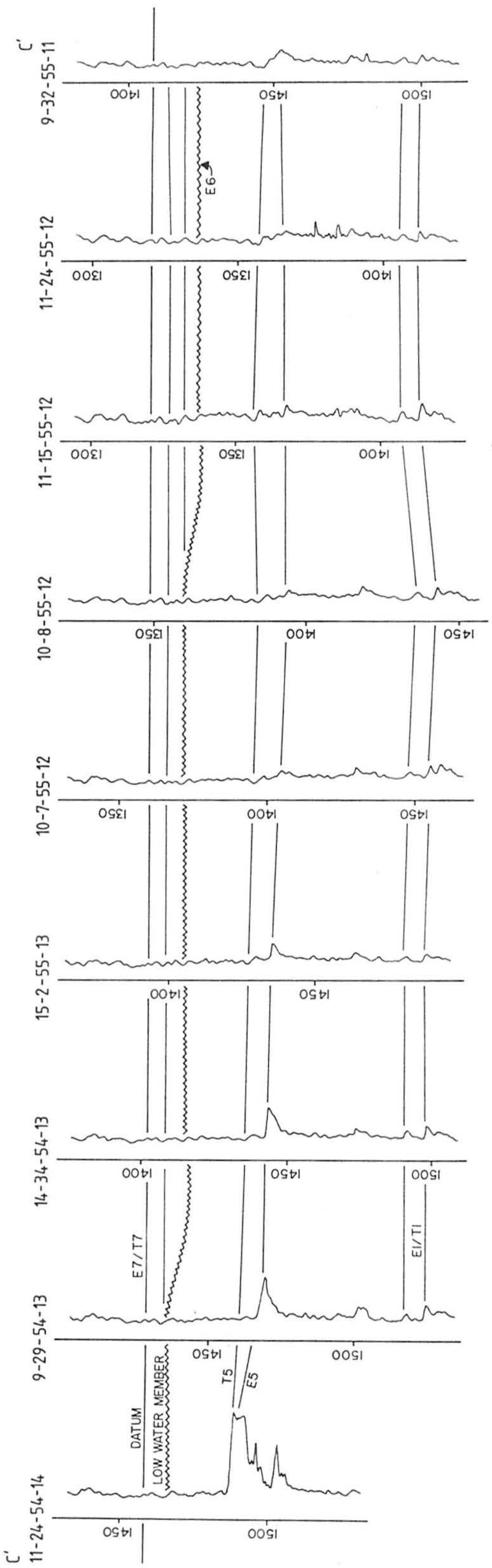
C'
9-32-55-11
11-24-55-12
11-15-55-12
10-8-55-12
10-7-55-12
15-2-55-13
14-34-54-13
9-29-54-13
11-24-54-14
C'
DATUM
LOW WATER MEMBER
T5
E5
E7/T7
E1/T1
E6

conglomerate accumulation on the E6 surface.

4.7 FORMATION OF THE E5 SURFACE

The erosion surface preserved in the Carrot Creek -- Cyn-Pem area could have formed in one of three ways; 1) fully sub-aerial erosion (fluvial downcutting), 2) fully marine (erosion on the shelf), or 3) in an intermediate position (shoreface erosion). These three possibilities will be discussed individually in detail in Chapter 8. A brief discussion is presented here, in order to interpret the morphology of the E5 surface so that the textures preserved in the conglomerates (Carrot Creek Member) overlying this surface may be discussed in terms of their depositional environment.

The sediments preserved in the Raven River Member (bioturbated mudstones and sandstones passing vertically upwards into hummocky cross stratified sandstones) suggest deposition of an overall regressive sequence in an open shelf environment. The hummocky cross stratified sandstones indicate deposition below fairweather wave base and above storm wave base. The remnant topography of bumps and hollows and the continuous trend of the bevel (with about 20 m of relief) suggests increased erosion of the bed. This erosional morphology implies a minimum sea level lowering to increase the ability of waves to scour the bed (fully submarine erosion) or a maximum lowering to allow fluvial downcutting (fully sub-aerial erosion).

A. FULLY SUB-AERIAL (Fluvial Downcutting)

The morphology of the the E5 surface does not resemble one of incised fluvial channels. Fluvial downcutting does not account for the presence of the bevel or the preservation of the basinward topography of bumps and hollows, which also trend roughly parallel to regional strike.

The other possibility is that the surface was cut sub-aerially and then reworked during a subsequent marine transgression. This is an added complication for which there is no real supporting evidence. There are no features preserved to suggest that rivers headed at the bevel. The hypothesis that the E5 surface formed as a result of fluvial downcutting and sub-aerial erosion with the gravels forming as fluvial bars, is rejected.

B. FULLY MARINE (Submarine Erosion)

Swagor et al. (1976) interpreted the erosion surface at the base of the conglomerates to have formed by submarine erosion on the open shelf. Although storm waves can scour the open shelf below fairweather wave base, the amount of relief (about 20 m) on the E5 surface, seems to make an open marine interpretation unlikely. Submarine erosion does not account for the continuous trend of the bevel. These features (amount of erosional relief and continuous trend of the bevel) suggest the presence of strongly localized erosion, rather than broad, open scouring on the shelf. The hypothesis that the erosion surface formed by submarine scour on the bed is rejected.

C. INTERMEDIATE (Shoreface Erosion)

The formation of the E5 surface as a result of shoreface erosion implies a drop in relative sea level, which caused the shoreface to move many tens of kilometers into the basin. In order to develop the preserved morphology of the E5 surface, the initial position of the maximum lowstand shoreface must have been located at Bigoray (refer to Fig.4.1), the basinward extent of the the bumps and hollows. Initial lowering of sea level must have been rapid so that the original shoreline could move quickly basinward, causing sediment bypassing of the shelf. If sea level lowering had been slow, (i.e., sediment supply kept pace with the rate of sea level lowering), then a steadily prograding coarsening upward sequence of offshore muds passing up into shoreface and shoreline deposits (such as that observed at Kakwa, Plint and Walker, 1986) would be expected. Such a sequence is not known to exist above the E5 surface, based on the regional correlations of Plint et al. (1986). Wave scour of the bed presumably resulted in the erosion of a new shoreface profile at maximum lowstand.

Bergman and Walker (1986, in press) interpreted the morphology of the E5 surface, particularly the remnant topography of bumps and hollows, to have formed during a period of stillstand or slow steady sea level rise

(Fig. 4.15). During this time, erosional shoreface retreat toward the southwest produced the remnant topography. This topography of bumps and hollows appears to be unusual. Kraft (1971) showed erosional "bumps" on the Pleistocene surface which are apparently associated with the Holocene transgression, but the relief on these bumps is only about 4 m. The bumps were interpreted by Bergman and Walker (1986, in press) as representing former positions of the shoreface. The irregular morphology of the surface was suggested by Bergman and Walker (1986, in press) to be due to armouring of the surface by gravel; other possibilities will be discussed in Chapter 8 of the thesis. The bevel marked the final position of the shoreface before marine transgression occurred, blanketing the conglomerate deposits with marine mudstones.

4.8 SUMMARY (Fig. 4.15)

1) Sequence "b" (Fig. 3.1) represents a progressive shallowing upward sequence through facies 1, 3, 4, and 5 (Fig. 4.15A).

2) The gritty siderite separating the sequences "b" and "a" (Fig. 3.1) is the result of a pause in deposition, possibly the result of a minor rise in sea level or a stillstand.

3) Sequence "a" (Fig. 3.1) represents another progressively shallowing upward sequence through bioturbated mudstones of facies 4 and 5, culminating in hummocky cross stratified sands suggesting deposition above storm wave base

Figure 4.15. Summary diagram of the erosional and depositional history in the Carrot Creek -- Cyn-Pem study area (after Bergman and Walker, in press). The details of the diagrams are presented in the text.

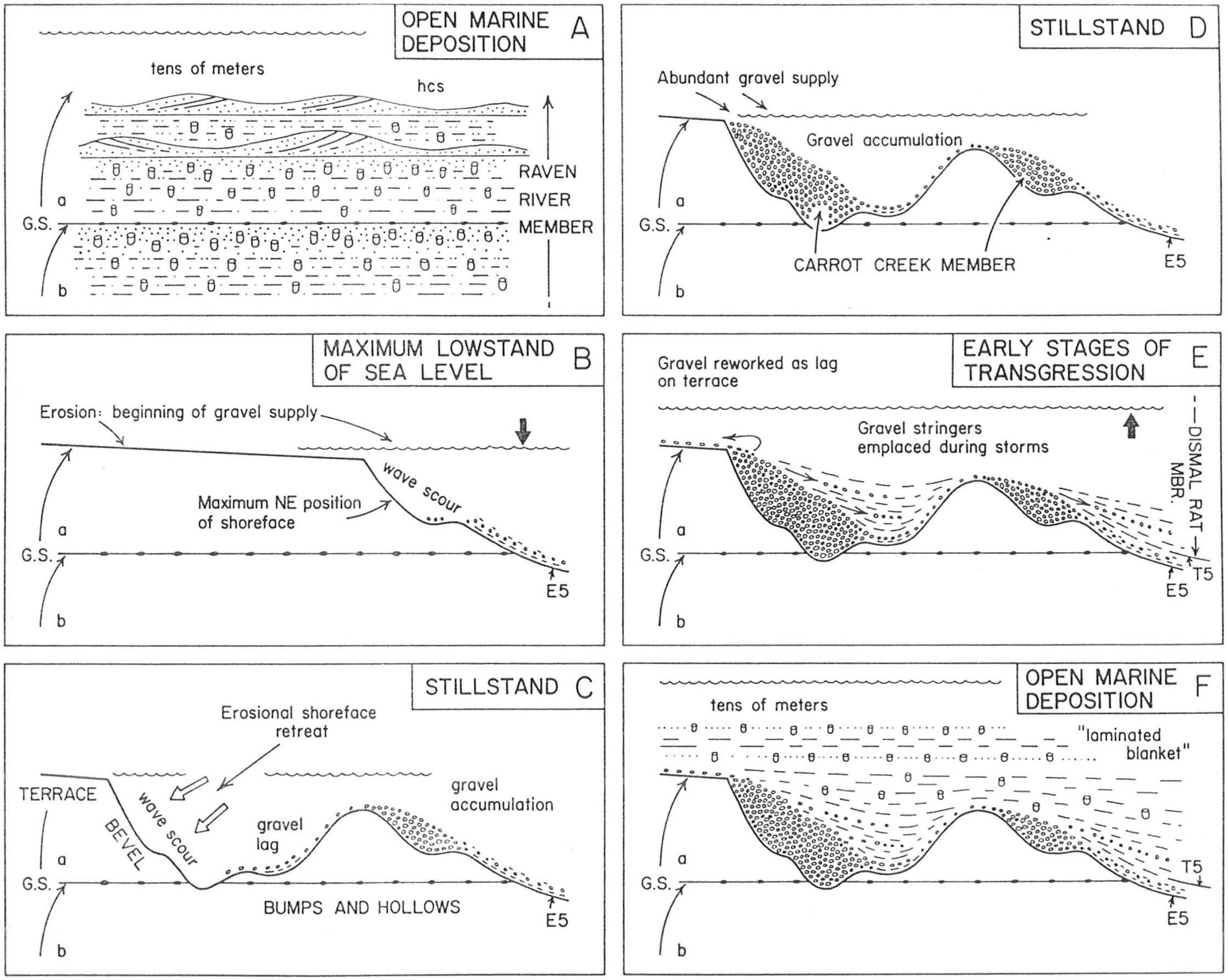
OPEN MARINE DEPOSITION A
tens of meters
hcs
RAVEN RIVER MEMBER
a
G.S.
b
STILLSTAND D
Abundant gravel supply
Gravel accumulation
CARROT CREEK MEMBER
E5
MAXIMUM LOWSTAND OF SEA LEVEL B
Erosion: beginning of gravel supply
wave scour
Maximum NE position of shoreface
EARLY STAGES OF TRANSGRESSION E
Gravel reworked as lag on terrace
Gravel stringers emplaced during storms
DISMAL RAT MBR.
T5
STILLSTAND C
Erosional shoreface retreat
TERRACE
BEVEL
wave scour
gravel lag
gravel accumulation
BUMPS AND HOLLOWS
OPEN MARINE DEPOSITION F
tens of meters
"laminated blanket"

(Fig. 4.15A).

4) A rapid drop in relative sea level resulted in a shift in the position of the shoreline basinwards (4.15B). The E5 surface is believed to have been formed by wave scouring on the bed to re-establish a new shoreface profile. During stillstand (Fig. 4.15C), this shoreface profile eroded back landwards leaving the bump and hollow topography, and the well established bevel where older sediments are truncated. Thus, the bumps are <u>not</u> newly formed offshore "ridges" rooted in the unconformable surface (data on cross section B, Fig. 4.3 and Foldout 2).

Why so irregular erosion in marine setting?

5) Also during stillstand (Fig. 4.15D), thick clast-supported conglomerate (up to 19m) was deposited against the landward side of the hollows.

6) During transgression, the gravel supply was cut off and the seaward sides of the hollows were filled with transgressive mudstones. During storms, gravel was reworked to form scattered pebbles and/or pebble stringers (facies 3P, 4P, and 5P) in the mudstones seaward of the thick gravels (Fig. 4.15 E). The transgression also reworked gravel back across the terrace from the thick accumulations against the bevel.

7) With continued transgression (Fig. 4.15 F) there is complete blanketing of the entire sequence by the laminated mudstones (facies 2).

8) After deposition of the laminated mudstones, further blanketing by massive mudstones (facies 1) occurred.

PART B: SEDIMENTOLOGY OF THE CARROT CREEK MEMBER

CHAPTER 5: DISCUSSION OF GRAVEL ENVIRONMENTS

5.1 INTRODUCTION

The Carrot Creek Member is bounded by the E5 erosion surface and the T5 transgressive surface (Fig. 2.3). It is composed of a chert pebble conglomerate with some interbedding of sand and mud. The thickness of this member varies from a thin veneer to about 20 m. A detailed discussion of the facies found in the Carrot Creek Member is presented in Chapter 6. Lateral variations within the member, and the relationship of the conglomerate to the E5 surface are discussed in Chapter 7. Detailed analysis of the cements (particularly the carbonate cements -- siderite and calcite) found within the conglomerates of the Carrot Creek and Burnstick Members of the Cardium Formation is being done by S. Zymela (Ph.D. in progress, pers. comm.) and hence will not be discussed herein.

The original objective of this thesis was to examine the conglomerate textures, particularly the fabric (as discussed in Chapter 1), in order to investigate the mechanism of emplacement of gravel into the basin. This proved to be impossible, as the conglomerates of the Carrot Creek Member showed very little preferred imbrication of the pebbles. These results made it difficult to define the depositional processes and environments of the gravel based on the textures of the gravels alone. The geometry of the erosion surface (discussed in Chapter 4) has proved to be the key to determining the depositional environment of the gravels. The conglomerates of the Carrot Creek Member are interpreted in this thesis as storm-dominated marine shoreface gravels, deposited during a rapid relative lowering of sea level.

During lowering or at max lowstand after base level erosion

This interpretation is based primarily on the geometry of the erosion surface on which the conglomerate bodies rest (Bergman and Walker, 1986; in press, and Chapter 4) and the regional stratigraphy proposed by Plint et al. (1986). Thus, the textures of the conglomerates could not be used to determine processes and environments. Rather, the environment is determined by the morphology of the erosion surface, and the textures of the conglomerates are presented to document what occurs in the shoreface environment.

To the best of my knowledge no one has previously described an ancient shoreface sequence similar to the one preserved at Carrot Creek. The existing literature provides a fairly limited documentation of conglomerates that are thought to have originated in coastal or nearshore environments. Nemec and Steel (1984) and Bourgeois and Leithold (1984) give good summaries of features believed to be associated with coastal conglomerates. A brief discussion of this literature is presented here to enable the reader to understand the extent to which the Carrot Creek Member is both the similar and different from other previously described coastal sequences -- both shoreface and beach. Differences between shelf, fluvial, and deep marine conglomerates will also be highlighted.

5.2 GRAVEL ENVIRONMENTS

As noted by Twenhofel (1947; p. 119), "... a conglomerate in itself has no environmental significance beyond the fact that the competency of a transporting agent was adequate to place its constituents where they are found ..." . The problem then, is to determine the depositional environment of the conglomerate. Conglomerate descriptors (summary in Harms et al., 1975, 1982) such as size, shape, roundness, sorting fabric, grading, stratification, pebble support (matrix versus clasts), the presence/absence of fossils (both body and trace), and preserved sedimentary structures in the conglomerates and interbedded sediments may provide some clues to the depositional environment of the gravels. These textures however, are <u>not</u> environmentally specific, and no one criterion is diagnostic of a depositional setting. The associations of conglomerates with other facies are perhaps the most reliable criteria for the determination of depositional environments (Twenhofel, 1947), and where available, faunal evidence is often diagnostic of gravel depositional environments (Bourgeois and Leithold, 1984).

Gravels are found in a wide variety of environments in both the continental and marine settings. Distinguishing between marine and non-marine conglomerates is often very difficult. The three general environmental settings (non-marine, marine, and marginal marine) will be discussed briefly below. The separation of these three settings is based primarily on textural features preserved in the conglomerates, and the association with surrounding sediments.

A. Non-marine Conglomerates

Non-marine conglomerates comprise mainly braided stream and mass flow sequences. The stratigraphic context of the conglomerates, in particular the association with sandstone sequences showing evidence of sub-aerial flood or soil-forming processes (such as, roots, caliche, paleosols, or dessication cracks), or containing a non-marine fauna or ichnofauna, may be sufficient to define the depositional setting (Nemec and Steel, 1984).

Braided river and braidplain conglomerates are the largest the group of non-marine conglomerates. They are characterized by gradual facies changes and decreasing grain size in a downstream direction. Braidplain deposits, although thinner than channel deposits, may have a lateral extent parallel to the paleoslope of as much as 500 km. For example, the Lower Cretaceous Cadomin Formation in the foothills of Alberta and Montana is sheet-like extending up to 300 km downslope from its source (Schultheis and Mountjoy, 1978).

Braided channel deposits occur in laterally fining and thinning sequences. Vertical sequences are fining upward, 2-3 m thick, and are dominantly structureless. In fluvial channels the smaller clasts may assume an "a" axis parallel, "a" axis imbricate pattern, however, the coarser clasts are generally aligned in fluvial with an "a" transverse, "b" imbricate pattern.

Braid bar deposits occur in laterally coarsening and thickening units with flat bases and convex-up top surfaces. Vertical sequences vary depending on locations within the bar complex, and the type of bar. Generally, vertical sequences are fining upward, 1-2 m thick, horizontally stratified or cross bedded units. Planar tabular cross stratification is more common in fluvial bars. Horizontal stratification consists of layers with different clast sizes or layers with alternating matrix filled and open work texture in fluvial conglomerates.

Fluvial gravels are mainly ungraded, with less common normal or inversely graded beds. Rust (1978) classified braided stream gravels into proximal and distal assemblages. Generalized vertical sequences of different types of braided fluvial systems were described by Miall (1977, 1978).

B. Deep Marine Conglomerates

Hein (1984) compared deep sea gravels and fluvial gravels. The most useful criteria recognized in the distinction of fluvial from deep sea conglomerates were grading types and gravel fabric patterns. Deep-sea conglomerates are mainly normally graded, with less common ungraded conglomerates and rare inversely or complexly graded beds. Deep sea channel conglomerates commonly have an "a" parallel, "a" imbricate fabric.

Deep sea channel deposits are composed of laterally fining and thinning deposits. Vertical sequences are commonly fining upward, with thickness of 5-10 m (Hein, 1982; Walker, 1984c). The main channel deposits are dominantly structureless.

Braid bar deposits in deep sea sediments occur in laterally coarsening and thickening units with flat bases and convex-up top surfaces. Vertical sequences vary depending upon locations within the bar complex and the type of braid bar. Generally, vertical sequences are fining upward, 1-2 m thick, horizontally stratified or cross bedded units. Graded trough cross stratified beds, graded horizontal stratification and irregular inclined cross stratification are common in deep-sea bar deposits. These features were not recognized in the fluvial conglomerates. Horizontal stratification consists of layers with different clast sizes or layers with alternating clast-supported and clast-dispersed texture. Open work texture was not observed in the deep-sea conglomerates.

Walker (1975a, b; 1977) proposed some generalized Bouma-like models for deep-sea conglomerates. The models were based on descriptors such as grading, statification and fabric. These models were later related by Walker (1978) to positions on a submarine fan. The models have changed little since they were proposed, but it should be noted that they are based on a limited amount of data.

They are ~~denigrated~~ by Shell Oil.

The non-marine and deep marine environments both deposit gravels in channels with associated bar complexes. The details of the morphology of the erosion surface preserved in the Carrot Creek -- Cyn-Pem study area does not support the presence of channels (Chapter 4). The textural sequences preserved in the conglomerates and the vertical and lateral relationships (described in Chapters 6 and 7) do not support either of these depositional settings. The only major depositional environment remaining is the coastal setting. Deposition of the conglomerates in this environment is supported by the morphology of the erosion surface (refer to Chapter 4). This environment will be discussed in more detail.

5.3 WAVE-DOMINATED NEARSHORE GRAVELS

Models for fluvial and deep sea deposition of gravels are relatively well established compared with models for the depostion of gravels in the high energy, wave dominated near shore environment. Nearshore gravels can be sub-divided into two separate depositional environments; the beach and the shoreface. The majority of publications on beach gravels have been from modern beach conglomerates rather than from ancient beach conglomerates, while the opposite is true for shoreface deposits. Marine beach gravels are rarely preserved, in the geologic record compared with the shoreface deposits, because only a very rapid rise of sea level could bring beach gravels below the level where they could not be eroded or moved shoreward. Combined with this modern beach gravels are more easily observed than shoreface gravels.

A. BEACH GRAVELS

The focus of research on gravel beaches has been on;

1) particle sorting on the beach as a function of size and shape (Bluck, 1967, 1969; Carr et al., 1970; Dobkins and Folk, 1970; Orford, 1975; Orford and Carter, 1982),

2) longshore transport and sorting of pebbles (Carr, 1969; 1971), and

3) Distinguishing beach gravels from fluvial gravels (Dobkins and Folk, 1970; Clifton 1973; Wescott and Ethridge, 1980; Ethridge and Wescott, 1981; Leckie and Walker, 1982; Maejima, 1982 and Bluck, 1982).

1) Particle sorting by size and shape.

Bluck (1967) provided a detailed description of downbeach zonation of particle size and shape on the surface layers of several modern beaches in South Wales. He described four zones (Fig. 5.1); from the landward edge moving seaward they are, 1) a large disc zone, characterized by cobble sized discs, 2) the imbricate zone composed mainly of imbricate disc shape pebbles, 3) the infill zone where spherical and rod shaped pebbles infill a framework of spherical cobbles, and 4) the outer frame composed of a spherical cobble frame. This downbeach zonation of pebbles is broadly accepted by workers on modern beaches, the controversy revolves around the cause of this sorting. Bluck (1967) felt that particle shape differentiation on the beach was the result of sorting by beach processes. Orford (1975) tested Bluck's hypothesis, that the degree of downbeach shape zonations were dependent on the wave energy recieved by the beach. He found that pebble shape zonation appeared to be not only a function of wave energy expended on the beach, but also depended on the way in which the energy was expended in terms of wave phase and breaker type. Dobkins and Folk (1970) supported the hypothesis of shape zonation on the beach, however they suggested that marine abrasion rather than sorting was the chief cause for the abundance of discs on the beaches. Kirk (1980) concluded that both the source of the clasts and process

Figure 5.1. Textural zonation of beach gravels at Sker Point, Wales (from Bluck, 1967).

STORM BEACH: SKER POINT

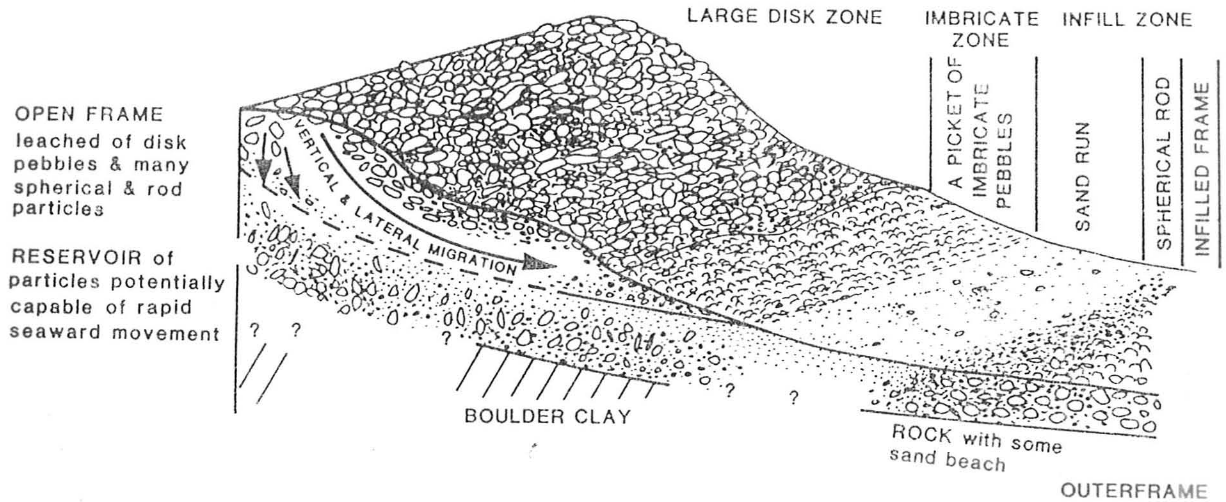

acting on the beach were important in determing particle-shape distribution on gravelly beaches. The results of this detailed work on modern beaches (sorting by particle size and shape, and its correlation with wave energy and type, and abrasion) have yet to be applied to ancient beach conglomerates.

2) Longshore transport and sorting of pebbles.

Carr (1969; 1971) discussed aspects of size grading, sorting, and transport of pebbles alongshore at Chesil Beach, England. Carr (1969) suggested that the alongshore pebble grading observed at Chesil beach was so pronounced because of the interaction of a number of features; firstly, the whole of the seaward face of the beach is subject to movement by breaking waves; secondly, the pebbles on the beach are subject to transport by longshore drift; thirdly, there is little addition new material pebble size and larger; and fourthly, most of the pebbles and cobbles are of flint and chert and have a similar specific gravity. Carr (1970) calculated rates of movement of 343 m per day for longshore transport of quartz granulites, but after 165 days the farthest distance travelled was only 3952 m from the origin. The lateral movement of individual pebbles was not believed to be necessarily greater under storm conditions. Carr (1970) found a linear correlation between pebble size (measured as long axis) and longshore movement over a short period of time. When the pebbles were spread over a greater distance, after a period of consistent wave approach in one direction, the pebbles were found to be distributed in an exponential relationship (Carr, 1970) with increasing size relative to distance moved. These papers considered only the processes on the exposed part of Chesil beach.

3) Distinguishing beach gravels from fluvial gravels.

Distinguishing features of beach and fluvial gravels were summarized by Ethridge and Wescott (1984, p. 221; Table 5.1). Gravel texture is probably the single most obvious feature used to distinguish beach and fluvial gravels. Pebbly beaches described from the Fahler Member of the Spirit River Formation, Central Alberta (Cant, 1984) are composed of well sorted, granular cherts, which may lack a matrix because of winnowing.

- Interpreted to be pebbly beaches!

Beaches may be classified as depositional or erosional (Wescott and Etheridge, 1980), on the basis of their morphology and textural characteristics. Erosional beaches by definition cannot be considered as areas of deposition; they are zones in which pre-existing deposits are modified by marine processes.

Depositional beaches are broad (15 to 50 m wide) and sandy with relatively gentle foreshore gradients (0.05 to 0.15). Grain size generally increases from the berm to the plunge point and decreases from the berm to the backshore. The sediments of depositional beaches include: 1) seaward

Table 5.1. Criteria for distinguishing beach gravels and fluvial channel gravels (data taken from Dobkins and Folk, 1970, and Clifton, 1973; after Etheridge and Wescott, 1981).

	Beach Gravels	Fluvial Gravels
* 1.	Well sorted	Poorly sorted
* 2.	Well segregated beds	Poorly segregated beds
* 3.	Continuous beds	Lenticular beds
* 4.	Gravels interbedded with gravelly sandstone - *rare*	Gravels interbedded with gravelly sandstone — *common*
* 5.	Erosional basal contacts - *rare*	Erosional basal contacts - *common*
* 6.	Repeated small-scale fining-up sequences - *rare*	Repeated small-scale fining-up sequences - *common* to *rare*
* 7.	Maximum clast size smaller than in adjacent channels	Maximum clast size larger than in adjacent beach
* 8.	Clayey or coaly laminae - *rare*	Clayey or coaly laminae - *common* to *rare*
9.	Imbrication - *seaward dipping*	Imbrication - *landward dipping*
10.	Sphericity - low	Sphericity - High
	Roundness - high	Roundness - low
* 11.	Horizontal beds of different size gravels or swash laminations	Horizontal beds or high angle trough cross-beds

* denotes criteria that can be identified in core

dipping, low angle thinly bedded units of sand in the foreshore zone; 2) horizontally bedded sand units in the berm and on the flat backshore zones; 3) landward dipping, low angle thinly bedded units of sand in the backshore zone; and 4) horizontally bedded gravel units with imbricated pebbles interbedded with sand units in all three beach zones. These gravel units are particularly common in storm-berm and lower foreshore deposits.

Erosional beaches are narrow (10 to 18 m wide) and are composed of very coarse sand to boulder sized clasts, with comparatively steep foreshore gradients (0.12 to 0.19). Sediments comprising erosional beaches are lag or talus deposits resulting from the erosion of fluvial deposits along beach scarps and the winnowing of finer grain sizes by wave action. The deposits are clast supported and the pores are filled with poorly sorted sand size matrix.

anything that is forming a beach sand!

B. SHOREFACE GRAVELS

The shoreface has been defined in the modern environment (Barrell, 1912) as the relatively steeply dipping, innermost portion of the continental shelf. The base of the shoreface is taken at the break in slope where the more steeply dipping shoreface merges with the relatively flat inner shelf. This break in slope generally occurs in water depths of about 15 to 20 m, the depth varies with the rigour of waves and currents. In the ancient rock record the base of the shoreface is taken as the point where sands pass seaward into muds. Walker (1985a) suggested that this transition was controlled by fairweather wave base, which is normally shallower than 20 m. The average thickness of a number of ancient sandstone deposits interpreted as shoreface deposits (discussed in Walker, 1985a) was 11 to 13 m. The depth values from both the modern environment and the ancient record suggest that the depth of the shoreface is about 10 to 20 m, and varies with the wave and current climate.

The shoreface may be sub-divided into two broad areas, based on the processes operating in these two areas. The lower shoreface is dominated by marine currents. Wave orbital currents are important in agitating the bottom, but generally will not result in net sediment transport. The upper shoreface is dominated by shoaling and breaking waves and less by marine currents. The boundary between these to areas is transitional, and is related to the intensity of waves and marine currents. In terms of effect on the bottom however, the transition generally occurs in depths of 10 to 15 m.

Conglomeratic deposits in the shoreface would be expected to reflect dominantly onshore-directed transport on the lower shoreface, with the increasing importance of longshore and offshore transport on the upper shoreface (Bourgeois and Leithold, 1984). Conglomerates of the lower shoreface tend to be associated with hummocky cross stratification (Nemec and Steel, 1984), and may include cross bedded conglomerate and pebbly sandstones. Upper shoreface deposits may reflect onshore, offshore or longshore processes. Deposits of the upper shoreface (Nemec and Steel, 1984) are generally clast supported conglomerate sheets, and are often normally graded. Trough cross bedded pebbly sandstones and high angle scours are often found in upper shoreface deposits.

Nearshore conglomeratic sequences with features suggestive of deposition on the shoreface have been described by several workers. Kumar and Sanders (1976) described crudely graded gravel layers in cores of shoreface sediments off Long Island, New York and interpreted these gravels as lag deposits formed during storm time. These beds were compared to similar features in the Quaternary and Tertiary sequences in New York, Virginia, and California. Dupre et al. (1980) described outer surf zone (lower shoreface) deposits in Pleistocene terraces of the Santa Cruz region, California, characterized by sand and fine gravel with landward and seaward dipping cross strata. Inner surf zone (upper shoreface) deposits in the same sequence were characterized by parallel laminated and cross bedded pebbly sand and by structureless gravel beds. Clifton (1981) interpreted rippled pebbly sandstone in Miocene strata of the Caliente Range, California to have been deposited in depths of about 8 m. He suggested that trough cross bedded pebbly sandstones and thin, laterally extensive gravel beds in these rocks were deposited in the surf zone of a high energy, nearshore system. Leckie (1983) and Leckie and Walker (1982) described "offshore gravel bars" (facies 8c of Leckie, 1983) from the Cretaceous Moosebar -- Lower Gates Formation of Alberta. These features were diagramatically suggested to have formed in depths ranging from 20 to 100 m. It was later suggested by Bourgeois and Leithold (1984) that these bars described by Leckie and Walker (1982) represent shoreface deposits. Leithold and Bourgeois (1984) described in detail shoreface gravels with examples from the Miocene of south-west Oregon. These examples are summarized by Bourgeois and Leithold (1984).

The marine shoreline environment allows the transport and deposition of gravel through the interaction of wave and marine current processes. This is reflected in the diversity of the preserved facies and the variability in the vertical sequence. The interaction of the shoreline processes is particularly true in the lower shoreface deposits where stratification tends to be better developed. The upper shoreface deposits are often massive to crudely stratified due to constant reworking of the clasts particularly during storm time. The next two chapters (chapters 6 and 7) will describe the conglomerate facies and facies sequences preserved in the Carrot Creek -- Cyn-Pem study area, and a discussion of how these facies and facies sequences are related to the processes operating on them. The areal distribution and lateral facies changes in the conglomerates will be discussed in terms of the relationship with the E5/T5 surfaces.

CHAPTER 6: FACIES DESCRIPTIONS AND FACIES SEQUENCES IN THE CARROT CREEK MEMBER

6.1 INTRODUCTION

One major purpose of this thesis is to examine the nature of the conglomerates preserved in the Carrot Creek area in terms of their geometry and aspect. A detailed description of the textures recognized in this facies, using both macroscopic features preserved in the core and petrographic descriptions, is presented in this chapter. Cardium conglomerates have been previously divided into three sub-facies by Walker (1983c), and Bergman and Walker (1986, in press), and into 8 sub-facies by Bergman (1984). These were preliminary classifications, based solely on core descriptions, therefore I suggest that in order to avoid confusion these earlier classifications be abandoned. The present scheme (Bergman, 1986, and this thesis) incorporates these previously recognized sub-facies.

The conglomerates have now been divided into 11 sub-facies, based on textures, pebble size, sorting, stratification, open work versus closed work, clast support versus matrix support, and the abundance of matrix. The Carrot Creek Member is composed of ten of these sub-facies; the gritty siderite (sub-facies 8 G.S.), described in Chapter 3, is not found in the Carrot Creek Member and will not be discussed in this chapter. Some of the sub-facies have been further subdivided into smaller units to distinguish more subtle features. These have not been designated as new sub-facies in order to preserve the affinity of the unit with the parent sub-facies.

An interpretation of the individual textural varieties described herein will not be given, unless well defined sedimentary structures are preserved. These structures will be identified in the description of the sub-facies. The preserved textures form as the result of the interaction of a variety of processes operating in the shoreface environment (section 4.8 of this thesis). The conglomerate sequences will be sub-divided into three types, based on the textural varieties preserved in the conglomerate sequence. The conglomerates textures preserved in these sequence types will be interpreted with respect to their position in the prograding and transgressive shoreface profile. In Chapter 7 the lateral facies relationships and the areal distribution of the conglomerates will be discussed in terms of the position in the shoreface and the relationship to the erosion surface.

6.2 DESCRIPTIONS

A summary table (Table 6.1) of the textural varieties preserved in the conglomerate is presented from both petrographic and core data. The percent porosity and matrix (Table 6.1) were also determined from thin section. These were determined as the intercept length. Three

Table 6.1. Summary table of the characteristics of the conglomerate textures observed in thin section.

TABLE 6.1: SUMMARY OF PETROGRAPHIC DESCRIPTIONS

SUB-FACIES	GRAIN SIZE (Ø UNITS)	SORTING	CLAST/MATRIX SUPPORTED	MATRIX COMPOSITION	% MATRIX	% POROSITY	ROUNDNESS	STRATIFICATION
$8C_1$	$\bar{X}$ = -0.66 (2.32 to -4.26)	σ = 0.195 moderate-poor	CLAST	VFU QUARTZ	3.6	13.5	well rounded to rounded	none observed
$8C_2$	$\bar{X}$ = -1.12 (0.74 to -3.54)	σ = 0.155 moderate	CLAST	VFU QUARTZ	3.8	10.7	well rounded to rounded	none observed
$8C_3$	$\bar{X}$ = -0.30 (2.32 to -3.58)	σ = 0.069 well sorted	CLAST	VFU QUARTZ	0.5	11.3	rounded to sub-rounded	none observed
8D	$\bar{X}$ = -0.96 (2.32 to -3.89)	σ = 0.151 moderate	CLAST	VFU QUARTZ	12.9	0.0	rounded to sub-rounded	none observed
8E	$\bar{X}$ = -1.09 (2.32 to -3.83)	σ = 0.165 moderate	CLAST	VFU QUARTZ	25.0	0.8	well rounded to sub-rounded	none observed
8F	$\bar{X}$ = -1.70 (0.74 to -3.26)	σ = 0.245 poorly sorted	MATRIX	VFU QUARTZ	90.0	0.0	well rounded to sub-rounded	crude to good inclined
$8G_1C$	$\bar{X}$ = -0.46 (2.32 to -3.58)	σ = 0.122 good	CLAST	VFU QUARTZ	1.95	11.9	well rounded to sub-rounded	good inclined
$8G_1F$	$\bar{X}$ = -0.12 (2.32 to -3.70)	σ = 0.073 well sorted	CLAST	VFU QUARTZ	10.0	6.0	sub-rounded	
$8G_2C$	$\bar{X}$ = -1.02 (2.32 to -2.77)	σ = 0.143 good-moderate	MATRIX	VFU QUARTZ	37.9	0.0	well rounded to sub-rounded	crude inclined
$8G_2F$	$\bar{X}$ = -0.25 (1.32 to -1.68)	σ = 0.060 well sorted	MATRIX	VFU QUARTZ	57.0	0.0	sub-rounded	none observed
$8K_L$	$\bar{X}$ = -0.59 (2.32 to -3.61)	σ = 0.163 moderate	CLAST	VFU QUARTZ	6.8	8.9	well rounded to sub-rounded	massive
$8K_U$	$\bar{X}$ = -0.14 (2.32 to -3.98)	σ = 0.156 moderate	CLAST	VFU QUARTZ	2.9	4.9	well rounded to sub-rounded	massive

traverses were made per thin section. The average of the three values was used as the percent porosity and matrix.

The grain size distribution curves for each sub-facies analyzed is shown in Figure 6.1. Grain size analysis was done from thin section on each sub-facies for purely descriptive puposes. Grain size distribution was determined from large thin sections, one from each facies where possible. These sections are shown along with core photos of each of the conglomerate textures. The thin sections were used as a negative to make an enlarged (5 times) print. The long axis of every grain longer than 1 mm on the print (or 0.2 mm in the thin section) was measured directly from the photo.

The measurements were entered and stored in a grain size program written in Turbo Pascal. The program was written to

1, store the data in a database,

2, convert the measured values into real values (i.e., divide the data set by 5),

3, calculate the mean and standard deviation (sorting), and

4, plot the cummulative distribution curve as a histogram.

The grain size (Ø units) was plotted against the percent number frequency (Fig. 6.1).

No attempt will be made to interpret the size analyses

Figure 6.1. Graph of the grain size (Ø units) versus the number percent frequencey for each of conglomerate sub-facies analysed in thin section. The median grain size is given for each curve when known. All curves are truncated at 1 Ø unit. A scale is given for the grain size under the first curve. C = coarser bed, F = finer bed, U = upper part of the sub-facies, L = lower part of the sub-facies.

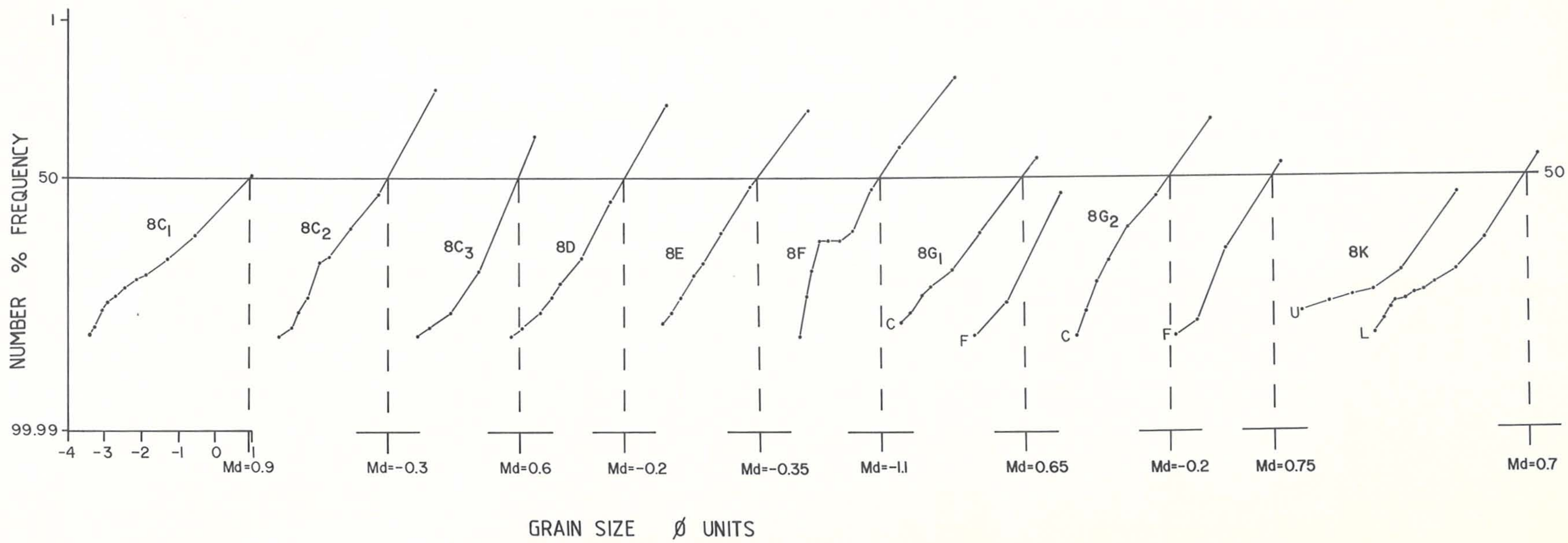

NUMBER % FREQUENCY
1
50
99.99
-4
-3
-2
-1
0
1
8C1
8C2
8C3
8D
8E
8F
8G1
8G2
8K
C
F
U
L
50
Md=0.9
Md=-0.3
Md=0.6
Md=-0.2
Md=-0.35
Md=-1.1
Md=0.65
Md=-0.2
Md=0.75
Md=0.7
GRAIN SIZE Ø UNITS

hydrodynamically. The sample size used in the determination of the grain size distribution was too small (limited to one large thin section per sub-facies) to be considered valid for hydrodynamic interpretations. Experimental work on coarse clastics is limited, and is mostly devoted to unidirectional flow situations. There is some experimental work on the initiation of motion of gravels in oscillatory flow conditions (Komar and Miller, 1973). A good summary of hydrodynamics and sediment transport is presented by Middleton and Southard, (1985).

Sub-Facies 8A -- Interbedded Pebbles, Sand, and Mud

This facies is generally found at the base of the conglomerate sequence. It can be divided into 3 units based on the type of material with which the conglomerate layers are interbedded (i.e., sand and mud, sand, and mud). The textural variety preserved in the conglomerates varies from bed to bed.

Unit $8A_1$ -- Interbedded Pebbles, Sand, and Mud (Fig. 6.2)

This is the most complexly interbedded of the three units. It is composed of 5 types of layers:

1) mud with sandy beds
2) mud with sandy beds and pebbles
3) sand beds
4) sand beds with floating pebbles
5) conglomerate beds.

Figure 6.2. Sub-facies 8A1 -- Interbedded Pebbles, Sand and Mud

A) Photo is taken from well 6-31-53-13, 1559 m. Scale bar is 3 cm. B) Photo is taken from well 2-29-52-13, 5456 ft. Core is 3 in. wide. C) Photo is taken from well 13-30-51-10, 1569 m. Scale bar is 3 cm. D) Photo is taken from well 13-30-51-10, 1568 m. Core is 3 in. wide.

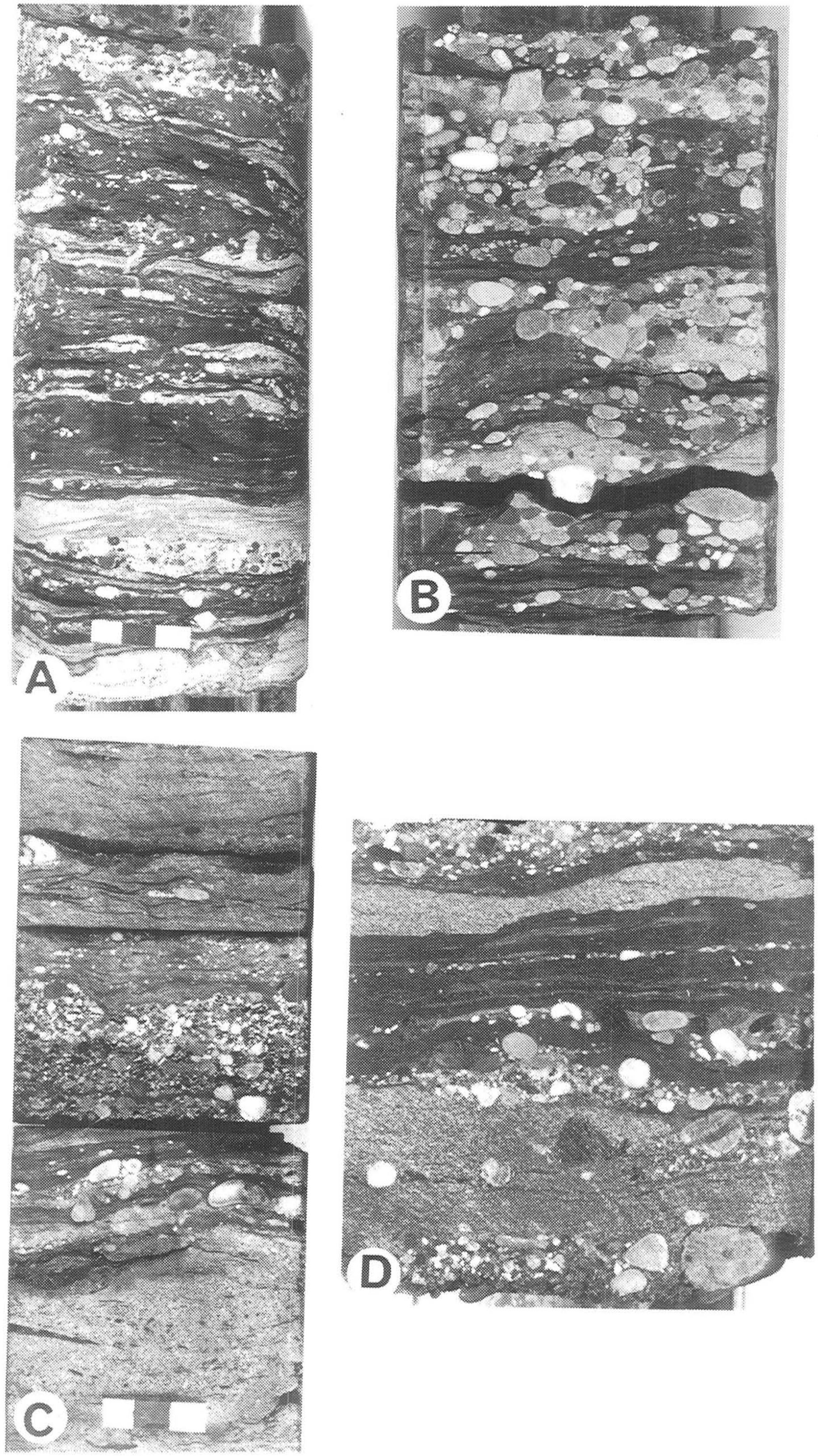
A
B
C
D

These five types of layers are variably interbedded. The interbedding is visible due to the alternation of coarse and fine beds. Abundant carbonaceous material (commonly wood fragments) and coalified wood fragments are often associated with this unit. The unit generally initiates the conglomerate sequence.

Bed thickness is on the scale of cm (3-4 cm maximum; generally only 1-2 cm thick). Stratification may be flat lying to low angle (to an observed maximum of about 17°) inclined. The thicker beds have sharp bases and grade upwards into the muddier beds. Some of the conglomerate beds are not graded, but are sharply draped with mud.

The chert grains range from sub-rounded coarse sand to well rounded pebbles with a long axis diameter of about 2.0 cm. The conglomerate beds are poorly sorted. No preserved orientation of the grains was observed. The matrix is very fine quartz sand. The sand also forms beds within the mudstone.

The muddy layers separating the coarser layers may contain sandy lenses (less than 1 mm thick), or a few scattered chert grains. In some instances the muds are black, with very little scattered coarse material, and appear to be composed of mud rip up clasts. Bioturbation is present.

Unit $8A_2$ -- Interbedded Pebbles and Sand (Fig. 6.3)

This unit is similar to unit $8A_1$, except that there are

Figure 6.3. Sub-facies $8A_2$ -- Interbedded Pebbles and Sand A) Photo is taken from well 6-31-53-13, 1557 m. Scale bare is 3 cm. B) Photo is taken from well 12-29-50-9, 1548 m. Scale bar is 3 cm. C) Photo is taken from well 13-30-51-10, 1568 m. Core is 3 in. wide. D) Photo is taken from well 6-29-52-13, 5458 ft. Core is 3 in. wide.

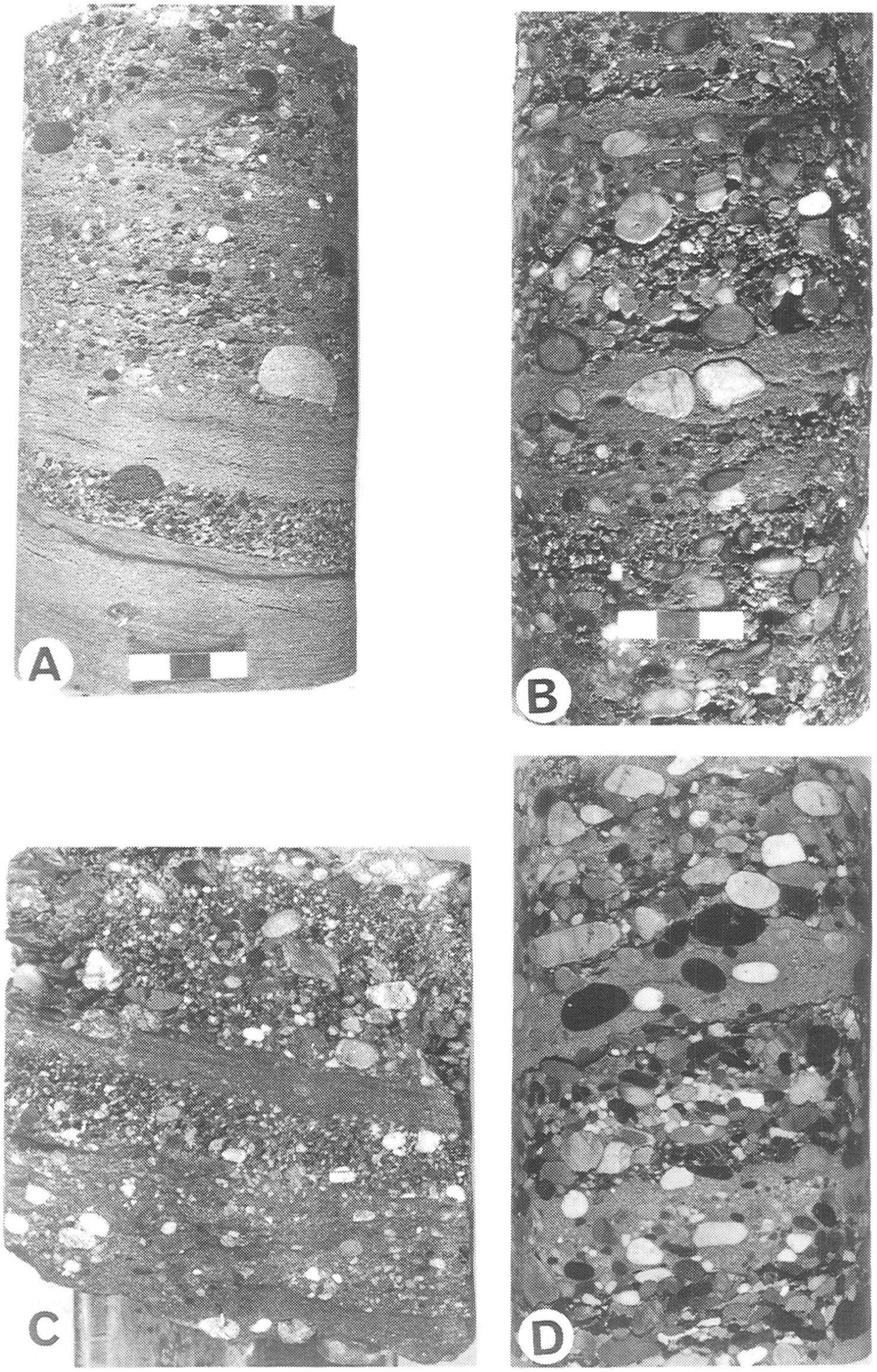
A
B
C
D

no muddy layers preserved. There may be a few shale partings and mud rip up clasts. The unit is composed of sharp based clast supported conglomerate beds grading into sandstone beds, or sandstone beds with a few chert pebbles. The beds may be flat lying to low angle inclined. Often carbonaceous debris (primarily wood) and coalified fragments are found in this unit.

The bed thickness of the conglomerates increases upwards from 2 to 5 cm at the base to 15 cm at the top. No discernable preserved fabric was observed. The conglomerate is poorly sorted with round to well rounded chert pebbles ranging in size from a long axis diameter of less than 1.0 cm to 3.5 cm.

The sandier facies are composed of very fine quartz sand, and may have well rounded floating chert pebbles (1-2 cm). The pebbles lie in the plane of the stratification where present. Bed thickness varies from 2 to 5 cm.

This unit generally overlies unit $8A_1$, or alternates with it.

Unit $8A_3$ -- Interbedded Pebbles and Mud (Fig. 6.4)

This unit differs from unit $8A_1$ by having less than 5% sand. It is composed of clast supported conglomerate beds interbedded with black mud. The conglomerate beds are poorly sorted, and are composed of well rounded chert pebbles with a mean long axis diameter of 1 to 2 cm. No preferred orientation of the grains was observed.

Figure 6.4. Sub-facies 8A3 -- Interbedded Pebbles and Mud A) Photo is taken from well 14-34-50-10, 4966 ft. B) Photo is taken from well 10-16-51-11, 5456 ft. Both photos are taken from 3 in. drill core.

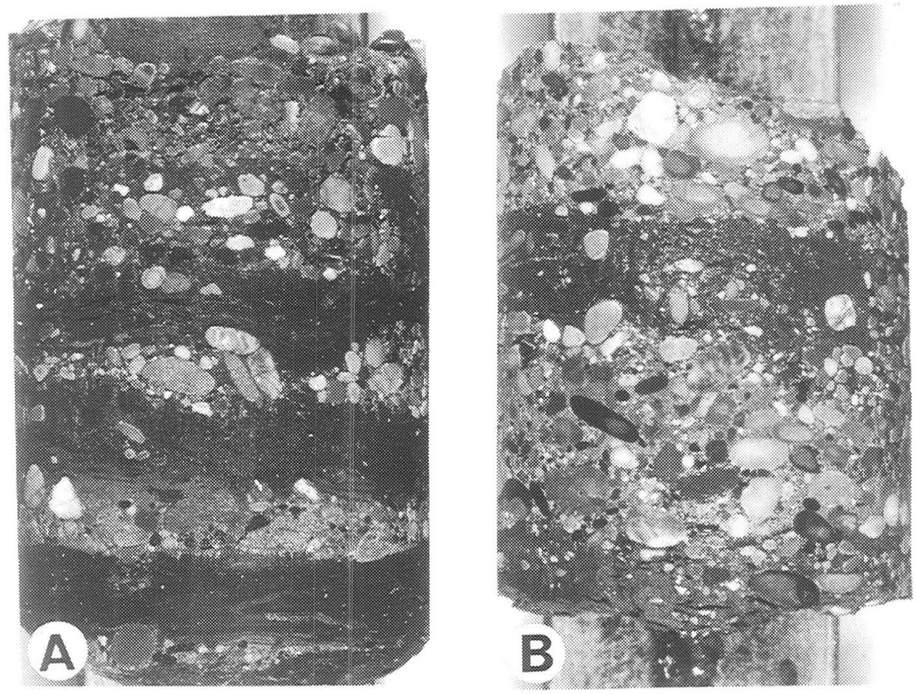
A
B

Both the conglomerate and mudstone bed thicknesses are in the 1 to 2 cm range. In many cases the beds have been reworked or the pebbles have sunk into the underlying muds, leaving only remnant conglomerate beds. The presence of this remnant bedding is the primary distinguishing feature between this unit and facies 8B.

Sub-Facies 8B -- Pebbly Mudstone (Fig. 6.5)

This facies is characterized by pebbles "floating" in mud, with no hint of an original stratification. The upper and lower contacts are gradational. The thickness of this facies varies considerably, but is generally within the range of 20 to 30 cm. This facies is poorly sorted, containing rounded to well rounded chert pebbles varying in size from a long axis diameter of 0.5 to 6.0 cm. In general the pebbles tend to be large compared with those of other facies. No discernable preferred fabric was observed, with pebble orientation ranging from horizontal to vertical.

Sub-angular, medium to coarse chert grains are found in varying amounts. There is less than 5% silt.

This facies is found at the top of the thick conglomerate sequence, and at the top of each of the overlying bioturbated mudstone facies (Facies 3P, 4P, and 5P). This facies does exhibit some variability in thickness, particularly in the overlying bioturbated facies (i.e., Facies 3P, 4P, and 5P), but no regional trends were observed. In some cases there is no thick clast supported

Figure 6.5. Sub-facies 8B -- Pebbly Mudstone

A) Photo is taken from well 16-33-50-10, 5052 ft. B) Photo is taken from well 4-9-52-12, 5534 ft. C) Photo is taken from well 12-36-50-10, 4929 ft. Above three photos were all taken from 3 in. drill core. D) Photo is taken from well 14-34-50-10, 4965 ft. Scale bar is 3 cm.

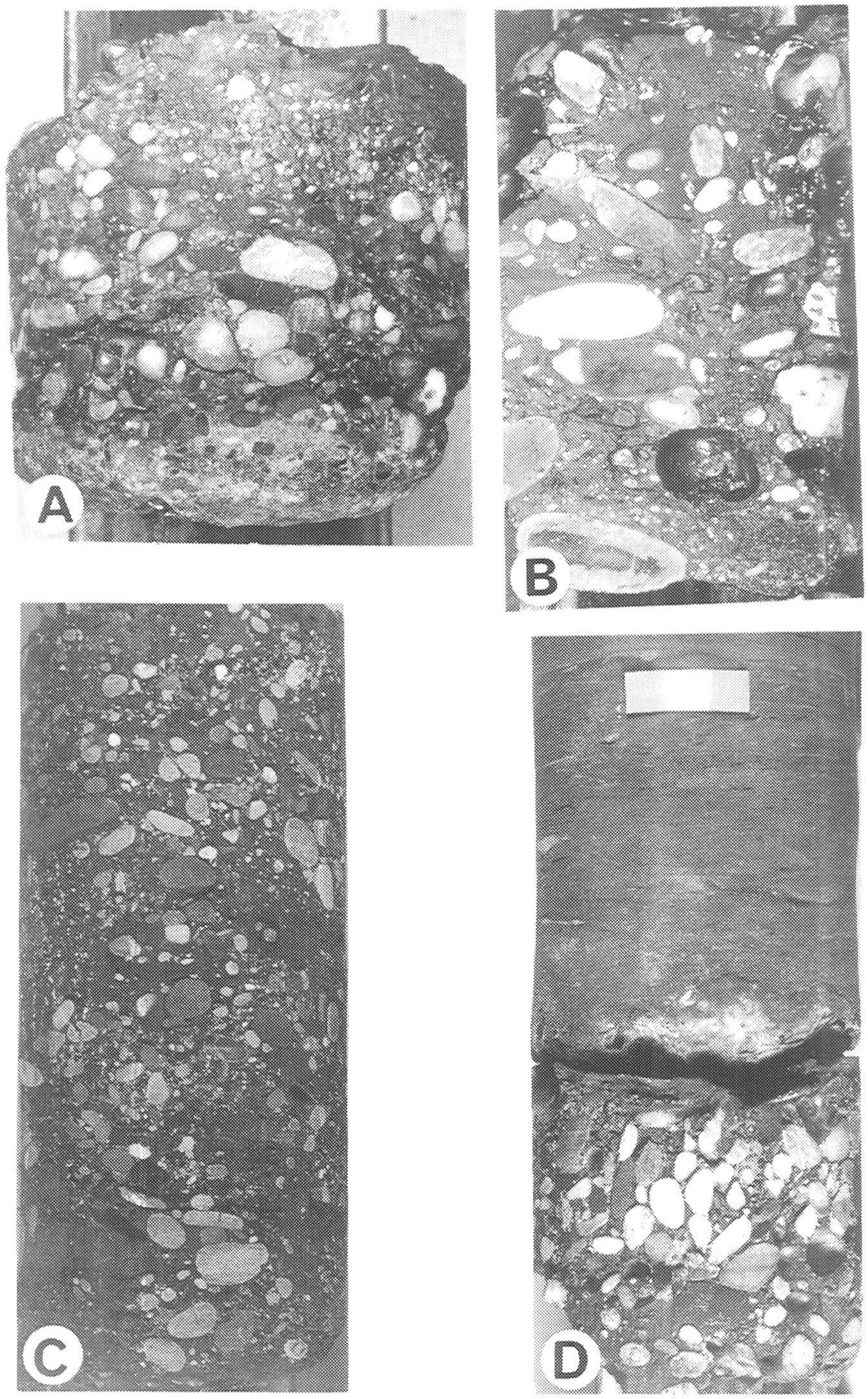
A
B
C
D

conglomerate; here the pebbly mudstone is the only record of coarse deposition. Technically this facies should be included in the Dismal Rat Member as the base of this sub-facies is the T5 surface.

Sub-Facies 8C -- Open Work

This facies has the highest porosity (13.5 %) of all those observed. It consists of clast supported conglomerate containing chert grains, with less than 5% very fine quartz sand matrix. The facies has been divided into 3 units, separated on the basis of grain size and sorting.

Unit $8C_1$ -- Coarse Grained, Open Work (Fig. 6.6)

This is the coarsest of the three units. Chert pebbles measured from core have a long axis diameter of 1 to 2 cms, are well rounded and ellipsoidal in shape. This unit may have larger pebbles floating in the framework, but in general is moderately sorted. Sub-rounded, very coarse chert sand is found in the pore spaces between the larger pebbles.

Bed thickness is variable, but is generally 2 to 5 cm. Beds are sharp based with tops that grade into sub-facies $8C_2$, $8C_3$, or 8E. No preferred fabric was recognized, with pebbles horizontal to vertical.

There is no mud associated with this unit. Sutured contacts may develop between chert grains, but are rare.

Unit $8C_2$ -- Mixed Grained, Open Work (Fig. 6.7)

This unit is intermediate between unit $8C_1$ and unit

Figure 6.6. Sub-facies $8C_1$ -- Coarse Grained Open Work
A) Photomicrograph is taken from well 16-30-53-13, 1558 m. Slide is 6.3 cm wide. B) Photo is taken from well 9-3-52-11, 1579 m. Core is 3 in. wide. C) Photo is taken from well 16-30-53-13, 1558 m. Scale bar is 3 cm.

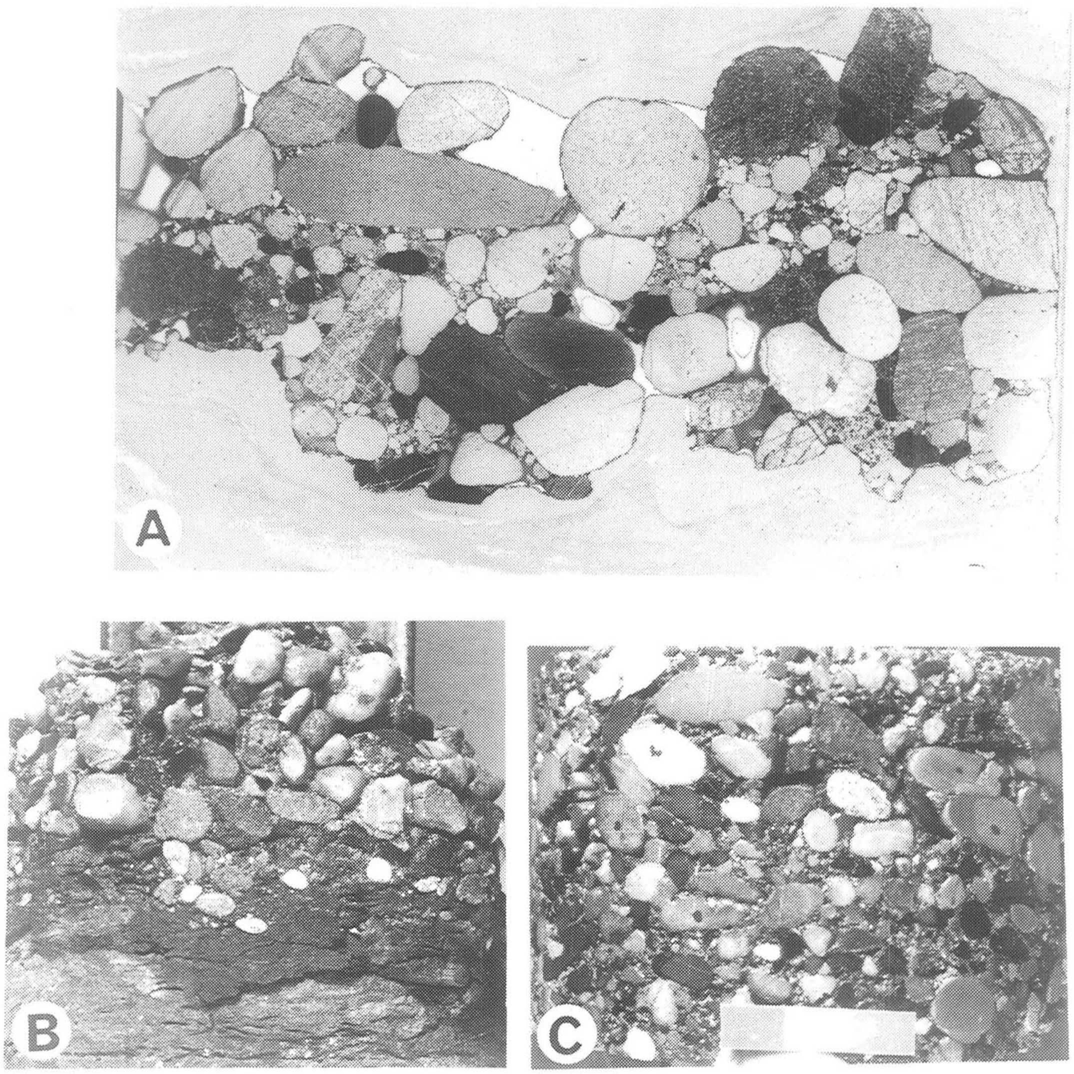
A
B
C

Figure 6.7. Sub-facies $8C_2$ -- Mixed Grained Open Work

A) Photomicrograph is taken from well 13-30-51-10, 1563 m. Slide is 3.9 cm wide. B) Photo is taken from well 9-3-52-11, 1571 m. C) Photo is taken from well 13-30-51-10, 1563 m. Both photos are taken from 3 in. drill core.

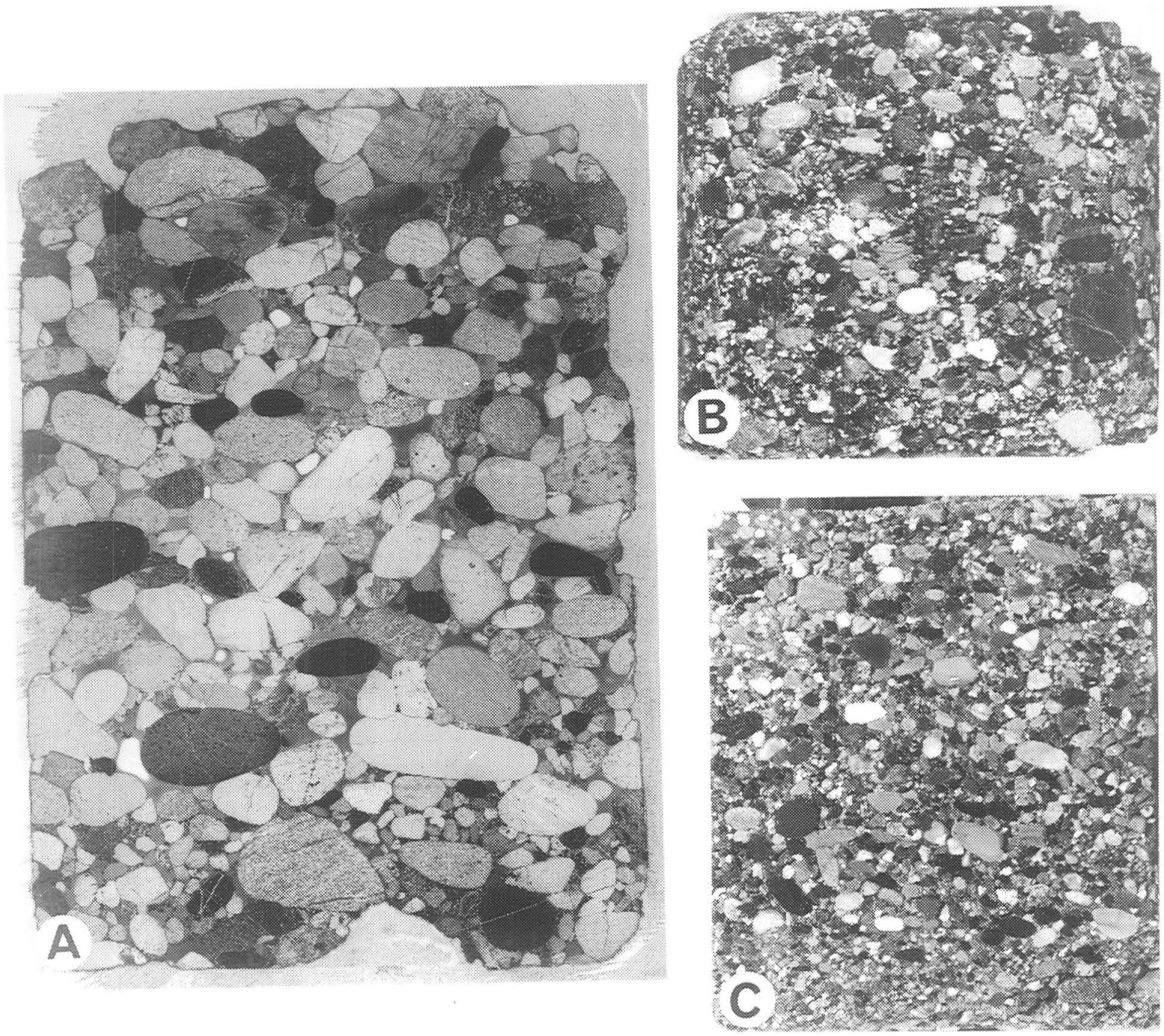

A
B
C

$8C_3$, and has a more variable aspect. Chert pebbles measured from core have a long axis diameter of 1 to 2 cms, are well rounded and ellipsoidal in shape. Some larger pebbles may be found floating in the unit. Sub-rounded, very coarse chert sand is found in the pore spaces between the larger pebbles. It is moderately sorted.

Bed thickness is variable, but generally ranges from 2 to 5 cm. The lower contact may or may not be sharp, depending on the nature of the underlying facies. No preferred fabric was observed, with clasts horizontal to inclined. This unit is often found associated with facies 8E.

Unit $8C_3$ -- Fine Grained, Open Work (Fig. 6.8)

This is the finest grained of the three units, composed of sub-rounded to sub-angular, very coarse chert sand. Some larger (0.5 to 1 to 2 cm) rounded to well rounded chert pebbles are often found floating in the unit. Rounded to sub-rounded chert granules have a long axis diameter of 0.1 cm. The unit is very well sorted.

Bed thickness is variable from 2 cm to greater than 14 cm. The unit is generally sharp based, and may show grading (normal or inverse). There was no preferred orientation of the grains observed. Mud is not associated with this unit. This unit is found associated with facies 8E, or gradational from $8C_1$ through $8C_2$.

Figure 6.8. Sub-facies $8C_3$ -- Fine Grained Open Work

A) Photomicrograph is taken from well 13-30-51-10, 1564 m. Slide is 6.1 cm wide. B) Photo is taken from well 9-3-52-11, 1578 m. C) Photo is taken from well 13-30-51-10, 1564 m. Both photos are taken from 3 in. drill core.

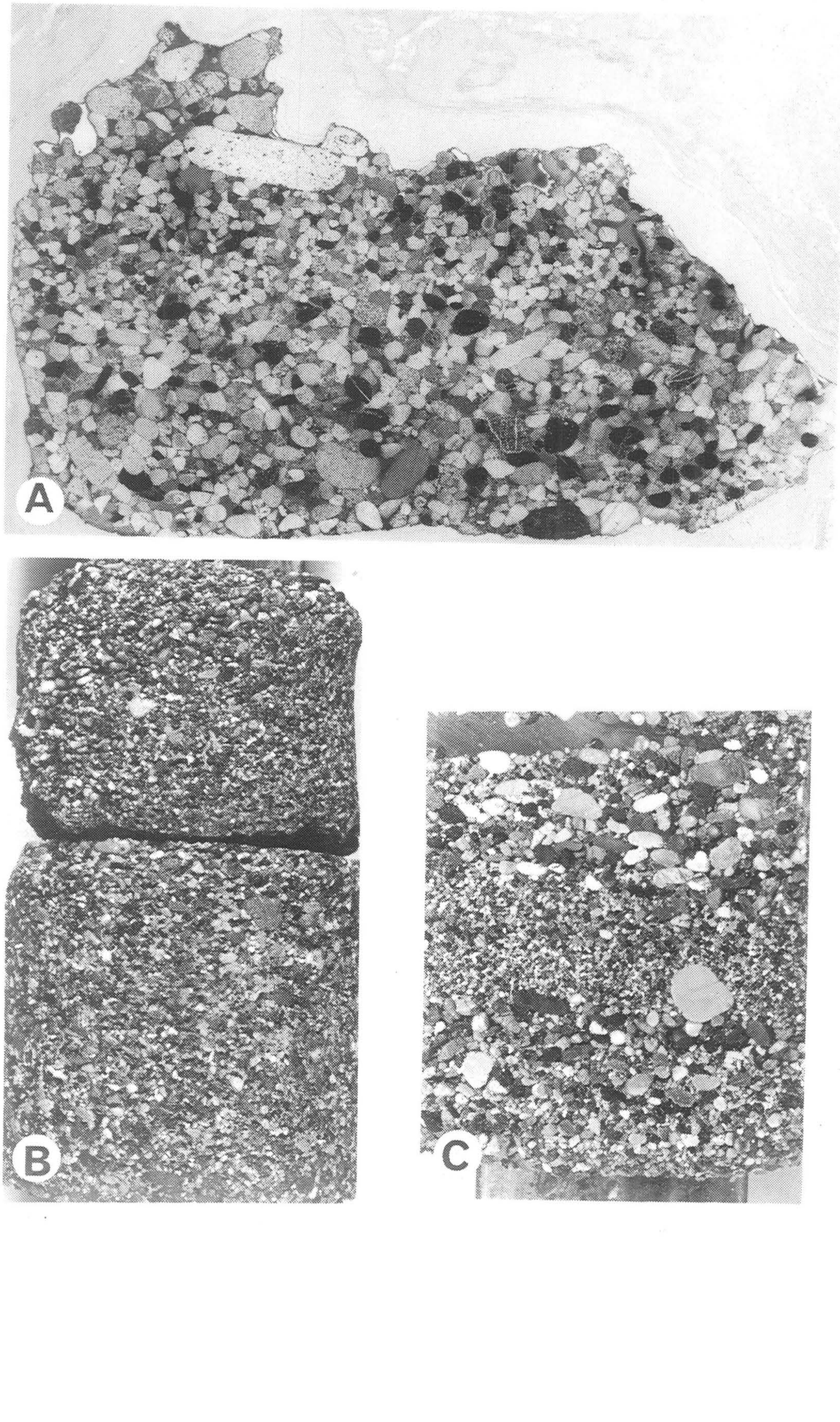
A
B
C

Sub-Facies 8D -- Closed Work (Fig. 6.9)

This is a clast supported facies. The upper and lower contacts are sharp. Bed thickness varies from 4 to 5 cm. This unit was not common in the study area.

The rounded to well-rounded chert pebbles measured in core range in size from less than 1.0 to approximately 2.0 cm. This facies is moderately sorted. The cherts show abundant grain to grain contacts; concave and microstylolitic contacts are common in this facies. Many of the chert pebble margins are corroded. There was no preferred orientation of the pebbles observed.

A very fine grained sand matrix of sub-angular quartz packs the interstices between the chert pebbles. There is no primary porosity preserved. Some clay minerals are present, accounting for the insoluble residue remaining on the microstylolitic contacts, and the corrosion of the chert pebble boundaries.

Generally, the unit is found in the lower interbedded part of the conglomerate sequence.

Sub-Facies 8E -- Closed Work, Matrix (Fig. 6.10)

This facies is similar to 8D but has greater percentage of sand matrix. The lower contact is generally gradational, while the upper contact is sharp or may grade into sub-facies 8F. Bed thickness is highly variable, ranging from cms to tens of cms. The sand content, the sedimentary structures preserved, grading and fabric are extremely

Figure 6.9. Sub-facies 8D -- Closed Work

A) Photomicrograph is taken from well 2-29-52-13, 5459 ft. Note the abundance of microstylolitic grain contacts associated with this facies. Slide is 3.4 cm wide. B) Photo is taken from well 2-29-52-13, 5459 ft. Scale bar is 3 cm. C) Photo is taken from well 2-29-52-13, 5460 ft. Core is 3 in. wide.

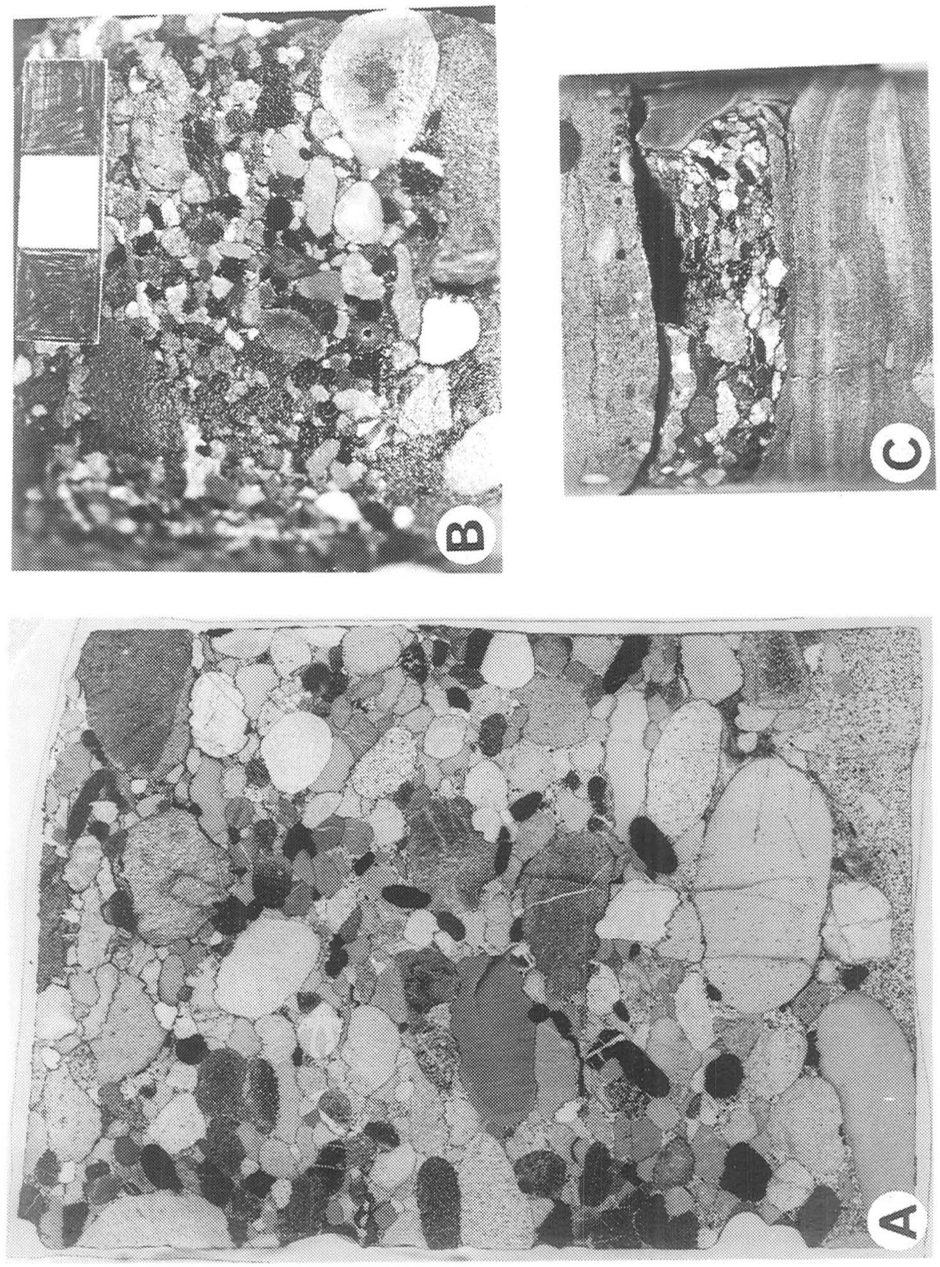
B
C
A

Figure 6.10. Sub-facies 8E -- Closed Work, Matrix

A) Photomicrograph is taken from well 16-30-53-13, 1560 m. Slide is 5.9 cm wide. B) Photo is taken from 2-29-52-13, 5455 ft. C) Photo is taken from well 9-3-52-11, 1573 m. Both photos are taken from 3 in. drill core.

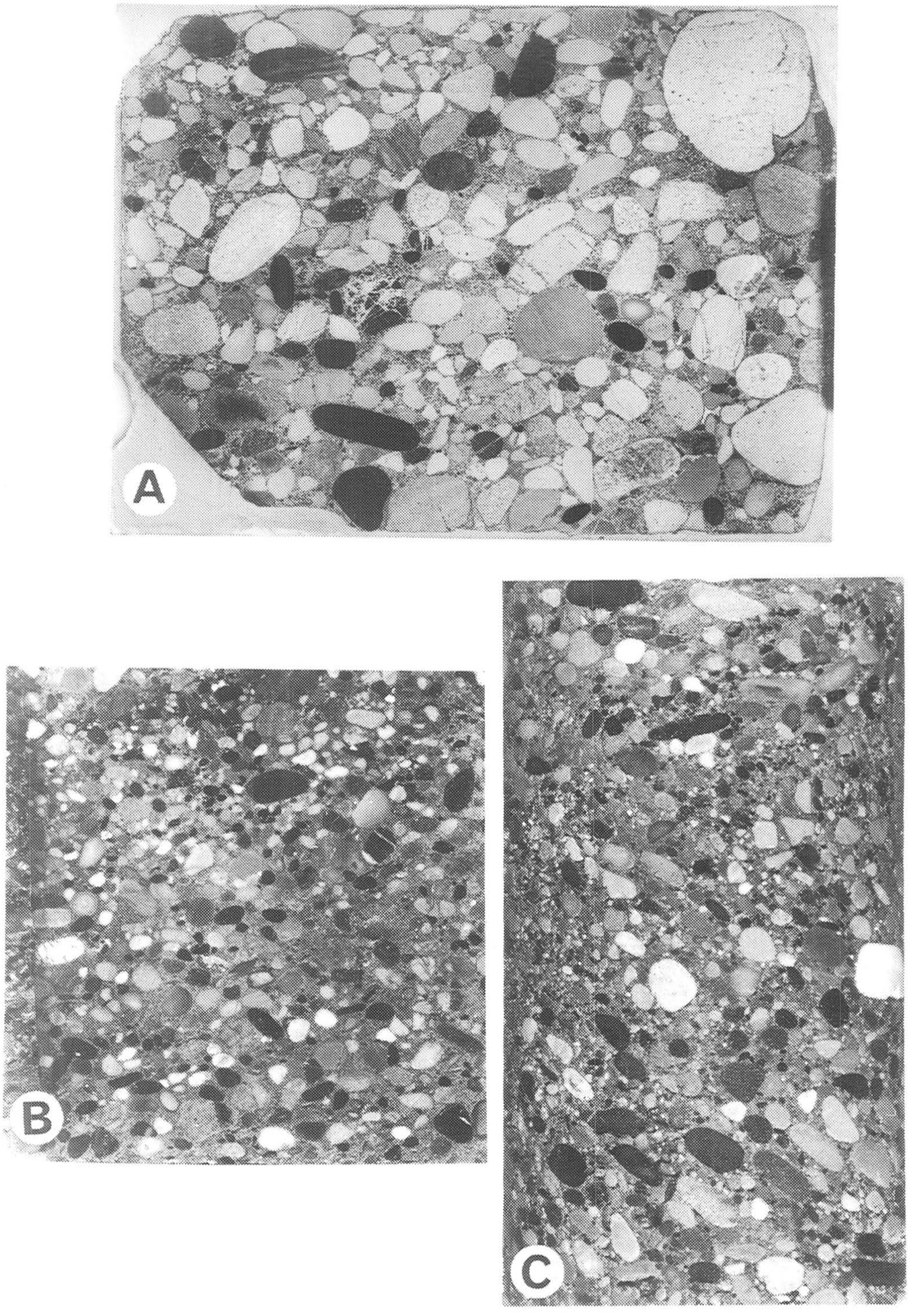
A
B
C

variable.

Sub-facies 8E is a clast supported, chert pebble conglomerate, with well-rounded ellipsoidal chert pebbles ranging in size from 0.4 to 3.5 cm. It is moderately sorted. The orientation of the pebbles was highly variable. In places no preferred orientation was observed, while in other areas the pebble fabric varied from flat lying to inclined. Pebbles with well developed imbrication may have angles as much as 50°. These pebbles have been observed to preserve both the "a" parallel - "a" imbricate ($a_{(p)}$, $a_{(i)}$) and the "a" transverse - "b" imbricate ($a_{(t)}$, $b_{(i)}$) fabric of Walker (1975). Size grading of the pebbles was not observed.

The matrix is composed of sub-angular very fine quartz grains. Very little mud is found in this facies, although some mud rip up clasts are present, as well as siderite nodules. Porosity is low (0.8%) and is sometimes occluded by microstylitization of the chert pebbles. This facies is associated with the openwork facies and is generally found overlying it or interbedded with the open work facies.

Sub-Facies 8F -- Pebbly Sandstone (Fig. 6.11)

This facies consists of pebbles "floating" in sand. The lower contact is sharp; the upper contact may be sharp or gradational. The thickness of this facies varies from 1.0 to 8.0 cms.

The pebbles consist of rounded to well-rounded,

Figure 6.11. Sub-facies 8F -- Pebbly Sandstone

A) Photomicrograph is taken from well 2-29-52-13, 5457 ft. Slide is 3.6 cm wide. B) Photo is taken from well 12-19-52-12, 1629 m. Core is 3 in. wide. C) Photo is taken from well 6-31-53-13, 1559 m. Scale bar is 3 cm.

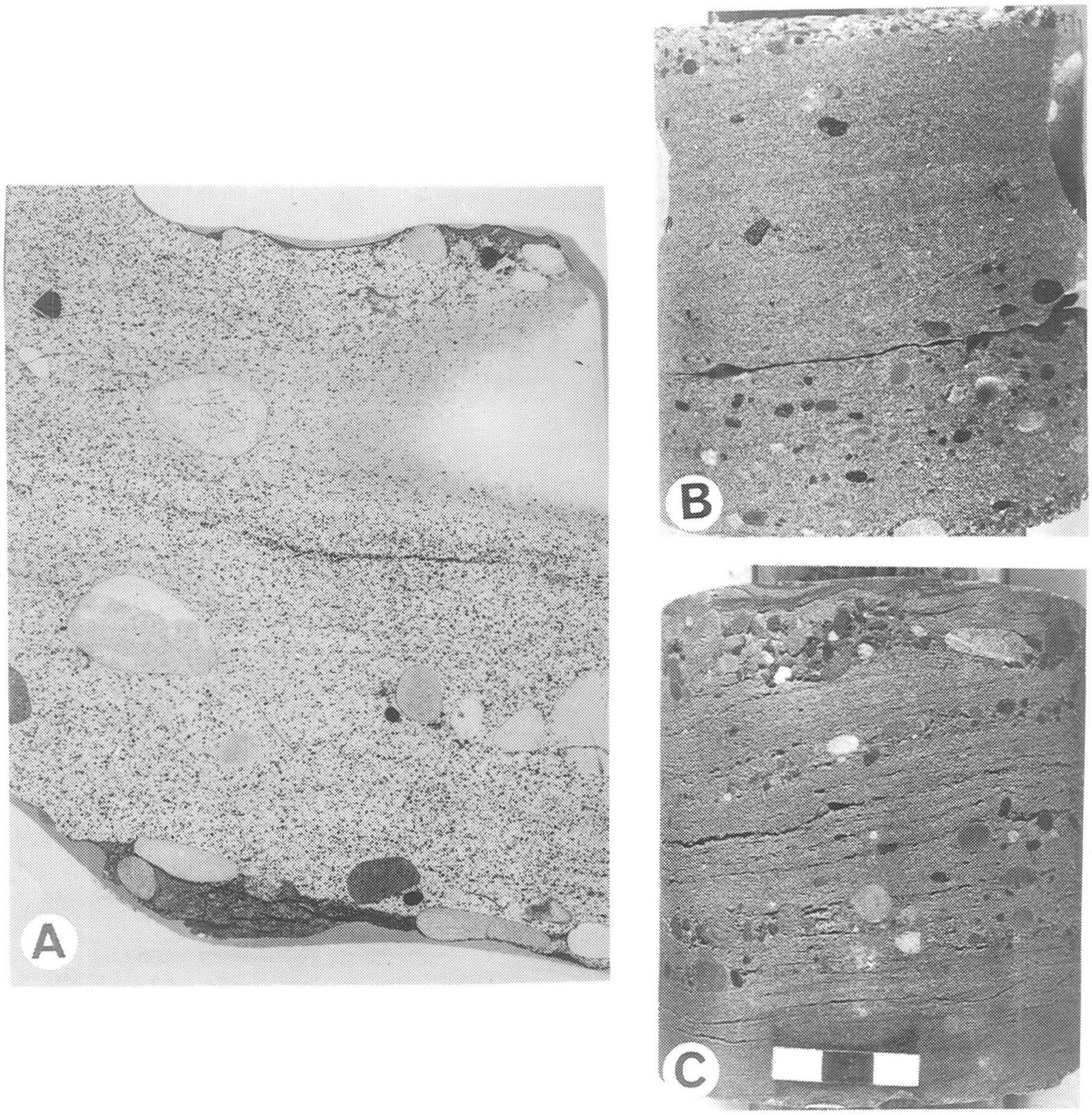
A
B
C

ellipsoidal cherts which vary from less than 1 cm to about 3 cm in diameter. The pebbles may be isolated or occur in a string along the stratification. The long axis lies in the plane of stratification of the sands. Sub-rounded coarse to very coarse chert grains may be present in this facies; their abundance is highly variable.

The sand is very fine quartz, and the grains are sub-angular to angular. The sands are generally parallel laminated, have low angle inclined stratification, or are wave rippled. The sands often have layers of carbonaceous and/or micaceous material concentrated on the bedding planes. Mud clasts are rarely present.

The pebbly sandstones (sub-facies 8F) generally occur lower in the conglomerate sequence, associated with the interbedded conglomerates. The low angle inclined stratification is interpreted as hummocky cross stratification and the pebbles are interpreted as lags at the base of these hummocky beds (see description in Dott and Bourgeois, 1982).

Sub-Facies 8G -- Interbedded Pebbles and Grits

This facies has been divided into two units, based on the amount of very fine quartz sand matrix. This facies shows a moderate to well developed stratification, marked by changes not only in pebble size, but also by changes in the percentage of matrix, and sorting.

Unit 8G1 -- Interbedded Pebbles and Coarse Sand (Fig. 6.12)

This unit is characterized by an interbedding of coarser grained and finer grained chert pebbles. Boundaries between beds are crude, but inclined stratification at about 17° is well developed. The pebbles lie in the plane of the stratification. Coarser beds appear to thin down dip across the width of the core (i.e., 2.5 to 1.5 cm and 2.6 to 0.6 cm), while the finer beds thicken down dip (0.4 to 1.4 cm). The angle of dip tends to become shallower upwards. This inclined stratification is interpreted as trough cross bedding. The minimum thickness of this sub-facies is 0.5 m, but the upper and lower contacts were commonly missing; much of the core now consists of cut plugs.

The well rounded chert pebbles have an average long axis diameter of 1.0 to 2.5 cm, measured from core. The coarse beds are moderately sorted. Bed thickness is relatively constant at 2.5 cm, with sharp bases and gradational tops.

The finer beds are composed of sub-angular to sub-rounded, medium to coarse chert sand. These beds are well sorted. The upper and lower contacts are sharp. The thickness varies from 0.5 to 1.0 cm upwards. There is an increase in the amount of matrix from the coarse layer and a decrease in the porosity.

Figure 6.12. Sub-facies $8G_1$ -- Interbedded Pebbles and Coarse Sand

A) Photomicrograph is taken from well 13-30-51-10, 1559 m. Slide is 3.9 cm wide. B) Photo is taken from well 13-30-51-10, 1559 m. C) Photo is taken from well 7-13-51-13, 1796 m. Scale bar is 3 cm.

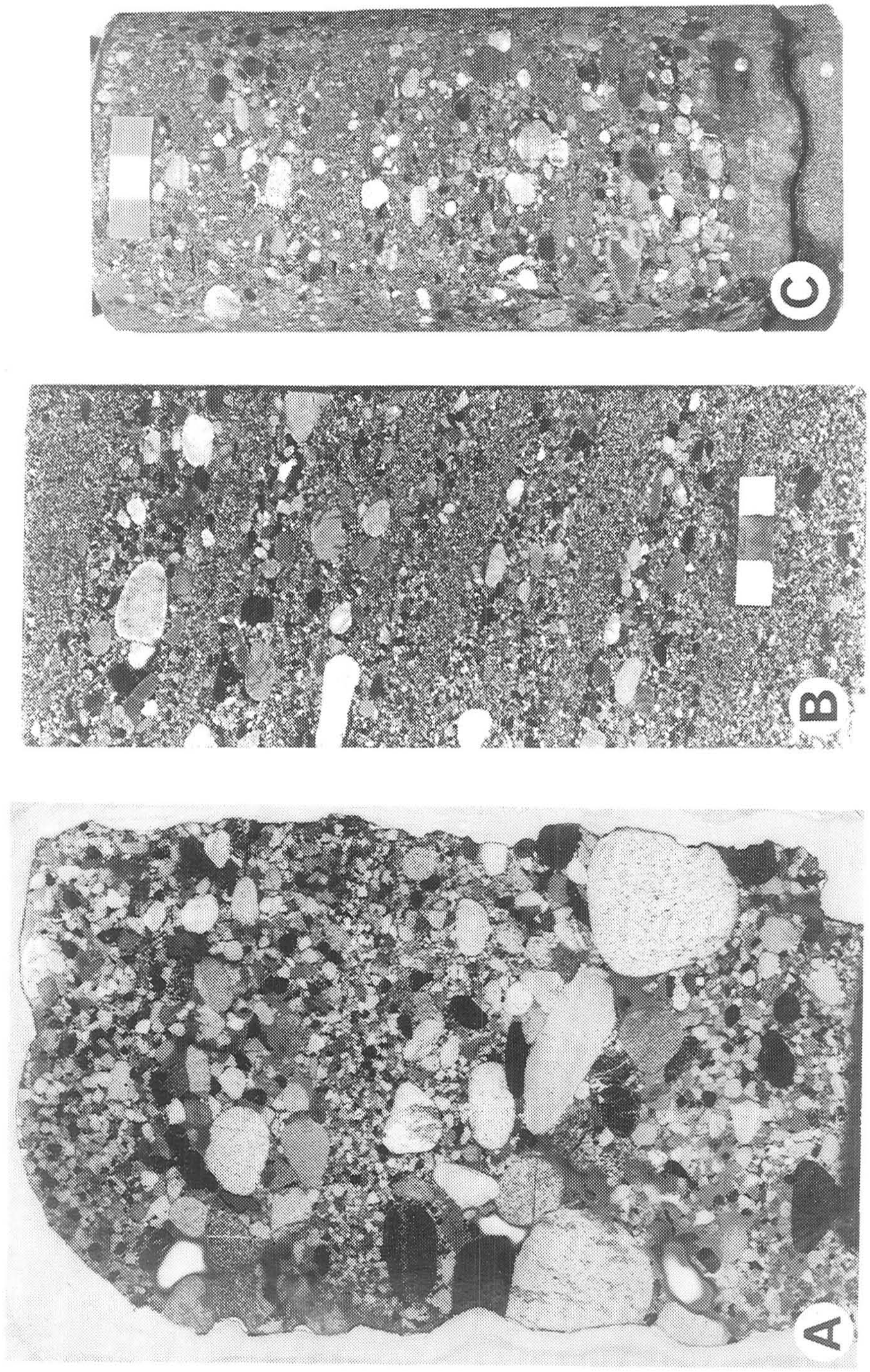
C
B
A

Unit $8G_2$ -- Interbedded Pebbles and Grits in a Sand Matrix (Fig. 6.13)

This is a <u>matrix</u> supported unit. The facies is crudely stratified. The stratification is flat lying to inclined at about 20°. The stratification is marked not only by changes in the pebble size, but also by changes in the percentage of matrix. The maximum preserved thickness of the unit is 0.5 m (cut plugs) and the upper and lower contacts are missing.

The coarse layers are composed of well rounded, ellipsoidal pebbles up to 4 cm measured from core, and very coarse to coarse grained, sub-rounded chert sand. The matrix is composed of very fine quartz sand, and comprises approximately 38% of the coarse layer.

Bed thickness varies from 1 to 7 cm, with gradational upper and lower contacts. The pebbles lie in the plane of the stratification.

The finer layers are composed of medium to very coarse sub-rounded chert sand. The percentage of matrix (vfU quartz sand) increases from 38% in the coarse layers to 57% in the finer layers.

Bed thickness in the fine layers varies from 0.3 to 5.0 cm, with gradational upper and lower contacts.

Sub-Facies 8K -- Coarse and Poorly Sorted (Fig. 6.14)

This facies is characterized by the absence of stratification. It is generally very thick (on the order of 6.0 m) and tends to occur toward the top of the conglomerate

Figure 6.13. Sub-facies 8G2 -- Interbedded Pebbles and Grit in a Sand Matrix

A) Photomicrograph is taken from well 6-29-52-13, 5446 ft. Slide is 2.2 cm wide. B) Photo is taken from well 2-29-52-13, 5455 ft. Core is 3 in. wide.

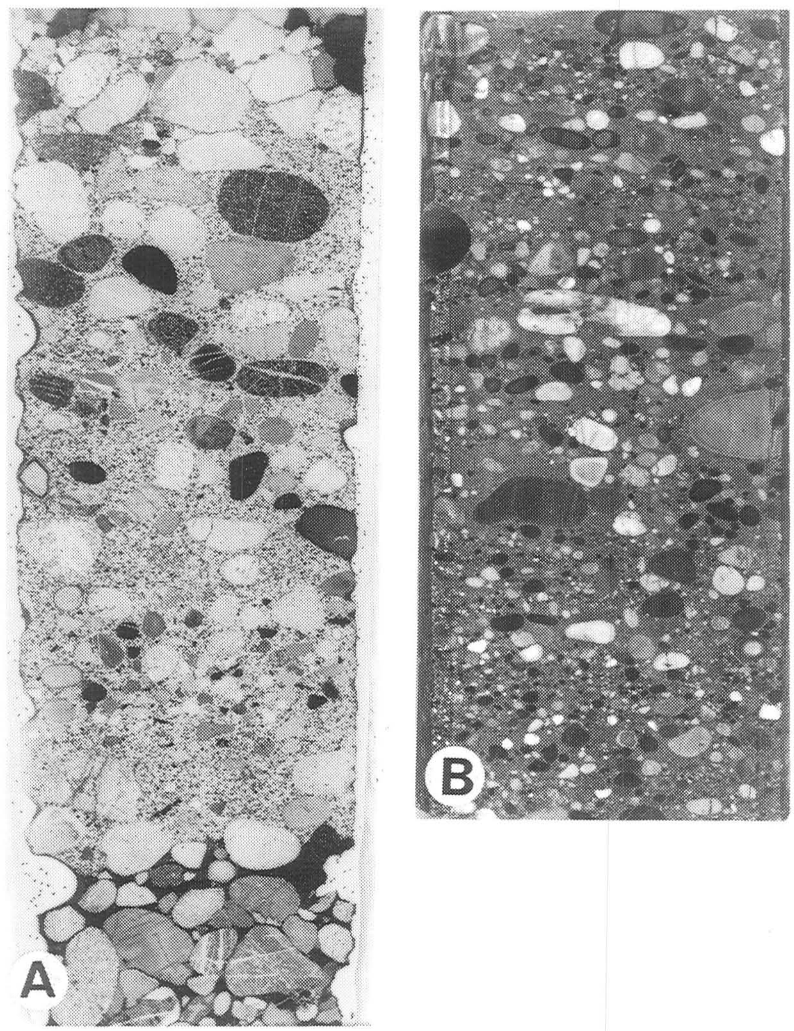
A
B

Figure 6.14. Sub-facies 8K -- Coarse and Poorly Sorted

A) Photomicrograph is taken from well 13-30-51-10, 1555 m. Slide is 3.6 cm wide. B) Photo is taken from well 13-30-51-10, 1555 m. Scale bar is 3 cm. C) Photo is taken from well 10-30-51-10, 1548 m. Core is 3 in. wide.

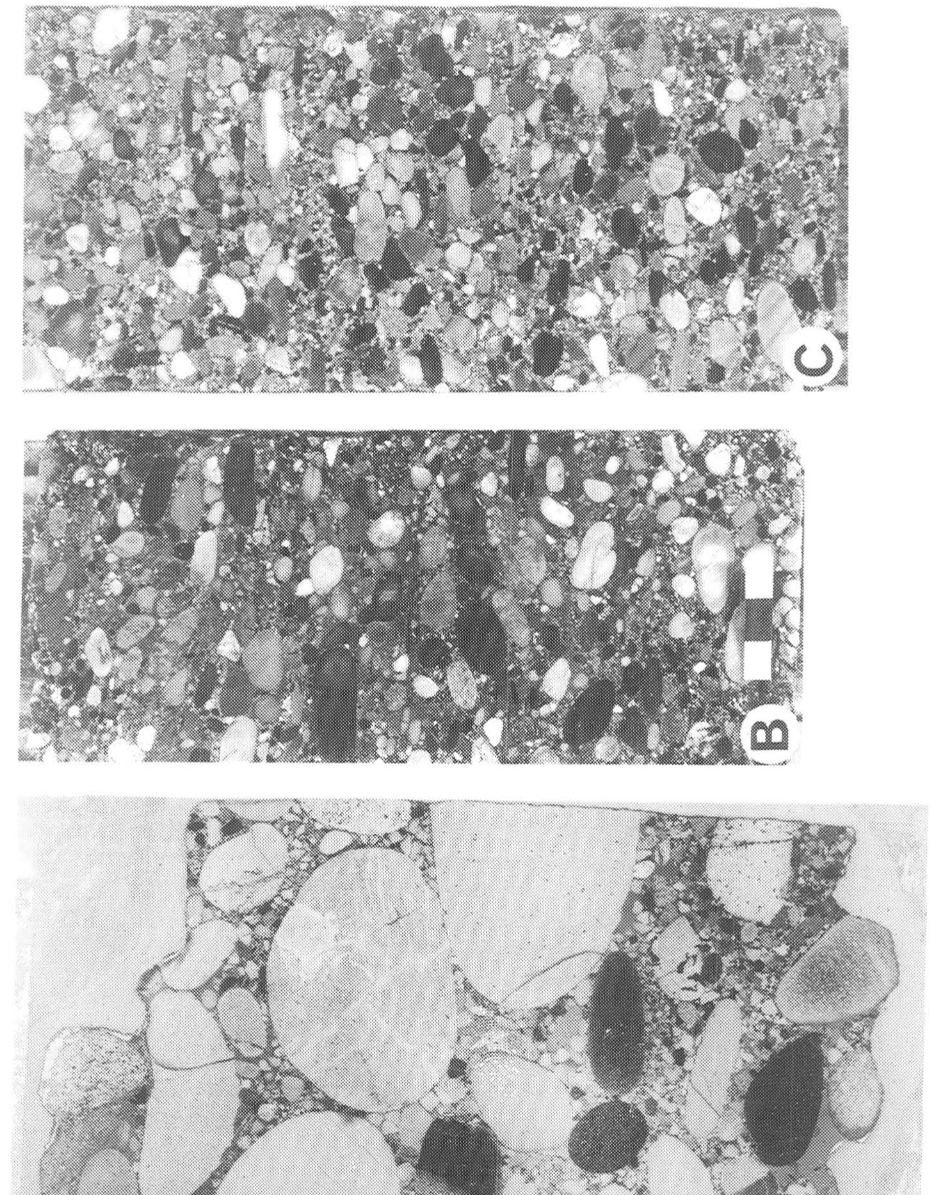
C
B
A

sequence. The upper and lower contacts are generally sharp. There are no obvious bedding planes and hence no obvious depositional breaks within this facies. There is a hint of a crude stratification in the lower third of this facies, but this is not well defined and boundaries are extremely diffuse.

Sub-facies 8K is clast supported. The chert pebbles are well rounded, varying in size from a long axis diameter measured in core from 1-2 cm at the base to 3-4 cm at the top of the facies. It is moderately sorted. Sphericity is greater than in other facies. No discernable fabric was observed, with pebbles ranging from horizontal to vertical.

The pore spaces, may be filled with sub-rounded coarse chert sand and by sub-angular fine quartz sand matrix.

There is no mud associated with this facies, either in the form of clasts or mud breaks.

Sub-Facies 8L -- Interbedded Open Work and Closed Work (Fig. 6.15)

This is a common facies in the thick clast supported conglomerates and forms the bulk of the conglomerate sequence. It is commonly 3-5 m thick. It is characterized by the interbedding of open work and closed work clast supported chert pebble conglomerates.

The bedding contacts may be crude, or commonly a sequence of sharp based open work beds grading to closed work beds is observed. The contacts may be inclined at

Figure 6.15. Sub-facies 8L -- Interbedded Open Work and Closed Work

A) Photo is taken from well 12-19-52-12, 1620 m. Core is 3 in. wide. B) Photo is taken from well 16-30-53-13, 1562 m. Scale bar is 3 cm. C) Photo is taken from well 7-20-51-11, 1678 m. Scale bar is 3 cm. D) Photo is taken from well 6-10-53-13, 1621 m. Core is 3 in. wide.

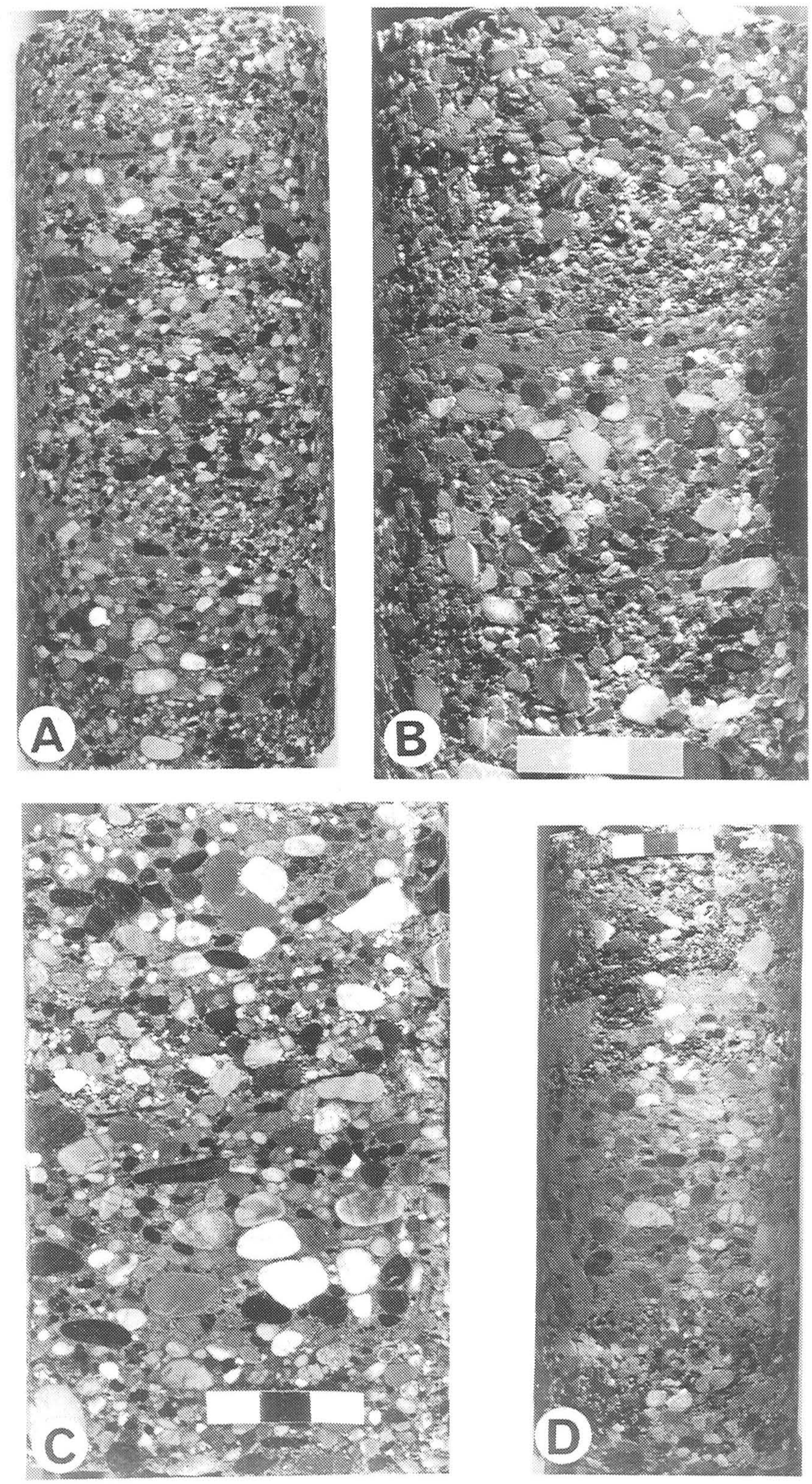
A
B
C
D

about 20° or scoured. Bed thicknesses of both the closed and open work layers are variable, but are usually on the scale of 4-6 cm.

In general, the open work beds are finer grained and better sorted. The closed work beds tend to have larger pebbles, and are not as well sorted. The contact between the two facies is marked by a change in the pebble size and sorting, and the presence or absence of matrix. The open work beds are similar to sub-facies 8C and the closed work beds are similar to sub-facies 8E.

Sub-Facies 8M -- Pebbles in Bioturbated Sandstone (Fig. 6.16)

This is not a particularly commmon facies in this area, but occurs more frequently in fields to the west of this study area (Plint and Walker, 1986). The facies is characterized by the occurrence of chert pebbles in completely bioturbated sandstones. There is no preservation of bedding within this sub-facies. The lower contact with the underlying facies is gradational. The upper contact is variable depending on the overlying unit. The thickness of this facies is highly variable, but in this area is of the order of 50 cm.

This facies is moderately sorted, containing rounded to well-rounded elliptical chert pebbles averaging 0.246 cm in size. Sub-angular fine grained quartz sand forms the matrix. No discernable fabric was observed, with chert

Figure 6.16. Sub-facies 8M -- Pebbles in Bioturbated Sandstone

A) Photo is taken from well 10-16-51-11, 5453 ft. B) Photo is taken from well 12-16-51-11, 5464 ft. C) Photo is taken from well 14-14-51-11, 5355 ft. Photos are taken from 3 in. drill core.

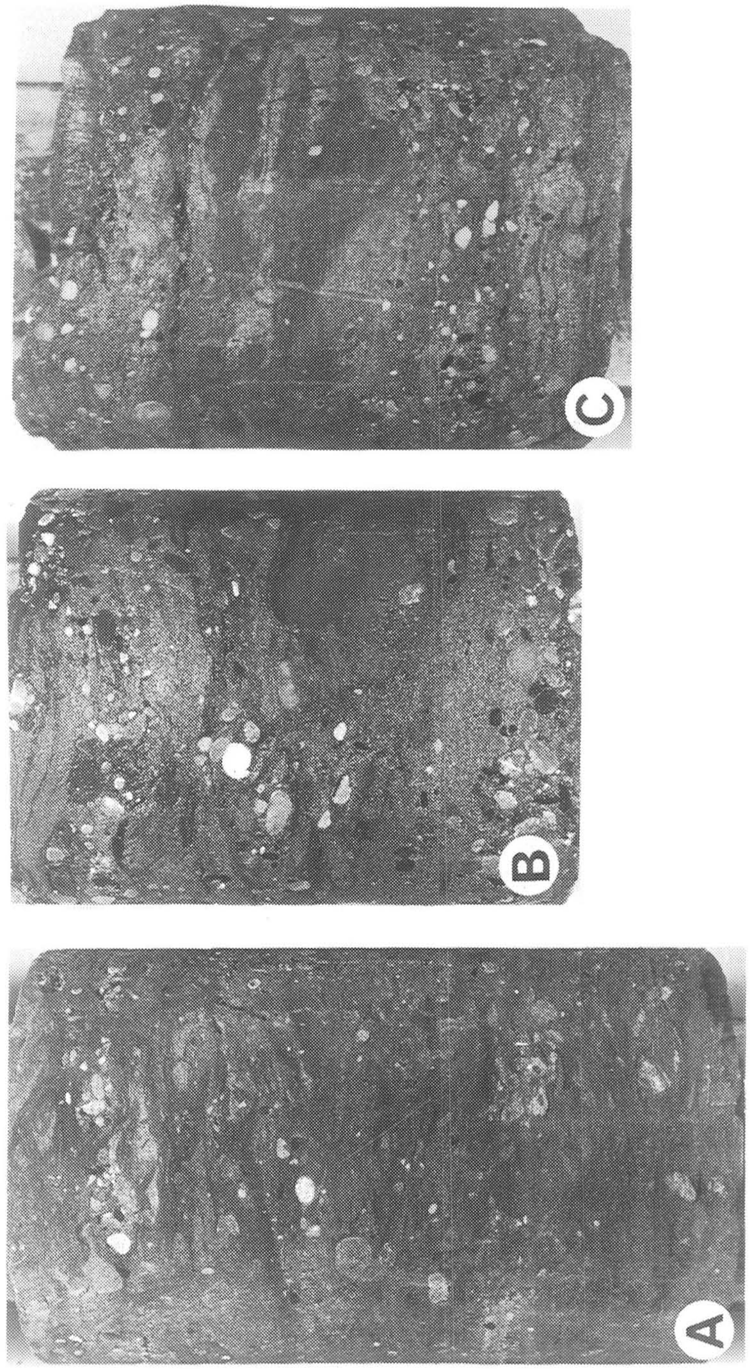
C
B
A

pebbles ranging from horizontal to vertical. Associated with this facies are abundant carbonaceous and micaceous material, and mud rip up clasts.

The overall aspect of this facies is thoroughly bioturbated. There are some hints of an original stratification but it is mostly sand, mud, and pebbles bioturbated together. Many of the burrows are pebble filled. Common burrow forms include, Terebellina, Chondrites, Rhizocorallium and Zoophycos.

6.3 CONGLOMERATE SEQUENCE

The previous section described the textural variety preserved in the Carrot Creek Member. No attempt was made to interpret the depositional environment of the individual textural varieties, although hummocky cross stratification was recognized in sub-facies 8F and trough cross bedding was preserved in sub-facies $8G_1$. In this section the textural varieties will be grouped into three textural sequence types. These textural sequence types will be used to separate the depositional environments preserved in the shoreface. In Chapter 7 the textural sequence types will be used to document the lateral variability of the thick shoreface conglomerate deposits. The conglomerate deposits of the Carrot Creek Member are interpreted as shoreface deposits (section 4.8 of this thesis). The shoreface environment was discussed in detail in Chapter 5.

In general, the thick (20 m) conglomerates, which preserve the full sequence (Type B, discussed later) coarsen upwards (Fig. 6.17), and this sequence is interpreted to represent a prograding conglomeratic shoreface. The mean grain size (cm), measured from core as long axis of the chert pebbles is plotted against the distance (m) of the pebbles above the erosion surface E5. The best fit least squares regression line is shown. The graph shows a progressive linear increase in grain size with increasing distance above the erosion surface E5.

This coarsening upward sequence has been sub-divided into two parts. The lower one-third of the conglomerate sequence shows well developed stratification and is interpreted to have formed on the lower shoreface. The upper two-thirds of the conglomerate sequence is massive to crudely stratified and is interpreted to have formed on the upper shoreface. The contact between the upper and lower shoreface deposits is transitional. The boundary between the upper and lower shoreface is related to the intensity of the waves, but in terms of effect on the bottom, depths of 10 to 15 m seem to mark a generalized division between the lower and upper shoreface (Swift and Niedoroda, 1985).

A. Lower Shoreface Deposits

The conglomerate textural sequence of the lower shoreface deposits of the Carrot Creek Member begins with sub-facies 8A. Sub-facies 8F is often associated with this

Figure 6.17. Graph of grain size (cm) versus the distance (m) above the E5 surface. The best fit least squares regression line is shown.

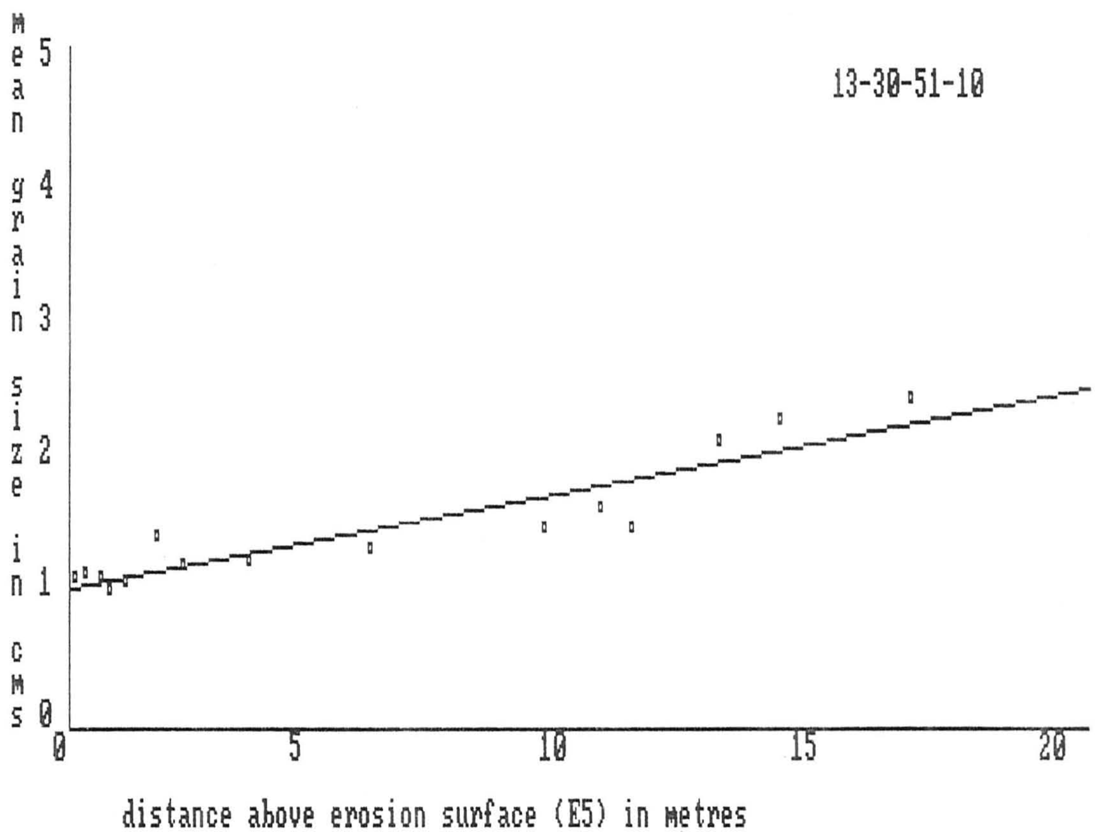
13-30-51-10
Mean grain size in cms
0
1
2
3
4
5
0
5
10
15
20
distance above erosion surface (E5) in metres

sub-facies and forms an intergral part of sub-facies $8A_2$. This sub-facies (8F) is often hummocky cross stratified with pebble lags at the base of these hummocky beds (see description in Dott and Bourgeois, 1982). Beds of sub-facies 8C, 8D, and 8E commonly develop in the lower third of the conglomerates, but there is no systematic development of these facies. In general the bed thickness of these facies tends to increase upwards. In some cores, well developed trough cross bedded sub-facies $8G_1$ occurs. In wells closer to the bevel (eg., 6-29-52-13) sub-facies $8G_2$ is preserved. The preserved thickness of this lower bedded conglomerate is about 5m.

All of these sub-facies are interpreted as part of the Lower Shoreface, because of the preservation of well developed stratification, and the position of these stratified beds at the base of the thick conglomerate sequence. The preserved thickness is in agreement with those described for lower shoreface deposits from both modern and ancient environments.

In the lower shoreface sediment transport is dominated by marine currents and less dominated by shoaling and breaking waves. Wave orbital currents are important in agitating the bottom, but generally will not produce sediment transport (Swift and Niedoroda, 1985). The deposits preserved in the lower shoreface tend to be better stratified and appear to suggest eposodic deposition of gravel possibly at storm time.

B. Upper Shoreface Deposits

The top two-thirds of the conglomerate of the Carrot Creek Member is massive (sub-facies 8K) to crudely stratified (sub-facies 8L). The textures preserved in this facies are interpreted to be due to constant reworking, presumably by continuous wave agitation. Preserved thicknesses are on the order of 10 to 15 m.

These two facies are believed to form the upper shoreface deposits, because of the lack of well developed stratification, and the position of these sub-facies in the upper part of the conglomerate sequence. The thickness of these deposits corresponds with those documented for both modern and ancient upper shoreface deposits.

The upper shoreface is dominated by shoaling and breaking waves, while marine currents tend to be less intense over the upper shoreface. The upper shoreface deposits are often massive to crudely stratified due to constant reworking of the clasts particularly during storm time.

C. Sequence Types Preserved in the Carrot Creek Member

The above described textural variety preserved in the shoreface conglomerates in the Carrot Creek -- Cyn-Pem study area are divided into three sequences. These sequences are based on core data only as they cannot be distinguished accurately on well logs.

TYPE A (Fig. 6.18): These are the veneer conglomerates which cover much of the E5 erosion surface. They are generally less than 1 m thick and are composed of sub-facies 8B, although sub-facies 8E may be preserved, particularly in the area of the terrace. This facies sequence is similar to facies 8D of Leckie (1983) and facies 5CV of Duke (1985), and like these authors, I interpret these conglomerates as a transgressive lag deposit. Core box photos of the conglomerate sequence type typical of wells found on the terrace and bumps are shown in Figures 3.15 and 3.17. Core box photos of the conglomerate sequence type found in the basin plain are shown in Figures 3.23 and 3.25.

T. lag on basin plain seaward of bumps & hollows max extent of shoreline regression.

TYPE B (Fig. 6.19): This sequence preserves both the Upper and Lower Shoreface deposits. The lower part of the sequence (up to about a maximum of 5 m) consists of stratified deposits, with dips (presumably seaward) of up to 17°. The sands preserved in these deposits are often hummocky cross stratified or wave rippled, with coarse lags at the base of the cross beds.

The lower contact (E5) often has pebbles bioturbated into the underlying shelf mudstones. The conglomerate sequence is intiated by interbedded conglomerates and sand with marine mudstones (sub-facies $8A_1$), and becomes sandier upwards. These interbedded deposits are usually associated with abundant carbonaceous debris, primarily wood fragments and coalified wood.

Figure 6.18. Conglomerate Facies Sequence Type A -- Type Well 8-30-50-13. See description in text. Vertical scale is in metres. The facies numbers are given on the right hand side of the litholog, and the position of the E5/T5 surface is shown. Core box photos of this sequence type are shown in Figs. 3.15, 3.17, 3.23,and 3.25. The conglomerate deposits in these wells are interpreted as transgressive lags.

8-30-50-13 — TYPE A

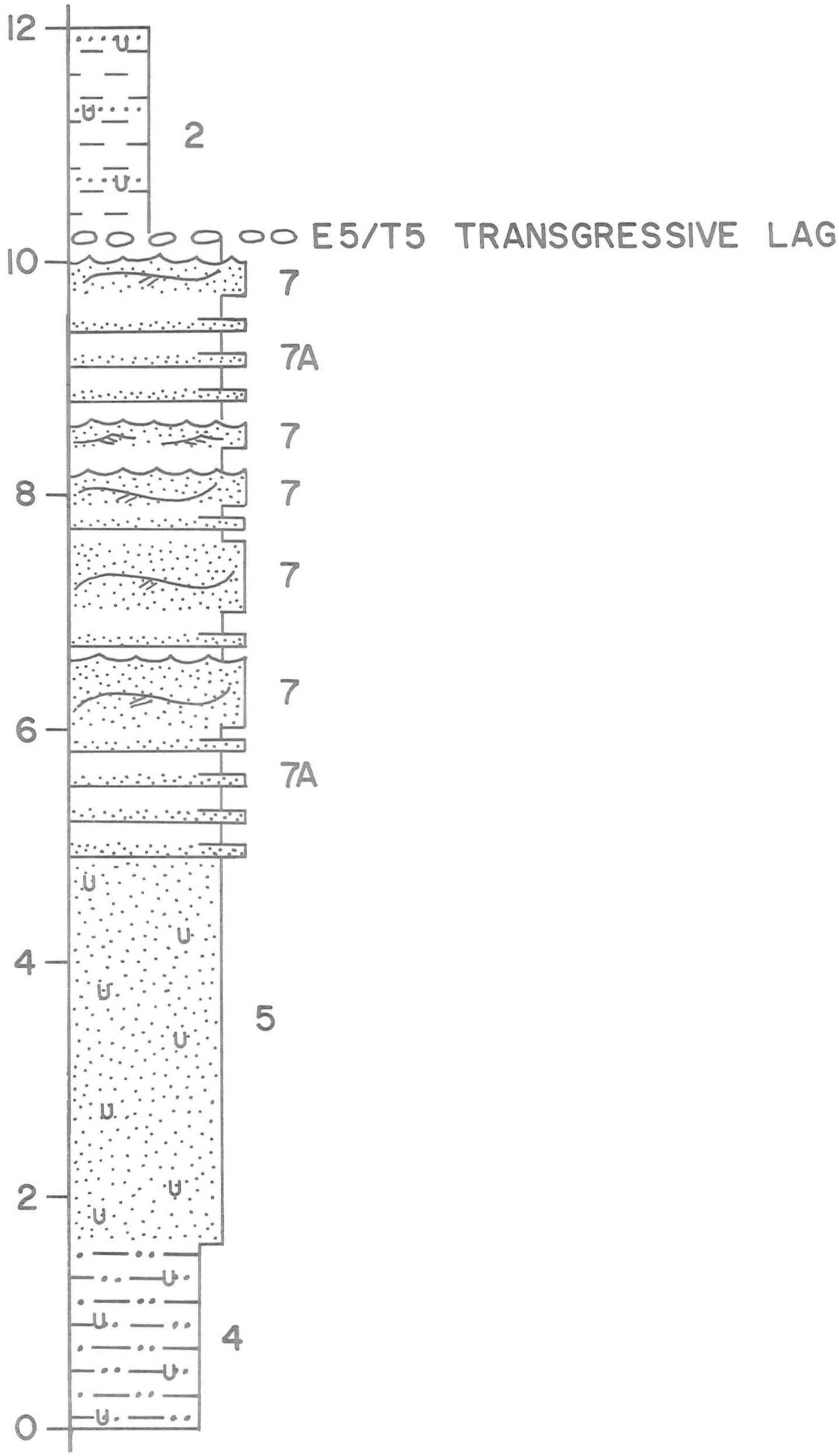

Figure 6.19. Conglomerate Facies Sequence Type B -- Type Well 13-30-51-10. See description in text. Vertical scale is in metres. The facies numbers are given on the right hand side of the litholog. The textural variety preserved in the conglomerates (facies 8) has been colour coded, according to the legend. The positions of the E5 and T5 surfaces are shown. Core box photos of this sequence type are shown in Fig. 3.19. The conglomerate deposits in this well have been separated into Upper Shoreface and Lower Shoreface; the boundary between the two is transitional.

13-30-51-10 — TYPE B

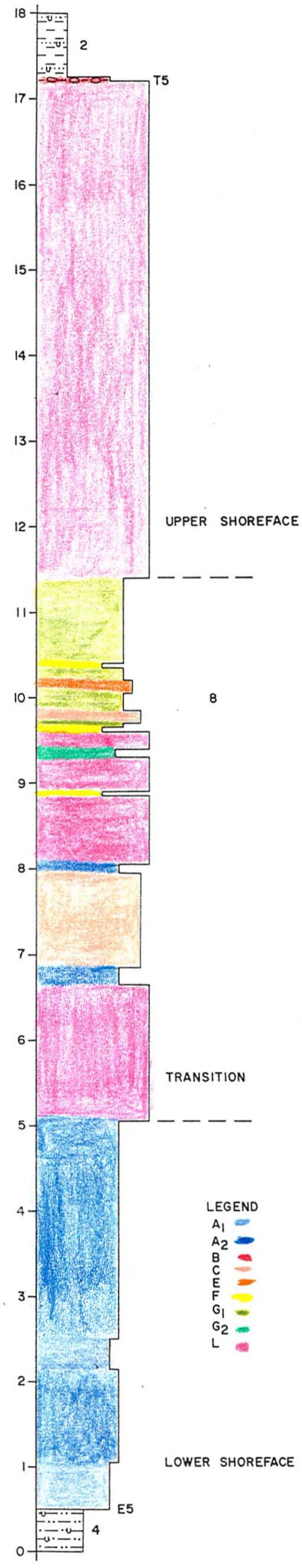

The upper portion of the sequence (about 10 - 15 m thick) is composed of crudely stratified (sub-facies 8L) to massive (sub-facies 8K) conglomerate. These deposits are interpreted as representing a high energy (presumably storm dominated) upper shoreface.

The contact between the upper and lower shoreface deposits is transitional with the conglomerate bed thickness increasing upwards until the stratification is difficult to discern. Where preserved the transition is often marked by sub-facies ($8G_1$).

These sequences are typically found in the landward side of the hollows adjacent to the bumps or banked up against the bevel. Sequences of this type are generally associated with the thickest gravel deposits. Core box photos of this conglomerate sequence type are shown in Figure 3.19.

TYPE C (Fig. 6.20): This sequence preserves only the massive (sub-facies 8K) or the crudely stratified conglomerates (sub-facies 8L). These are interpreted as Upper Shoreface deposits. The lower contact (E5) is often bioturbated, with pebbles bioturbated down into the underlying shelf mudstones, or the contact is sharp. These sequences are greater than a metre in thickness and tend to occur on the terrace or the back of bumps. Core box photos of this conglomerate sequence type are shown in Figure 3.21.

The conglomerates of the Carrot Creek Member are capped

Figure 6.20. Conglomerate Facies Sequence Type C -- Type Well 8-7-51-10. See description in text. Vertical scale is in metres. The facies numbers are given on the right hand side of the litholog. The textural variety preserved in the conglomerates (facies 8) has been colour coded; refer to legend given in Fig. 6.19. The positions of the E5 and T5 surfaces are shown. Core box photos of this sequence type are shown in Fig. 3.21. The conglomerate textures in this well have been interpreted as representing deposits of the upper shoreface.

8-7-51-10 — TYPE C

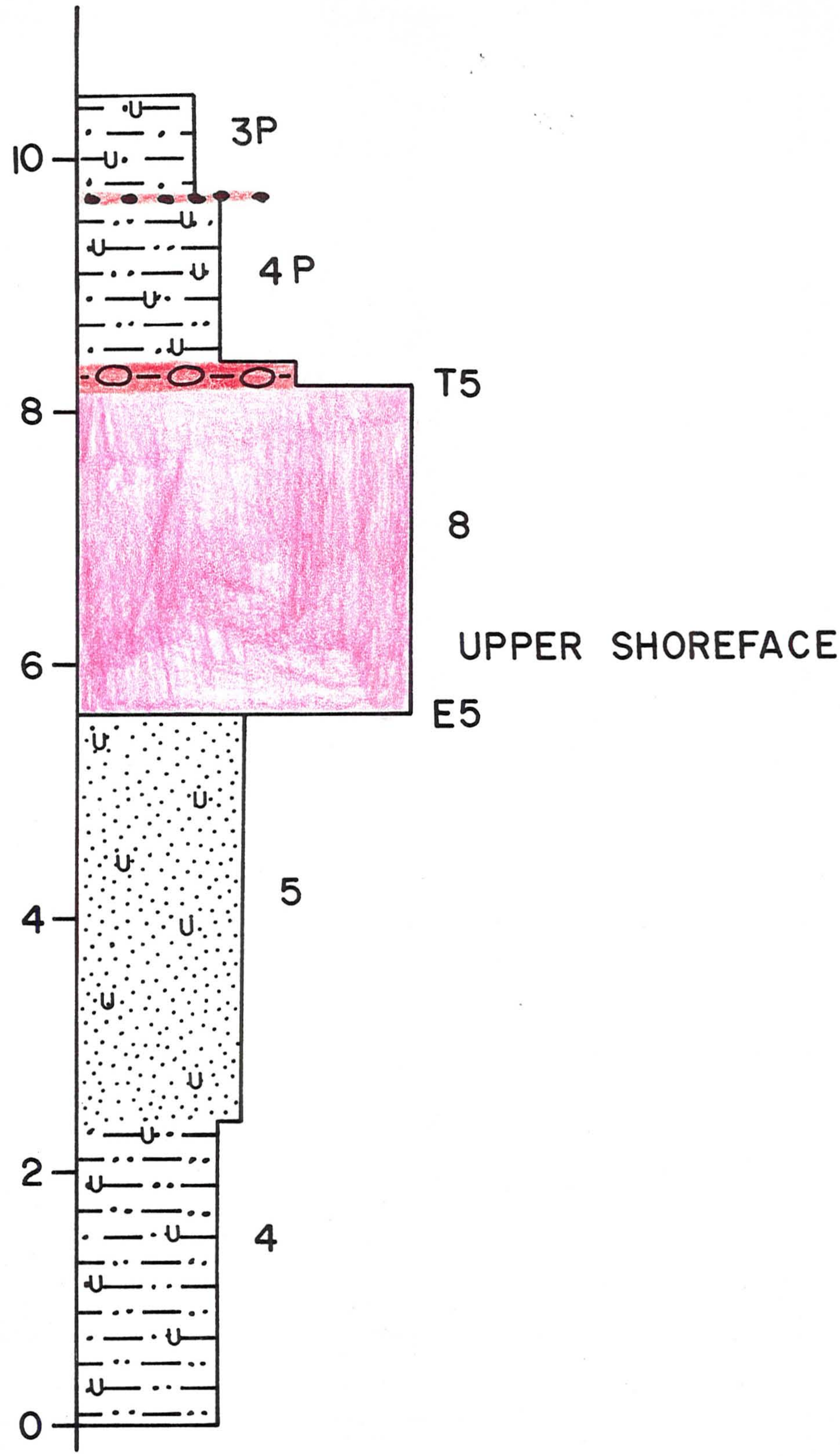

by pebbly mudstones (sub-facies 8B). This facies is also present in the overlying mudstones of sub-facies 3P, 4P, and 5P, and at the transition between these facies. These mudstones are all believed to have formed during the subsequent transgression (Part A), and are the result of reworking of the thick conglomerates associated with the bevel and the hollows.

These sequences describe the vertical textural variability of the conglomerate deposits. The relationship of these vertical sequences to each other and the relationship to the E5 surface will be discussed in the following chapter.

CHAPTER 7 -- LATERAL VARIATION WITHIN THE CARROT CREEK MEMBER

7.1 INTRODUCTION

The previous chapter described the textural varieties and the variation in the vertical sequences preserved in the conglomerates of the Carrot Creek Member. As discussed in Chapter 4 (Fig. 4.10), the conglomerate thickness varies from a thin veneer covering the entire study area to localized pools of conglomerate up to 19 m thick. The term pool is used herein to describe the localized patches of thick conglomerates. It has no connection with oil pools described by the E.R.C.B. The purpose of this Chapter is examine the details of the lateral variation present in the conglomerates, and the relationship to the E5 surface.

Why not use 'pods' instead of pools - reduces the confusion.

7.2 AREAL DISTRIBUTION OF THE CONGLOMERATE

The thick conglomerates are patchily distributed in ellipsoidal pools over an approximately 20 km wide band from the bevel to the basinward edge of the bumps and hollows. The size of these pools averages 5.0 (2.5 - 8.5) km X 1.2 (0.6 - 2.0) km. The pools trend northeast-southwest, parallel or sub-parallel to the trend of the bevel. The conglomerates in these pools were interpreted as shoreface deposits, based primarily on the geometry of the E5 surface (Chapter 4), the interbedding of the conglomerate with marine mudstones (Chapter 6, sub-facies $8A_1$), and the vertical textural sequence in the conglomerates (Chapter 6). The conglomerate pools appear to occur in three linear trends (Fig. 7.1). There is no progressive thinning or thickening of the conglomerates along this trend. The conglomerates rest in one sided scours banked against the landward side of the hollows, and thin basinwards.

The lateral relationships of the conglomerate sequences and the relationship of the conglomerates to the erosional surface were examined in a series of cross sections drawn both normal to the strike, and parallel to the strike of individual pools. Three pools were chosen (one from each linear trend), based primarily on the amount and distribution of preserved core present in each pool. The cross-sections are located in Figure 7.1. The sections are hung on the E7/T7 Datum (Chapter 4). The depth indicated on either side of the cross sections is the depth below the E7/T7 surface. Where there is conglomerate missing in the core boxes, unless otherwise shown, the missing section is always taken at the top of the conglomerate. This is done to be consistent, as there is no way of determining from the core where the missing sections are. The textural varieties are colour coded (Fig. 7.2) on the cross sections.

7.3 CROSS SECTIONS THROUGH POOL A NORMAL TO THE BEVEL (Fig. 7.3)

This pool is located in the area of the bevel (Fig. 7.1), and marks the third position of the linear

Figure 7.1. Conglomerate isopach map showing the distribution of the conglomerate pools. The location of the bevel is shown by a dashed line. Contour interval is 5 m. The positions of the three linear trends of the pools is shown (labelled 1, 2, or 3) and the pool studied for each trend is labelled A, B, or C. The location of each of the cross sections examined in the pools is shown.

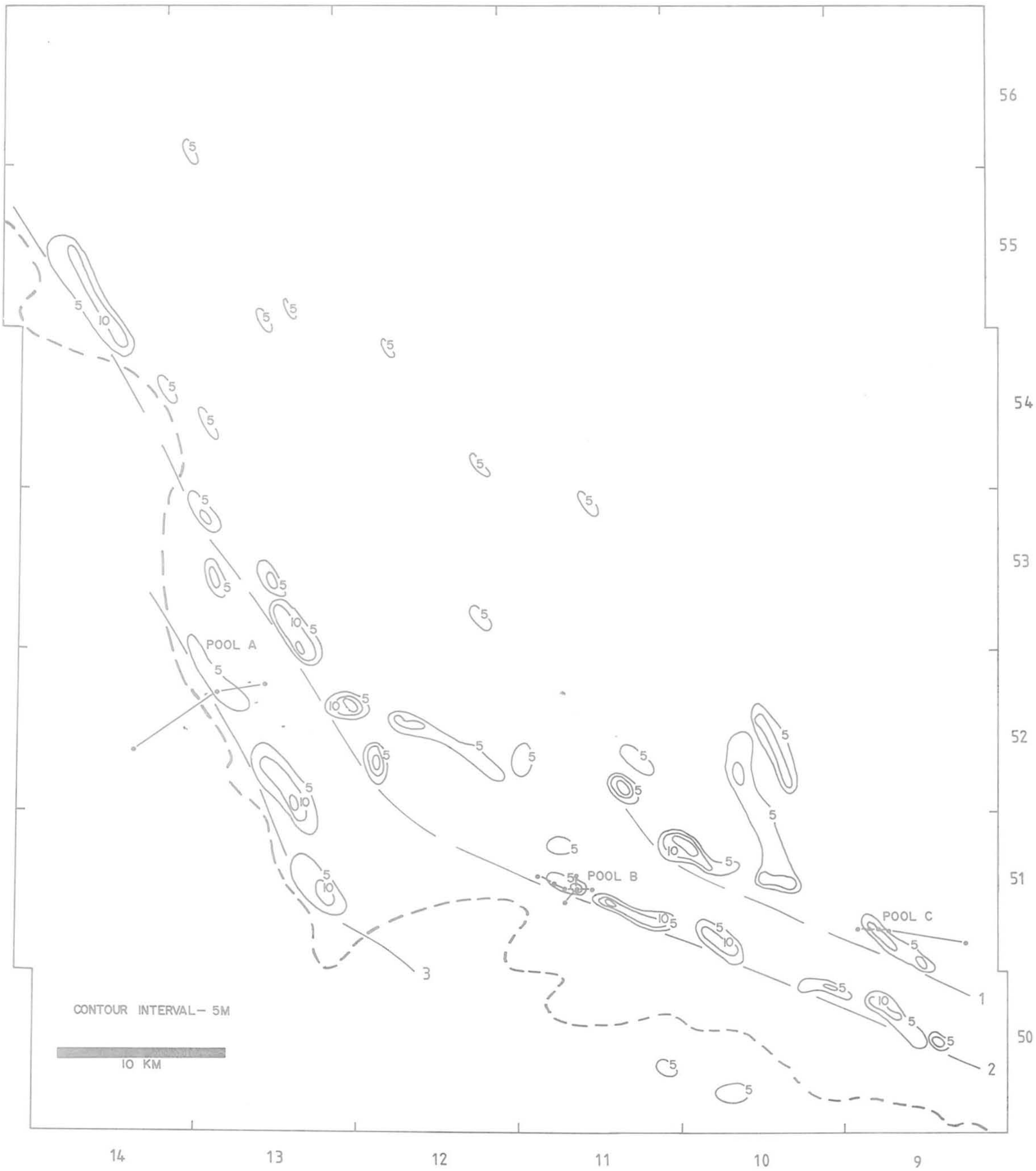

56
55
54
53
52
51
50
14
13
12
11
10
9
POOL A
POOL B
POOL C
1
2
3
CONTOUR INTERVAL– 5M
10 KM

Figure 7.2. Colour key to the conglomerate textures preserved in the cores used in the cross sections shown in Figs. 7.3 to 7.6, and located in Fig. 7.1.

COLOUR CODE TO CONGLOMERATE TEXTURES

$8A_1$ ---
$8A_2$ ---
$8A_3$ ---
8B ---
8C ---
8D ---
8E ---
8F ---
$8G_1$ ---
$8G_2$ ---
8K ---
8L ---
8M ---

trend, of the conglomerate pools preserved in the Carrot Creek study area. This is the only area where the matrix supported conglomerate, sub-facies $8G_2$, occurs.

The conglomerate sequence type preserved is controlled by the morphology of the erosion surface. The deeper scours preserve the full sequence (Type B) as in well 6-29-52-13. Here, the preserved thickness of the lower shoreface deposit is 2.3 m. and the upper shoreface deposit is 5.6 m. Wells 4-14-52-14 and 12-27-52-13 are Type A wells with conglomerate veneers. The thick conglomerates (well 6-29-52-13) are banked up against the landward side of the bevel and thin basinwards. The fining upward transgressive pebbly mudstones (well 12-27-52-13) of the Dismal Rat Member onlap the thick conglomerates of the Carrot Creek Member. All of the facies described above are overlain by the "laminated blanket" (Laminated Dark Mudstones, facies 2).

7.4 CROSS SECTIONS THROUGH POOL B

This pool is representative of those located on the second linear trend, and it lies basinwards of pool A and the bevel (Fig. 7.1). The conglomerates in this area develop good cross-bedding (sub-facies $8G_1$) in the area of transition from lower shoreface to upper shoreface deposits. The transitional portion of the shoreface is much better preserved in this area than in the pools adjacent to the bevel. Sections both normal and parallel to the

Figure 7.3. Cross section through Pool A, normal to the bevel as located in Fig. 7.1. Vertical scale is in metres. There is no implied horizontal scale. The facies numbers are shown on the right hand side of the litholog. The positions of the E5 and T5 surfaces are shown. The deposits of the Raven River Member are interpreted as representing aggrading shelf deposits. The conglomerates are shown to be separated from these deposits by the E5 surface. The conglomerates are divided into lower and upper shoreface deposits, and the boundary between these two deposits is transitional. The transgressive mudstones, well 12-27, onlap the thick conglomerates preserved in well 6-29. The entire sequence is buried by the "laminated blanket" (facies 2). "A" refers to the upper coarsening upward sequence preserved in the Raven River Member.

POOL A - NORMAL TO BEVEL

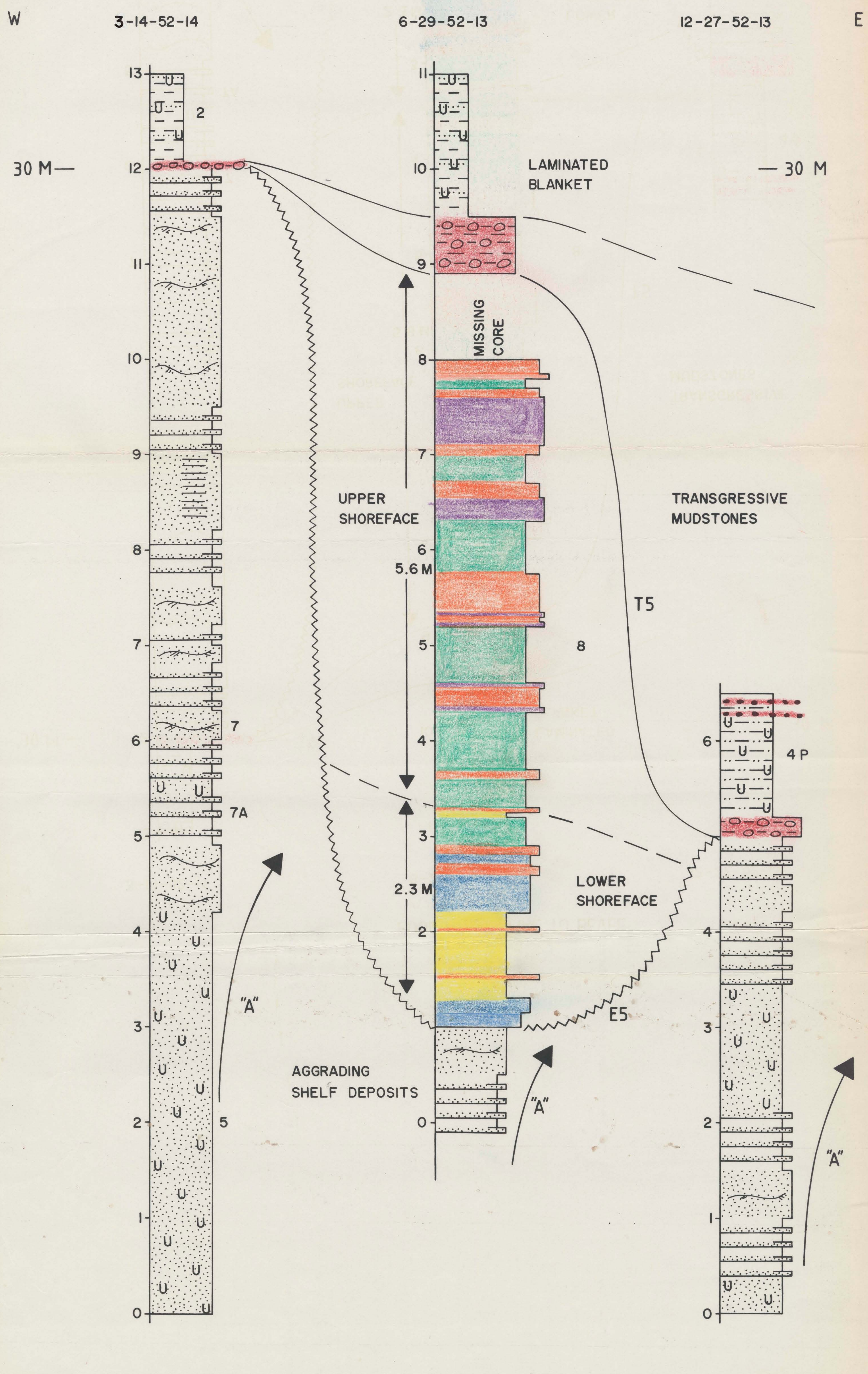

regional trend of the bevel (located in Fig. 7.1) are presented.

A) POOL B, NORMAL TO THE BEVEL (Fig. 7.4)

The depth of erosion on the E5 surface determines the type of conglomerate sequence preserved. The full sequence (Type B) is preserved in well 2-21. The thickness of the lower shoreface preserved in this well is 2.2 m. The lower shoreface deposits thin shoreward into the erosion suface (well 12-16). The conglomerates thin basinwards and the E5 and T5 surfaces become coincident. The fining upward transgressive pebbly mudstones of the Dismal Rat onlap the the thick conglomerates of the Carrot Creek Member.

The preserved maximum thickness of the upper shoreface in this area is 9.3 m in well 2-21. The thick deposits of the upper shoreface are predominantly crudely stratified conglomerates of sub-facies 8L. The thickness of the open-work conglomerates of sub-facies 8C and the closed work conglomerates of sub-facies 8E is more variable in the lower section of the upper shoreface. Landward the shoreface passes laterally into 0.4 m of closed work conglomerate of sub-facies 8E. Basinwards the upper shoreface passes laterally into fining upward transgressive pebbly mudstones (10-21).

The shoreface deposits in this pool are more complex than those preserved in pool A. As shown in well 12-16 the upper shoreface deposits are overlain by what is interpreted in the present classification scheme as lower shoreface deposits. The deposits then pass vertically into fining upward transgressive pebbly mudstones of the Dismal Rat Member (Chapters 3 and 4). The lower shoreface sequence and transgressive pebbly mudstones are interpreted to have been deposited from a more landward pool. The entire sequence is then buried by the "laminated blanket" (Laminated Dark Mudstones of facies 2).

B) POOL B, PARALLEL TO BEVEL (Fig. 7.5)

This section demonstrates that along the strike of the pool the thick conglmerates do not thin laterally into transgressive mudstones, but are banked up against the of bumps. The deepest scour preserves the full sequence (Type B) of lower to upper shoreface (wells 2-21, 4-21, and 7-20). The apparent topography seen on the gritty siderite horizon between wells 12-20 and 7-20 is believed to be the result of compaction from the overlying conglomerates. The amount of erosion on the E5 surface between these wells is only 8 m; the preserved thickness of the "a" sequence is about 12 m (well 4-28-50-12, Appendix 2)

7.5 CROSS SECTIONS THROUGH POOL C NORMAL TO THE BEVEL (Fig. 7.6)

This pool marks the most basinward position of the linear trends of the conglomerate pools shown in Figure 7.1. In this area the E5 surfaces scours deepest into the underlying Raven River Member. The "a" sequence

Figure 7.4. Cross section through Pool B, normal to the bevel as located in Fig. 7.1. Vertical scale is in metres. There is no implied horizontal scale. The facies numbers are shown on the right hand side of the litholog. The positions of the E5 and T5 surfaces are shown. The deposits of the Raven River Member are interpreted as representing aggrading shelf deposits. The conglomerates are shown to be separated from these deposits by the E5 surface. The conglomerates are divided into lower and upper shoreface deposits, and the boundary between these two deposits is transitional. The transgressive mudstones, well 10-21, onlap the thick conglomerates preserved in well 2-21. The lower shoreface deposits and transgressive mudstones preserved in well 12-16 represent deposition from a more landward pool. The entire sequence is buried by the "laminated blanket" (facies 2). G.S. = Gritty Siderite, "A" and "B" refer to the two coarsening upward sequences preserved in the Raven River Member.

POOL B-NORMAL TO BEVEL

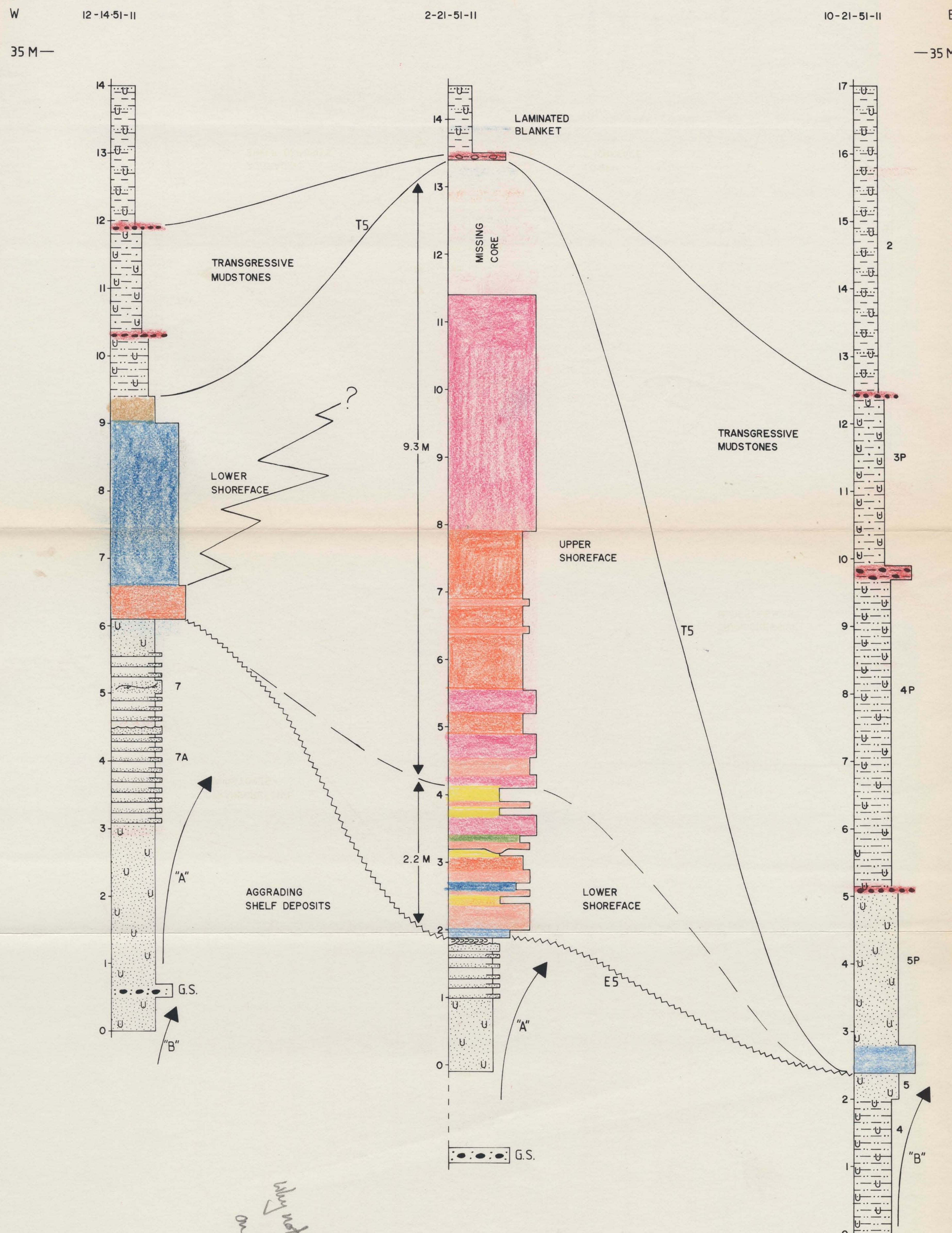

Why not hang on Gritty Shale?

Figure 7.5. Cross section through Pool B, parallel to the bevel as located in Fig. 7.1. Vertical scale is in metres. There is no implied horizontal scale. The facies numbers are shown on the right hand side of the litholog. The positions of the E5 and T5 surfaces are shown. The deposits of the Raven River Member are interpreted as representing aggrading shelf deposits. The conglomerates are shown to be separated from these deposits by the E5 surface. The conglomerates are divided into lower and upper shoreface deposits, and the boundary between these two deposits is transitional. The conglomerates do not thin along strike into transgressive mudstones, but are banked up against the bumps. The transgressive mudstones overlie the the conglomerates and the entire sequence is buried by the "laminated blanket" (facies 2). The relief on the gritty siderite horizon (G.S.) is believed to be the result of differential compaction. "A" and "B" refer to the two coarsening upward sequences preserved in the Raven River Member.

POOL B – PARALLEL TO BEVEL

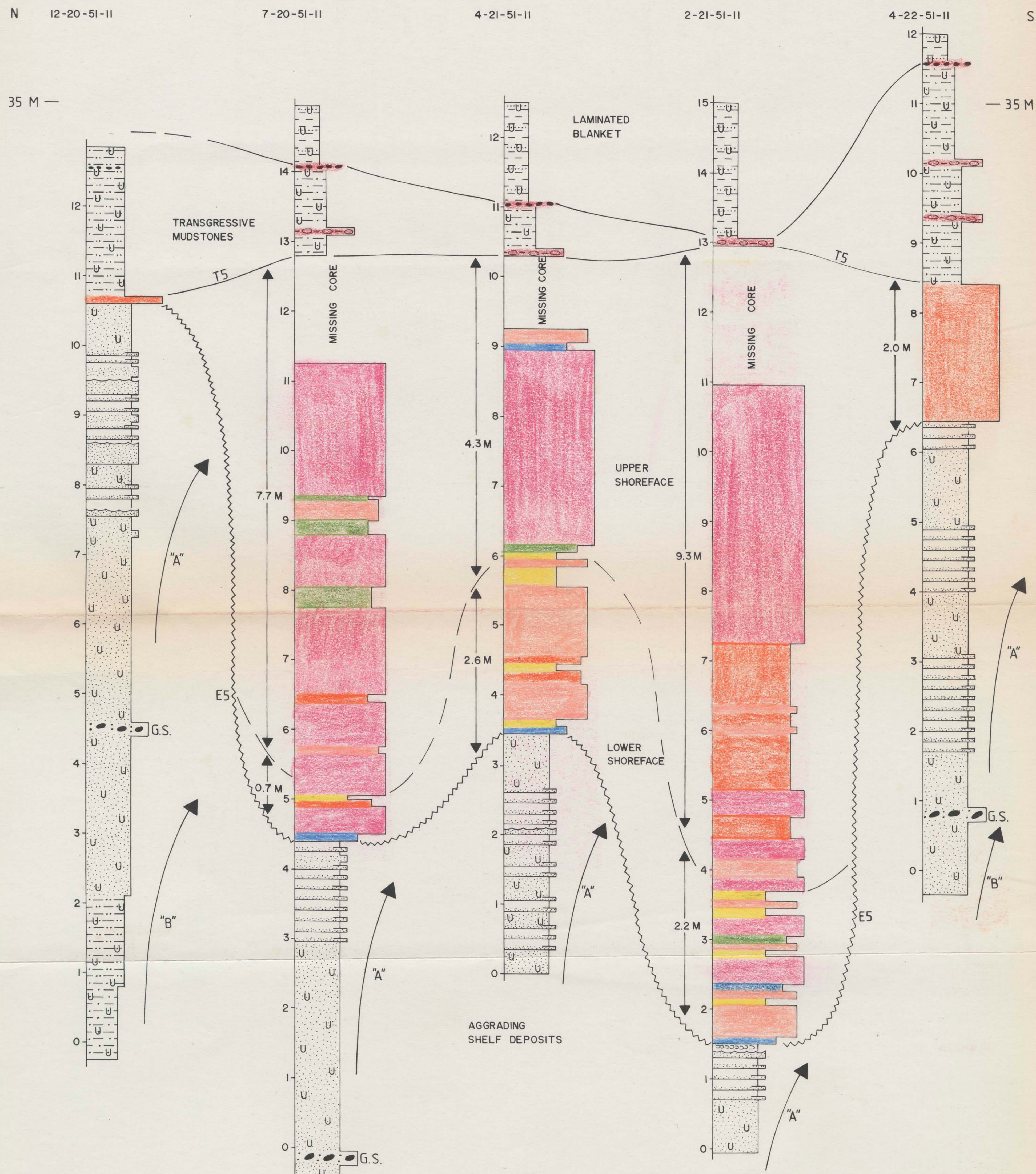

Hang on?

and the gritty siderite horizon have been removed, and E5 lies in the lower "b" sequence of the Raven River Member (Chapter 3). This section best demonstrates the one sided nature of the hollows. The sequence type preserved in the conglomerates is controlled by the depth of erosion on the E5 surface.

The full sequence (Type B) is preserved in well 11-8. Unfortunately, much of the section containing the conglomerate was lost during drilling, therefore the junction between the lower and upper shoreface deposits cannot be determined. The minimum preserved thickness of the lower shoreface is 2 m, and is composed entirely of sub-facies $8A_1$. The lower shoreface dies into the erosion surface both landward and seaward of well 11-8. The upper shoreface deposits are preserved in wells 11-8, 10-8, and 9-8. The deposits of the upper shoreface are crudely stratified (sub-facies 8L), with a maximum preserved thickness in well 11-8 of 10.5 m.

The E5/T5 surfaces are essentially coincident in well 1-11 (Type A) basinward of the conglomeratic shoreface deposits. In this well a thick (11.4 m) sequence of fining upward transgressive pebbly mudstones of the Dismal Rat Member (Chapters 3 and 4) is developed. The shoreface deposits in wells 9-8, and 10-8 are overlain by 6.6 m (10-8) of transgressive pebbly mudstones. Landward (westwards) of 11-8 the thin (0.2 m) conglomerate deposits found in well

9-7 (Type A) are overlain by a thick (7.7 m) sequence of transgressive pebbly mudstones. These mudstones are believed to be younger than the pebbly mudstones shown in well 1-11, 9-8, and 10-8, and appear to represent the onlap deposits of the next more landward pool. The whole sequence is then covered by "laminated blanket" (Laminated Dark Mudstones of facies 2).

7.6 SUMMARY OF THE SHOREFACE CONGLOMERATE DEPOSITS

The sequence of conglomerate deposits preserved in the three pools, from each of the three linear trends shown in Figure 7.1, are similar. A map showing the distribution of sequence type is shown in Figure 7.7. From this map and the cross sections presented above, it can be seen that the type of sequence preserved is a response to the depth of scour on the erosion surface. The full sequence (Type B) is preserved in the deepest scours, which is coincident with the axis of the gravel pools. A cartoon normal to the bevel showing the fill of the pools is given in Figure 7.8. This diagram is not intended as an interpretation of the pools. It is only intended as a simplification of the cross sections through the pools described earlier. Wells are superimposed on the cartoon to illustrate the sequence type expected depending on where the well was drilled with respect to the erosion surface.

Generally, the sequence begins with sub-facies $8A_1$, suggesting depostion at the boundary between the inner shelf

Figure 7.6. Cross section through Pool C, normal to the bevel as located in Fig. 7.1. Vertical scale is in metres. There is no implied horizontal scale. The facies numbers are shown on the right hand side of the litholog. The postions of the E5 and T5 surfaces are shown. The deposits of the Raven River Member are interpreted as representing aggrading shelf deposits. The conglomerates are shown to be separated from these deposits by the E5 surface. The conglomerates are divided into lower and upper shoreface depostis, and the boundary between these two deposits is transitional. The transgessive mudstones of wells 1-11, 9-8, 10-8 are shown to onlap the thick conglomerates preserved in wells 9-8, 10-8, 11-8. The transgressive mudstones preserved in well 9-7 are believed to represent deposition from a more landward pool. The entire sequence is buried by the "laminated blanket" (facies 2). "B" refers to the lower coarsening upward sequence preserved in the Raven River.

POOL C – NORMAL TO BEVEL

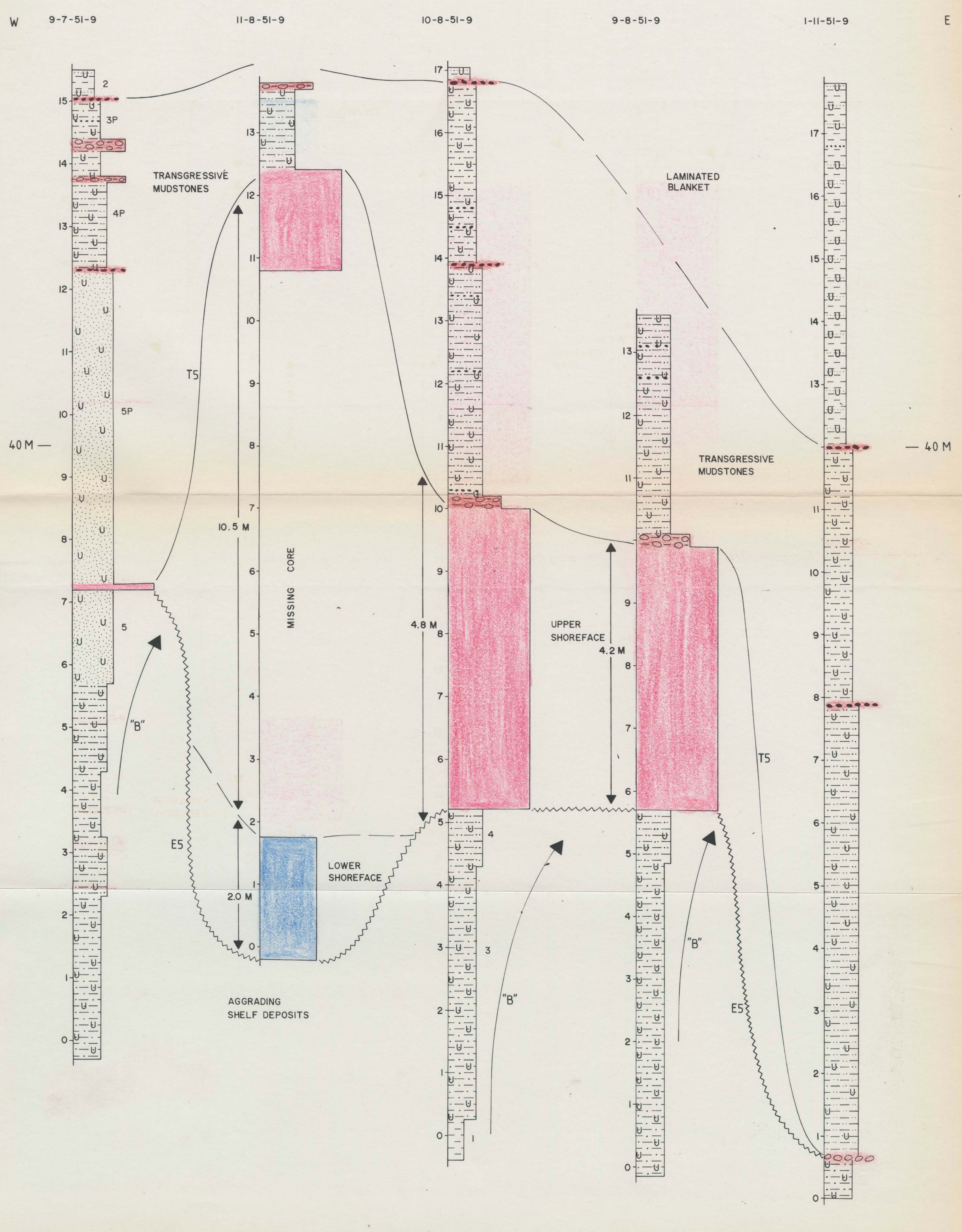

Figure 7.7. Conglomerate Facies Sequence Map. This map shows the areal distribution of the conglomerate facies sequence types described in Chapter 6. The 5 m contour line of the conglomerate thickness is drawn for refence to the location of the pools. The map is based entirely on core descriptions.


56
55
54
53
52
51
50
14
13
12
11
10
9
POOL A
POOL B
POOL C
10 KM
•-A
▲-B
■-C
CONGLOMERATE FACIES SEQUENCE MAP

Figure 7.8. Schematic cross section of the sequences preserved in a conglomerate pool. This is not intended as an interpretive diagram, only as a simplification of the vertical relationships of the conglomerate textures preserved in the pools.

SCHEMATIC CROSS SECTION OF CONGLOMERATE POOL — NORMAL TO THE BEVEL

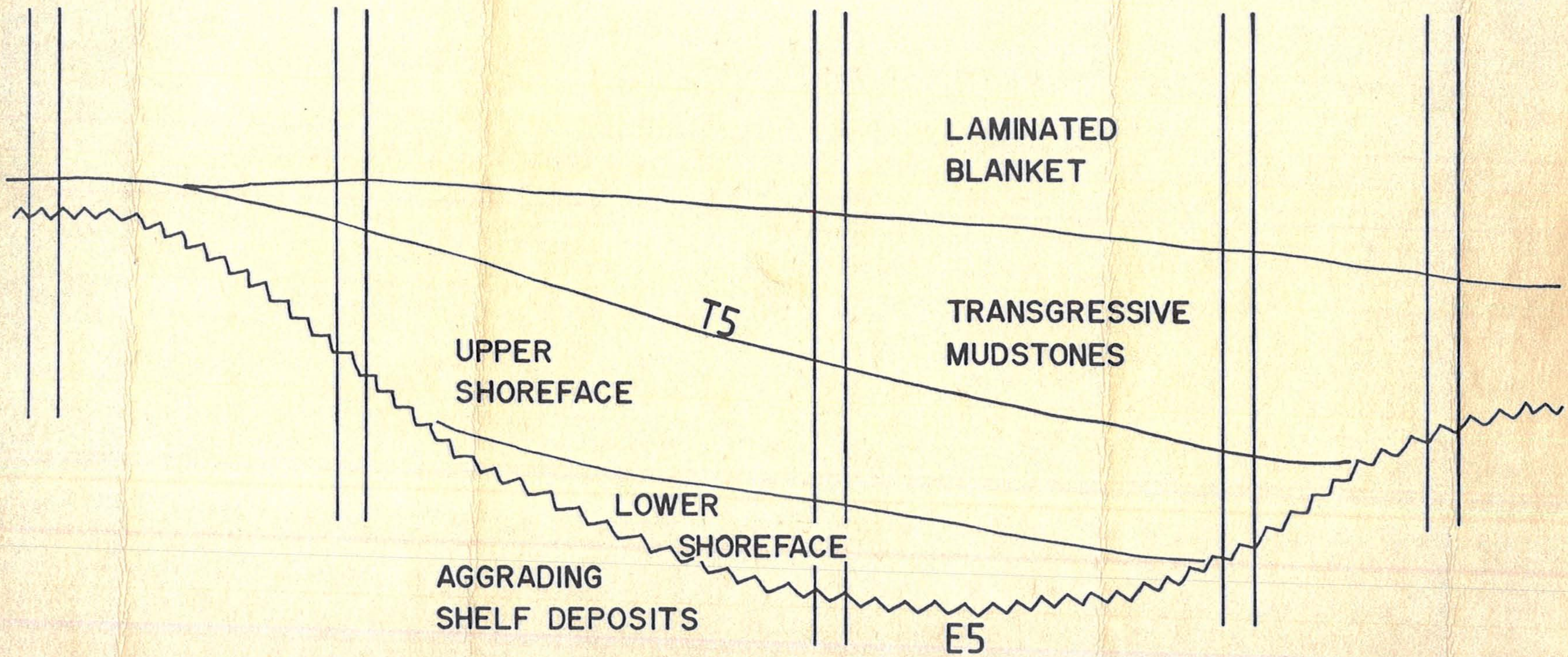

and the toe of the shoreface. The thickness of the lower shoreface deposits in the Carrot Creek Member varies from less than a metre to about 5 m. As the conglomerate progrades the thickness of the conglomerate beds increases and the amount of mud and bioturbation decreases. Interbeds are sandy rather than muddy. The upper portion of the lower shoreface and base of the upper shoreface is marked by trough cross bedded gravels (sub-facies $8G_1$) and is interpreted as marking the transition zone from the lower to upper shoreface.

The preserved thickness of the upper shoreface deposits in the Carrot Creek Member varies from 6 to 12 m. The deposits of the upper shoreface are crudely stratified (sub-facies 8L) to massive (sub-facies 8K), with no recognizable sedimentary structures observed. This is probably the result of the dominance of wave processes, continually reworking the gravels on the shoreface. The most variability in these deposits occurs at the base of the deposit where the facies are transitional from the upper to lower shoreface.

The deposits preserved in the most basinward pools are believed to be more complex due to deposition from more landward pools. This is best displayed in Fig. 7.4, well 12-16, where upper shoreface deposits are believed to be overlain by lower shoreface deposits and transgressive pebbly mudstones, in the present sequence interpretation.

A detailed discussion of this idea will be presented in Chapter 8. During continued transgression the entire sequence is overlain by the laminated blanket (facies 2; Chapter 3).

In the concluding chapter the morphology of the erosion surface described in Chapter 4 (Part A) and the description of the conglomerate deposits (Part B) overlying this surface will be intergrated. The synthesis of these two separate lines of evidence will be used to develop the overall depositional environment of the Carrot Creek Member.

CHAPTER 8 -- DISCUSSION OF THE CARDIUM DEPOSITIONAL HISTORY AT CARROT CREEK

8.1 INTRODUCTION

The purpose of this chapter is to discuss the depositional history of the Carrot Creek Member of the Cardium Formation in the Carrot Creek -- Cyn-Pem study area (T. 50-56, R. 9-14, W5). The discussion will focus on the formation and resulting morphology of the E5 surface, particularly the bumps and hollows and how the E5 surface compares with the pre-Holocene erosional surface and other ancient examples. The relationship of the conglomerates to the E5 surface will be considered. In conclusion a comparison of the Cardium conglomerates to other coarsening upward deposits in the Western Interior Seaway will be given. Those deposits interpreted as having formed many tens of kilometres from a contemporaneous shoreline, and which are coarser than the supposed time equivalent shoreline deposits are of particular interest.

The depositional environment of the Carrot Creek Member is inferred from the formation and resulting morphology of the E5 surface (Chapter 4). A brief discussion of the depositional history of the Carrot Creek Member was presented by Bergman and Walker (1986; in press, fig. 13). A synopsis of the results of this thesis follows immediately, and the rest of the chapter is devoted to the details.

SYNOPSIS OF THE INTERPRETATION

The deposits of the Raven River Member are interpreted as representing aggrading shelf sediments. These deposits are truncated by an erosion surface (E5), which is believed to have formed during a rapid fall in relative sea level, causing the shoreline to move into the basin. The maximum basinward position of the shoreface is at Bigoray (Fig. 4.1). During stillstand a new shoreface profile was established in the basin at Bigoray and this profile was blanketed by prograding gravel deposits (Carrot Creek Member). A series of rapid rises of relative sea level occurred, separated by periods of stillstand during which time new shoreface profiles were established landwards (southwestwards) of Bigoray. Thus, the bump and hollow topography represents more basinward positions of the shoreface. The final preserved position of the shoreface in the Carrot Creek area is marked by the long continuous bevel. Each of the shoreface profiles was blanketed by gravel deposits (Carrot Creek Member). The transgressive rises are marked by the onlap of the transgressive pebbly mudstones of the Dismal Rat Member. Westwards of Carrot Creek the transgression appears to be slow and continuous.

8.2 FORMATION OF THE E5 SURFACE

The palaeotopography of the E5 surface (Chapter 4) as defined from cross sections (Figs. 4.2 to 4.5; Foldouts 1 to

4), an isopach map (Fig. 4.6; Foldout 5) and mesh diagrams (Figs. 4.8 and 4.9), consists of a broad terrace located in the southwest corner of the study area, bounded basinwards by a northwest-southeast trending bevel. A remnant topography of bumps and hollows is preserved basinwards of the bevel, and the topography gradually flattens into a broad, relatively flat expanse, the basin plain. The relief on this surface relative to a horizontal upper datum (E7/T7) is about 20 m.

The deposits of the Raven River Member below the E5 surface, particularly the preservation of hummocky cross stratified sandstones, suggest deposition in an open marine setting on a broad storm dominated shelf below fairweather wave base and above storm wave base (Krause, 1983; Krause and Nelson, 1984; Keith, 1985; Walker, 1983 b,c). The formation of the erosional topography of the E5 surface requires increased erosion of the bed rather than the deposition of very fine sand. A marked change in the wave climate from that suggested by the deposits of the Raven River Member is therefore necessary to form the erosion surface. At minimum, lowering of relative sea level results in enhanced wave erosion of the bed (fully submarine); at maximum, lowering of relative sea level results in lowered base level, sub-aerial exposure of the former sea floor, and fluvial downcutting (fully sub-aerial) into shelf mudstones to produce the observed erosional topography.

Thus the E5 surface could have formed in one of three situations:

1. fully marine (submarine erosion of the shelf)
2. fully sub-aerial (fluvial downcutting)
3. intermediate (shoreface erosion).

Each of these three possibilites is discussed in detail below, with respect to the preserved morphology of the E5 surface and the overlying deposits.

1. Submarine Erosion

Storm waves can scour the open shelf below fairweather wave base. Storm events are recognized in the geologic record as deposits which are "unusual" compared with the overall lithologic sequence (eg., a sharp-based graded bed with a basal shell coquina surrounded by metres of bioturbated shelf mudstones). Storm deposits are preserved below fairweather wave base in depths where daily reworking is minimal or absent. The literature suggests four types of evidence that may be used to identify storm deposits on the shelf. These are discussed briefly below.

A. *In situ* winnowing of the sea floor, marked by the formation of shell lags.

Kreisa (1981) and Brenner and Davies (1973) describe shells parallel to bedding and convex up. The shells are commonly unbroken and not abraded suggesting *in situ* winnowing without transport. The fauna comprising the shell beds are similar to the surrounding interbedded shells. Kreisa (1981) also noted that the shells are mud-coated or mud-filled and this mud is identical to that of the underlying shale. Brenner and Davies (1973) and Kreisa (1981) suggest bed thicknesses on the order of cms to a few tens of cms.

B. Transported shell accumulations commonly with the shells in sharp based graded calcarenite beds.

These type of deposits have been described by Kelling and Mullin (1975), Cant (1980), Brenner and Davies (1973), and Aigner (1982a). The bed thickness ranges from a few cms to several tens of cms. The bases of the beds are sharp and commonly erosive with both tool and scour marks. Scours up to several metres wide and several tens of cms deep are common. Kelling and Mullin (1975) and Aigner (1982a) describe a sequence of internal structures for storm deposits similar to the internal sequence described for turbidites (Bouma, 1962). The storm layers are interbedded with shelf mudstones.

C. Storm scouring leading to the formation of hardgrounds and condensed horizons.

Aigner (1982b) suggested that storm scouring of the softer substrate down to well-compacted or semi-lithified levels may contribute to hardground formation. Condensed horizons with many zonal faunas present within an unusually thin sedimentary sequence have been attributed to storm scouring of a soft substrate (Hagdorn, 1982; Gebhard, 1982).

D. Sharp based hummocky cross stratified beds commonly interbedded with bioturbated mudstones (Wright and Walker, 1981). This is typical of the deposits of the Raven River Member found underlying the E5 surface.

In general, storm erosion on the shelf produces broad open scours up to several metres wide and several tens of cms deep. Storm beds range from a few cms to several tens of cms thick and are commonly interbedded with the background sediments.

Swagor et al. (1976) suggested that the erosion surface beneath the Carrot Creek conglomerates (here termed E5) formed by submarine erosion on the shelf. Submarine erosion of the open shelf does not account for the continuous strike of the bevel. The bevel indicates the presence of strongly localized continuous erosion, rather than broad open scouring on the shelf.

Submarine erosion might account for the remnant topography of bumps and hollows basinwards of the bevel. The amount of relief (about 20 m) on this surface however, seems to make an open marine interpretation unlikely. The third objection to forming the E5 surface by submarine erosion is geometric. The area of maximum sediment removal occurs out in the basin plain, while the area of least sediment removal occurs on the terrace (in what would presumably be shallower water depths where wave energy should be greater). If the surface were formed by submarine erosion on the shelf, then in the area of the basin plain, the storm waves must remove the entire "a" sequence, the gritty siderite, and part of the "b" sequence. This is a minimum of 12 m of sediment. The argument could be raised that the "a" sequence dies out in the basin. In the area of the bumps and hollows however, the "a" sequence is preserved in the bumps. This suggests that the sequence extended at least as far as the edge of the bumps and hollows. Landwards, the amount of erosion decreases significantly. On the terrace the topographic relief is generally less than a metre. Thus the maximum amounts of erosion would occur in the deepest part of the basin. The amount of erosion required and the morphology of the surface is not compatable with the descriptions of storm features recognized on the shelf.

Swagor et al. (1976), Smith (1986), and Hayes and Smith (1987) have suggested that gravels were transported from the shoreline across the shelf by storm enhanced process, such as rip currents. The thick conglomerate deposits (Carrot Creek Member) are not typical of deposits described as transported storm deposits. The conglomerate does not represent in situ winnowing. There is no evidence of pebbles ever having been present in the mudstones and sandstones of the Raven River Member. The thickness of the deposits are an order of magnitude larger than those typically described from the literature for storm deposits. The style of bedding found in the storm layers (i.e., interbedded with the background sediments) is not typical of the thick conglomerate sequences. For these reasons the E5 surface is believed not to be the result of submarine erosion, and the conglomerates (Carrot Creek Member) are not the result of storm transport across the shelf.

2. Fluvial Downcutting

The idea that the E5 surface at Carrot Creek was formed by fluvial downcutting was rejected by Swagor et al. (1976) due to the absence of evidence (eg., roots, coals, soils) to support sub-aerial exposure and erosion. The morphology of the erosion surface documented in this thesis supports the rejection of fluvial downcutting as the erosional mechanism. If the E5 surface had formed as a result of fluvial incision, some suggestion of channelling would be expected, particularly on the terrace. The terrace is a relatively flat surface, with no evidence of a fluvial system preserved on it, and there is also no evidence of incision into or through the bevel. A dendritic flow pattern of fluvial drainage could be superimposed around the bump and hollow topography with either a southeast or northeast flow direction. There is no indication of where these rivers would head or where they would terminate on the relatively flat basin plain.

The literature provides very little information about the formation and morphology of erosion surfaces produced by sea level variation. In the few published cases where these erosion surfaces have been documented (Nelson and Bray, 1970; Kraft, 1971; and Suter and Berryhill, 1985 for the pre-Holocene erosion surface; and McCubbin 1969; and Weimer and Flexer, 1985 for the Cretaceous) the resulting topography is believed to be the result of fluvial downcutting during lowstand. I will briefly present the evidence provided by these authors supporting the fluvial interpretation, firstly for the pre-Holocene surface, and secondly for the Cretaceous. I will then attempt to relate this information to the E5 surface.

Nelson and Bray (1970) considered that the three most important factors controlling the distribution of the Holocene sediments were topography, variations in the rate of rise of the sea, and currents. Of these three factors I am presently concerned only with the topography of the surface. The Pleistocene-Holocene contact in the Sabine-High Island area of the Gulf of Mexico was described by Nelson and Bray (1970) as very flat. The unconfomrity surface dips gently seaward with approximately the same degree of slope as that of the present-day sea floor. The most prominent feature on this otherwise flat erosion surface is the buried channel of the Sabine River. The topography of this channel is not reflected on the present day sea floor. The channel was interpreted by Nelson and Bray (1970) as a former river valley that ranged from 4 to 8 miles (6.4 to 12.9 km) in width and had several tributaries, some as much as 9 miles (14.4 km) long within this area. The location of the late Wisconsinan fluvial systems in this area were mapped in detail by Suter and Berryhill (1985) and the positions of these ancient streams across the continental shelf are shown in their figure 1. The depths of the large fluvial feeder channels recorded by Suter and Berryhill (1985) are more than 50 m.

Kraft (1971) described a similar pre-Holocene topography on the Atlantic shelf off the coast of Delaware. Like Nelson and Bray (1970), Kraft (1971) suggested that the thickness and areal extent of the Holocene sedimentary deposits were to a large extent controlled by the morphology of the Pleistocene unconformity surface. The Pleistocene surface in this area is irregular, indicating cross sections of channels. Deeply incised river valleys with local relief of up to 140 ft (43 m) are common on the shelf in this area, and can be projected into the emergent surface to form a continuation of the trellis-dendritic drainage pattern believed to be typical of the pre-Holocene surface. Another example of pre-Holocene fluvial downcutting into shelf sediments during lowstand is the Laurentian Channel on the Nova Scotian shelf (Slatt, 1984; Uchupi, 1968).

In all of these cases the Holocene sediments attain their greatest thickness in the buried channels. The initial fill of the incised channels on the shelf is believed to be fluvial. Nelson and Bray (1970) recorded a basal quartz sand, of unknown thickness, confined to the buried Sabine River Channel. Overlying this basal quartz sand was a patchy distribution of peat up to 5 ft (1.5 m) thick. Overlying this sequence were the Holocene marine sediments. Kraft (1971) records shallow marine-estuarine sediments associated with the fluvial channels.

Coal/peat as [illegible]

There is even less documentation in the literature of the formation and morphology of ancient unconformity surfaces than in the modern. The most detailed analysis of the formation and morphology of an erosion surface is the ancient is that of McCubbin (1969). The only other public study to illustrate the nature of the erosion surface is that of Weimer and Flexer (1985).

McCubbin (1969) illustrated with cross sections and isopach maps the palaeotopography of the pre-Niobrara erosion surface in northwest New Mexico. He suggested that the surface was formed by fluvial downcutting in a strike-valley setting. This surface consists of cuesta like ridges separated by intervening valleys, with the steeper slopes (about 2°) facing northeastwards (basinwards). The erosional relief on this surface was greater than 100 ft (30 m). The valleys are deepest in the middle and become shallower along trend.

Weimer and Flexer (1985) suggest that the erosion surface at the base of the Turner sandstone in the Eastern Powder River Basin, Wyoming, developed during a mid-Turonian sea level lowstand. The morphology of the erosion surface is shown only on cross sections. Weimer and Flexer (1985) suggest that northeast trending valleys were cut into the deeper water marine deposits during the lowstand and were subsequently filled during sea level rise. Without maps detailing of the nature of the erosion surface, it is difficult to compare their surface with that at Carrot Creek.

In both studies the sediments overlying these ancient erosion surfaces are coarser grained shallow marine sandstones. Weimer and Flexer (1985) suggest that the lower Turner Member is brackish to marine (tidal flat to estuary) in-filling valleys cut into the underlying marine sediments.

Both of the erosion surfaces described in the ancient are significantly different in morphology and overlying fill from the pre-Holocene ersosion surface. The pre-Niobrara erosion surface consists of cuesta-like ridges separated by intervening valleys. The basal Niobrara sandstone is a wedge of sediment bounded by a cuesta-like ridge on the pre-Niobrabra erosion surface along the southwest (landward side), thinning gradually basinwards passing into basin mudstones. Compare this surface with the pre-Holocene incised channels on the Gulf of Mexico shelf, or off the coast of Delaware. The fill of the pre-Holocene channels is fluvial, while the overlying sediments of the Cretaceous erosion surfaces are interpreted as shallow marine. The differences in the morphology of the ancient surfaces compared with the pre-Holocene erosion surface, suggest that the ancient examples may not necessarily be the result of sub-aerial erosion and fluvial downcutting.

The morphology of the E5 surface does not resemble one of incised fluvial channels as described for the pre-Holocene surface. Fluvial downcutting does not account for the "one-sided" geometry of the bevel or the basinward topography of bumps and hollows trending roughly parallel to the strike of the bevel. The term "one-sided geometry" is used here to describe a more steeply dipping erosion surface on one side (the bevel on the southwestern side) passing laterally basinwards into shelf muds on the other side, <u>without</u> a more steeply dipping erosional margin (northeastern side) as would be expected in a channellized system with palaeoflow to the southeast.

Cross sections through the conglomerate pools parallel to the trend of the bevel (Fig. 7.5) might suggest a channel morphology, with drainage to the northeast. These channels however cannot be traced into the basin plain or onto the terrace. There is no preserved evidence in the Carrot Creek area of where these rivers would head on the terrace or where they would terminate on the basin plain.

The sediments overlying this erosion surface (E5) are interpreted as shallow marine. The gravels in the lower part of the conglomerate sequence are interbedded with marine mudstones and sandstones containing wave formed structures (eg., wave ripples). The conglomerate deposits are found in discrete pools, not as long continuous ribbon sands like the strike-valley deposits described by Exum and Harms (1968). Rather the conglomerates form a wedge of sediment bounded by a more steeply dipping erosion surface on the southwest side.

For the above reasons I suggest that the morphology on the E5 surface is not the result of sub-aerial exposure and fluvial downcutting. I also suggest that the surfaces described by McCubbin (1969) and Weimer and Flexer (1985) may be the result of processes other than sub-aerial exposure and fluvial downcutting.

McCubbin (1969) suggested that "...the pre-Niobrara topography was unlike topography formed by marine erosion" (p. 2135). I believe this statement to mean that the topography was not the result of storm erosion on the shelf. The interpretation preferred by McCubbin (1969) was that "...the topography was formed largely by subaerial erosion, and was later modified by marine processes during the early Niobrara transgression" (p. 2135). McCubbin suggested that major topographic features were clearly present at the time of deposition of the basal Niobrara sandstone bodies and played a major role in determining sandstone distribution.

Like the pre-Niobrara erosion surface, the possibility exists that the Carrot Creek erosion surface (E5) was cut sub-aerially (fluvial downcutting) during lowstand and then modified by the subsequent marine transgression. This is an added complication, however, for which there is no supporting evidence preserved on E5 surface. If this evidence existed, it has been removed by the subsequent transgression. There is no preserved evidence to suggest that rivers head at the bevel and continue westwards or southwestwards across the Cardium shelf. The hypothesis that the E5 surface formed as a result of sub-aerial exposure is not supported by the data presented in this thesis.

3. Shoreface Erosion

The deposits of the Raven River Member directly underlying the E5 surface are believed by most workers to have been deposited in an open marine setting on a storm-dominated shelf (Krause, 1983; Krause and Nelson, 1984; Keith, 1985; Walker, 1983a, b, c). The formation of the E5 surface as a result of shoreface erosion implies a drop of relative sea level, causing the shoreface to move many tens of kilometres into the basin. In order to develop the preserved morphology of the E5 surface, the position of the shoreface at maximum lowstand must have been located at the basinward edge of the bumps and hollows (Bigoray, Fig. 4.1). Initial lowering of relative sea level must have been greater than sediment supply, causing the shoreline to move quickly basinwards resulting in sediment bypassing of the shelf. If sea lowering had been less than or equal to sediment supply, then a steadily prograding coarsening upward sequence of offshore muds passing up into shoreface and beach and lagoonal deposits would have been expected (eg., Kakwa and Musreau Members of the Cardium Formation, Plint and Walker, 1986). This type of sequence has not been observed in regional correlations (Plint et al., 1986) of the Raven River Member or the Carrot Creek Member of the Cardium Formation. Wave scour of the bed presumably resulted in the erosion of a new shoreface profile at maximum lowstand.

The formation of the E5 surface by shoreface erosion is consistent with the morphology and geometry of this surface. The maximum amount of sediment removal by a retreating shoreface would be expected to be seaward of the last preserved position of the shoreface (bevel). The basin sediments are removed by erosion as the shoreface retreats and these eroded sediments are transported basinwards. The formation of the remant topography of bumps and hollows by simple erosional retreat of the shoreface is difficult to explain. Two problems arise from this interpretation.

Firstly, how did the bump and hollow topography form, and secondly, why are the bumps and hollows not continuous along strike. A discussion of the bumps and hollows is given below. The continuous strike of the bevel indicates the presence of strongly localized erosion, and is consistent with erosion at the shoreface. The relatively flat terrace landward of the bevel is formed by erosional translation of the shoreface during sea level rise. The main problem arising from this interpretation concerns the formation and preservation of the bumps and hollows as a result of simple erosional retreat of the shoreface.

Bergman and Walker (1986; in press) interpreted the morphology of the E5 surface, particularly the remnant topography of bumps and hollows as having formed during a period of stillstand or sea level rise. During this time, erosional shoreface retreat toward the southwest produced the remnant topography. There is, however, no known erosional topography of bumps and hollows of this scale associated with the Holocene transgression. The pre-Holocene erosional surface described by Nelson and Bray (1970) and Kraft (1971) is relatively flat. The irregular topography preserved on the pre-Holocene surface is believed to be the result of fluvial incision during lowstand. Kraft (1971) illustrates a remnant topography associated with the Holocene transgression, but the relief on this surface is only about 4 m.

The bumps preserved on the E5 surface were interpreted by Bergman and Walker (1986; in press) as representing former positions of the shoreface. They suggested that the irregular morphology of the surface was due to partial gravel armouring of the bed, leaving erosional remnants during erosional shoreface retreat. The bevel marks the final position of the shoreface before marine transgression occurred, blanketing the entire sequence (Raven River Member and Carrot Creek Member) with marine mudstones of the Dismal Rat Member.

The morphology of the E5 surface is consistent with the hypothesis that it was formed by erosional retreat of the shoreface. Two problems arise from this interpretation of the E5 surface, firstly, the formation of the bump and hollow topography and secondly, the lack of continuity of the bumps along strike. The morphology of the E5 surface will be examined in more detail in the following sections, particularly the bump and hollow topography, in order to better understand how this topography might have formed.

8.3 FORMATION OF THE BUMP AND HOLLOW TOPOGRAPHY

The E5 surface is interpreted above as having formed by shoreface erosion. It was suggested (Bergman and Walker, 1986; in press) that the topography preserved on the surface was the result of lowering of relative sea level, shoreface erosion, and gravel armouring of the bed. This poses problems both regionally and locally.

On a regional scale (Fig. 8.1), with respect to an upper horizontal datum (E7/T7), the top of the Raven River Member appears to be a planar surface which has been dissected by the E5 surface (Fig. 8.1). The erosion associated with the E5 surface cuts into the same stratigraphic level of the Raven River Member across the basin. Each of these erosional cuts is interpreted as representing a shoreface profile. It does not seem reasonable to suggest that sea level dropped to erode a shoreface profile at Carrot Creek and rose to leave Pembina as a high and then dropped to erode a shoreface profile at Willesden Green and rose to preserve the sands in Willesden Green. Sea level would have to drop again in order erode another shoreface profile at the edge of Ferrier and then rise again. This interpretation would leave Pembina exposed as an island, while a shoreface profile was being established at Willesden Green. An island at Pembina would decrease the ability of the waves to scour at Willesden Green. If waves were capable of establishing a shoreface profile at Willesden Green, why was Pembina not eroded? The probability of preserving Pembina as an island while a shoreface profile was established at Willesden Green would be very low. The bump and hollow topography preserved in Carrot Creek poses similar problems to those described above but on a smaller scale.

Figure 8.1. Schematic cross section showing the morphology of the E5 surface across the basin with respect to an upper horizontal planar datum.

REGIONAL MORPHOLOGY OF THE E5 SURFACE
WITH RESPECT TO A HORIZONTAL DATUM

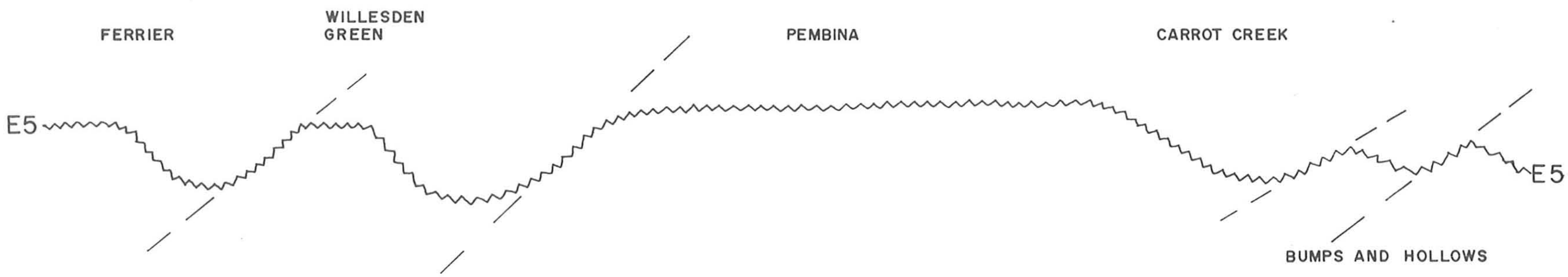

COULD THIS REPRESENT AN ORIGINALLY TILTED "STEPPED" EROSION SURFACE?

If the E5 surface were "stepped", then sea level would not have to fluctuate up and down. Instead, the surface could be produced by an initial lowering, followed by subsequent sea level rises separated by stillstands. If the E5 surface is stepped, this implies that the deposits of the Raven River Member must have had an original basinward dip, because erosion on the E5 surface occurs at the same stratigraphic level throughout the basin. The erosional cuts are believed to be formed by wave scour in the shoreface. In this interpretation, the tangent to the backs of the fields would represent the initial horizontal "bite" (where "bite" refers to the scouring of a new shoreface profile in the underlying Raven River sediments) and the distance between the tangents would indicate the amount of sea level rise. The possibility that the E5 surface was stepped was examined in detail locally for the bumps and hollows.

The morphology of the E5 surface in the Carrot Creek area (described above), is based on an assumed horizontal upper datum (E7/T7). The markers (and presumably the sedimentary facies) are roughly parallel to this datum. The E5 surface was shown in Chapter 4 to scour down to variable depths into the underlying stratigraphy of the Raven River Member. This resulted in the apparent irregular topography of bumps and hollows (refer to cross section B, Fig. 4.3, Foldout 2) preserved in the Carrot Creek -- Cyn-Pem study area.

The present discussion will now assume that the gritty siderite horizon (sub-facies 8 G.S., Fig. 3.13) is a planar surface, which has become dissected by the E5 erosion surface. This assumption appears to be reasonable because, the sub-facies is regionally extensive (except where removed by erosion) capping the top of a coarsening upward "b" sequence, is of relatively constant thickness (about 20 cm) and is interpreted as representing a period of non-deposition in the basin during a rapid rise of relative sea level. Within the study area there is no evidence of erosion at this horizon. The gritty siderite is always found gradationally overlying facies 5 of the "b" sequence.

The dissection of the "b" sequence, gritty siderite, and "a" sequence, resulting in the irregular topography of bumps and hollows presents problems. How is this topography related to relative sea level change and shoreface erosion?

Three possibilities of forming the bump and hollow topography as a result of stepping were considered;

1) Simple rotation of the backs of the bumps to the horizontal, using the average dip of the backs of the bumps as the implied original dip of the Raven River Member;

2) Calculating a regional dip of the underlying Raven

River Member from the basin plain and fitting the bumps and hollows into this regional dip;

3) Initial upward tilting of the underlying Raven River (which from now on will be referred to as "the surface") coupled with an episodic downward rotation.

Each of these possibilities will be discussed in detail below.

1) Simple Rotation

A portion of cross section B (Fig. 4.3, Foldout 2) was replotted (Fig. 8.2A) taking lateral spacing of the wells into consideration. The gritty siderite horizon was chosen as datum and the E5 surface was then replotted with respect to it. Plotting the surface this way revealed a similar topography of bumps and hollows to that resulting from plotting relative to the E7/T7 surface. From the plot of E5 relative to the gritty siderite, it was apparent that the slopes of the tangents to the backs of the bumps were essentially parallel (Fig. 8.2A). The slope of the tangents was calculated, giving an average slope of 0.024 (1.34°). If the tangents to the back of the bumps are rotated through 1.34°, making them horizontal (Fig. 8.2B), there is an implied original regional basinward dip of 1.34° of the gritty siderite and presumably the "a" and "b" sequences of the Raven River Member. The vertical exaggeration in both sketches (Fig. 8.2 A and B) is large as a surface dipping at 1.34° would be difficult to draft and study at

Figure 8.2. A) The E5 surface, from a portion of cross section B (Fig. 4.3) was replotted with the gritty siderite layer taken as horizontal, and the distance between wells scaled. The slope of the tangents on the backs of the bumps was calculated. The average slope was 1.34°. B) The tangents to the bumps were rotated to the horizontal (through 1.34°) giving an implied original dip of the gritty siderite of 1.34° basinwards. This results in a stepped profile for the E5 surface, very similar to that predicted by Swift et al. (1973) for the Holocene transgression. In both sections the vertical exaggeration is large. G.S. = Gritty Siderite, "A" and "B" refer to the coarsening upward sequences in the Raven River Member.

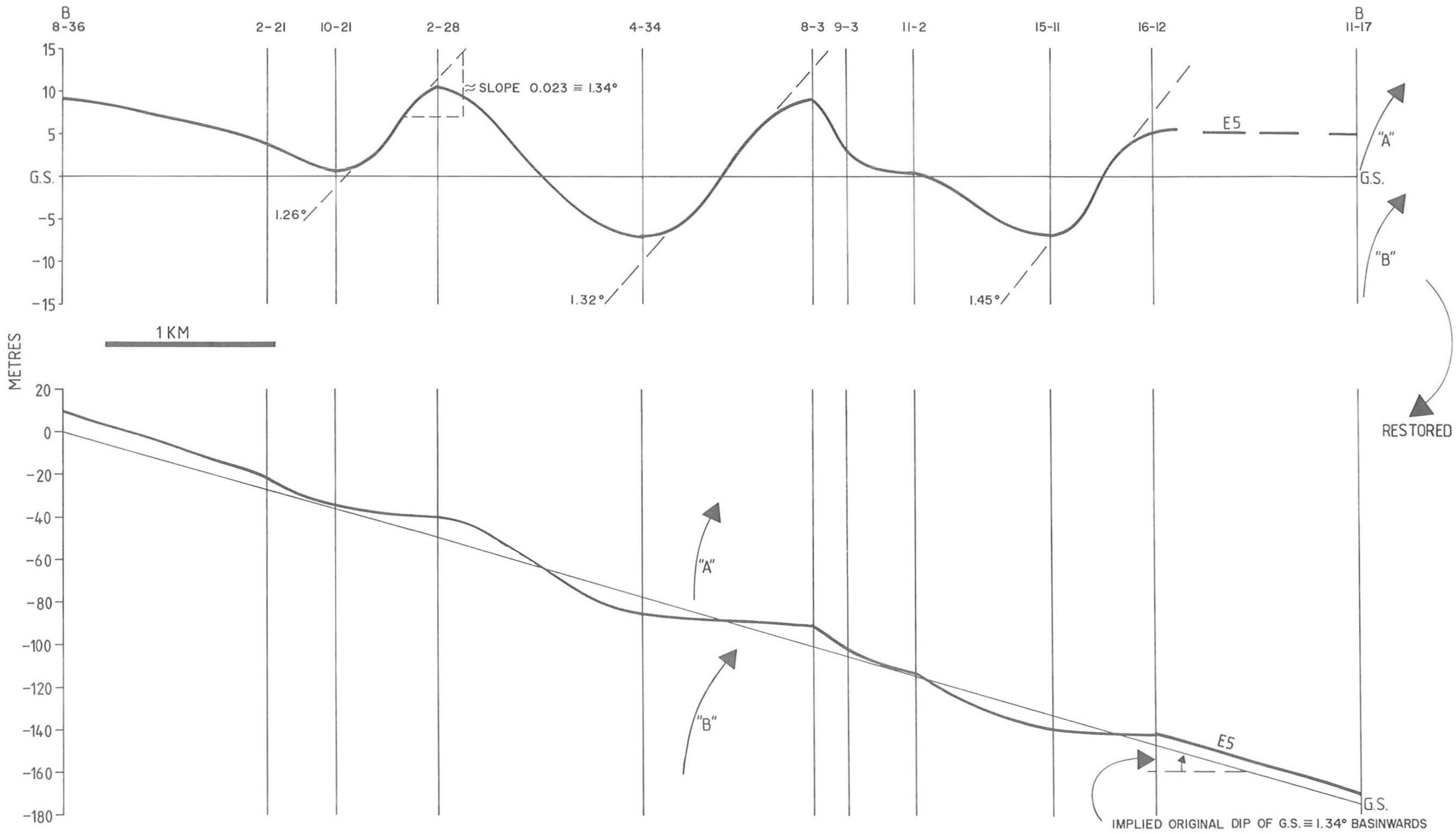

B
8-36
2-21
10-21
2-28
4-34
8-3
9-3
11-2
15-11
16-12
B
11-17
15
10
5
G.S.
-5
-10
-15
≈ SLOPE 0.023 ≡ 1.34°
1.26°
1.32°
1.45°
E5
"A"
G.S.
"B"
1 KM
METRES
RESTORED
20
0
-20
-40
-60
-80
-100
-120
-140
-160
-180
"A"
"B"
E5
G.S.
IMPLIED ORIGINAL DIP OF G.S. ≡ 1.34° BASINWARDS

true scale. Plotting the E5 surface with respect to an originally dipping seaward stratigraphy changes the topography of the surface from one of bumps and hollows to what appears to be a series of incised stepped shoreface profiles (Fig. 8.2).

Two main problems arise from interpreting the E5 surface in this manner. Firstly, the implied original regional dip of 1.34° basinwards of the gritty siderite and the Raven River Member is steep. If projected to an assumed highstand shoreline position at the edge of the deformed belt (show in Fig. 2.1) about 100 km to the west, then the Raven River sediments preserved in the Carrot Creek area would have been originally deposited in about 2,050 m of water. The edge of the deformed belt is the closest place to Carrot Creek where a highstand position of the shoreline could have been located. Basinwards of the deformed belt the Raven River sediments are marine. Considering the regional similarity of the deposits of the Raven River Member, and the preservation of hummocky cross stratification and wave ripples in the sandstones (facies 7 and 7A), water depths of 2050 m in the Carrot Creek -- Cyn-Pem area seem extremely unlikely.

Secondly, the shoreface "steps" preserved in the Carrot Creek area are relatively large (for example, 46 m over the relatively short distance of 2.24 km; refer to wells 2-28, 4-34 and 8-3 in Figure 8.2). The size of this step implies that sea level rose 46 m, assuming a constant regional dip, before the next shoreface profile was established. This is a very large rise.

The base of the shoreface is defined in modern studies as the break in slope where the more steeply dipping (2.86°) shoreface profile merges with the comparatively flat (0.0286°) inner shelf (definition and average slopes from Swift and Niedoroda, 1985). The possibility was examined that perhaps the dip values calculated from the tangents to the backs of the bumps were landward of this break in slope, and that the values were taken from the the more steeply dipping shoreface profile, not the flatter open marine profile. In this way the value of 1.34° does not represent the original slope of the gritty siderite and the dip of the Raven River deposits. The amount of sea level rise associated with the steps would then be an apparent rise, <u>not</u> the actual rise.

The result of this hypothesis is shown by geometric reconstruction and trigonometric analysis (Fig. 8.3). The tops of the bumps are labelled C and D. The angle measured on the backs of the bumps (β) is taken as a dip somewhere in the shoreface (line GF is a tangent to the curved profile CD in Case 1), relative to an originally dipping stratigraphy. The regional dip of the original stratigraphy is given as α. The angle (γ) is the intersection of the tangent to the shoreface profile with the originally dipping

Figure 8.3. Geometric reconstruction of the bump and hollow topography. Case 1, the tangent to the back of the bumps is rotated 1.34° to the horizontal, giving an implied regional basinward dip of the gritty siderite and Raven River Member of 1.34°. The height of the bite (CA) is the amount of sea level rise. Case 2, the tangent to the back of the bump (GF) represents a dip on the more steeply dipping shoreface rather than regional dip (EF). The bite height (GE) represents only an apparent rise in sea level. If the regional dip (α) is smaller than the calculated dip (β), then the apparent bite (GE) is smaller than the real bite (CA).

CASE I - DIP ON BACK OF BUMP GIVES REGIONAL DIP

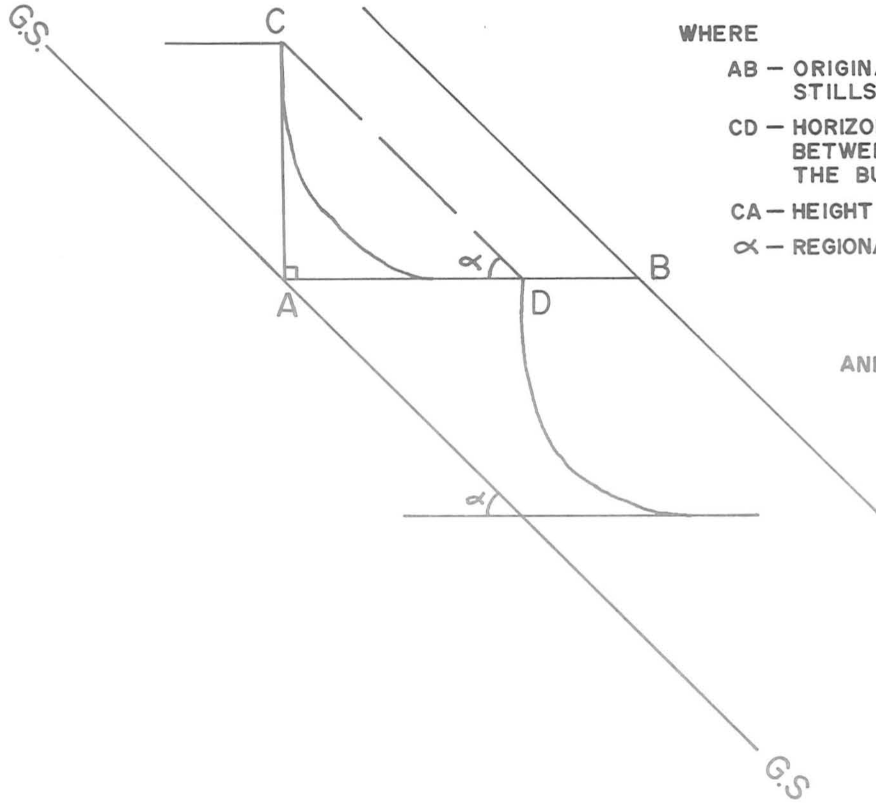

WHERE

AB — ORIGINAL HORIZONTAL STILLSTAND BITE

CD — HORIZONTAL DISTANCE BETWEEN THE TOPS OF THE BUMPS

CA — HEIGHT OF THE BITE

α — REGIONAL DIP

AND

$CA = CD \cdot \sin\alpha$

CASE 2- DIP ON BACK OF BUMP GIVES SHOREFACE DIP

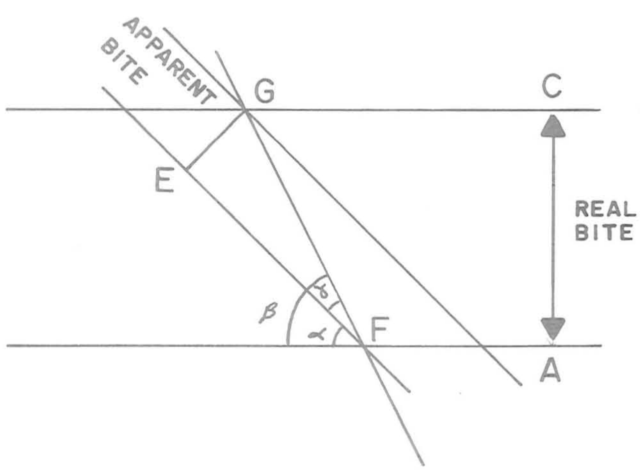

WHERE

CA — HEIGHT OF THE BITE

GE — APPARENT HEIGHT OF THE BITE

α — REGIONAL DIP

β — SHOREFACE DIP

γ — INTERSECTION OF SHOREFACE AND REGIONAL BEDDING

THUS, IF $\beta > \alpha$

THEN $CA > GE$

REAL BITE > APPARENT BITE

AND

$$CA = \frac{GE}{\sin\gamma} \cdot \sin\beta$$

stratigraphy. Point E is the intersection of the tangent to the next shoreface with the originally dipping stratigraphy. Line GE is the vertical separation between the two shoreface tangents and represents the size of the apparent bite. From this reconstruction, if $\beta > \alpha$, then the size of the real step will be larger than the apparent step. Thus the limiting position for the size of the step occurs when the back of the bump is rotated to the horizontal. From this analysis if the amount of rise calculated from the data is only an apparent rise, then the actual rise would be much larger.

For the above reasons this mechanism seemed unlikely for the formation of the bumps and hollows.

2) Shallow Regional Dip

The original basinward dip of the Raven River Member was determined from a portion of cross section A (Fig. 4.2) across the relatively flat basin plain located in the northeast corner of the study area. The dip calculated from this section was 0.04° (refer to wells 9-29-54-9 and 16-27-54-9 on cross section A, Fig. 4.2). This is believed to be a more realistic regional dip. Swift and Niedoroda (1985) record a dip of 0.0286° or lower for the shelf. If the shoreline is again taken at the edge of the deformed belt (Fig. 2.1), a distance of about 100 km, the use of 0.04° as the value of regional dip for the deposits of the Raven River Member implies that the depth of water in the

Carrot Creek area during Raven River time was about 60 m. This depth value is consistent with the formation and preservation of hummocky cross stratification observed at the top of the Raven River Member. The calculation of the the original dip of the Raven River stratigraphy is being considered in more detail by S.M. Leggitt (M.Sc. in progress, pers. comm., 1987) and D.J. McLean (M.Sc. in progress, pers. comm., 1987).

The problem arising from plotting the E5 surface with respect to an assumed originally dipping stratigraphy of 0.04° is that the topography of bumps and hollows is similar to that preserved when there is no implied basinward dip. Rotating the E5 surface through 0.04° does not solve anything. For this reason, this method does not seem a reasonable mechanism for forming the bump and hollow topography.

3) Tilting and Subsidence

This is the mechanism suggested to be responsible for the formation and preservation of the bump and hollow topography. In both of the previous methods, a dip was calculated from the cross sections and then applied as a static value to the entire basin. In this mechanism, an original regional dip (α) was calculated for the Raven River Member. By uplift in the rising Cordillera to the west, this dip (α) was then increased to a maximum value ($\beta + \alpha$), causing a fall of relative sea level. The newly emergent surface (top of the Raven River) subsequently rotates downwards until the initial regional dip is restored. This downward rotation is episodic, giving rise to periods of relative sea level rise during downward rotation of the surface, separated by periods of stillstand when little or no rotation is taking place. Throughout the rest of this discussion the assumption is made that depth is constant with respect to a "hinge" basinward of Cardium subcrop, and hence fairweather wave base is fixed with respect to the hinge. The following discussion of the formation of the bumps and hollows will consider;

A) how the erosional envelope is formed,

B) how this mechanism leads to the formation of the bump and hollow topography, and

C) both the positive aspects and the problems of forming the bumps and hollows in this way.

A) Formation of the erosional envelope

The method of forming and preserving the bump and hollow topography is shown diagrammatically in Figure 8.4. The depositional dip of the basin is increased to $\beta + \alpha$

where α is the regional dip

β is the amount of tilting

This initial upward tilting results in a relative sea level fall, and movement of the shoreface into the basin. The dip is held constant for a period of time (relative stillstand) in order to establish a initial horizontal shoreface bite

Figure 8.4. Summary diagram of the formation of an erosional envelope. The details of the diagram are presented in the text. The jagged line is used to represent missing section. The position of the hinge is further out in the basin.

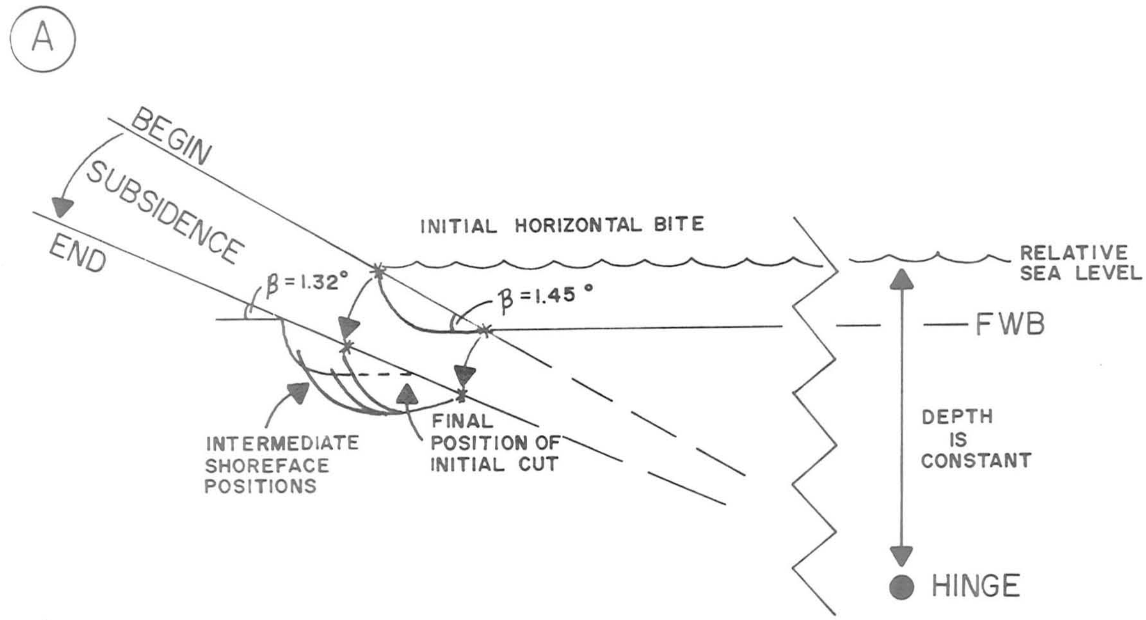
A
BEGIN
SUBSIDENCE
END
INITIAL HORIZONTAL BITE
RELATIVE SEA LEVEL
β = 1.32°
β = 1.45°
FWB
INTERMEDIATE SHOREFACE POSITIONS
FINAL POSITION OF INITIAL CUT
DEPTH IS CONSTANT
HINGE

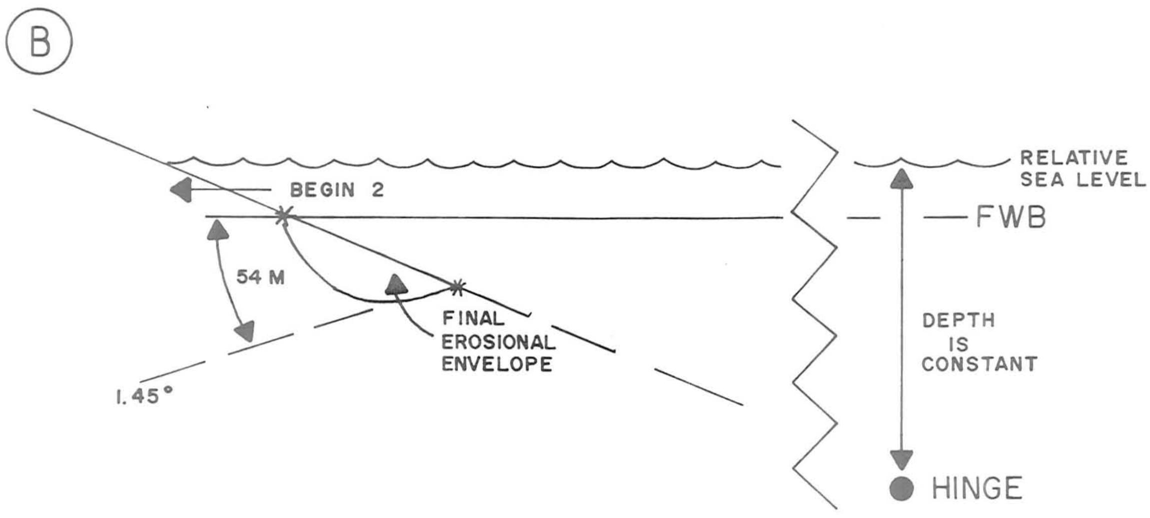
B
RELATIVE SEA LEVEL
BEGIN 2
FWB
54 M
FINAL EROSIONAL ENVELOPE
DEPTH IS CONSTANT
1.45°
HINGE

(Fig. 8.4A). The size of this initial cut will be a function of the depth of fairweather wave base and the length of stillstand. The surface begins to rotate downwards (subside) after the initial tilting, causing a rise in relative sea level. As the surface rotates downwards the initial horizontal bite is rotated downwards as well (Fig. 8.4A). The asterisks mark the positions of the initial horizontal bite. These are shown in their rotated position as the surface subsides. The initial horizontal cut rotates downwards with the surface and becomes what is now the back of a bump.

Intermediate positions of the shoreface are established during the downward rotation (Fig. 8.4A). Translation of the shoreface continues until there is a pause in subsidence (stillstand) and another horizontal bite occurs (shoreface position 2). These intermediate positions of the shoreface combine to form the preserved erosional envelope (Fig. 8.4B). The size of the erosional envelope is a function of time, and the rate of subsidence (thus proportional to a relative sea level rise), it is <u>not</u> a measure of the depth of fairweather wave base.

B) Formation of the Bump and Hollow Topography

The formation and preservation of the bump and hollow topography is summarized in Figure 8.5, and will be described below. The angles calculated in Fig. 8.2 will be used in this discussion. The initial regional dip (α) of

Figure 8.5. Summary diagram of the erosional history in the Carrot Creek -- Cyn-Pem study area, resulting in the formationa and preservation of the bump and hollow topography. The details of the diagrams are presented in the text.

(A)

DEPOSITIONAL ENVIRONMENT OF THE RAVEN RIVER MEMBER AT CARROT CREEK

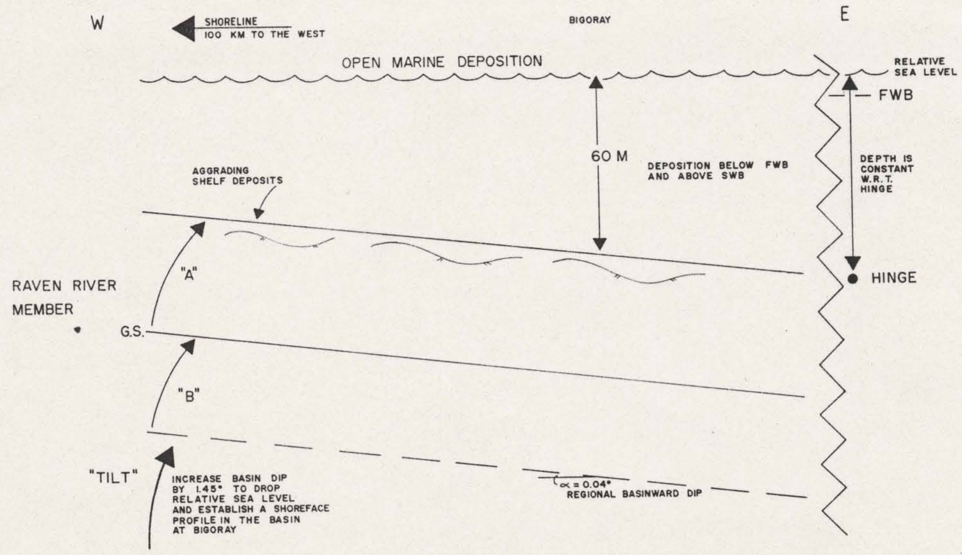

(B)

W STILLSTAND AT MAXIMUM LOWSTAND E

W STILLSTAND AT SHOREFACE POSITION 2 E

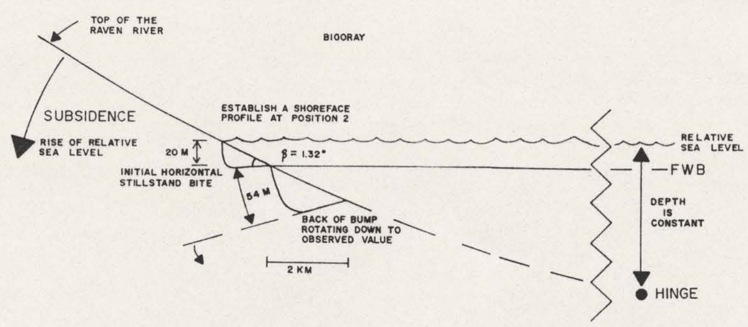

(D)

W STILLSTAND AT SHOREFACE POSITION 3 E

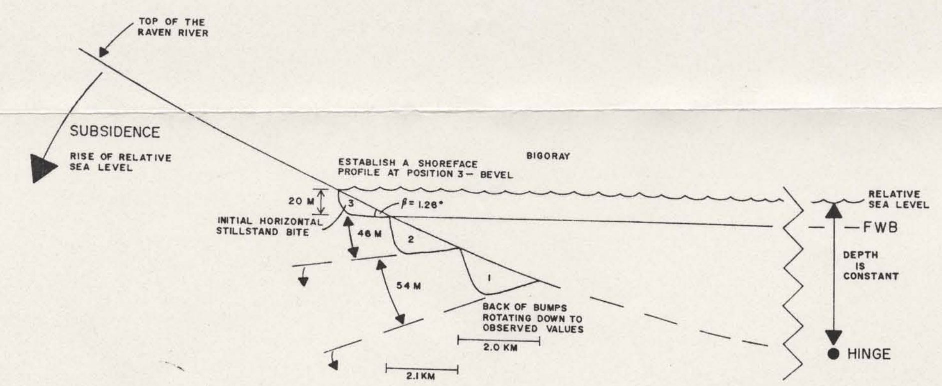

(E)

W CONTINUOUS SUBSIDENCE E

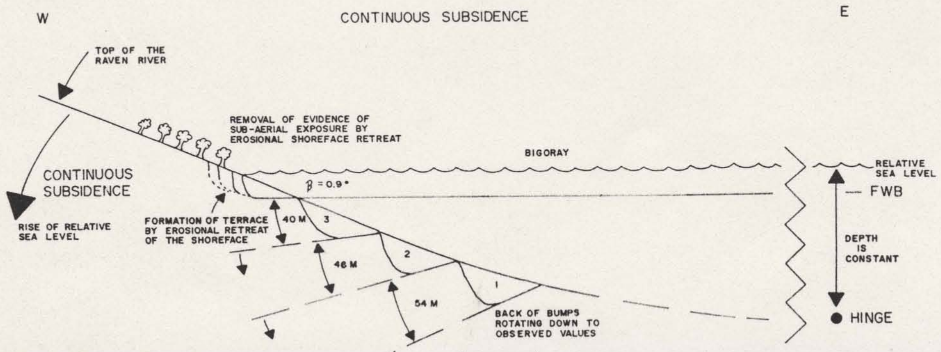

the Raven River Member will be taken as 0.04°. The absolute value of α is not crucial to this discussion. The details of the formation of the erosional envelope were shown in Figure 8.4. In this sequence of diagrams (Fig. 8.5) only the initial cut and the resulting erosional envelope are shown.

The deposits of the Raven River Member represent aggrading shelf sediments, deposited under open marine conditions below fairweather wave base and above storm wave base (preservation of hummocky cross stratified sands, facies 7, at the top of the Raven River Member). If the shoreline position at Raven River time is taken at the edge of the deformed belt, about 100 km to the west (Fig. 2.1), then hummocky cross stratified sandstones of the Raven River Member at Carrot Creek would have been deposited in about 60 m of water (Fig. 8.5A). A fixed hinge position is assumed to be present basinwards of Bigoray. Depth is constant with respect to this hinge and hence fairweather wave base is fixed with respect to the hinge.

Upwarping of the basin sediments increased the regional dip by 1.45° (Fig. 8.5A). This results in a drop of relative sea level and a shift in the shoreline basinwards to Bigoray. The depth with respect to the hinge remains constant. The relative drop is the result of a change in the intersection point between the land surface and the sea.

After tilting the sediments, an initial horizontal stillstand bite was established at Bigoray (Fig. 8.5B). The surface then rotated downwards, resulting in a rise of relative sea level and erosional southwestward translation of the shoreface. The erosional envelope rotated downwards with the surface (Fig. 8.5C). There was a pause in the downward rotation when the dip of the surface had dropped to 1.32°. Another horizontal stillstand bite was established at shoreface position 2 (Fig. 7.1). Slow subsidence began again, resulting in a relative sea level rise and shoreface translation.

The downward rotation paused again at 1.26° and a horizontal bite is carved at shoreface position 3 (Fig. 7.1). The two previously formed erosional envelopes rotated downwards again with the surface (Fig. 8.5D). Subsidence resumed and appears to have been more continuous from this time.

The terrace formed during the slow continuous subsidence of the surface. Erosional shoreface translation removed any evidence of sub-aerial exposure (Fig. 8.5E). With continued subsidence the erosional envelopes continued to rotate downwards with the surface until regional basin dip is restored, producing the observed topography of bumps and hollows.

C) Advantages and Complications associated with this Interpretation

The formation of the bump and hollow topography by initial upward tilting and episodic subsidence solves a number of problems associated with the formation and preservation of this topography. Unfortunately, a few questions also arise. I will consider first the advantages of the above mechanism of generating and preserving this topography, and then present some of the problems associated with this interpretation in the Carrot Creek area.

ADVANTAGES

1. Forming the topography in this way allows for an initial regional dip of the Raven River Member independent of the dips associated with the bump and hollow topography.

2. Upward tilting of the sediments results in a relative sea level drop and basinward migration of the shoreline. Episodic subsidence allows the establishment of the initial shoreface profiles during stillstand, and continuous subsidence allows erosional shoreface translation during relative sea level rise.

3. The size of the erosional envelope between the horizontal stillstand bites is not an indication of the depth of fairweather wave base, rather the size of the step is related to time and the rate of subsidence. The amount of shoreface translation is related to time, the rate of shoreface erosion, and the rate of subsidence (rate of relative sea level rise).

4. The episodic downward rotation is consistent with the formation and preservation of the bumps and hollows. As the

surface rotates downwards (Fig. 8.6), the initial horizontal bite rotates downwards with the surface and forms what is now preserved as the back of a bump. The dips of the tangents to the backs of the bumps decrease progressively southwestwards both locally (Fig. 8.2) and regionally. S.M. Leggitt (pers. comm., 1987) has recorded dips on the back of bumps across Pembina of 0.97°, 0.82°, and 0.14°. The dips are progressively decreasing in a southward direction.

COMPLICATIONS

The hypothesis discussed above for the formation of the E5 surface is based on only one cross section (Fig. 8.2) through the bumps and hollows. It assumes that the top of the Raven River Member is a shallow seaward dipping <u>planar</u> surface. Two complications arise when this hypothesis is expanded to cover the entire area of study. Firstly, the bumps and hollows are not continuous along strike. Secondly, the dip values on the backs of the bumps decrease along strike on either side of cross section B.

The along strike discontinuity of the bumps and hollows poses problems. In a shoreface interpretation it would be expected that the positions of the shoreface would be marked by a long continuous scarp, such as the bevel, rather than a series of discontinuous bumps and hollows. On the conglomerate isopach map, the thick conglomerate pools line up on three linear trends (Fig. 7.1) which were interpreted

Figure 8.6. Summary diagram of the mechanism of formation of the bumps and hollows. The dips shown to the backs of the bumps are those calculated in Figure 8.2. The relative positions of the terrace, bevel, and bumps and hollows are shown. Depth is constant with respect to the hinge. Relative sea level rise is the result of the subsidence. The backs of the bumps represent the initial horizontal bites at stillstand, and the hollows (erosional envelope) form as a result of shoreface translation during relative sea level rise.

SUMMARY DIAGRAM OF THE MECHANISM OF FORMATION OF THE BUMPS AND HOLLOWS

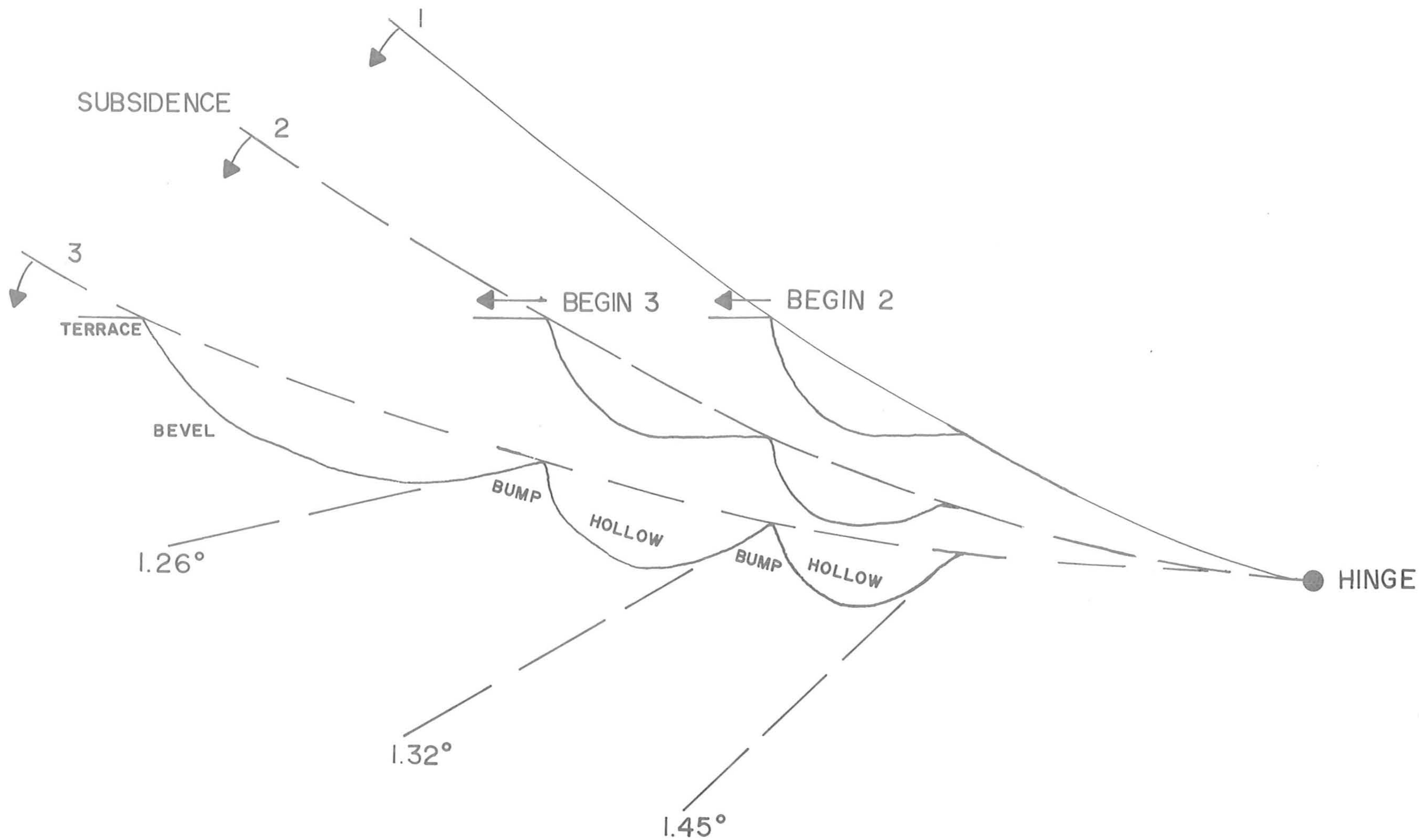

as representing positions of the shoreface in the basin. These trends however, are difficult to discern on the contour map of the erosion surface. The dip values and the wells from which they were calculated are shown in Fig. 8.7, with the relative position of the shoreline shown as a double line. The locations of the shorefaces determined from the map of the erosion surface differ slightly in position from those determined from the conglomerate pools, but the trends are similar.

The discontinuity of the bumps and hollows may be a result of the data available. Some of the isolated hollows are probably more continuous than shown by the contour patterns.

The angles of the backs of the bumps were calculated with respect to the gritty siderite for cross sections A and D (Figs. 4.2 and 4.4 respectively). The dip values calculated for the three sections decrease landwards as predicted by the hypothesis. The complication arises from the along strike variation in dips.

The values calculated from cross section D are consistent with values recorded by S.M. Leggitt (pers. comm., 1987) for Pembina. There appears to be a gradual decrease in the dip values southeastwards, suggesting a tilting of the surface to the southeast.

The dip values calculated from cross section A to the north of cross section B give markedly different results from both cross section B and D (Fig. 8.7). The change in values northwards appears to be abrupt rather than gradual as shown in the south. The morphology of the surface changes abruptly to the north as well. The well defined bump and hollow topography recorded in the south is a more gently undulating surface to the north. These differences suggest that some sort of decoupling of the surface has occurred across the field. A number of possibilities were considered to explain the along strike variation;

1) strike slip faulting,

2) thrust faulting, and

3) differential compaction over a pre-existing topography.

Each of these possibilities will be discussed below.

1) Strike Slip Fault

The possibility of a sinistral strike slip fault separating the northern and southern areas of the field was considered. The argument for this fault was the apparent offset of the conglomerate pools along strike (Fig. 7.1, and Fig. 8.7). From this map, the horizontal offset on the fault would have been about 10 km. The problem with this interpretation is that the fault cannot be traced basinwards or landwards. The projection of this fault westwards would cut the Kakwa shoreface. There is no offset of the Kakwa shoreface in the area projected for the trace of the fault. Considering the amount of displacement that would be

Figure 8.7. The dips on the backs of the bumps with respect to the gritty siderite are shown for cross sections A, B, and C are shown, along with the implied position of the shoreface (double line). Note the along strike variation of the dip values and the lack of continuity of the bumps. Northwards of cross section B (blocked line) the dips are very low and the topography of bumps and hollows is becoming less pronounced.

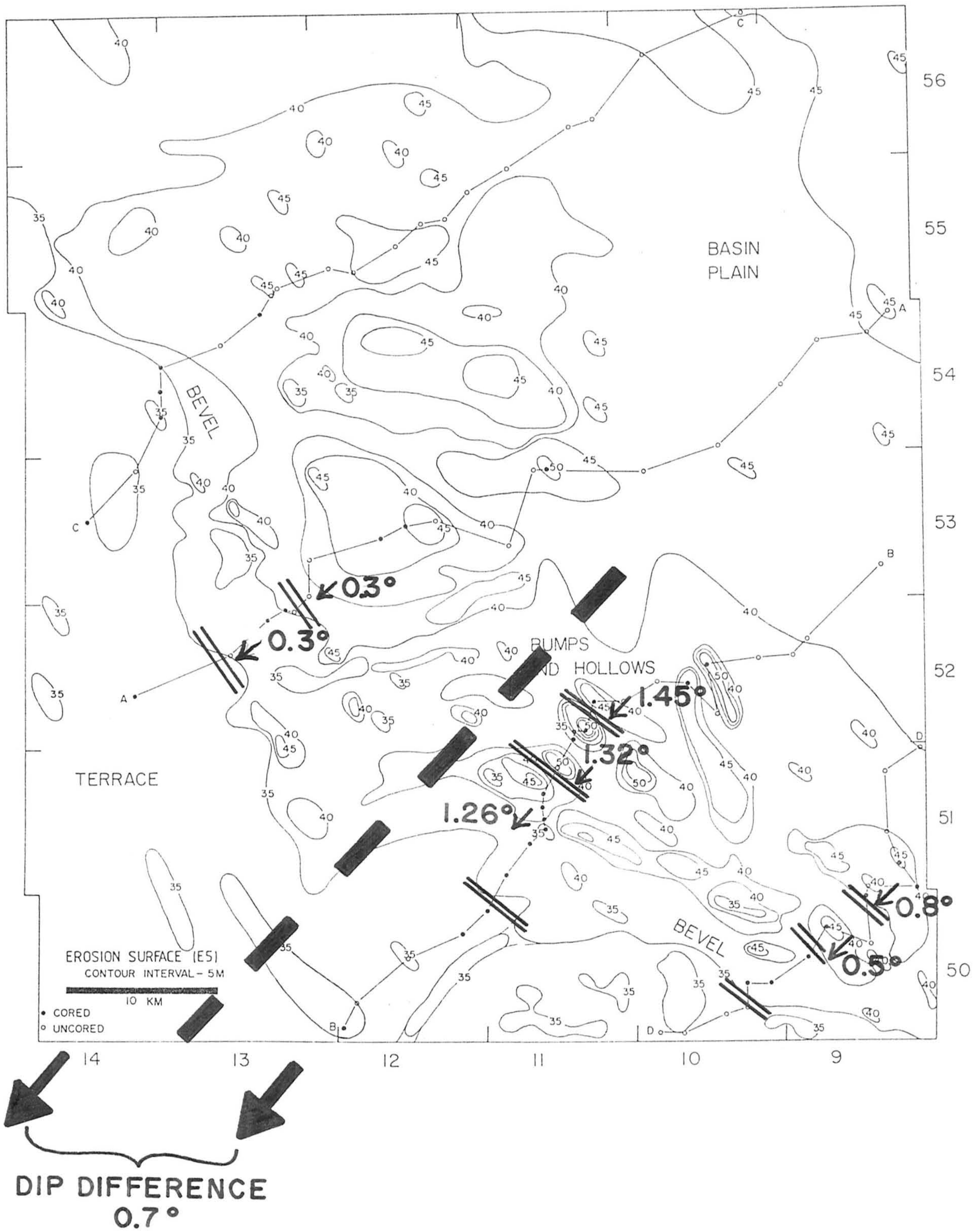
BASIN
PLAIN
BEVEL
TERRACE
BUMPS
AND HOLLOWS
BEVEL
0.3°
0.3°
1.45°
1.32°
1.26°
0.8°
0.5°
EROSION SURFACE (ES)
CONTOUR INTERVAL - 5M
10 KM
• CORED
○ UNCORED
14
13
12
11
10
9
56
55
54
53
52
51
50
DIP DIFFERENCE
0.7°

necessary to give the preserved morphology, the lack of mapability poses serious problems. For this reason, the hypothesis that the observed along strike variation in topography and dip was the result of a strike slip fault in the Carrot Creek area was rejected.

2) Thrust Faulting

Another mechanism considered for decoupling the northern part of the field from the southern part was the possibility of post-Cardium thrust faulting. The thrust slice would have to have slid across the top of the Kakwa shoreface (no offset of the Kakwa shoreface) in the west and continue basinwards into the Carrot Creek area. At Carrot Creek the thrust fault breaks into two separating the field into two sections. The southern thrust slice moved farther into the basin than the northern thrust slice. Again regional correlations show no evidence for this thrust. Thrust faulting does not account for the along strike variation in depositional dip, or the along strike variation of the bumps and hollows. For these reasons, the hypothesis that thrust faulting was responsible for the along strike variation in topography and dip was rejected.

3) Differential Compaction

In the present discussion, the assumption is made that the top of the Raven River is a seaward dipping planar surface. However, if the top of the Raven River is not planar, than variations in along strike dips would be expected.

Pembina oil field is situated on top of a group of Devonian Nisku pinnacle reefs (Nielson and Porter, 1984; Exploration Staff, Chevron Standard Limited, 1979). The location of these pinnacle reefs is shown in Figure 8.8. The present study area is outlined and the position of the northwestern edge of the bumps and hollows is shown. Note that northeast of the edge of the bumps and hollows (Fig. 8.7) there are no pinnacle reefs preserved in the Winterburn Basin (Fig. 8.8), and that the best development of bumps and hollows coincides with the area of pinnacle reefs (Figs. 8.7 and 8.8).

Sediments draping the reefs will reflect the topography of the reefs through differential compaction. With time, the topography is flattened out as sediments accumulate in the basin. By Raven River time differential compaction over the reefs results in a broad gently undulating surface, such that the area over the reefs is a relative high while northwards the surface is a relative low (Fig. 8.9).

The original basin dips also vary across this break in slope. The slope on the northwestern side of the edge of the bumps and hollows is rotated downwards compared with the southeastern side (Fig. 8.9). This topography is also presumably the result of differential compaction over a pre-existing topography (presumably following a Devonian reef trend). The change in dip of the two surfaces is less

Figure 8.8. Location map showing the position of Devonian Nisku reefs in the study area. Note that the northward edge of the bumps and hollows (dashed line) is coincident with the edge of the pinnacle reefs developing on the Nisku shelf, and the edge of the Winterburn carbonate shale basin. (map taken from Exploration Staff, Chevron Standard Ltd., 1979).

DIP INTO WINTERBURN BASIN

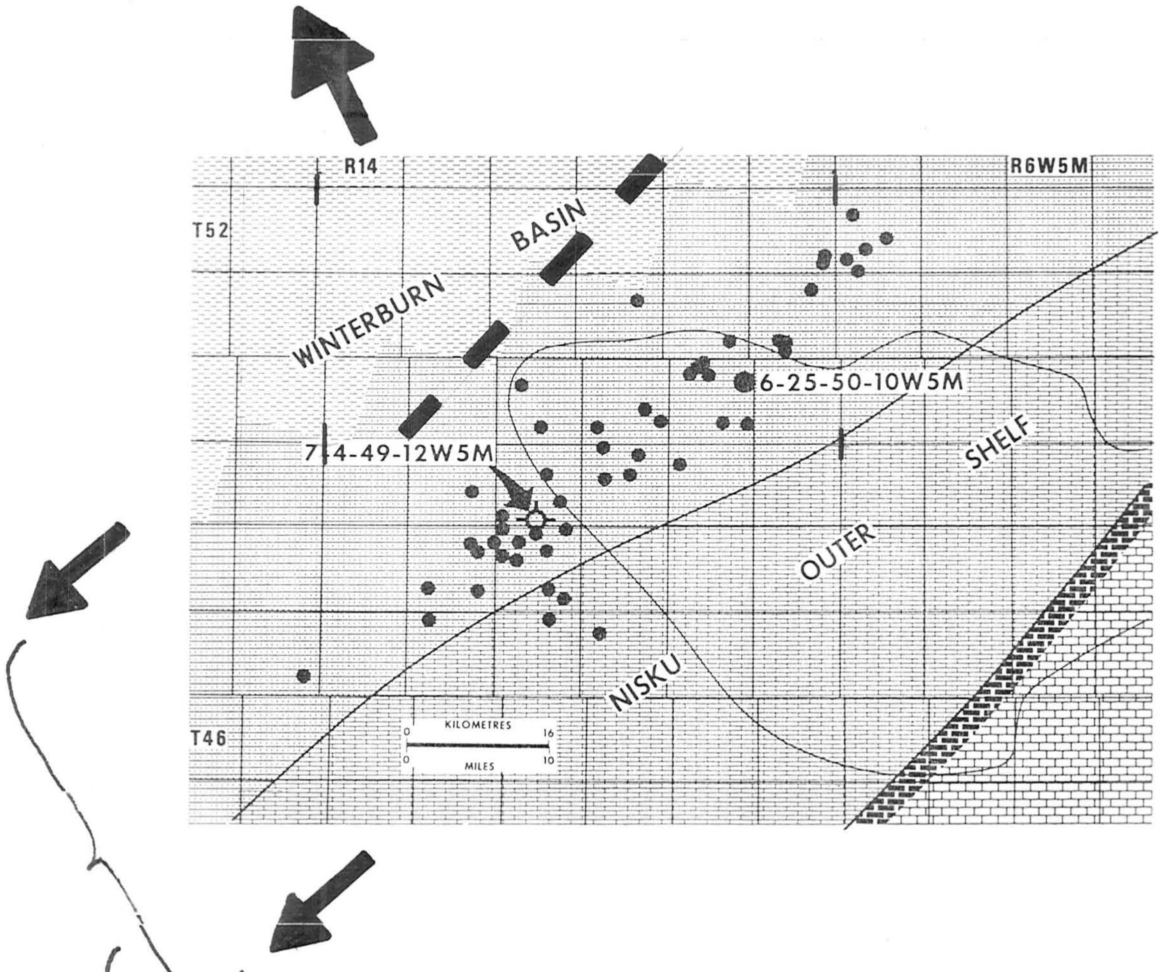

DIP DIFFERENCE ALONG
NE/SW TREND OF 0.7°

Figure 8.9. Cartoon showing the inferred depositional morphology of the top of the Raven River due to differential compaction over the underlying Devonian reef complexes, prior to erosion by the E5 surface. The relative positions of the shorefaces drawn on. The more steeply dipping portions of the surface the erosional envelopes will translate predominantly upwards, while on the more gently dipping surface to the north, shoreface translation is predominantly horizontal.

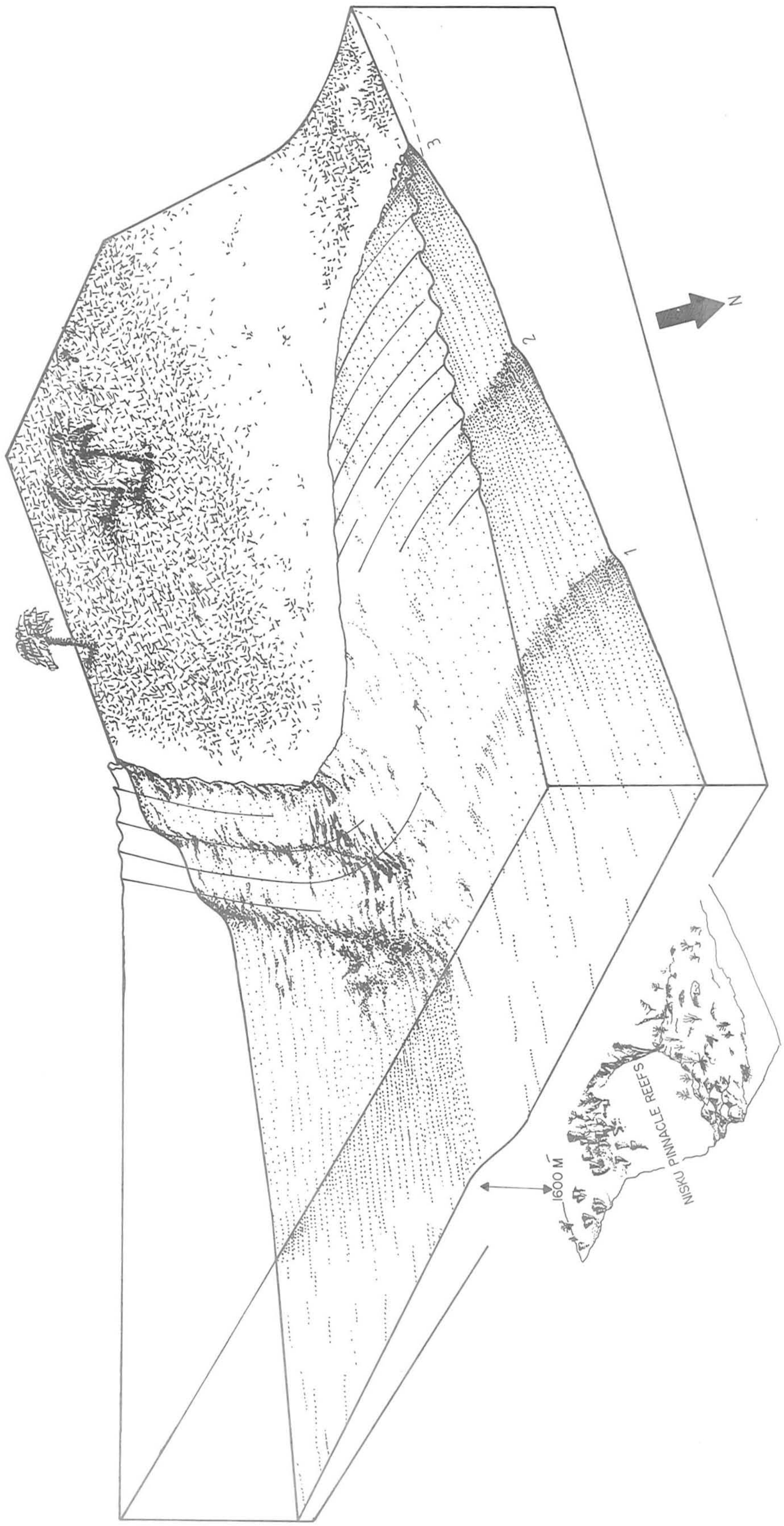

3
2
1
N
1600 M
NISKU PINNACLE REEFS

than 1°. Hence, the values obtained for the amount of upward tilting of the surface vary along strike. That is, the more steeply dipping seaward part of the surface (southeastern side) will record steeper dips, while the less steeply basinward dipping part of the surface (northwestern side) will record shallower dips (Fig. 8.9).

The morphology of shoreface profiles cut into the undulating Raven River Member would also vary along strike. In areas where the dips are steep the shoreface profile will translate upwards during subsidence, forming narrow, deep erosional envelopes. However, where the dip of the surface is shallow the shoreface will translate horizontally during subsidence, resulting in broad, shallow erosional envelopes. The positions of the shoreface will appear to be offset due to wrapping around of the shoreline profile on the variably dipping topography (Fig. 8.9).

This hypothesis requires further study of the underlying sediments to assess the validity of the argument.

8.4 Relationship of the Carrot Creek Member to the E5 Surface

The conglomerates of the Carrot Creek Member are interpreted in this thesis as shoreface deposits. The conglomerates were presumably deposited during the formation of the initial horizontal shoreface bite (Fig. 8.4), and during the subsequent translation of the shoreface whilst relative sea level rose. The transgressive pebbly mudstones (Dismal Rat Member) now blanket the conglomerates that were preserved in earlier erosional envelopes when later shoreface profiles are forming. This interpretation is based primarily on 1), the morphology and the interpretation of the formation of the E5 surface directly underlying the conglomerates; 2), the interbedding of the conglomerates with marine mudstones, and to a lesser extent 3), on the regional stratigraphy (Plint et al., 1986). This discussion will consider three aspects of the conglomerates;

1) the areal distribution of the thick conglomerate pools,

2) the deposits preserved in a "typical" pool, and

3) the relationship of the pools to the E5 surface.

1) Areal Distribution

The E5 surface is covered by pebbles of the Carrot Creek Member. The conglomerates vary in thickness from a thin veneer to thick (up to 20 m) localized elongate pools trending northwest-southeast. The pools are associated with the deepest scours on the the E5 surface. The average size of the pools is 5.0 km long by 1.2 km wide. Each of these pools is interpreted as representing a shoreface deposit, based primarily on the "one-sided geometry" of the gravel deposits.

The map of the areal distribution of the conglomerates (Fig. 7.1) shows that the individual gravel pools occur on one of three linear trends, labelled 1, 2, or 3 on the map. Each of these trends is interpreted as marking a former position of the shoreface in the Carrot Creek area. The position of these three linear trends do not coincide exactly with the position of the trends predicted from the structure contour map (Fig. 8.7). However, the trends are similar. Position 1, at the seaward edge of the bumps and hollows, is believed to mark the position of the maximum lowstand shoreface, while position 3, the bevel, marks the final position of the shoreface.

2) Deposits of a "Typical" Pool

The conglomerate sequences preserved in each of the pools are similar, regardless of which position of the shoreface the pool is taken from (refer to cross sections in Chapter 7, Figs. 7.3 to 7.7). The conglomerate sequence is sub-divided into upper and lower shoreface deposits, based on

1) the textural variation, particularly the development of stratification;
2) the position of these textures in the overall conglomerate sequence; and
3) the thickness of the deposits (described in Chapter 6).

The boundary between the upper and lower shoreface deposits is transitional. Overall the conglomerate sequence coarsens upwards (Fig. 6.17).

The lower shoreface deposits are generally less than 5 m thick and are characterized by well developed low angle inclined stratification. These deposits are generally found at the base of the sequence, directly overlying the E5 surface. The deposits of the upper shoreface are about 10 m thick and are characterized by crudely stratified to massive conglomerates, and comprise the upper part of the conglomerate sequence.

There is no record of a beach preserved in the Carrot Creek area. If a beach has been preserved, it was not recognized. It is more likely, however, that the beach was eroded and/or reworked during relative sea level rise. There is no evidence of sub-aerial exposure (eg., roots, coals, soils) preserved in the Carrot Creek area. These features are believed to have been removed by erosional shoreface translation during sea level rise (Fig. 8.5E).

Gravel is continuously supplied to the shoreface, however, the thickness of the conglomerates preserved in the hollows however is not a function of the depth of fairweather wave base or the size of the erosional step. In this interpretation as the surface subsides, erosional shoreface translation occurs. The lower shoreface deposits of the initial horizontal cut sink below fairweather wave base as the surface rotates downwards. The conglomerates of the upper shoreface of the initial horizontal cut are reworked during shoreface translation, as the surface rotates downwards, resulting in a relative sea level rise, and hence a relative rise in fairweather wave base. Thus, the textural sequences preserved in the hollows are a function of reworking in a translating shoreface (Fig. 8.10). The lower shoreface deposits are preserved only in the deepest parts of the hollows, where the deposits have sunk below fairweather wave base, as the the surface rotated downwards, and hence were not subject to wave reworking in the translating shoreface.

3) Relationship of the Conglomerate pools to the E5 surface

Gravel is deposited in the initial horizontal shoreface bite and is reworked as the shoreface translates during subsidence and relative sea level rise. A pause in subsidence results in a relative stillstand. At this time, upper shoreface gravels deposited during the final stages of subsidence would be reworked landwards as a transgressive lag (Fig. 8.10), as the new initial horizontal stillstand bite is cut. The lag deposits are overlain by lower shoreface deposits (Fig. 8.10) from the newly forming erosional envelope. With resumed subsidence the lower shoreface deposits sink below fairweather wave base and pass vertically upwards into the transgressive pebbly mudstones of the Dismal Rat Member (Fig. 8.10).

This is demonstrated most effectively in well 12-16 (Fig. 7.4), located at shoreface position 2, where deposits interpreted as upper shoreface (based on the preserved

Figure 8.10. Conglomerate fill of an erosional envelope. The thickness of the conglomerates preserveved in an erosional envelope is not a function of fairweather wave base. During subsidence there is a relative sea level rise and shoreface translation reworking the gravels in the shoreface. It is this constant reworking in the translating shoreface that gives the preserve textural relationships of the conglomerates in the hollows.

GRAVEL FILL OF AN EROSIONAL ENVELOPE

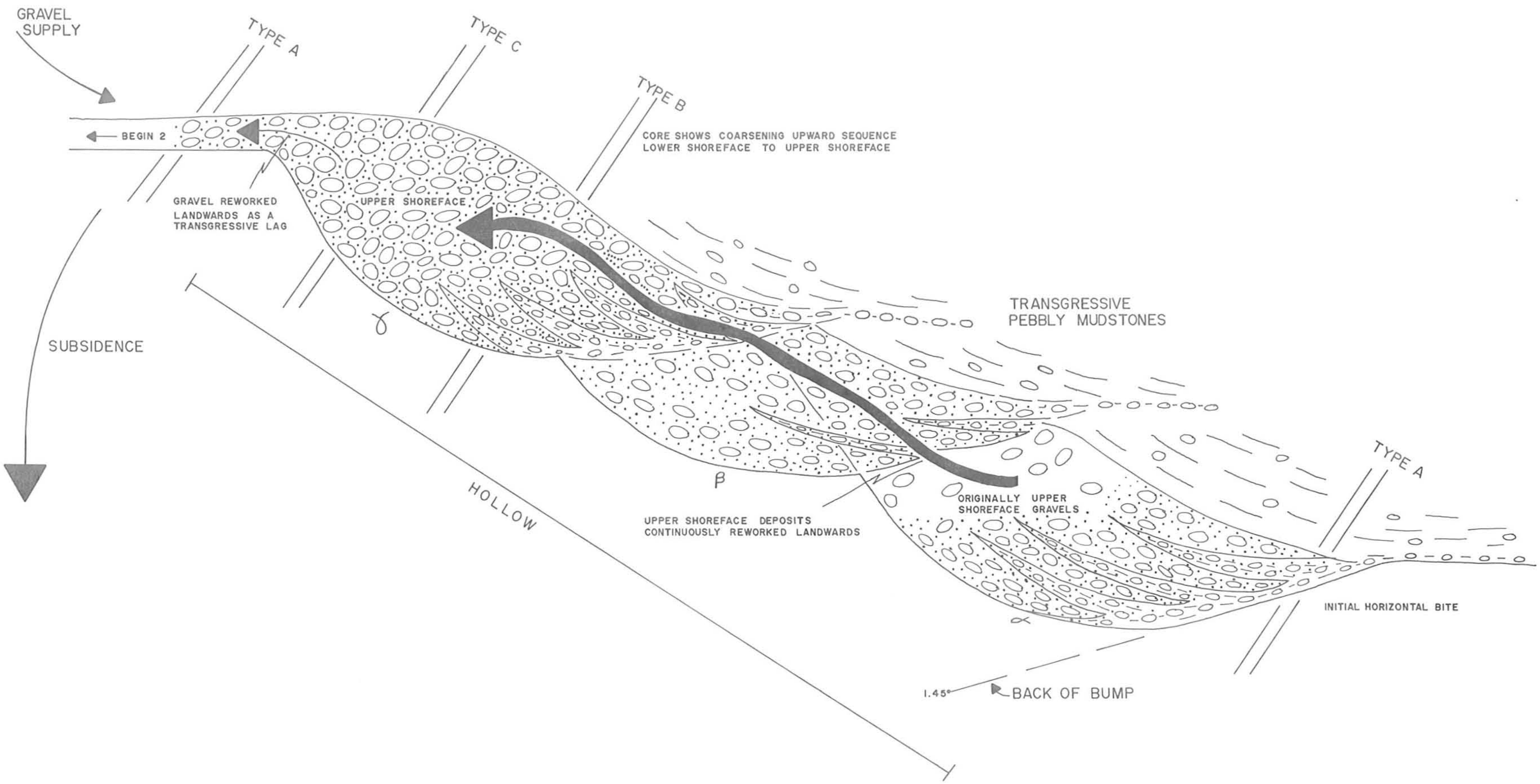

conglomerate textures) are overlain by deposits interpreted as lower shoreface (with the interpretation based on the conglomerate textures). The lower shoreface deposits pass vertically upwards into transgressive pebbly mudstones. The upper shoreface deposits were deposited when the shoreface was at position 2, and reworked landwards as the initial cut of shoreface 3 was being established. The lower shoreface deposits and the transgressive mudstones were deposited from a more landward position of the shoreface. The same situation occurs at Bigoray (shoreface position 1) where the landward conglomerate is covered by a thick sequence of transgressive pebbly mudstones, and passes laterally basinwards into a thick conglomerate (Figure 7.6, wells 9-7 and 11-8). The thick conglomerates preserved in well 11-8 were deposited when the shoreface was at position 1 (Bigoray), while the thick sequence of transgressive pebbly mudstones preserved in well 9-7 were deposited from a more landward shoreface position.

8.5 SOURCE OF THE GRAVEL

The problem of how the gravel is supplied to the shoreface has not been specifically adressed in this thesis. Regional correlation of the Cardium (Plint et al., 1986; Duke, 1985a), however, leaves two options for supplying gravel to the Carrot Creek shoreface. The gravels may be transported from the northwest by longshore drift, or the gravels may be transported directly from the west by incised fluvial channels during lowstand. These two possibilities will be considered individually below.

1) Longshore Drift

The idea of longshore drift from the northwest was suggested by A.G. Plint (pers. comm., 1986). In the Peace River area of Northern Alberta there is an outcrop of thick conglomerate (Baytree Member of Stott, 1963) believed by Plint to be stratigraphically equivalent to the Carrot Creek Member. This conglomerate is interpreted as fluvial and gives consistent flow directions to the southwest. Basinwards, the Baytree conglomerates appear to become dominated by marine wave processes.

A.G. Plint (pers. comm., 1986) suggested that the Baytree River was the source of the Carrot Creek conglomerate, and that the conglomerates were transported approximately 400 km from Baytree southeastwards to Carrot Creek by longshore drift. However, there is no evidence of gravel shoreface deposits between Carrot Creek and Baytree. Modern gravel transport by longshore drift in the shoreface occurs over relatively small distances. Using the transport rates determined by Carr (1971) for Chesil beach, transport of the gravel from Baytree to Carrot Creek could take anywhere from 3.2 to 45 years. These figures apply only to the movement of one pebble. Transport of the conglomerates to the Carrot Creek shoreface by longshore drift from Baytree (approximately 400 km) during lowstand, implies a time lag between the formation of the shoreface profile and the arrival of gravel. This hypothesis does not fit well with the method suggested above of forming the bump and hollow topography.

2) Fluvial Supply

A drop in relative sea level by increased seaward tilting of the basin sediments would result in a drop of base level, and hence an increased gradient that would allow the transport of gravel directly to the shoreline. If fluvial supply directly from the west is the source of the Carrot Creek conglomerates, based on regional correlation (Plint et al., 1986), all evidence of this fluvial system and sub-aerial exposure has been removed by erosional shoreface translation during a relative sea level rise (Fig. 8.5E).

If the highstand shoreface position is again assumed to be at the edge of the deformed belt (Fig. 2.1), then the conglomerates would only have to be transported about 100 km to the depositional site at Carrot Creek. The gradient decreases with each successive landward position of the shoreface. This has two effects on the conglomerates. Firstly, the thickness of the gravel deposits would also decrease landwards from Bigoray southwestwards across Pembina (Fig. 2.1), as the gradient decreases. Secondly, there appears to be a slight decrease landwards in the average size of the largest pebbles (apparent long axis) observed in core, from the seaward edge of the bump and hollows (2.5 cm) to the edge of the bevel (2.1 cm; Fig. 8.11).

Nemec and Steel (1984) suggested that thick sequences of conglomerate in shallow marine settings are likely to be the product of a pronounced fluvial flooding. In systems of fluvial -- wave interaction, gravels may accumulate laterally from the channel mouth. These accumulations may be represented in the Carrot Creek area by the thick localized conglomerate pools. The pools tend to line up not only along strike, but also down dip (Fig. 7.1), and may mark the relative positions of fluvial discharge into the system. Conglomerates of this origin will have characteristics suggesting a wave-dominated settings (Nemec and Steel, 1984).

8.6 COMPARISON WITH THE PRE-HOLOCENE EROSION SURFACE

The topography of bumps and hollows associated with the E5 surface forms in response to tectonic uplift in the Cordillera and <u>relative</u> sea level variation in a foreland basin. This type of surface would not be expected to form on a pre-Holocene erosion surface on a passive continental margin. The formation of the individual shoreface profiles on the E5 surface are believed to form by similar erosional processes as described for the pre-Holocene erosion surface (Swift et al., 1972; Swift et al., 1973; Rampino and Sanders, 1980). The preserved topographies of these

Figure 8.11. Map showing the average of the ten largest grains (measured as long axis from core) for each of the three preserved positions of the conglomerate shown on Figure 7.1.

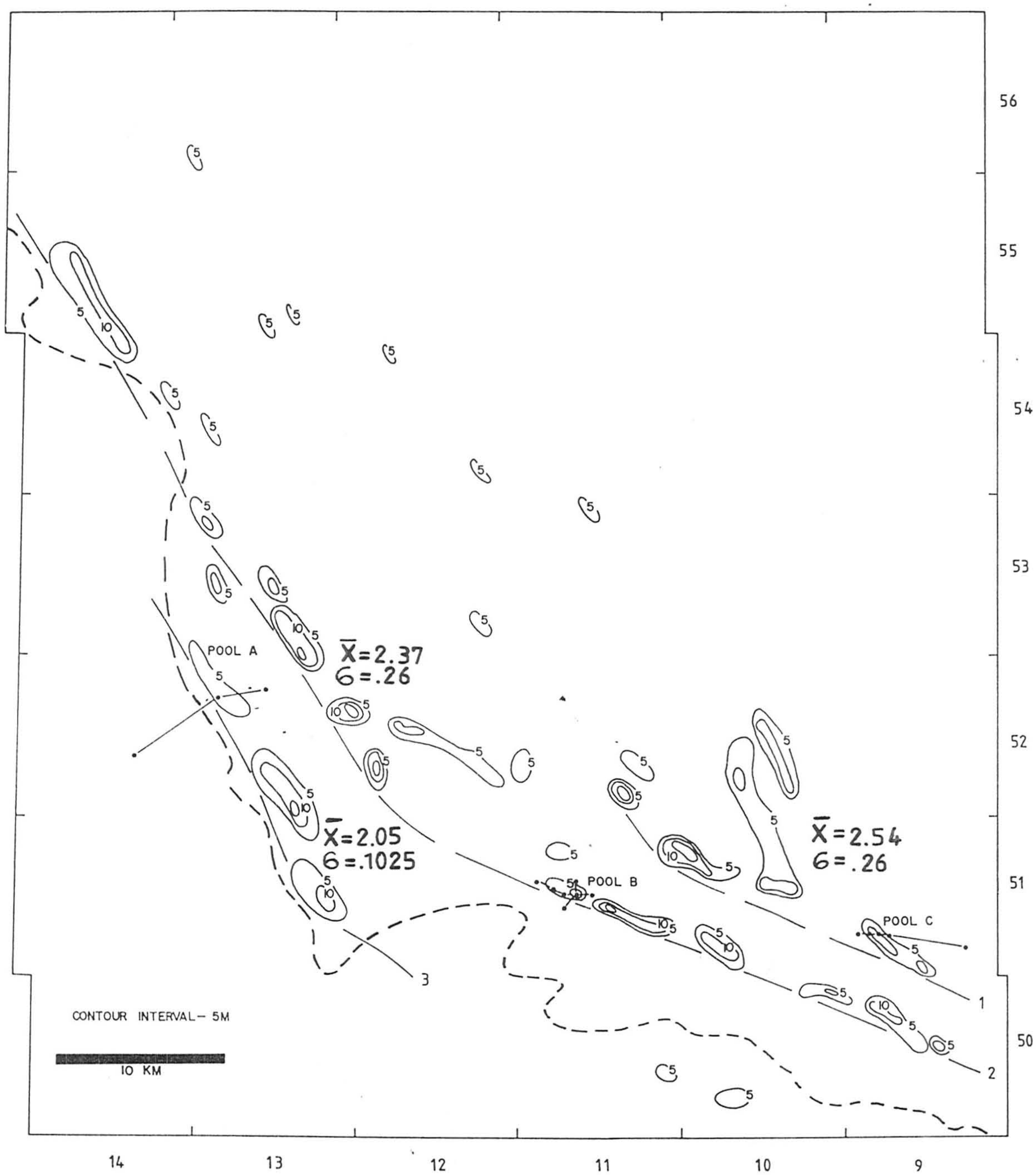

56
55
54
53
52
51
50
14
13
12
11
10
9
POOL A
POOL B
POOL C
X̄=2.37
6=.26
X̄=2.05
6=.1025
X̄=2.54
6=.26
1
2
3
CONTOUR INTERVAL- 5M
10 KM

shoreface profiles in a foreland basin and on the passive continental shelf are very different.

TOPOGRAPHY ON THE PRE-HOLOCENE EROSION SURFACE

Veatch and Smith (1939) and McClennan and McMaster (1971) suggested that the shelf surface was not a simple seaward inclined surface; instead it consisted of nearly horizontal "terraces" separated by more steeply dipping inclined surfaces (Fig. 8.12). Swift et al. (1972) and Swift et al. (1973, fig. 2), however, interpreted the terraces as "...reflecting periods of transgression when the equilibrium shoreface profile translated shoreward. During periods of near stillstand shoreface translation was dominantly upwards. As transgression resumed, shoreface translation returned to horizontal mode" (p. 229). This is contrary to the interpretation presented above for the bumps and hollows where the "terraces" (backs of bumps) are interpreted as forming by shoreface erosion during stillstand, and the "steps" (erosional envelope) are formed during erosional translation of the shoreface during relative sea level rise. In both methods of continuous erosional shoreface retreat any evidence of beach, or sub-aerial deposits would be removed by shoreface translation.

Sanders and Kumar (1975) and Rampino and Sanders (1980) suggested that rather than continuous erosional retreat of the shoreface as suggested by Swift et al. (1972) and Swift

Figure 8.12. Generation of a shelf scarp by depositional stillstand and upward profile translation during a period of gerneral transgression and landward profile translation (from Swift et al., 1973). The relative positions of transgressions and stillstands for the bumps and hollows are shown below.

A

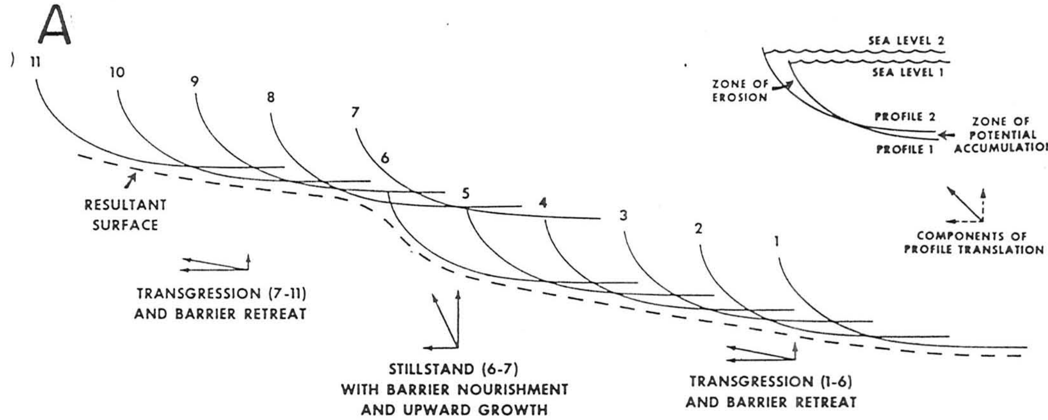
11
10
9
8
7
6
5
4
3
2
1
SEA LEVEL 2
SEA LEVEL 1
ZONE OF EROSION
PROFILE 2
PROFILE 1
ZONE OF POTENTIAL ACCUMULATION
COMPONENTS OF PROFILE TRANSLATION
RESULTANT SURFACE
TRANSGRESSION (7-11) AND BARRIER RETREAT
STILLSTAND (6-7) WITH BARRIER NOURISHMENT AND UPWARD GROWTH
TRANSGRESSION (1-6) AND BARRIER RETREAT

B

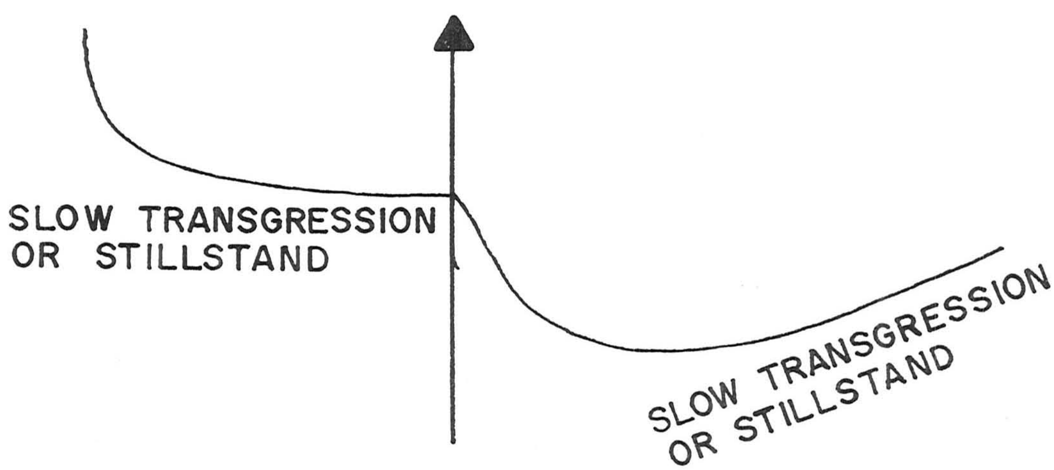
RAPID TRANSGRESSION
SLOW TRANSGRESSION OR STILLSTAND
SLOW TRANSGRESSION OR STILLSTAND

et al. (1973), shoreface erosion occurred as a series of successive leaps. Rampino and Sanders (1980) termed this type of shoreface movement "stepwise retreat". The surf zone jumps landwards during a rapid rise of sea level resulting in the "in-place" drowning of barrier islands and allowing the preservation of beach and lagoonal deposits, by landward overstepping of the surf zone.

There is no evidence (i.e., no preservation of beach or sub-aerial deposits) in the Carrot Creek area to suggest stepwise shoreface retreat in the sense of Rampino and Sanders (1980). In light of the method of forming the bumps and hollows, this type of erosional retreat would not be expected, as sea level rise is the result of gradual subsidence.

The studies of the formation of the pre-Holocene erosion surface on the modern Atlantic Shelf (Kraft, 1971; Swift et al., 1972; Swift et al., 1973; and Rampino and Sanders, 1980) differ from the Carrot Creek study area in two fundamental aspects:

1) primary control of sea level variation, and

2) the tectonic setting.

These are discussed below.

1) Eustatic versus Tectonic Control

The Holocene rise of sea level is a eustatic pheneomenon resulting from glacial melting after the last glaciation. Subsidence of the crust occurs in the basin and has little effect on the position of sea level at the shoreface. Subsidence in this setting serves to increase the water depth in the basin. The mechanism of forming the bumps and hollows outlined above, invokes tectonics as the primary control of sea level. Sea level remains constant with respect to a fixed point in the basin, with the observed regressions and transgressions forming as the result of initial upwarping and subsidence. Although eustatic sea level changes have been proposed for the Turonian (Vail et al., in press; Hancock and Kauffman, 1979), the tectonic overprinting would mask the passive eustatic effects (Jeletzky, 1978). The contribution of eustatic sea level rise in the formation of the E5 surface was not examined.

2) Passive Margin versus Foreland Basin

Modern continental shelves on passive margins differ markedly from foreland basins with respect to the position of the hinge and the area of maximum subsidence. Passive margins (eg., North Atlantic Shelf) that have rifted and are thermally subsiding are hinged at their landward side marging (Pitman, 1978) and the maximum subsidence, controlled by the cooling thermal boundary layer, is beneath the seaward margin. Foreland basins are hinged on the seaward side of the sediment pile and subsidence is induced by loading of the continental craton by successive thrust slices (Jordan, 1981), and is greatest on the landward margin. A brief discussion of the Western Interior Foreland Basin is presented below in order to establish the tectonic framework for the deposition of the Cardium Formation in the Alberta Basin.

FORELAND BASINS

Foreland basins are elongate subsiding troughs flanking the cratonic side of orogenic thrust belts, and are characteristic of mountain belts worldwide. Sediments in the foreland basin reflect the history of uplift and erosion, and hence, deformation of the adjacent orogenic zone. Two end-members of foreland basins are recognized (Dickinson, 1974), occurring in distinctly different tectonic settings. Retroarc basins form on the cratonic side of foreland thrust belts that are adjacent to magmatic areas (eg., sedimentary basin forming on the east side of the sub- Andean thrust belt of the Andes). Peripheral basins form beside foreland thrust belts that are adjacent to suture zones (eg., modern Indo-Gangetic basin south of the Himalayas). Retroarc basins develop during normal subduction of oceanic crust beneath a continent, whereas peripheral basins form during continental collision.

The Cretaceous western interior basin was an elongated, asymmetrical trough which lay to the east of the Cordilleran Orogenic Belt. The seaway occupied a modified Andean type (retroarc basin) foreland basin (Jordan, 1981; Beaumont, 1979, 1981). The main tectonic elements in the Alberta

Basin show that the area is fundamentally two-dimensional, with the structural trend following a northwest-southeast direction. The model of foreland basin formation and the effects on sedimentation will be described below.

A) Flexural Model of Foreland Basin Formation

Price (1973) suggested that foreland basins formed as a consequence of downwarp driven by tectonic thickening of the crust in the thrust belt. The hypothesis of crustal flexure has been subsequently modelled quantitatively (eg., Beaumont, 1979, 1981; Jordan, 1981; Quinlan and Beaumont, 1984) for a variety of sedimentary basins, and a brief summary of the model is presented below.

To a first order approximation the lithosphere behaves like a uniform elastic plate at time scales greater than 10^4 years (Walcott, 1976; Jordan, 1981). Beaumont (1979, 1981) inferred that the lithospere behaved viscoelastically, with the effective clastic thickness of the plate being a function of its thermal state, therefore the thickness of the plate varies with time. The results of both models suggest that the flexural rigidity of the crust is on the order of 10^{23} Nm (Jordan, 1981) and 10^{25} Nm (Beaumont, 1981). These values correspond to an elastic lithosphere about 22 to 48 km thick (Jordan, 1981). The relaxation time constant τ was given as 27.5 MA (Beaumont, 1981). It is difficult to separate the variables relevant to elastic-viscoelastic debate (eg., age and elastic thickness) from other variables (eg., thermal history, initial lithospheric thickness, plate motions), and the results obtained by both models are similar, hence no further distinction is made between the two.

Of greater significance is the basic explanation of subsidence and uplift within the basin. The flexural model demonstrates that erosion of the fold thrust belt unloads the lithosphere causing uplift and concomitant erosion in the basin (Beaumont, 1979, 1981; Jordan 1981). Regional isostatic compensation is the principal driving force of the subsidence as the lithosphere accomodates loading by flexure (Jordan, 1981).

The topographic profiles generated immediately after thrust events (Jordan, 1981; fig. 14) using the elastic/ viscoelastic flexure models include 1), a high mountain range overlying the thrust faults, 2) a gently sloping region of sedimentation (less than 1.5° dipping basinwards) corresponding to alluvial and coastal plain deposits, and 3), a flat region corresponding to an ancient sea floor. The model correlates well with the subdivision of foreland basin into 6 broad areas (Kauffman, 1985, fig. 2), based on marine water depths, sedimentation and subsidence rates, and tectonic stability. These are listed below from west to east:

1) Cordilleran thrust belt providing immense amounts of terrigenous clastic sediments.

2) Rapidly subsiding foreland basin formed by crustal loading from the advancing thrust slices.

3) Eastern edge of the foreland basin forms an incipient forebulge zone which first divides the transgressing seaway, and the marine depositional basin into western (foreland) and eastern troughs.

4) The west central trough along the basin axis where fine-grained clastic marine sediments develop. This centre of subsidence lies outboard of the predicted basinal models described above. Some sort of mechanism for mid-basin subsidence is required.

5) A broad migrating, east-central tectonic hinge zone, where subsidence is moderate and episodic west of the hinge zone, and occurred sporadically at very low levels on the eastern platform. The hinge is a region of tectonic adjustment to the pulses of subsidence and loading in the basins to the west.

6) The tectonically stable platform occupying the eastern part of the seaway. Subsidence is low and episodic.

B) Effects on Sedimentation

Active tectonism in the Cordilleran orogenic belt characterized the entire Cretaceous Period, and had a strong effect on sedimentation and subsidence in the basin (Kauffman, 1984, 1985). Several major periods occurred during the Cretaceous resulting in massive eastward incursions of coarse clastics into fluvial lowlands, marginal marine, and shallow water marine environments in the Western Interior Basin. During periods of relative tectonic "quiesence", thinner fine-grained clastics were deposited (Kauffman, 1985). The marine phases and underlying molasse phases were interpreted in the flexural models in terms of a combination of basement downwarping, clastic influx and eustatic sea level rise (Beaumont, 1981). Tectonically active intervals are associated with relative sea level rise, while tectonically passive intervals are associated with relative sea level fall (Kauffman, 1985).

Shoreline positions varied complexly in the Cretaceous (McGookey, 1972) and the positions of the shorelines can be correlated with major thrusting events in the Cordillera. The positions of the shorelines are shown on the topographic profiles for the Meade and Absoraka thrusts (Jordan, 1981, fig. 15b,c). This diagram shows that the predicted topographic breaks clearly correspond to predicted paleoshoreline positions in the basin. In general, the surface slope and local relief diminish to the east.

High resolution event stratigraphy can be used to measure subsidence events, in both the foreland and axial basins. Tectonic rebound (uplift of structural highs and depression of adjacent basins) in both the incipient forebulge zone, and in the structural hinge zone of the eastern basin can be recognized by event stratigraphy.

IMPLICATIONS OF THE PROPOSED MODEL IN A FORELAND BASIN SETTING

A direct comparison of the proposed tectonic evolution of the bumps and hollows in the Carrot Creek area with other existing models of foreland basins (eg., Jordan, 1981; Beaumont, 1981) is extremely difficult. Existing models of foreland basins describe the whole basin, and hence are on a much larger scale than the area described in this thesis. To the best of my knowledge, no one else has proposed such a detailed direct coupling between tectonic control of relative sea level, the formation and resulting morphology of the erosion surface, and the effects on sedimentation in the basin. Although the data presented in the thesis, and in other Cardium studies (Leggitt, pers. comm.; McLean, pers. comm.) support the proposed interpretation, some problems arise when this interpretation is considered on a regional scale. These problems go beyond the scope of the thesis, and open up intriguing new areas of research. A brief description of some of the problems is presented below.

1. An increase in the dipping surface to 1.45° is very steep. If this dipping surface was projected back 100 km westward to the present edge of the deformed belt, it would result in a mountain chain with average heights of about 2500 m. The problem is compounded because the dip of the surface would be expected to increase landwards (westwards).

2. Increasing the dip of the Raven River Member to 1.45°

would increase the gradients of the rivers to about 25 m per km. This gradient is equivalent to that found on the mid-portion of alluvial fans. River gradients this steep would be capable of transporting boulders out to Carrot Creek, not just 1 to 2 cm pebbles.

3. The third problem concerns the length of time available to form the E5 surface. The total time available to deposit the Cardium Formation is about 1 Myr. Within the Cardium Formation there are 7 regionally extensive erosion surfaces (Plint et al., 1986). The length of time available for the formation of the six Cardium sequences between the seven erosion surfaces (given equal time for each) is about 167,000 years. This implies a lot of vertical crustal movement in a very short period of time (i.e., construction and erosion of a 2500 m high mountain chain). Two points should be made clear. Firstly, I do not propose that all of the Cardium erosion surfaces formed by this mechanism, and secondly, the effects of eustatic variation of sea level have not been taken into account. As stated earlier in the thesis, there is an overall eustatic lowering of sea level during the Turonian (Kauffman, 1977; Weimer, 1984).

The problems described above are valid criticisms of the proposed mechanism of creating the E5 surface. They may not necessarily suggest that the proposed tectonic evolution is invalid (and therefore be abandoned); rather, these problems may reflect our lack understanding of smaller scale flexures within foreland basins. Further studies similar to this may eventually serve to "fine-tune" our understanding of the controls of crustal movements in foreland basins. Finally, the reader is reminded of the basic problem. If shoreface erosion occurred without tilting (Fig. 8.1), then numerous rises and falls of sea level would be required to form the E5 surface. To overcome this problem, the possibility of making a stepped surface was considered (Fig. 8.2), with an implied basinward tilting of the markers. The erosional morphology of the E5 surface, both locally and regionally, suggests that some sort of tilting was necessary to form this surface.

8.7 COMPARISON WITH OTHER DEPOSITS IN THE WESTERN INTERIOR SEAWAY

Publically available structure maps are available for only three other surfaces. The surfaces are from the Bad Heart Formation, Alberta (Plint and Walker, in press), the Viking Formation, Alberta (Raddysh, 1986), and the Gallup Sandstone, New Mexico (McCubbin, 1969; Tillman, 1985). A similar surface has been suggested to be associated with the Holocene transgression (Kraft, 1971; Swift et al., 1972; Swift et al., 1973).

The (Upper Cretaceous) Bad Heart Formation is about 100 m stratigraphically above the Cardium Formation. The relief on the Bad Heart erosional surface is about 40 m. Plint and Walker (in press) demonstrated a topography on this surface similar to that preserved on the E5 surface at Carrot Creek and divided the surface into a terrace, bevel, and bumps and hollows. It differs from the Carrot Creek surface (E5) in that there does not appear to be a thick concentration of coarse material above the erosion surface. The amount of relief on the surface suggests that at least part of it was cut sub-aerially.

The (Lower Cretaceous) Viking Formation in the Gilby A and B fields was shown by Raddysh (1986) to have an erosion surface similar to that preserved at Carrot Creek (E5). This surface has a relief of about 11 m, and using the terminology described herein can be divided into a terrace, bevel and basin plain. Coarse, pebbly sandstones are stacked up against the bevel, forming a long narrow sand body toatlly encased in marine mudstones. The bevel was interpreted by Raddysh (1986) as a shoreface cut during a lowstand of sea level, with the coarse material worked along the shoreface by waves. Subsequent transgression resulted in burial of the sand body by marine mudstones. Joffre field, immediately along trend from Gilby toward the southeast, is underlain by two erosion surfaces, but these have only been documented in cross section, rather than isopach maps (Downing, 1986).

The overall sequence preserved in the Cardium Formation is one of basinal aggradation, sea level lowering, erosion (E5), and transgression (T5). The thick conglomerate deposits of the Carrot Creek Member preserved in this area are not gradationally rooted in the underlying coarsening upward sequence of bioturbated mudtones and sandstones, and hummocky cross stratified sands. Gradational rooting of the coarse material has been suggested for many of the Cretaceous coarsening upward shelf sandbodies in the Western Interior Seaway, for example, Shannon (Spearing, 1976; Tillman and Martinsen, 1984; Seeling, 1978; Shurr, 1984; Hobson et al., 1982), Viking (Beaumont, 1984), Duffy Mountain (Boyles and Scott, 1982), Frontier (Tillman and Almon, 1979; Barlow and Haun, 1966), and Cardium (Berven, 1966; Krause and Nelson, 1984).

In the Carrot Creek -- Cyn-Pem study, the conglomerates are separated from the underlying coarsening upward sequence by a major erosion surface, formed as a result of initial upward tilting of the surface and gradual subsidence to preserve the bump and hollow topography. This interpretation makes comparison with the other Western Interior deposits difficult. Whether this interpretation applies to other deposits in the Western Interior Seaway cannot be assessed without knowing firstly, if these deposits are gradationally rooted in the underlying shales, and secondly, if there is an unconformity present at the base of the coarse deposits. Detailed maps of the morphology of the erosion surface are needed. The ideas presented in this thesis should be considered as a possibility for forming coarse deposits surrounded by marine shales particularly, when the basin deposits are coarser than the implied time-equivalent shoreline deposits (eg., Frontier Formation).

CHAPTER 9 -- SUMMARY OF CARROT CREEK DEPOSITIONAL HISTORY AND OTHER CONCLUSIONS

9.1 INTRODUCTION

This chapter is presented to highlight the major points of this thesis. The first objective of this thesis was to determine the depositional history of the Carrot Creek Member, of the Cardium Formation in the Carrot Creek Oil Field. This is given below. Other conclusions derived from the specific study of the sediments at Carrot Creek are listed in section 9.3.

9.2 SUMMARY OF THE DEPOSITIONAL HISTORY AT CARROT CREEK

1. Sequences "b" and "a" of the Raven River Member (Fig. 8.5A) document progressive shallowing upwards under open shallow marine conditions. Sequence "b" coarsens upward from facies 1 through facies 3, 4, and 5. Sequence "a" coarsens upwards through bioturbated mudstones of facies 4 and 5, culminating in hummocky cross stratified sands suggesting deposition above storm wave base.
2. The "a" and "b" sequences of the Raven River Member are separated by a gritty siderite horizon (sub-facies 8G.S.) (Fig. 8.5A). The gritty siderite is interpreted as representing a pause in deposition due presumably to a minor rise in relative sea level or a stillstand.
3. Sequence "b", the gritty siderite, and sequence "a", make up a package believed to have an original basinward dip (α) of 0.04° basinwards (Fig. 8.5A). This implies

deposition of the Raven River Member in depths of water on the order of 60 m, if the highstand shoreline position is taken at its closest possible position, at least 100 km to the west at the edge of the deformed belt (Fig. 2.1). The top of the Raven River Member prior to erosion is believed to be gently undulating as a result of differential compaction reflecting the topography of the underlying Devonian Nisku reefs. Absolute sea level remains constant with respect to a hinge basinwards of Carrot Creek.

4. With uplift in the Cordillera, the regional dip was increased to $\beta + \alpha$. This resulted in a drop of relative sea level causing the shoreface to move basinwards to the seaward edge of the bumps and hollows (Bigoray). An initial horizontal shoreface bite formed during stillstand. Gravel is supplied to the basin shoreface as a result of the increased gradient.

5. Gradual subsidence resulted in a rise of relative sea level and erosional translation of the shoreface. The initial horizontal cut rotated downwards as the surface (top of the Raven River Member) subsided. The initial shoreface profile and the translating profiles were preserved as an erosional envelope. Gravel was reworked in the shoreface as sea level rose.

6. There was a pause in subsidence and another initial horizontal bite occurred at shoreface position 2. Subsidence began again, resulting in shoreface translation

and downward rotation of the erosional envelope. The gravel deposits in erosional envelope 1 were overlain by the transgressive pebbly mudstones (Dismal Rat Member) while the shoreface was forming at position 2.

7. There was a pause in subsidence and another initial horizontal bite occurred at shoreface position 3 (bevel). Subsidence began again, resulting in shoreface translation and downward rotation of erosional envelopes 1 and 2. The transgressive pebbly mudstones blanketed the conglomerates in erosional envelopes 2 and 3.

8. There was a pause in subsidence and another initial horizontal bite occurred. Continuous subsidence resulted in erosional shoreface translation which gave rise to the relatively flat terrace. Any evidence of sub-aerial exposure and fluvial downcutting was removed by erosional retreat of the shoreface. The erosional envelopes rotated downwards as subsidence continued until regional basin dip was restored. During continued subsidence the entire sequence was blanketed by the "laminated blanket" (facies 2), as open marine conditions return to the basin.

9.3 OTHER CONCLUSIONS

1. The conglomerates (Carrot Creek Member) in the Carrot Creek Oil Field were originally interpreted as an offshore "terrace bar" with transport of the gravels accross the shelf during storms (Swagor et al., 1976). Superficially, the coarsening upward deposits at Carrot Creek are similar

to other such ridges described from the western interior seaway. The deposits at Carrot Creek, however, differ from other similar deposits in the Western Interior Seaway in that the conglomerates are not gradationally rooted in the underlying shelf sediments; rather, they are separated from these shelf deposits by a major erosion surface (E5). The presence or absence of such unconformities at the base of other such ridges must be investigated when considering the the depositional history of linear "offshore ridges".

2. Swagor et al. (1976) first suggested that the conglomerates were separated from the underlying shelf sediments by an erosion surface (E5). They suggested a submarine origin of this erosion surface. The geometry of the E5 surface does not appear to be the result of storm scouring on the shelf; rather, it appears to be consistent with shoreface erosion. The E5 surface was interpreted herein as forming during a lowering of relative sea level as a result of tectonic uplift in the Cordillera and relative sea level rise during subsidence.

3. There is not enough time to form all seven E/T surfaces in the Cardium eustatically. Eustatic sea level variation does not account for the formation of the bump and hollow topography. Tectonic control of sea level seems to be the best mechanism of forming the topography on the E5 surface.

4. The morphology of bumps and hollows appears to be the result of lithospheric flexure. An initial increased

basinward tilt of the sediments caused a relative lowering of sea level and the establishment of a shoreface profile in the basin. The hollows formed by shoreface translation during subsidence and relative sea level rise.

5. A modern analogue of the erosional bump and hollow topography will not be found on passive margin continental shelves (eg., Atlantic Shelf), because of the differences in the tectonic setting. The formation of the bumps and hollows was by initial upward tilting and slow subsidence in a foreland basin setting. In the passive margin setting the hinge is landward of sediment deposition, hence subsidence results in a deepening of the basin, but has little effect on the position of the shoreline. In foreland basins however, the hinge is seaward of sediment deposition, hence subsidence results in movement of the shoreline, while the depth in the basin, with respect to the hinge, remains constant.

REFERENCES

AIGNER, T., 1982a. Calcareous Tempestites: Storm-dominated stratification in Upper Muschelkalk Limestones (Middle Trias, SW-Germany). In: G. Einsele and A. Seilacher (eds.) Cyclic and Event Stratification. New York, Springer, 180-198.

AIGNER, T., 1982b. Event stratification in Nummulite accumulations and in shell beds from the Eocene of Egypt. In: G. Einsele and A. Seilacher (eds.) Cyclic and Event Stratification. New York, Springer, 248-262.

ALMON, W.R., 1979. Petrophysical evidence of cementation differences in the Cardium Sandstone. Canadian Well Logging Society, 7th Formation evaluation symposium, Calgary, p. K1-K4.

BARLOW, J.A., and HAUN, J.D., 1966. Regional stratigraphy of Frontier Formation and relation to Salt Creek Field Wyoming. Bulletin of the American Association of Petroleum Geologists, 50(10), 2185-2196.

BARRELL, J., 1912. Criteria for the recognition of ancient delta deposits. Geological Society of America Bulletin, 23, 377-446.

BEACH, F.K., 1957. Stands by Tubidity. Canadian Oil and Gas Industries, 10 (2), 39-40.

BEACH, F.K., 1955. Cardium a turbidity current deposit.

Journal of the Alberta Society of Petroleum Geologists, 3, 123-125.

BEAUMONT, C., 1981. Foreland basins. Geophysical Journal of the Royal Astronomical Society, 65, 291-329.

BEAUMONT, C., 1979. The evolution of sedimentary basins on a viscoelastic lithosphere: theory and examples. Geophysical Journal of the Royal Astronomical Society, 55, 471-497.

BEAUMONT, E.A., 1984. Retrogradational shelf sedimentation: the Lower Cretaceous Viking Formation, central Alberta. In: Siliciclastic Shelf Sediments. Society of Economic Palaeontologists and Mineralogists, Special Publication 34, 163-178.

BERG, R.R., 1975. Depositional environment of Upper Cretaceous Sussex Sandstone, House Creek Field, Wyoming. American Association of Petroleum Geologists, Bulletin, 59, 2099-2110.

BERGMAN, K.M., 1986. Facies and "sand-body" geometry of the Carrot Creek -- Cyn-Pem area, south-central Alberta. McMaster University, Tech. Memo. 86-1, 50 p.

BERGMAN, K.M., 1984. Upper Cretaceous (Turonian) Cardium Formation, central Alberta. McMaster University, Tech. Memo. 84-1, 35 p. With Supplement, 32 p.

BERGMAN, K.M., and WALKER, R.G., in press. The importance of sea-level fluctuations in the formation of linear conglomeratic bodies; Carrot Creek Member of the

Cardium Formation, Cretaceous Western Interior Seaway, Alberta, Canada. Journal of Sedimentary Petrology.

BERGMAN, K.M., and WALKER, R.G., 1986. Cardium Formation conglomerates at Carrot Creek Field: offshore linear ridges or shoreface deposits? In: T.F. Moslow and E.G. Rhodes (eds.) Modern and Ancient Shelf Clastics. Society of Economic Palaeontologists and Mineralogists Core Workshop No. 9, 217-268.

BERVEN, R.J., 1966. Cardium sandstone bodies, Crossfield-Garrington area, Alberta. Bulletin of Canadian Petroleum Geology, 14, 208-240.

BLUCK, B.J., 1982 (abstract). Gravel assemblages in beach and fluvial sediments. 11th International Sedimentological Congress, Hamilton, Canada, Book of Abstracts, p. 53.

BLUCK, B.J., 1969. Particle rounding in beach gravels. Geological Magazine, 106, 1-14.

BLUCK, B.J., 1967. Sedimentation of beach gravels: examples from South Wales. Journal of Sedimentary Petrology, 37, 128-156.

BOUMA, A.H., 1962. Sedimentology of some flysch deposits. Amsterdam, Elsevier, 168 pp.

BOURGEOIS, J., and LEITHOLD, E.L., 1984. Wave-worked conglomerates -- depositional processes and criteria for recognition. In: E.H. Koster and R.J. Steel (eds.) Sedimentology of Gravels and Conglomerates.

Canadian Society of Petroleum Geologists, Memoir 10, 331-343.

BOYLES, J.M., and SCOTT, J.A., 1982. A model for migrating shelf-bar sandstones in upper Mancos Shale (Campanian), northwestern Colorado. American Association of Petroleum Geologists, Bulletin, 66, 491-508.

BRENNER, R.L., 1978. Sussex Sandstone of Wyoming -- examples of Cretaceous offshore sedimentation. American Association of Petroleum Geologists, Bulletin, 62, 181-200.

BRENNER, R.L., and DAVIES, K.K., 1973. Storm generated coquinoid sandstone: genesis of high energy marine sediments from the Upper Jurassic of Wyoming and Montana. Bulletin of the Geological Society of America, 84, 1685-1697.

CAMPBELL, C.V., 1971. Depositional model -- Upper Cretaceous Gallup beach shoreline, Ship Rock area, northwestern New Mexico. Journal of Sedimentary Petrology, 41, 395-404.

CANT, D.J., 1984. Development of shoreline -- shelf sand bodies in a Cretaceous epeiric sea deposit. Journal of Sedimentary Petrology, 54(2), 541-556.

CANT, D.J., 1980. Storm dominated shallow marine sediments of the Arisaig Group (Silurian-Devonian) of Nova Scotia. Canadian Journal of Earth Science, 17, 120-131.

CARR, A.P., 1971. Experiments on longshore transport and sorting of pebbles: Chesil Beach England. Journal of Sedimentary Petrology, 41, 1084-1104.

CARR, A.P., 1969. Size grading along a pebble beach: Chesil Beach England. Journal of Sedimentary Petrology, 39, 297-311.

CARR, A.P., GLEASON, R., and KING, A., 1970. Significance of pebble size and shape sorting by waves. Sedimentary Geology, 4, 89-101.

CLIFTON, H.E., 1981. Progradational sequences in Miocene shoreline deposits, southeastern Caliente Range, California. Journal of Sedimentary Petrology 41, 651-670.

CLIFTON, H.E., 1973. Pebble segregation and bed lenticularity in wave worked versus alluvial gravel. Sedimentary Geology, 20, 173-187.

CLIFTON, H.E., HUNTER, R.E., and PHILLIPS, R.L., 1971. Depositional structures and processes in the non-barred high-energy nearshore. Journal of Sedimentary Petrology, 41, 651-670.

DENGLER, A.T., WILDE, P., NODA, E.K., and NORMARK, W.R., 1984. Turbidity currents generated by Hurricane Iwa. Geo Marine Letters, 4, 5-11.

DE WIEL, J.E.F., 1956. Viking and Cardium not turbidity current deposits. Journal of the Alberta Society of Petroleum Geologists, 4, 173-175.

DICKINSON, W.R., 1974. Plate tectonics and sedimentation. Society of Economic Palaeontologists and Mineralogists, Special Publication, 22, 1-27.

DOBKINS, J.E., and FOLK, R.L., 1970. Shape development on Tahiti-Nui. Journal of Sedimentary Petrology, 40, 1167-1203.

DOWNING, K.P., 1986. The depositional history of the Lower Cretaceous Viking Formation at Joffre, Alberta, Canada. Unpublished Masters Thesis, McMaster University, 138 pp.

DOTT, R.H., and BOURGEOIS, J., 1982. Hummocky stratification: significance of its variable bedding sequences. Bulletin of the Geological Society of America, 93, 663-680.

DUKE, W.L., 1985a. Sedimentology of the Upper Cretaceous (Turonian) Cardium Formation in outcrop in southern Alberta. Ph.D. Thesis, McMaster University,

DUKE, W.L., 1985b. Hummocky cross stratification, tropical hurricanes and intense winter storms. Sedimentology, 32, 167-194.

DUPRE, W.R., CLIFTON, H.E., and HUNTER, R.E., 1980. Modern sedimentary facies of the open Pacific coast and Pleistocene analogs from Monterey Bay, California. In: M.E. Field et al. (eds.) Quaternary Depositional Environments of the Pacific Coast. Pacific Section, Society of Economic Palaeontologists and Mineralogists, Pacific Coast Palaeogeography, 4, 105-120.

ETHRIDGE, F.G., and WESCOTT, W.A., 1984. Tectonic setting, recognition and hydrocarbon reservoir potential of fan-delta deposits. In: E.H. Koster and R.J. Steel (eds.) Sedimentology of Gravels and Conglomerates. Canadian Society of Petroleum Geologists, Memoir 10, 217-235.

ETHRIDGE, F.G., and WESCOTT, W.A., 1981 (abstract). Tectonic setting, recognition and hydrocarbon potential of fan-delta deposits. In: Sedimentary Tectonics: Principles and Applications. Laramie, Wyoming; Department of Geology, University of Wyoming, Wyoming Geological Association and Geological Survey of Wyoming, p. 11.

EXPLORATION STAFF, CHEVRON STANDARD LIMITED, 1979. The geology, geophysics and significance of the Nisku reef discoveries, West Pembina area, Alberta Canada. Bulletin of Canadian Petroleum Geology, 27(3), 326-359.

EXUM, F.A., and HARMS, J.C., Comaparison of marine-bar with valley-fill stratigraphic traps, western Nebraska. Bulletin of the American Association of Petroleum Geologists, 52 (10), 1851-1868.

FLEMMING, B.W., 1980. Sand transport and bedform patterns on the continental shelf between Durban and Port Elizabeth (southeast African Continental Margin). Sedimentary Geology, 26, 179-205.

FORRISTALL, G.Z., HAMILTON, R.C., and CARDONE, V.J., 1977. Continental Shelf currents in Tropical Storm Delia: observations and theory. Journal of Physical Oceanography, 87, 532-546.

FOUCH, T.D., 1983. Patterns of synorogenic sedimentation in Upper Cretaceous rocks of central and northeastern Utah. In: M. Reynolds and E. Dolly (eds.) Mesozoic Palaeogeography of west-central United States, Denver, Colorado. Society of Economic Palaeontologists and Mineralogists, Rocky Mountain Section, Special Publication, 305-336.

FOX, W.T., 1983. At the sea's edge. Prentice Hall, Englewood Cliffs, New Jersey, p. 93-124.

GEBHARD, G., 1982. Glauconitic condensation through high energy events in the Albian near Clars (Escragnolles, Var, SE-France). In: G. Einsele and A. Seilacher (eds.) Cyclic and Event Stratification. New York, Springer, 286-298.

GRANT, W.D., and MADSEN, O.S., 1979. Combined wave and current interaction with a rough bottom. Journal of Geophysical Research, 84, 1797-1808.

GREENWOOD, B., 1984 (abstract). Hummocky cross stratification: Shelf or Surf. Sedimentology of Shelf Sands and Sandstones, Research Symposium, Calgary, Canada. Canadian Society of Petroleum Geologists, Program and Abstracts, p. 39.

GRIFFITH, L.A., 1981. Depositional environment and conglomerate diagenisis of the Cardium Formation, Ferrier Field, Alberta. Unpublished M.Sc. Thesis, University of Calgary, 131p.

HAGDORN, H., 1982. The "Bank der Kleinen Terebrateln" (Upper Muschelkalk, Triassic) near Schwabisch Hall (SW Germany) -- a tempestite condensation horizon. In: G. Einsele and A. Seilacher (eds.) Cyclic and Event Stratification. New York, Springer, 263-285.

HALLAM, A., 1984. Pre-Quaternary sea level changes. Annual Review of Earth and Planetary Sciences, 12, 205-243.

HALLAM, A., 1963. Major epeirogenic and eustatic changes since the Cretaceous and their possible relationship to crustal structure. American Journal of Science, 261, 397-423.

HAMBLIN, A.P., and WALKER, R.G., 1979. Storm-dominated shallow marine deposits: the Fernie-Kootenay (Jurassic) transition, southern Rocky Moutains. Canadian Journal of Earth Sciences 16 (9), 1637-1690.

HANCOCK, J.M., 1975. The sequence of facies in the Upper Cretaceous of northern Europe compared with that in the Western Interior. In: W.G.E. Caldwell (ed.) The Cretaceous System in the Western Interior of North America. Geological Association of Canada, Special Paper 13, 83-118.

HANCOCK, J.M., AND KAUFFMAN, E.G., 1979. The great transgressions of the Late Cretaceous. Geological Society of London, Journal, 136, 175-186.

HARDING, S.R.L., 1955. Pembina -- Regional Geology. Canadian Oil and Gas Industries, 8 (6), 67-72.

HARMS, J.C., SOUTHARD, J.B., and WALKER, R.G., 1982. Structures and sequences in clastic rocks. Society of Economic Palaeontologists and Mineralogists, Short Course 9, 249p.

HARMS, J.C., SPEARING, J.B., SOUTHARD, J.B., and WALKER, R.G., 1975. Depositional environments as interpreted from primary sedimentary structures and stratification sequences. Society of Economic Palaeotologists and Mineralogists, Short Course 2, 161p.

HAYES, B.J.R., and SMITH,D.G., (in press). Discussion: Cardium Formation 6. Stratigraphic framework of the Cardium in subsurface. Canadian Society of Petroleum Geologists Bulletin.

HAYES, M.O., 1967. Hurricanes as geological agents: case studies of Hurricanes Carla, 1961, and Cindy, 1963. Texas Bureau of Economic Geology, Report of Investigations No. 61, 54 p.

HEEZEN, B.C., MENZIES, R.J., SCHNEIDER, E.D., EWING, W.M., and GRANELLI, N.C.J., 1964. Congo submarine canyon. Bulletin of the American Association of Petroleum Geologists, 48 (7), 1126-1149.

HEEZEN, B.C., 1956. Corrientes de turbidez del Rio

Magdelena. Societa Geografica de Colombia, Boll., 51-52, 135-143.

HEIN, F.J., 1984. Deep-sea and fluvial braided channel conglomerates: A comparison of two case studies. In: E.H. Koster and R.J. Steel (eds.) Sedimentology of Gravels and Conglomerates. Canadian Society of Petroleum Geologists, Memoir 10, 33-49.

HEIN, F.J., 1982. The Cambro-Ordovician Cap Enrage Formation, Quebec, Canada: conglomeratic deposits of a braided submarine channel with terraces. Sedimentology, 29, 309-329.

HOBSON, J.P., FOWLER, M.L., and BEAUMONT, E.A., 1982. Depositional and statistical exploration models, Upper Cretaceous offshore sandstone complex, Sussex Member, House Creek Field, Wyoming. American Association of Petroleum Geologists, Bulletin, 66, 689-707.

HOWARTH, M.J., 1982. Tidal currents on the Continental Shelf. In: A.H. Stride (ed.) Offshore Tidal Sands. London, Chapman and Hall, p. 10-26.

HUNTER, R.E., and CLIFTON, H.E., 1982. Cyclic deposits and hummocky cross-stratification of probable storm origin in Upper Cretaceous rocks of the Cape Sebastian area, southwestern Oregon. Journal of Sedimentary Petrology, 52, 127-143.

HUNTER, R.E., CLIFTON, H.E., and PHILLIPS, R.L., 1979. Depositional processes, sedimentary structures, and predicted vertical sequences in barred nearshore systems, southern Oregon coast. Journal of Sedimentary Petrology, 49, 711-726.

JELETZKY, J.A., 1978. Causes of Cretaceous oscillations of sea level in Western and Arctic Canada and some general geotectonic implications. Geological Survey of Canada, Paper 77-18, 38p.

JONES, R.M.P., 1980. Basinal isostatic adjustment faults and their petroleum significance. Bulletin of Canadian Petroleum Geology, 28 (2), 211-251.

JORDAN, T.E., 1981. Thrust loads and foreland basin evolution, Cretaceous western United States. American Association of Petroleum Geologists, Bulletin, 65, 2506-2520.

KAUFFMAN, E.G., 1985. Cretaceous evolution of the Western Interior Basin of the United States. In: L.M. Pratt et al. (eds.) Fine-grained deposits and biofacies of the Cretaceous Western Interior Seaway: evidence of cyclic sedimentary processes. Society of Economic Palaeontologists and Mineralogist, Field Trip 9, iv-xi.

KAUFFMAN, E.G., 1984. Palaeobiogeography and evolutionary response dynamic in the Cretaceous Western Interior Seaway of North America. In: G.E.G. Westermann (ed.) Jurassic-Cretaceous biochronology and palaeogeography of North America. Geological Association of Canada, Special Paper 27, 273-306.

KAUFFMAN, E.G., 1977. Geological and biological overview: Western Interior Cretaceous Basin. Mountain Geologist, 14, 75-99.

KEITH, D.A.W., 1985. Sedimentology of the Cardium Formation, Willesden Green Field, Alberta. M.Sc. Thesis, McMaster University, 233p.

KELLING, G., and MULLIN, P.R., 1975. Graded limestones and limestone-quartzite couplets: possible storm-deposits from the Moraccan Carboniferous. Sedimentary Geology, 13, 161-190.

KIRK, R.M., 1980. Mixed sand and gravel beaches: morphology, processes and sediments. Progress in Physical Geography, 4, 189-210.

KOLLA, V., BUFFER, R.T., and LADD, J.W., 1984. Seismic stratigraphy and sedimentation of Magdelena Fan, Southern Columbian Basin, Caribbean Sea. Bulletin of the American Association of Petroleum Geologists, 68 (3), 316-332.

KOMAR, P.D., 1976. Beach Processes and Sedimentation. Prentice Hall, Englewood Cliffs, New Jersey, 429 p.

KOMAR P.D., and MILLER, M.C., 1973. The threshold of sediment movement under oscillatory water waves. Journal of Sedimentary Petrology, 43(4), 1101-1110.

KOSTER, E.H., and STEEL, R.J., 1984. Sedimentology of gravels and conglomerates. Canadian society of Petroleum Geologists, Memoir 10, 441p.

KRAFT, J.C., 1971. Sedimentary facies patterns and geologic history of a Holocene marine transgression. Geological Society of America Bulletin, 82, 2131-2158.

KRAUSE, F.F., 1984. Pembina Cardium. Recovery Efficiency Study: A geological and engineering synthesis Volume 1, 189p.

KRAUSE, F.F., 1983. Sedimentology of a Tempestite: episodic deposition in the Cardium Formation, Pembina Oilfield Area, west central Alberta. In: J.R. McLean and G.E. Reinson (eds.) Sedimentology of Selected Mesozoic Clastic Sequences. Calgary, Alberta. Canadian Society of Petroleum Geologists, 43-65.

KRAUSE, F.F., and NELSON, D.A., 1984. Storm event sedimentation: lithofacies association in the Cardium Formation, Pembina area, west-central Alberta, Canada. In: D.F. Stott and D.J. Glass (eds.) The Mesozoic of Middle North America. Canadian Society of Petroleum Geologists, Memoir 9, 485-511

KREISA, R.D., 1981. Storm-generated sedimentary structures in subtidal marine facies with examples from the middle and upper Ordovician of south-western Virginia. Journal of Sedimentary Petrology, 51, 823-848.

KUMAR, N., and SANDERS, J.E., 1976. Characteristics of shoreface storm deposits: modern and ancient examples. Journal of Sedimentary Petrology, 46, 145-162.

LANGFORD-SMITH, T., and THOM, B.G., 1969. New South Wales coastal morphology. Geological Society of Australia, 16, 572-580.

LANPHERE, M.A., and JONES, D.L., 1978. Cretaceous time scale from North America. In: G.V. Cohee and M.F. Glaessner (eds.) The Geological Time Scale. American Association of Petroleum Geologists, Studies in Geology 6, 259-268.

LEITHOLD, E.L., and BOURGEOIS, J., 1984. Characteristics of coarse-grained sequences deposited in nearshore, wave-dominated environments -- examples from the Miocene of south-west Oregon. Sedimentology, 31, 749-775.

LECKIE, D.A., 1983. Sedimentology of the Moosebar and Gates Formations (Lower Cretaceous). Ph.D. Thesis, McMaster University, 515p.

LECKIE, D.A., and WALKER, R.G., 1982. Storm and tide dominated shorelines in Cretaceous Moosebar-Lower Gates interval -- outcrop equivalents of deep basin gas trap in western Canada. American Association of Petroleum Geologists Bulletin, 66 (2), 138-157.

LINDSAY, J.F., PRIOR, D.B., and COLEMAN, J.M., 1984. Distributary mouth bar development and role of submarine landslides in delta growth, South Pass, Mississippi Delta. Bulletion of the Association of Petroleum Geologists, 68 (11), 1732-1734.

LYELL, C., 1832. Principles of Geology 2nd ed. London, 3 Volumes.

MAEJIMA, W. 1982. Texture and stratification of gravelly beach sediments, Enju Beach, Kii Peninsula, Japan. Osaka City University, Journal of Geosciences, 25, 35-51.

McCAVE, I.N., 1971. Sand waves in the North Sea off the coast of Holland. Marine Geology, 10, 199-225.

McLENNEN, C.E., and McMASTER, R.L., 1971. Probable Holocene transgression effects in the geomorphic features of the continental shelf off New Jersey, United States. Maritime Sedimentology, 7, 69-72.

McCUBBIN, D.G., 1969. Cretaceous strike-valley sandstone reservoirs, northwestern New Mexico. Bulletin of the American Association of Petroleum Geologists, 53 (10), 2114-2140.

McGOOKEY, D.P., 1972. Cretaceous System. In: W.W. Mallory (ed.) Geologic Atlas Rocky Mountain Region. Rocky Mountain Association of Geologists, Special Publication, 190-228.

McLAUGHLIN, K.V., 1986. The effects fo sea level changes on the sedimentology of the Cardium Formation; norhteastern Pembina, Alberta. B.Sc. Thesis, McMaster University, 66p.

MIALL, A.D., 1986. Eustatic sea level changes interpreted from Seismic Stratigraphy: A critique of the methodology with particular reference to the North Sea Jurassic record. American Association of Petroleum Geologists Bulletin, 70 (2), 131-137.

MIALL, A.D., 1984. Principles of Sedimentary Basin Analysis. Springer-Verlag, New York, 329-365.

MIALL, A.D., 1978. Lithofacies types and vertical profile models in braided river deposits: a summary. In: A.D. Miall (ed.) Fluvial Sedimentology, Canadian Society of Petroleum Geologists, Memoir 5, 597-604.

MIALL, A.D., 1977. A review of the braided river depositional environment. Earth Science Reviews, 13, 1-62.

MICHAELIS, E.W., 1957. Cardium sedimentation in the Pembina River area. Journal of the Alberta Society of Petroleum Geologists, 5, 73-77.

MICHAELIS, E.W., and DIXON, G., 1969. Interpretation of depositional processes from sedimentary structures in the Cardium sand. Bulletin of Canadian Petroleum Geology, 17, 410-443.

MIDDLETON, G.V., 1973. Johannes Walther's law of correlation of facies. Geological Society of America Bulletin, 84, 979-988.

MIDDLETON, G.V., and SOUTHARD, J.B., 1984. Mechanics of sediment movement, Second Edition. Society of Economic Palaeontologists and Mineralogists, Short Course No. 3, 401p.

MORTON, R.A., 1981. Formation of storm deposits by wind-forced currents in the Gulf of Mexico and the North Sea. In: S.D. Nio et al. (eds.) Holocene Marine Sedimentation in the North Sea Basin. International Association of Sedimentologists, Special Publication 5, 385-396.

MOORE, D.G., 1961. Submarine slumps. Journal of Sedimentary Petrology, 31 (3), 343-357.

MURRAY, S.P., 1970. Bottom currents near the coast during Hurricane Camille. Journal of Geophysical Research, 75, 4579-4582.

NELSON, F.H., and BRAY, E.E., 1970. Stratigraphy and history of the Holocene sediments in the Sabine-High Island area, Gulf of Mexico. In: J.P. Morgan (ed.) Deltaic Sedimentation, Modern and Ancient. Society of Economic Palaeontologists and Mineralogists, Special Publication 15, 48-77.

NEMEC, W., and STEEL, R.J., 1984. Alluvial and coastal conglomerates: their significant features and some comments on gravelly mass-flow deposits. In: E.H. Koster and R.J. Steel (eds.) Sedimentology of Gravels and Conglomerates. Canadian Society of Petroleum Geologists Memoir 10, 1-31.

NIELSEN, A.R., 1957. Cardium stratigraphy of the Pembina field. Journal of the Alberta Society of Petroleum Geologists, 5, 64-72.

NIELSEN, A.R., and PORTER, J.W., 1984. Pembina oil field -- in retrospect. In: D.F. Stott and D.J. Glass (eds.) The Mesozoic of Middle North America. Canadian Society of Petroleum Geologists, Memoir 9, 1-13.

OBRADOVICH, J.D., and COBBAN, W.A., 1975. A time scale for the Late Cretaceous of the Western Interior of North America. In: W.G.A. Caldwell (ed.) The Cretaceous System in the Western Interior of North America. Geological Association of Canada, Special Paper, 13, 31-54.

OFF, T., 1963. Rhythmic linear sand bodies caused by tidal currents. American Association of Petroleum Geologists Bulletin, 47, 324-341.

ORFORD, J.D., 1975. Discrimination of particle zonation on a pebble beach. Sedimentology, 22, 441-463.

ORFORD, J.D., and CARTER, R.W.G, 1982. Coastal overtop and washover sedimentation on a fringing sandy gravel barrier coast, Carnsore Point, southwest Ireland. Journal of Sedimentary Petrology, 52, 265-278.

PALMER, A.R., 1983. The decade of North American geology. 1983 geological time scale. Geology, 11, 503-504.

PANTIN, H.M., 1983. Conditions for the ignition of catastrophically erosive turbidity currents -- Comment. Marine Geology, 52, 281-290.

PANTIN, H.M., 1979. Interaction between velocity and effective density in turbidity flow: Phase plume analysis, with criteria for autosuspension. Marine Geology, 31, 59-99.

PARKER, G., 1982. Conditions for the ignition of catatrophically erosive turbidity currents. Marine Geology, 46, 307-327.

PITMAN, W.C., 1978. Relationship between eustacy and stratigraphic sequences of passive margins. Geological Society of America Bulletin, 89, 1320-1403.

PLINT, A.G., and WALKER, R.G., in press. Morphology and origin of an erosion surface cut into the Bad Heart Formation during major sea level change, Santonian of west-central Alberta, Canada. Journal of Sedimentary Petrology.

PLINT, A.G., and WALKER, R.G., 1986. Cardium Formation 8. Facies and environments of the Cardium shoreline and coastal plain in the Kakwa Field and adjacent areas, Northwestern Alberta. Bulletin of Canadian Petroleum Geology.

PLINT, A.G., WALKER, R.G., and BERGMAN, K.M., (in press). Reply to Brad J.R. Hayes and David G. Smith, and to James M. Rine, Kenneth P. Helmold, and Grant Bartlett. Canadian Society of Petroleum Geologists Bulletin.

PLINT, A.G., WALKER, R.G., and BERGMAN, K.M., 1986. Cardium Formation 6: Stratigraphic framework of the Cardium in subsurface. Bulletin of Canadian Petroleum Geology, 34 (2), 213-225.

PRICE, R.A., 1973. Large-scale gravitational flow of supracrustal rocks, southern Canadian Rockies. In: K.A. de Jong and R. Scholten (eds.) Gravity and Tectonics. New York, John Wiley, p. 491-502.

QUINLAN, G.M., and BEAUMONT, C., 1984. Appalachian thrusting, lithospheric flexure and the Paleozoic stratigraphy of the eastern interior of North America. Canadian Journal of Earth Science, 21, 973-996.

RADDYSH, H., 1986. Sedimentology of the Viking Formation at Gilby "A" and "B" fields, Alberta. Unpublished B.Sc. Thesis, McMaster University, 241 pp.

RAMPINO, M.R., and SANDERS, J.E., 1980. Holocene transgression in south-central Long Island, New York. Journal of Sedimentary Petrology, 50 (4), 1063-1080.

RINE, J.M., 1986 (abstract). Effects of rising sea level on facies distribution within the Cardium Formation of west central Alberta, Muskeg River area. Canadian Society of Petroleum Geologists Reservoir, 13 (2), 1-3.

RINE, J.M., HELMOLD, K.P., and BARTLETT, G., (in press). Cardium Formation 6. Stratigraphic framework of the Cardium in subsurface: Discussion. Canadian Society of Petroleum Geologists Bulletin.

ROSENTHAL, L.R.P., and WALKER, R.G., in press. Lateral and vertical facies sequences in the Upper Cretaceous Chungo Member, Wapiabi Formation, southern Alberta. Canadian Journal of Earth Sciences.

RUST, B.R., 1978. A classification of alluvial channel systems. In: A.D. Miall (ed.) Fluvial Sedimentology. Candian Society of Petroleum Geologists, Memoir 5, 187-198.

SANDERS, J.E., and KUMAR, N., 1975. Evidence of shoreface retreat and in-place "drowning" during Holocene submergence of barriers, shelf off Fire Island, New York. Geological Society of America Bulletin, 86, 65-76.

SCHULTHEIS, N.H., and MOUNTJOY, E.W., 1978. Cadomin conglomerate of western Alberta -- a result of early Cretaceous uplift of the main ranges. Bulletin of Canadian Petroleum Geology, 26, 297-342.

SEELING, A., 1978. The Shannon Sandstone, a further look at the environment of deposition at Heldt Draw Field, Wyoming. Mountain Geologist, 15, 133-144.

SHEPARD, F.P., and EMERY, K.O., 1973. Congo submarine canyon and fan valley. Bulletin of the American Association of Petroleum Geologists, 57 (9), 1679-1691.

SHURR, G.W., 1984. Geometry of shelf sandstone bodies in the Shannon Sandstone of southeastern Montana. In: R.W. Tillman and C.T. Siemers (eds.) Siliciclastic Shelf Sediments. Society of Economic Palaeontologists and Mineralogists, Special Publication 34, 63-84.

SINHA, R.N., 1970. Cardium Formation, Edson area, Alberta. Geological Survey of Canada, Paper 68-30, 63p.

SLATT, R.M., 1984. Continental shelf topography: key to understanding distribution of shelf sand-ridge deposits from Cretaceous Western Interior Seaway. American Association of Petroleum Geologists Bulletin, 68 (9), 1107-1120.

SLOSS, L.L., 1984. Comparative anatomy of cratonic unconformities. In: J.S. Schlee (ed.) Interregional Unconformities and Hydrocarbon Accumulation. American Association of Petroleum Geologists, Memoir 36, 1-6.

SLOSS, L.L., 1963. Sequences in the cratonic interior of North America. Geological Society of America Bulletin, 74, 93-113.

SMITH, D., 1986 (abstract). The palaeogeography and hydrocarbon potential of the Cardium Formation (Upper Cretaceous) of the Alberta Basin. Canadian Society of Petroleum Geologists 1986 Convention, Program and Abstracts, p. 80

SOARES, P.C., LANDIM, P.M.B., and FULFARO, V.J., 1978. Tectonic cycles and sedimentary sequences in the Brazilian intracratonic basins. Geological Society of America Bulletin, 89, 181-191

SOUTHARD, J.B., 1984 (abstract). Laboratory studies of oscillatory flow bed configurations and their bearing on stratification in shallow marine sands. Canadian Society of Petroleum Geologists, Shelf Sands and Sandstone Symposium, Programs and Abstracts, p. 65.

SPEARING, D.R., 1976. Upper Cretaceous Shannon Sandstone: an offshore shallow marine sand body. Wyoming Geological Association, 28th Annual Field Conference, Guidebook, 65-72.

STERLING, G.H., and STROHBECK, G.E., 1975. The failure of the South Pass 7 Platform B in Hurricane Camille. Journal of Petroleum Technology, 27, 263-268.

STOTT, D.F., 1963. The Cretaceous Alberta Group and equivalent rocks, Rocky Mountain Foothills, Alberta. Geological Survey of Canada, Memoir 317, 306p.

STOTT, D.F., 1956. Bighorn Formation in the central Foothills of Alberta. Guide book, 6th Annual Field Conference, Alberta Society of Petroleum Geologists, 33-38.

STRIDE, A.H., 1982. Offshore tidal sands. London, Chapman and Hall, 222 pp.

SUESS, E., 1906. The face of the earth. Clarendon Press, Oxford.

SUTER, J.R., and BERRYHILL, H.L., 1985. Late Quaternary shelf-margin deltas, Northwest Gulf of Mexico. American Association of Petroleum Geologists Bulletin, 69(1), 77-91.

SWAGOR, N.S., 1975. The Cardium conglomerate of the Carrot Creek Field, central Alberta. M.Sc. Thesis, University of Calgary, 151p.

SWAGOR, N.S., OLIVER, T.A., and JOHNSON, B.A., 1976. Carrot

Creek Field, Central Alberta. In: M.M. Lerand (ed.) The Sedimentology of Selected Clastic Oil and Gas Reservoirs in Alberta. Canadian Society of Petroleum Geologists, p. 78-95.

SWIFT, D.J.P., and NIEDORODA, A.W., 1985. Fluid and sediment dynamics on continental shelves. In: R.W. Tillman et al. (eds.) Shelf Sands and Sandstone Reservoirs. S.E.P.M. Short Course No. 13, p. 47-134.

SWIFT, D.J.P., YOUNG, R.A., CLARKE, T., and VINCENT, E., 1981. Sediment transport in the Middle Atlantic Bight of North America: synopsis of recent observations. In: S.D. Nio, R.T.E. Schuttenhelm, and T.C.E. Van Weering (eds.) Holocene Marine Sedimentation in the North Sea Basin. International Association of Sedimentologists, Special Publication 5, 361-383.

SWIFT, D.J.P., DUANE, D.B., and McKINNEY, T.F., 1973. Ridge and swale topography of the Middle Atlantic Bight, North America: secular response to the Holocene hydraulic regime. Marine Geology, 15, 227-247.

SWIFT, D.J.P., KOFOED, J.W., SAULSBURY, F.P. and SEARS, P., 1972. Holocene evolution of the shelf surface, central and southern Atlantic shelf of North America. In: D.J.P. Swift, D.B. Duane, and O.H. Pilkey (eds.) Shelf Sediment Transport: Process and Pattern. Dowden, Hutchinson and Ross, Stroudsburg, Pennsylvania, U.S.A., 499-573.

SWIFT, D.J.P., STANLEY, D.J., and CURRAY, J.R., 1971. Relict sediments on continental shelves: a reconsideration. Journal of Geology, 79, 322-346.

TILLMAN, R.W., 1985. A spectrum of shelf sands and sandstones. In: R.W. Tillman et al. (eds.) Shelf Sands and Sandstone Reservoirs. Society of Economic Palaeontologists and Mineralogists Short Course No. 13, 1-46.

TILLMAN, R.W., and ALMON, W.R., 1979. Diagenesis of Frontier Formation offshore bar sandstones, Spearhead Ranch field, Wyoming. In: P.A. Scholle and P.R. Schluger (eds.) Aspects of Diagenesis. Society of Economic Palaeontologists and Mineralogists, Special Publication 26, 337-378.

TILLMAN, R.W., and MARTINSEN, R.S., 1984. The Shannon shelf-ridge sandstone complex, Salt Creek Anticline area, Powder River Basin, Wyoming. In: R.W. Tillman and C.T. Siemers (eds.). Siliciclastic Shelf Sediments, Society of Economic Palaeontologists and Mineralogists Special Publication No. 34, p. 85-142.

TILLMAN, R.W., SWIFT, D.J.P., and WALKER, R.G., 1985. Shelf Sands and Sandstone Reservoirs. Society of Economic Palaeontologists and Mineralogists Short Course No. 13, 708 p.

TWENHOFEL, W.H., 1947. The environmental significance of conglomerates. Journal of Sedimentary Petrology, 17 (3), 119-128.

TYE, R.S., RANGANATHAN, V., and EBANKS, W.J., 1986. Facies analysis and reservoir zonation of a Cretaceous shelf sand ridge: Hartzog Draw Field, Wyoming. In: T.F. Moslow and E.G. Rhodes (eds.) Modern and Ancient Shelf Clastics: A core workshop. Society of Economic Palaeontologists and Mineralogists Core Workshop No. 9, 169-216.

UCHUPI, E., 1968. Atlantic continental shelf and slope of the United States -- physiography. U.S. Geological Survey Professional Paper 529-C, 30 pp.

UCHUPI, E., and AUSTIN, J.A., 1979. The stratigraphy and structure of the Laurentian cone region. Canadian Journal of Earth Sciences, 16, 1726-1752.

VAIL, P.R., MITCHUM, R.M., and THOMPSON, S., 1977a. Seismic stratigraphy and global changes of sea level, part three: relative changes of sea level from coastal onlap. American Association of Petroleum Geologists, Memoir 26, 63-82.

VAIL, P.R., MITCHUM, R.M., and THOMPSON, S., 1977b. Seismic stratigraphy and global changes of sea level, part four: global cycles of relative changes of sea level. American Association of Petroleum Geologists, Memoir 26, 83-98.

VAN HINTE, J.E., 1976. A Cretaceous time scale. American

Association of Petroleum Geologists Bulletin, 60, 498-516.

VEATCH, A.C., and SMITH, P.A., 1939. Atlantic submarine valleys of the United States, and the Congo submarine valley. Geological Society of America, Special Paper 7, 101 pp.

VINCENT, C.E., YOUNG, R.A., and SWIFT, D.J.P., 1982. On the relationship between bedload and suspended sand transport on the inner shelf, Long Island, New York. Journal of Geophysical Research, 87, 4163-4170.

WALCOTT, R.I., 1976. Lithospheric flexure, analysis of gravity anomalies, and the propagation of seamount chains. In: G.H. Sutton, M.H. Manghnani, and R. Moberly (eds.) The Geophysics of the Pacific Ocean Basin and its Margin. American Geophysical Union, Geophysical Monograph Series, 19, 431-438.

WALKER, R.G., 1986. Cardium Formation 7. Progress report compiling data from outcrop and subsurface in southern Alberta. McMaster University, Tech. Memo 86-3, 97p.

WALKER, R.G., 1985a. Geological evidence for storm transportation and deposition on ancient shelves. In: R.W. Tillman et al. (eds.) Shelf Sands and Sandstone Reservoirs. S.E.P.M. Short Course No. 13, p. 243-302.

WALKER, R.G., 1985b. Cardium Formation 5. Channel cut and filled by turbidity currents in the Cretaceous Western Interior Seaway, Ricinus Field, Alberta. American

Association of Petroleum Geologists, Bulletin, 69, 1963-1981.

WALKER, R.G., 1985c. Cardium Formation 4. Review of the facies and depositional processes in the southern Foothills and Plains, Alberta, Canada. In: R.W. Tillman et al. (eds.) Shelf Sands and Sandstone Reservoirs. S.E.P.M. Short Course No. 13, p. 353-402.

WALKER, R.G., 1984a. Shelf and shallow marine sands. In: R.G. Walker (ed.) Facies Models, 2nd Edition. Geoscience Canada Reprint Series 1, Geological Association of Canada, 141-170.

WALKER, R.G., 1984b. General Introduction: Facies, Facies Sequences and Facies Models. In: R.G. Walker (ed.) Facies Models, 2nd edition. Geoscience Canada Reprint Series 1, Geological Association of Canada, 1-10.

WALKER, R.G., 1984c. Turbidites and associated coarse clastic deposits. In: R.G. Walker (ed.) Facies Models, 2nd edition. Geoscience Canada Reprint Series 1, Geological Association of Canada, 171-188.

WALKER, R.G., 1983a. Cardium Formation 1. "Cardium a turbidity current deposit" (Beach, 1955): a brief history of ideas. Bulletin of Canadian Petroleum Geology, 31, 205-212.

WALKER, R.G., 1983b. Cardium Formation 2. Sand body geometry in the Garrington-Caroline-Ricinus area, Alberta -- the "ragged blanket" model. Bulletin of Canadian Petroleum Geology, 31, 14-26.

WALKER, R.G., 1983c. Cardium Formation 3. Sedimentology and stratigraphy in the Garrington-Caroline area, Alberta. Bulletin of Canadian Petroleum Geology, 31, 213-230.

WALKER, R.G., 1982. Hummocky and swaley cross stratification. In: R.G. Walker (ed.) Clastic units of the Front Ranges, Foothills and Plains in the area between Field, B.C. and Drumheller, Alberta. International Association of Sedimentologists, 11th International Congress on Sedimentology (Hamilton, Canada), Guidebook to Excursion 21A, p. 22-30.

WALKER, R.G., 1978. Deep water sandstone facies and ancient submarine fans: models for exploration for stratigraphic traps. American Association of Petroleum Geologists, Bulletin, 62, 932-966.

WALKER, R.G., 1977. Deposits of upper Mesozoic resedimented conglomerates and associated turbidites in south western Oregon. Geological Society of America Bulletin, 88, 273-285.

WALKER, R.G., 1975a. Generalized facies models for resedimented conglomerates of turbidite association. Geological society of America Bulletin, 86, 737-748.

WALKER, R.G., 1975b. Upper Cretaceous resedimented conglomerates at Wheeler Gorge, California: description and field guide. Journal of Sedimentary Petrology, 45, 105-112.

WALKER, R.G., DUKE, W.L., and LECKIE, D.A., 1983. Hummocky stratification: significance of its variable bedding sequences: discussion. Bulletin of the Geological Society of America, 94, 1245-1249.

WEIMER, R.J., 1984. Relation of unconformities, tectonics and sea-level changes, Cretaceous of Western Interior, U.S.A. In: J.S. Schlee (ed.) Interregional Unconformities and Hydrocarbon Accumulation. American Association of Petroleum Geologists, Memoir 36, 7-35.

WEIMER, R.J., and FLEXER, A., 1985. Depositional patterns and unconformities, Upper Cretaceous, Eastern Powder River Basin, Wyoming. 36th Annual Field Conference, Wyoming Geological Association Guidebook, 131-147.

WESCOTT, W.A., and ETHRIDGE, F.G., 1980. Fan-delta sedimentology and tectonic setting -- Yallahs fan delta. southeast Jamaica. American Association of Petroleum Geologists Bulletin, 64, 374-399.

WINN, R.D., STONECIPHER, S.A., and BISHOP, M.G., 1983. Depositional environments and diagenesis of offshore sand ridges, Frontier Formation, Spearhead Ranch Field, Wyoming. Mountain Geologist, 20, 41-58.

WRIGHT, L.D., AND COLEMAN, J.M., 1972. River delta morphology: wave climate and the role of the subaqueous profile. Science, 176, 282-284.

WRIGHT, M.E., and WALKER, R.G., 1981. Cardium Formation (Upper Cretaceous) at Seebe, Alberta -- storm-transported sandstones and conglomerates in shallow marine depositional environments below fairweather wave base. Canadian Journal of Earth Sciences, 18, 795-809.

APPENDIX 1 -- WELL LOCATIONS

The well locations are sorted according to township and range. The facies sequence type preserved in each well is given under the well type. The resistivity log picks for the E7/T7 (datum) surface and the E5 surface are given where possible. The cored interval is listed in feet or metres as given for the well. In some wells the log picks are given in metres and the cored interval in feet. This occurs when an offset well has been drilled at a later date, but a second core was not cut. The most recent well logs were used to pick the surfaces. All wells are located west of the fifth meridian. An asterisk beside the well location indicates good conglomerate development. This list comprises all of the publically available core as of December, 1985, for townships 50 to 56, ranges 9 to 14W5.

WELL LOCATION	WELL TYPE	E7/T7	E5	CORED INTERVAL	
02-01-50-09	1A			4805 - 4858	FT
04-01-50-09	1A				
06-01-50-09	1A	4692	4812		FT
08-01-50-09	1A	4652	4778		FT
14-01-50-09	3A				
16-01-50-09	3A	4658	4780	4767 - 4801	FT
02-02-50-09	1A				
04-02-50-09	1A				
06-02-50-09	1A	4789	4900	4891 - 4941	FT
08-02-50-09	1A				
14-02-50-09	3A	4781	4908	4863 - 4939	FT
16-02-50-09	3A	1438	1477		M
06-03-50-09	1A	4897	5004		FT
08-03-50-09	1A	4811	4930		FT
14-03-50-09	3B	4809	4940		FT
06-04-50-09	1A	4938	5046		FT
08-04-50-09	1A	4960	5070		FT
14-04-50-09	1A				
16-04-50-09	1A	4892	5002		FT
06-05-50-09	3B	5107	5222		FT
08-05-50-09	1A	4999	5110		FT
10-05-50-09	1A				
14-05-50-09	3A	4991	5103		FT
02-06-50-09	3A	5224	5338		FT
14-06-50-09	1A	5127	5243		FT
16-06-50-09	3A	5074	5193		FT
06-07-50-09	3A	5096	5212	5200 - 5260	FT
06-08-50-09	3A	4950	5070		FT

06-09-50-09	3A	4865	4990	4950 - 5010	FT
16-10-50-09	3A	1450	1486		M
06-11-50-09	3A	4777	4900		FT
08-11-50-09	3A	4717	4836		FT
14-11-50-09	1A			4836 - 4886	FT
16-11-50-09	1A	4692	4811	4770 - 4805	FT
06-12-50-09	1A	4668	4789	4754 - 4824	FT
08-12-50-09	1A	4690	4820		FT
14-12-50-09	1A	4663	4782		FT
16-12-50-09	1A	4644	4763		FT
06-13-50-09	3A	4689	4820	4789 - 4834	FT
08-13-50-09	3A	4642	4767		FT
14-13-50-09	3A			4788 - 4848	FT
16-13-50-09	3A	4650	4772		FT
06-14-50-09	3A	4720	4844	4823 - 4865	FT
08-14-50-09	3A			4794 - 4846	FT
14-14-50-09	1A	4722	4840		FT
06-15-50-09	3A	1447	1487	1476 - 1494	M
10-15-50-09*	1A	1443	1479		M
12-15-50-09*	1A	1447	1487		M
16-15-50-09	3A	4730	4870		FT
12-16-50-09	3A	4791	4924		FT
14-16-50-09	3A	4756	4891	4878 - 4898	FT
16-16-50-09	3A	4748	4880		FT
08-19-50-09	3A	4800	4928	4900 - 4955	FT
14-19-50-09	3A	1470	1509		M
08-20-50-09	3A				
09-20-50-09	1A	5147	5292		FT
14-20-50-09	1A				
06-21-50-09*	1B	4760	4890		FT
08-21-50-09*	2A	4766	4894		FT
16-21-50-09*	2A				
06-22-50-09*	2A	4740	4878	4840 - 4848	FT
08-22-50-09*	2A	4714	4840		FT
10-22-50-09	3A	1443	1481	1470 - 1479	M
14-22-50-09	3A	4759	4887		FT
06-23-50-09	1A	5254	5390		FT
08-23-50-09	3A	4693	4824	4810 - 4870	FT
06-25-50-09	3A	1428	1470		M
06-26-50-09	3A	4707	4840	4752 - 4812	FT
05-29-50-09	1A	5333	5473		FT
06-29-50-09*	2A			4825 - 4885	FT
08-29-50-09*	2B	4762	4915		FT
10-29-50-09*	2B	1449	1495	1477 - 1493	M
12-29-50-09*	2B			1520 - 1557	M
14-29-50-09	3A				
06-30-50-09	3A				
10-30-50-09	3A	4732	4860		FT
14-30-50-09*	1A	5220	5345		FT
16-30-50-09*	2B	4717	4870		FT
04-31-50-09*	2A	4757	4884	4845 - 4911	FT
06-31-50-09	3A	4744	4875	4835 - 4895	FT

03-32-50-09	3B	1473	1514		M
10-34-50-09	3A	1422	1464	1452 - 1470	M
13-34-50-09	3A	1424	1464	1455 - 1473	M
09-35-50-09	3A	4670	4800		FT
12-35-50-09	3A	4660	4791		FT
11-36-50-09	3A	4654	4784		FT
03-01-50-10	1A	1597	1631		M
06-01-50-10	1A	5260	5373	5365 - 5415	FT
08-01-50-10	1A	5270	5383		FT
16-01-50-10	1A	5197	5312		FT
06-02-50-10	1A	5349	5447		FT
08-02-50-10	1A	5304	5404		FT
10-02-50-10	1A				
14-02-50-10	1A	5359	5456		FT
16-02-50-10	1A	5352	5462		FT
06-03-50-10	1A				
08-03-50-10	1A				
14-03-50-10	1A				
06-04-50-10	1A				
08-04-50-10	1A	5270	5380		FT
14-04-50-10	1A				
16-04-50-10	1A				
06-05-50-10	1A	5283	5399		FT
08-05-50-10	1A			5382 - 5417	FT
14-05-50-10	1A				
16-05-50-10	1A				
06-06-50-10	3A	5360	5459		FT
08-06-50-10	1A	5315	5425		FT
06-07-50-10	1A	5361	5463	5450 - 5480	FT
08-07-50-10	1A			5404 - 5445	FT
16-07-50-10	1A				
06-08-50-10*	2A	5320	5443		FT
08-08-50-10	2A				
14-08-50-10	2A				
16-08-50-10	2A				
06-09-50-10*	1B	5248	5370		FT
14-09-50-10	1B			5328 - 5388	FT
02-10-50-10	3A	1621	1655		M
06-10-50-10	1A			5405 - 5422	FT
07-10-50-10	3A	5312	5423		FT
06-11-50-10	1A	5273	5384	5372 - 5417	FT
08-11-50-10	1A	5195	5310		FT
14-11-50-10	1A	5239	5359		FT
04-12-50-10	1A	1595	1630		M
06-12-50-10	1A	5192	5310	5282 - 5332	FT
08-12-50-10	1A	5152	5269		FT
10-12-50-10	3A	1573	1610		M
06-13-50-10	3A	5082	5203	5181 - 5231	FT
06-14-50-10	3A	5179	5298	5285 - 5341	FT
04-17-50-10	1A	1638	1673		M
09-17-50-10	3A	1605	1643		M
06-18-50-10	1A	5432	5532		FT

14-18-50-10	3A			5593 - 5643	FT
16-18-50-10	3A	5342	5461	5440 - 5491	FT
06-19-50-10	1A	5436	5542	5530 - 5580	FT
14-19-50-10	1A	5356	5469	5452 - 5493	FT
02-20-50-10	3A	5270	5390		FT
06-20-50-10	3A	5283	5400		FT
12-20-50-10	1A	5290	5401	5390 - 5458	FT
16-20-50-10	1A	5316	5431	5412 - 5462	FT
16-21-50-10	3A			5350 - 5402	FT
09-22-50-10	3A	1590	1628	1621 - 1625	M
10-23-50-10	3B	4854	5007		FT
04-25-50-10	3B	1492	1531		M
06-25-50-10	3B	4878	5010	4962 - 5022	FT
11-25-50-10	3B	1475	1515		M
14-25-50-10	1A	4810	4931	4912 - 4946	FT
16-25-50-10	1A	4780	4900	4882 - 4918	FT
06-26-50-10	3B	5030	5170	5135 - 5185	FT
08-26-50-10	3B	1505	1545		M
09-26-50-10	3B	1496	1636		M
14-26-50-10	3B			5003 - 5054	FT
16-26-50-10	3B			4950 - 4976	FT
14-28-50-10	3A	1563	1599		M
15-28-50-10	3A	1571	1609		M
14-29-50-10	3A	1607	1642		M
08-30-50-10	3A	5283	5408	5385 - 5445	FT
01-32-50-10	3A	5110	5230	5204 - 5264	FT
14-32-50-10	3A			5260 - 5320	FT
05-33-50-10	3A	5082	5202		FT
14-33-50-10	3A			5058 - 5118	FT
16-33-50-10	1B			5020 - 5095	FT
06-34-50-10	1A	1511	1544		M
08-34-50-10	1A	4876	4988		FT
14-34-50-10*	2B			4947 - 5018	FT
16-34-50-10*	2B			4920 - 4991	FT
01-35-50-10	1A	4830	4942	4915 - 4965	FT
06-35-50-10*	1B	4831	4958		FT
10-35-50-10*	2A			4899 - 4949	FT
14-35-50-10	1A				
16-35-50-10	3B	4780	4919	4916 - 4931	FT
06-36-50-10*	2A	4786	4930	4864 - 4940	FT
08-36-50-10*	2A	4773	4908	4869 - 4920	FT
12-36-50-10	3A			4915 - 4949	FT
16-36-50-10	3A			4845 - 4895	FT
06-01-50-11	1A				
14-01-50-11	1A			5467 - 5527	FT
16-01-50-11	1A				
06-02-50-11	1A	5474	5594	5570 - 5620	FT
08-02-50-11	1A			5506 - 5557	FT
14-02-50-11	1A			5543 - 5592	FT
16-02-50-11	1A			5491 - 5543	FT
06-03-50-11	1B	1709	1744	5693 - 5744	FT
08-03-50-11	1B			5625 - 5701	FT

11-03-50-11	1A	1697	1731		M
14-03-50-11	1A			5611 - 5661	FT
16-03-50-11	1B			5572 - 5622	FT
06-04-50-11	1A	5654	5768	5760 - 5810	FT
08-04-50-11	1A			5734 - 5794	FT
14-04-50-11	1A				
16-04-50-11	1A			5673 - 5720	FT
06-05-50-11	1A	5661	5774	5767 - 5819	FT
08-05-50-11	1A	5668	5781		FT
14-05-50-11	1A			5792 - 5791	FT
16-05-50-11	1A	5646	5760	5746 - 5771	FT
02-06-50-11	1A			5741 - 5791	FT
04-06-50-11	1A	5687	5798	5787 - 5837	FT
08-06-50-11	1A				
09-06-50-11	1A	5672	5785	5773 - 5833	FT
10-06-50-11	1A				
12-06-50-11	1A			5750 - 5800	FT
15-06-50-11	1A	1726	1761		M
16-06-50-11	1A	5672	5785		FT
02-07-50-11	1A			5794 - 5844	FT
04-07-50-11	1A	5650	5761	5750 - 5800	FT
10-07-50-11	1A	5704	5815	5808 - 5858	FT
12-07-50-11	1A				
06-08-50-11	1A	5659	5758	5753 - 5812	FT
08-08-50-11	1A	5640	5745	5721 - 5781	FT
14-08-50-11	1A	5639	5756	5732 - 5802	FT
15-08-50-11	1A	1717	1751		
16-08-50-11	1A	1710	1747	1744 - 1762	M
06-09-50-11	1A	5578	5690	5671 - 5695	FT
08-09-50-11	1A			5617 - 5667	FT
16-09-50-11	1A	5513	5616		FT
06-10-50-11	1A	5493	5600		FT
08-10-50-11	1A			5532 - 5582	FT
14-10-50-11	1B			5571 - 5621	FT
16-10-50-11	1A			5517 - 5580	FT
06-11-50-11	1A	5410	5520	5506 - 5558	FT
08-11-50-11	1A				
09-11-50-11	1A	1649	1682		M
14-11-50-11	1A			5491 - 5551	FT
16-11-50-11	1A				
06-12-50-11	1A	5390	5500	5480 - 5530	FT
07-12-50-11	1A	1649	1682		M
08-12-50-11	1B			5500 - 5571	FT
10-12-50-11	1A				
12-12-50-11	1A	1651	1686		M
14-12-50-11	1A			5500 - 5560	FT
16-12-50-11	1A			5523 - 5595	FT
06-13-50-11*	2A	5461	5580	5550 - 5567	FT
08-13-50-11	1B			5511 - 5525	FT
14-13-50-11	1A			5610 - 5662	FT
16-13-50-11*	1B	1657	1691		M
06-14-50-11	1A	5417	5520	5500 - 5547	FT

08-14-50-11	1A			5540 - 5590	FT
14-14-50-11	1A			5530 - 5570	FT
16-14-50-11	1A			5562 - 5612	FT
06-15-50-11	1A	5464	5572	5561 - 5611	FT
08-15-50-11	1A	1652	1689	5517 - 5567	FT
16-15-50-11	1A	1649	1681	5516 - 5566	FT
06-16-50-11	1A	5600	5690	5673 - 5723	FT
06-17-50-11	1A	5617	5729	5705 - 5755	FT
13-17-50-11	1A	1719	1750		M
02-18-50-11	1A			5793 - 5843	FT
04-18-50-11	1A			5784 - 5825	FT
10-18-50-11	1A	1733	1767	1760 - 1779	M
12-18-50-11	1A			5792 - 5842	FT
04-19-50-11	1A	5688	5789	5775 - 5835	FT
02-21-50-11	1A	5539	5649	5610 - 5689	FT
02-22-50-11	1A	1651	1684		M
06-22-50-11	1A	5437	5540	5537 - 5587	FT
14-22-50-11	1A			5552 - 5602	FT
06-23-50-11	1A	5452	5558	5546 - 5600	FT
08-23-50-11	1A			5613 - 5665	FT
14-23-50-11	1A	5525	5635	5620 - 5668	FT
16-23-50-11	1A			5662 - 5686	FT
06-24-50-11	1A	5499	5610	5598 - 5630	FT
08-24-50-11	1A			5613 - 5645	FT
14-24-50-11	1B			5618 - 5659	FT
16-24-50-11	1A			5536 - 5585	FT
06-25-50-11	1A	5446	5555	5550 - 5600	FT
08-25-50-11	1A	5383	5503	5465 - 5515	FT
14-25-50-11	1B			5515 - 5565	FT
08-26-50-11	1A	5550	5666	5662 - 5712	FT
14-26-50-11	1B			5640 - 5700	FT
16-26-50-11*	2A			5600 - 5685	FT
08-27-50-11	3A	5434	5563		FT
10-29-50-11	1A	5490	5610	5572 - 5622	FT
06-30-50-11	1A	1710	1745		M
10-31-50-11	1A	5543	5654		FT
10-32-50-11	1A				
10-33-50-11*	3A	5444	5571	5545 - 5604	FT
02-34-50-11	3A			5576 - 5635	FT
06-34-50-11	3A	1670	1709	1699 - 1717	M
10-34-50-11	3A			5549 - 5609	FT
06-35-50-11	1A	5448	5558	5537 - 5597	FT
14-35-50-11	1A	5511	5634	5601 - 5660	FT
04-36-50-11	1A	5422	5527	5518 - 5578	FT
10-01-50-12	1A			5756 - 5806	FT
16-04-50-12	1A	1743	1780		M
12-06-50-12	1A	5970	6090	6063 - 6185	FT
10-07-50-12	1A	1777	1812		M
10-11-50-12	1A	1755	1789		M
02-12-50-12	1A			5761 - 5811	FT
04-12-50-12	1A	5753	5865		FT
12-13-50-12	1A			5855 - 5892	FT

02-14-50-12	1A				
10-14-50-12	1A			5822 - 5892	FT
01-15-50-12	1A	5710	5823		FT
16-15-50-12	1A				
14-20-50-12	1A	5770	5875		FT
08-21-50-12	1A	1750	1786		M
10-21-50-12	1A			5825 - 5872	FT
07-23-50-12	1A	1740	1775		M
04-25-50-12	1A	5710	5816	5794 - 5907	FT
08-26-50-12	1A	5696	5800	5786 - 5837	FT
04-28-50-12	1A			5900 - 6000	FT
12-30-50-12	1A	5890	5998		FT
03-31-50-12	1A	1808	1842	1830 - 1848	M
03-34-50-12	1A	1726	1759	1752 - 1771	M
08-36-50-12	1A	5590	5700	5686 - 5762	FT
08-15-50-13	1A	1838	1874		M
08-30-50-13	1A	1835	1868	1860 - 1878	M
16-33-50-13	1A	5937	6045	6023 - 6083	FT
07-06-50-14	1A	6657	6767		FT
02-25-50-14	1A	6085	6204		FT
09-35-50-14	1A	1837	1872	1870 - 1888	M
02-01-51-09	3A	4678	4808	4750 - 4855	FT
02-03-51-09*	2A	1421	1460		M
05-03-51-09*	2A	1423	1466	1455 - 1473	M
12-03-51-09	3B	1424	1465		M
06-04-51-09	3B	4852	4980		FT
08-04-51-09*	2A	1424	1465	1450 - 1462	M
10-04-51-09*	2B	4665	4812		FT
11-04-51-09*	2B	1420	1462		M
13-04-51-09*	2B	1420	1465	1450 - 1476	M
15-04-51-09*	2B	1426	1471	1467 - 1477	M
09-07-51-09	3B	1445	1487	1470 - 1494	M
06-08-51-09	3A	1431	1470	1454 - 1472	M
08-08-51-09*	2B	1424	1471	1454 - 1470	M
09-08-51-09*	2B	1427	1472	1464 - 1482	M
10-08-51-09*	2B	1426	1471	1455 - 1479	M
11-08-51-09*	2B	1429	1477	1463 - 1474	M
02-09-51-09	3B	1424	1467	1458 - 1476	M
05-09-51-09*	2B	1430	1475		M
01-11-51-09	3B	4810	4967	4910 - 4970	FT
06-14-51-09	3B	4560	4691		FT
02-17-51-09	3B	4732	4860		FT
01-18-51-09	3B	1446	1487	1477 - 1495	M
13-18-51-09	3B	1451	1488	1476 - 1494	M
10-21-51-09	3B	4551	4676	4662 - 4711	FT
14-26-51-09	3B	1355	1394		M
07-29-51-09	3B	4605	4730	4700 - 4740	FT
16-30-51-09	3B	4634	4765		FT
02-31-51-09	3B	4664	4789		FT
10-31-51-09	3B	1394	1432		M
11-31-51-09	3B	1411	1449		M
07-34-51-09	3B	4468	4594		FT

15-36-51-09	3B	1384	1424		M
04-02-51-10	1B	4850	4970		FT
14-02-51-10	3A	1465	1507		M
10-03-51-10	3B			5082 - 5132	FT
12-03-51-10*	2B				
03-04-51-10	3A	1539	1576		M
05-04-51-10	3A	1554	1591		M
06-04-51-10*	2A	5000	5130	5094 - 5154	FT
08-04-51-10*	2A			5066 - 5140	FT
14-04-51-10*	2A	5013	5164	5103 - 5178	FT
16-04-51-10*	2A			5080 - 5131	FT
08-05-51-10	3A	5120	5240	5213 - 5330	FT
14-05-51-10*	2A			5235 - 5303	FT
16-05-51-10*	2B	5074	5225	5177 - 5242	FT
06-07-51-10	3B	5190	5338	5290 - 5339	FT
08-07-51-10*	2B	5154	5290	5267 - 5320	FT
14-07-51-10*	2B			5254 - 5313	FT
16-07-51-10	3A	5130	5256	5228 - 5283	FT
06-08-51-10*	2B	5105	5262		FT
08-08-51-10*	2B				
10-08-51-10*	2B				
12-08-51-10*	2B			5218 - 5278	FT
02-09-51-10	3B			5138 - 5162	FT
06-09-51-10	3B	5074	5223	5182 - 5232	FT
12-09-51-10*	2B			5185 - 5245	FT
08-10-51-10	3A	1494	1531		M
02-11-51-10	3A	4840	4965		FT
06-11-51-10	3A	1466	1506		M
04-14-51-10	3A	1482	1523		M
13-14-51-10	3B	1498	1541		M
15-14-51-10	3B	1521	1565		M
16-14-51-10	3A	1516	1556		M
16-15-51-10	3A	1519	1560		M
02-17-51-10	3B	5120	5259	5184 - 5312	FT
04-18-51-10	3B	5184	5327	5294 - 5354	FT
06-19-51-10	3A	5101	5232		FT
16-19-51-10	3A	1520	1555		M
07-20-51-10	3A	1540	1580		M
14-20-51-10*	2A	1510	1554		M
16-20-51-10*	2A	1503	1545		M
06-21-51-10	3A	1518	1559		M
08-21-51-10*	2A	1524	1563		M
14-21-51-10*	2A	1523	1563		M
06-22-51-10*	2B	1520	1568		M
10-22-51-10*	2B	1523	1569	1553 - 1567	M
11-22-51-10*	2B	1525	1573		M
13-22-51-10	3B	1526	1565	1550 - 1580	M
02-23-51-10*	2B	1513	1557		M
03-23-51-10*	2B	1518	1564	1550 - 1568	M
04-23-51-10*	2B	1515	1561	1544 - 1553	M
10-23-51-10	3A	4854	5005	4970 - 5030	FT
07-26-51-10	3B	1465	1510	1497 - 1515	M

02-29-51-10	3A	1501	1544		M
06-29-51-10*	2A	1502	1545	1531 - 1547	M
06-30-51-10*	2A	1516	1562		M
07-30-51-10*	2A	1512	1560		M
10-30-51-10*	2B	1507	1558	1534 - 1552	M
13-30-51-10*	2B	1518	1569	1546 - 1570	M
02-31-51-10	3A	1505	1545		M
04-31-51-10*	2B	1510	1560	1545 - 1548	M
13-31-51-10	3B	1496	1544	1528 - 1546	M
06-33-51-10	3A	1493	1529		M
14-34-51-10*	2A	1472	1518	1505 - 1533	M
04-03-51-11	1A	5452	5575	5550 - 5610	FT
10-03-51-11	1A	1681	1722		M
06-05-51-11	1B	5535	5662		FT
13-05-51-11	1B	5517	5640	5531 - 5704	FT
07-07-51-11	1B	5487	5607		FT
13-08-51-11	1A	1653	1692		M
06-09-51-11	1A	5423	5546		FT
12-09-51-11	1A	5413	5531		FT
14-11-51-11*	1B	5269	5389	5370 - 5420	FT
16-11-51-11*	2A	5247	5392		FT
06-12-51-11*	2B	5266	5410	5356 - 5405	FT
08-12-51-11	3B	5240	5380	5350 - 5402	FT
14-12-51-11*	2B	5223	5375		FT
16-12-51-11*	2B	5193	5343	5309 - 5354	FT
04-13-51-11*	2B	1595	1640	1632 - 1647	M
06-14-51-11*	2B	5237	5400		FT
08-14-51-11*	2B	5231	5381	5337 - 5387	FT
12-14-51-11*	2B	1600	1645	1625 - 1657	M
14-14-51-11	3B	5210	5354	5315 - 5365	FT
02-15-51-11*	2A	5316	5444	5413 - 5463	FT
10-15-51-11*	2A	5264	5420	5362 - 5470	FT
04-16-51-11*	1B	5390	5510	5490 - 5538	FT
10-16-51-11	1A	5342	5453	5437 - 5487	FT
12-16-51-11*	1B	5345	5470	5444 - 5494	FT
10-17-51-11	1A	1633	1671		M
07-18-51-11	1A	5457	5573		FT
10-19-51-11	1A	1671	1710		M
07-20-51-11*	1B	1632	1674	1655 - 1684	M
10-20-51-11*	1B	5345	5475	5446 - 5496	FT
12-20-51-11	1A	5438	5560	5549 - 5599	FT
02-21-51-11*	1B	5290	5430	5390 - 5440	FT
04-21-51-11*	1B	5300	5432	5400 - 5450	FT
10-21-51-11	3B	5240	5385	5330 - 5400	FT
02-22-51-11*	2A	5236	5370	5332 - 5382	FT
04-22-51-11*	1B	5276	5400	5369 - 5419	FT
08-25-51-11*	1B	1532	1574		M
14-25-51-11	3A	1547	1585		M
16-25-51-11*	2B	1531	1576		M
03-26-51-11	3A	1570	1609		M
04-26-51-11	3A	5155	5287		FT
02-28-51-11	1A	1596	1631	1629 - 1648	M

04-28-51-11	1A	5293	5408	5375 - 5430	FT
06-28-51-11*	1B	1599	1635		M
12-28-51-11*	2A	1597	1646		M
02-29-51-11*	1A	5363	5482	5473 - 5523	FT
04-29-51-11	3A	5416	5545	5467 - 5535	FT
10-29-51-11*	1B	5277	5408		FT
12-29-51-11	1A	5349	5472	5455 - 5485	FT
04-30-51-11	1A	5488	5612		FT
10-30-51-11	1A	5422	5500	5537 - 5587	FT
12-31-51-11	3B	5345	5483		FT
02-32-51-11	3A			1657 - 1675	M
04-32-51-11	3A	5328	5465	5435 - 5465	FT
04-33-51-11	1A	1618	1656		M
04-34-51-11	3B	1605	1655		M
02-36-51-11*	2B	1530	1574	1569 - 1571	M
06-36-51-11	3A	1538	1573		M
09-36-51-11*	2A			1551 - 1569	M
14-36-51-11	3A	1529	1564	1555 - 1574	M
11-06-51-12*	1B	1763	1798		M
04-08-51-12	1A	5733	5835	5822 - 5872	FT
10-12-51-12	1A	5548	5658		FT
07-13-51-12	1A	5610	5722		FT
02-14-51-12	1A	1717	1752		M
15-20-51-12	3A	1730	1770		M
10-21-51-12	3A	5650	5770		FT
10-22-51-12	1A	1728	1765	5762 - 5813	FT
07-25-51-12	1A	1682	1720		M
06-26-51-12	3A	1730	1769		M
16-26-51-12	3B	5562	5693		FT
06-28-51-12	3B	1723	1763		M
10-33-51-12	3A	5700	5833	5787 - 5846	FT
16-34-51-12	3A	5628	5760		FT
16-35-51-12	3A	1681	1721		M
06-36-51-12	3A	1658	1700		M
12-36-51-12	3A	5497	5628	5582 - 5654	FT
07-01-51-13	1B	1804	1840	1811 - 1829	M
06-04-51-13	1A	1800	1836		M
10-11-51-13	1A	5884	5990	5970 - 6025	FT
07-13-51-13*	1B	1761	1798	1782 - 1800	M
11-13-51-13*	1B	1769	1813		M
02-20-51-13	1A	1830	1863		M
02-22-51-13	1A	1795	1829		M
12-23-51-13*	1B	1796	1835		M
10-24-51-13	3A	5850	5980		FT
08-35-51-13*	1B	1789	1827	1810 - 1827	M
09-35-51-13	3A	1763	1807	1794 - 1808	M
11-35-51-13*	1B	1749	1794		M
16-11-51-14	1A	1813	1848		M
15-13-51-14	1A	6010	6113	6070 - 6130	FT
10-23-51-14*	1A	6050	6157		FT
13-01-52-09	3B	1387	1428		M
15-01-52-09	3B	1377	1418		M

06-03-52-09	3B	1365	1405		M
10-04-52-09	3B	4491	4620		FT
10-05-52-09	3B	4515	4638		FT
01-08-52-09	3B	1372	1410		M
06-10-52-09	3B	4480	4609		FT
14-11-52-09	3B	4480	4613		FT
06-12-52-09	3B	1374	1414		M
07-12-52-09	3B	1370	1411		M
07-13-52-09	3B	1346	1387		M
06-14-52-09	3B	4483	4618		FT
10-19-52-09	3B	4442	4570		FT
10-21-52-09	3B	4415	4547		FT
07-24-52-09	3B	4333	4470		FT
06-29-52-09	3B	4401	4534		FT
07-35-52-09	3B	4357	4495		FT
04-36-52-09	3B	4350	4488		FT
15-02-52-10	3B	4628	4750	4730 - 4822	FT
14-05-52-10	3B	1475	1515		M
10-06-52-10	3B	4834	4978	4920 - 4980	FT
06-09-52-10*	2A	1450	1496		M
07-10-52-10	3B	4666	4788		FT
04-11-52-10*	2B	1410	1460		M
11-16-52-10*	2B	1412	1461	1451 - 1468	M
11-17-52-10	3B	1420	1457		M
09-19-52-10	3B	1414	1451		M
05-22-52-10*	2B	1390	1442	1426 - 1444	M
11-24-52-10	3B	4489	4618		FT
06-02-52-11*	1B	1538	1575		M
11-02-52-11*	2B	1520	1571	1552 - 1569	M
08-03-52-11	1A	1545	1577	1570 - 1588	M
09-03-52-11*	2A	1534	1577	1565 - 1583	M
12-03-52-11	3A	5108	5231	5167 - 5287	FT
13-04-52-11	3A	5131	5248	5250 - 5349	FT
05-06-52-11	3B	5265	5394	5371 - 5427	FT
09-06-52-11	3B	5222	5348	5321 - 5401	FT
13-07-52-11*	2A	1577	1616	1607 - 1625	M
15-07-52-11*	2A	1568	1608	1595 - 1609	M
09-08-52-11	3B	1550	1590		M
11-08-52-11	3B	1559	1599		M
07-10-52-11	3B	4987	5124		FT
15-11-52-11*	2B	4850	5010	4982 - 5054	FT
16-12-52-11	3B	4787	4905		FT
06-17-52-11	3B	1550	1593		M
02-18-52-11*	2B	1559	1603	1597 - 1615	M
11-18-52-11*	2A	1560	1600	1590 - 1603	M
03-19-52-11	3A	1555	1591		M
10-19-52-11	3B	5067	5195		FT
03-20-52-11	3A	1523	1558		M
13-20-52-11	3A	5008	5138	5050 - 5160	FT
10-21-52-11	3A	1490	1528	1510 - 1538	M
16-21-52-11	3B	4874	5003	4974 - 5034	FT
13-25-52-11*	2B	1425	1469	1471 - 1480	M

14-28-52-11	3B	4883	5010	4945 - 5095	M
03-29-52-11	3B	1515	1553		M
06-30-52-11	3B	1527	1565		M
11-30-52-11	3A	1516	1552		M
06-31-52-11	3A	1501	1537		M
10-32-52-11	3B	1477	1517		M
07-34-52-11	3B	4773	4898		FT
06-01-52-12	3A	5339	5470		FT
09-01-52-12	1A	1605	1641	1630 - 1648	M
07-02-52-12	3A	1653	1691		M
10-03-52-12	1A			5594 - 5654	FT
07-04-52-12	1A	1707	1743		M
16-07-52-12*	1B	5310	5450	5400 - 5516	FT
02-08-52-12*	1B	5428	5545	5480 - 5600	FT
10-08-52-12*	2A	5381	5500	5466 - 5517	FT
12-08-52-12*	2B	1629	1676		M
04-09-52-12	1A	5438	5544	5522 - 5562	FT
07-11-52-12	1A				
02-12-52-12*	2B	1598	1645	1627 - 1646	M
04-12-52-12	1A	5300	5420	5380 - 5481	FT
06-12-52-12*	2A	1604	1646		M
15-12-52-12	1A	5300	5416		FT
04-13-52-12	3B	1587	1629		M
01-14-52-12*	2A	1592	1632	1624 - 1632	M
03-14-52-12*	2A	1604	1643	1644 - 1661	M
10-14-52-12	3A	1583	1618		M
12-14-52-12	3A	1590	1625		M
09-15-52-12*	2A	1605	1641		M
11-15-52-12*	1B	1605	1640		M
16-16-52-12*	2A	1611	1645		M
04-17-52-12*	2B	5290	5437	5374 - 5440	FT
10-17-52-12	3B	1596	1635		M
12-17-52-12	3B	5262	5390	5334 - 5418	FT
02-18-52-12*	1B			5384 - 5466	FT
10-18-52-12*	2A	5237	5355	5355 - 5401	FT
02-19-52-12	3A	1587	1620		M
04-19-52-12	1B			5360 - 5394	FT
06-19-52-12	1B	1591	1628		M
12-19-52-12*	2A	1575	1621	1614 - 1632	M
06-20-52-12	1A	1580	1613		M
08-20-52-12*	2A	1580	1621		M
13-20-52-12	3A	5151	5275		FT
16-20-52-12	1A	1571	1606		M
02-21-52-12*	2B	1595	1638		M
06-21-52-12*	2A	1588	1628		M
10-21-52-12*	2A	5189	5312	5292 - 5347	FT
05-22-52-12	3B	5230	5360	5329 - 5392	FT
11-22-52-12	3B	1583	1622		M
08-23-52-12	3B	1576	1613		M
15-23-52-12	3B	5116	5247	5215 - 5275	FT
16-23-52-12	3A	1564	1600		M
03-24-52-12	3A	1563	1599	1588 - 1606	M

09-24-52-12	3B	1551	1593		M
12-24-52-12*	2A	1558	1600	1595 - 1616	M
07-25-52-12	3B	1531	1569		M
02-26-52-12	3A	1541	1580		M
10-26-52-12	3A	1525	1562		M
11-26-52-12	3A	1527	1567		M
07-27-52-12	3A	1546	1584		M
03-28-52-12	3B	5140	5270	5235 - 5295	FT
06-28-52-12	3A	1566	1607		M
16-29-52-12	3B	1551	1595		M
11-32-52-12	3A	1537	1577		M
01-34-52-12*	2A	1522	1564		M
04-35-52-12	3B	1518	1564		M
05-36-52-12	3B	1512	1558		M
04-02-52-13*	2A	1716	1765	1727 - 1745	M
02-03-52-13	1A	1736	1765	1761 - 1777	M
10-03-52-13*	2A	1705	1744	1726 - 1740	M
11-03-52-13*	1B	1715	1754	1738 - 1760	M
04-08-52-13	1A	5592	5700		FT
16-08-52-13*	1A	1681	1716		M
08-09-52-13*	1B	1695	1731		M
09-09-52-13*	1B	1674	1712		M
05-10-52-13*	2A	1694	1735		M
12-10-52-13*	2A	1673	1715		M
10-13-52-13	1A	5297	5408	5375 - 5420	FT
14-14-52-13	1A	1617	1649	1642 - 1660	M
06-16-52-13	1A	1648	1680	1670 - 1688	M
10-21-52-13	1B			5382 - 5442	FT
13-21-52-13*	1B	5334	5450	5425 - 5480	FT
14-24-52-13*	1B	5182	5307		FT
16-24-52-13*	2A	1576	1618	1607 - 1613	M
01-25-52-13*	1B	1565	1602		M
06-25-52-13	3A	5140	5269	5220 - 5269	FT
14-25-52-13*	1B	5087	5210	5174 - 5224	FT
16-25-52-13	3A	1545	1582		M
16-26-52-13	1A	1560	1595		M
12-27-52-13	3A	5250	5370	5349 - 5399	FT
02-29-52-13*	1B	5342	5462	5430 - 5473	FT
06-29-52-13*	1B	5333	5460	5421 - 5462	FT
07-34-52-13*	1A	5188	5306	5293 - 5352	FT
01-35-52-13*	1B	1556	1592		M
06-35-52-13*	1B	1563	1598		M
10-35-52-13*	2A	5095	5240	5195 - 5267	FT
14-35-52-13*	2A	1559	1601	1587 - 1605	M
03-14-52-14	1A	1693	1723	1717 - 1735	M
08-18-52-14	3A	1764	1801	1799 - 1818	M
07-22-52-14	1A	1711	1745		M
06-32-52-14	1A	5560	5675	5650 - 5686	FT
10-36-52-14	1A	5371	5473	5455 - 5515	FT
10-08-53-09	3B	4292	4430		FT
06-11-53-09	3B	4310	4446		FT
02-21-53-09	3B	1273	1316		M

10-22-53-09	3B	4116	4252		FT
14-23-53-09	3B	1257	1298		M
06-29-53-09	3B	4082	4214		FT
15-35-53-09	3B	1213	1254		M
14-36-53-09	3B	1202	1244		M
16-07-53-10	3B	4550	4685		FT
01-08-53-10	3B	1376	1415		M
05-13-53-10	3B	4276	4408		FT
08-15-53-10	3B	1337	1377		M
06-16-53-10	3B	4417	4550		FT
06-17-53-10	3B	1352	1393		M
10-18-53-10	3B	4514	4650		FT
10-21-53-10	3B	4343	4477		FT
10-23-53-10	3B	1283	1324		M
06-24-53-10	3B	1272	1314		M
08-25-53-10	3B	4100	4239		FT
06-26-53-10	3B	1273	1317		M
11-26-53-10	3B	4168	4307		FT
06-27-53-10	3B	1298	1339		M
10-27-53-10	3B	4236	4372		FT
04-29-53-10	3B	4320	4456		FT
10-29-53-10	3B	4252	4390		FT
07-31-53-10	3B	4240	4380		FT
07-35-53-10	3B	4130	4283		FT
02-05-53-11	3B	4805	4949	4912 - 4944	FT
10-05-53-11	3B	4772	4923		FT
07-07-53-11	3B	4791	4915		FT
10-09-53-11	3B	4632	4762		FT
06-17-53-11	3B	1415	1453		M
11-22-53-11	3B	4551	4690		FT
11-25-53-11	3B	4339	4490		FT
16-31-53-11	3B			1382 - 1400	M
06-33-53-11	3B	1358	1403		M
08-33-53-11*	2B			1395 - 1409	M
07-01-53-12	3B	4866	5018		FT
12-01-53-12	3B	4856	4985	4958 - 5013	FT
08-08-53-12	3B	1519	1561		M
05-09-53-12	3B	4942	5078	5060 - 5156	FT
07-09-53-12	3B	1495	1535		M
01-11-53-12*	2B	4824	4962	4926 - 4999	FT
05-11-53-12	3B	1484	1522		M
10-15-53-12	3B	4767	4920		FT
10-16-53-12	3B	4800	4943	4903 - 4967	FT
11-16-53-12*	2B	4825	4969		FT
12-16-53-12	3A	4850	4990	4958 - 5010	FT
10-20-53-12	3A	4787	4925	4870 - 4990	FT
12-20-53-12	3B	4795	4936	4887 - 4947	FT
04-22-53-12	3B	4739	4881	4820 - 4880	FT
06-23-53-12	3B	4745	4895		FT
10-25-53-12	3B	4583	4732		FT
06-33-53-12	3B	4620	4760	4695 - 4795	FT
10-35-53-12	3B	1384	1430		M

06-01-53-13	3B	5033	5170	5136 - 5197	FT
10-02-53-13*	2B	5090	5234		FT
01-03-53-13	3A	1571	1610	1602 - 1619	M
06-04-53-13	1A	1602	1637	1632 - 1650	M
08-04-53-13	1A	1592	1628		M
16-05-53-13	1A	1588	1620	1617 - 1633	M
06-06-53-13	1B	5230	5347	5305 - 5356	FT
10-07-53-13*	1B	1572	1608		M
07-08-53-13	3A	5262	5380	5365 - 5430	FT
10-09-53-13	1A	5240	5347	5355 - 5394	FT
06-10-53-13*	2A	1579	1622	1613 - 1624	M
14-10-53-13	3A	1562	1600	1590 - 1608	M
06-11-53-13	3A	1548	1590	1577 - 1595	M
14-12-53-13	3A	1515	1551		M
10-13-53-13	1A	5392	5510		FT
10-14-53-13	3B	4950	5083	5044 - 5105	FT
06-15-53-13*	2A	1552	1594	1581 - 1601	M
10-15-53-13	3A	5060	5185	5194 - 5249	FT
10-16-53-13	1A	1572	1605		M
05-17-53-13*	1B	1566	1605	1597 - 1615	M
10-17-53-13	1A	1576	1610	1601 - 1624	M
05-18-53-13	1B	1579	1615	1612 - 1630	M
11-18-53-13*	1B	1581	1615	5270 - 5330	M
10-19-53-13	3A	1536	1573		M
10-20-53-13	3B	5067	5200	5180 - 5240	FT
06-21-53-13	3B	1555	1596		M
11-21-53-13	1A	5068	5170	5155 - 5215	FT
08-29-53-13	3A	1526	1565		M
07-30-53-13	3A	5051	5170		FT
16-30-53-13*	2A	1526	1567	1556 - 1564	M
06-31-53-13*	2A	1519	1557	1549 - 1566	M
12-32-53-13	3B	4943	5070	5042 - 5092	FT
03-33-53-13	3B	1497	1540		M
02-36-53-13	3B	4765	4917	4885 - 4944	FT
10-01-53-14	1A	5292	5395	5378 - 5438	FT
03-02-53-14	1A	1627	1658	1645 - 1663	M
10-11-53-14	1A	5332	5438		FT
10-19-53-14	1A	5264	5371		FT
06-21-53-14	1A	5198	5310	5296 - 5340	FT
06-23-53-14	1A	5261	5375	5385 - 5406	FT
10-24-53-14	1A	5170	5281	5243 - 5316	FT
08-26-53-14	1A	1550	1581	1572 - 1586	M
10-30-53-14	1A	5210	5310	5309 - 5369	FT
11-34-53-14	1A	5093	5210		FT
06-35-53-14	1B	1529	1565		M
07-36-53-14	1A	1541	1575		M
06-02-54-09	3B	1204	1247		M
06-03-54-09	3B	4001	4140		FT
15-03-54-09	3B	1208	1250		M
10-09-54-09	3B	3994	4133		FT
10-10-54-09	3B	3965	4105		FT
06-11-54-09	3B	1198	1241		M

10-13-54-09	3B	3843	3984		FT
11-14-54-09	3B	1186	1228		M
07-15-54-09	3B	3957	4095		FT
10-17-54-09	3B	3984	4120		FT
11-18-54-09	3B	1210	1251		M
03-22-54-09	3B	1224	1265		M
10-22-54-09	3B	3923	4059		FT
16-27-54-09	3B	1178	1223		M
09-29-54-09	3B	1230	1271		M
08-32-54-09	3B	1240	1284		M
10-35-54-09	3B	3810	3950		FT
07-03-54-10	3B	1250	1292		M
03-25-54-10	3B	1228	1269		M
16-32-54-10	3B	1218	1259		M
10-34-54-10	3B	4167	4300		FT
07-05-54-11	3B	4421	4546		FT
06-06-54-11	3B	1340	1378	1372 - 1389	M
10-07-54-11	3B	1319	1360		M
05-10-54-11	3B	4249	4384		FT
10-11-54-11	3B	4229	4380		FT
04-13-54-11	3B	1292	1332		M
11-15-54-11	3B	1311	1350		M
06-17-54-11	3B	4270	4418		FT
06-19-54-11	3B	1306	1353		M
11-20-54-11	3B	1299	1345		M
10-26-54-11	3B	1265	1310		M
07-29-54-11	3B	1306	1345		M
14-29-54-11	3B	1300	1338		M
06-30-54-11	3B	1307	1346		M
16-31-54-11	3B	1309	1349		M
10-34-54-11	3B	1250	1290		M
14-01-54-12	3B	1345	1383	1370 - 1389	M
08-02-54-12	3B	1364	1405	1398 - 1416	M
16-02-54-12*	2B	1357	1400	1389 - 1405	M
12-03-54-12*	2B	4550	4683		FT
06-04-54-12	3B	4602	4739		FT
04-08-54-12	3B	4628	4771		FT
14-08-54-12	3A	4587	4700		FT
02-09-54-12	3A	1384	1422		M
05-11-54-12	3A	1358	1395		M
06-12-54-12	3A	1335	1371		M
05-13-54-12	3B	4344	4474		FT
06-13-54-12	3B	1322	1361		M
10-13-54-12	3B	4320	4467		FT
06-14-54-12	3A	1334	1375		M
06-15-54-12	3A	4449	4569		FT
12-17-54-12	3A	4555	4678		FT
02-18-54-12	3A	4602	4720		FT
04-18-54-12	3A	4618	4732		FT
10-18-54-12	3A	4578	4690		FT
13-18-54-12	3A	1403	1440		M
02-19-54-12	3A	4559	4680		FT

04-19-54-12	3B	4575	4710		FT
10-19-54-12	3A	4540	4670		FT
04-20-54-12	3A	4535	4668		FT
11-25-54-12	3B	1310	1349		M
07-27-54-12	3B	4390	4540		FT
06-28-54-12	3B	1352	1399		M
11-29-54-12	3B	1365	1410		M
04-30-54-12	3A	4540	4664		FT
11-30-54-12	3A	4530	4654		FT
10-31-54-12	3A	4531	4650		FT
06-32-54-12*	2A	1363	1405		M
12-32-54-12	3A	1375	1415		M
16-36-54-12	3B	1300	1340		M
04-01-54-13	3A	4746	4867		FT
11-02-54-13	3A	4744	4877	4832 - 4892	FT
16-02-54-13	3A	1441	1483		M
07-04-54-13	3A	4850	4974		FT
06-05-54-13	3A	4873	4997	4960 - 5020	FT
06-06-54-13	3A	1494	1529		M
06-07-54-13	3A	1474	1509		M
10-07-54-13*	2A	4807	4932		FT
06-09-54-13	3A	1467	1506		M
09-13-54-13	3A	1405	1442		M
10-14-54-13	3A	4660	4772	4788 - 4828	FT
08-18-54-13*	2A	1467	1503		M
10-21-54-13	3B	1430	1470		M
08-24-54-13	3A	4580	4700		FT
10-24-54-13	3A	4573	4692		FT
12-24-54-13	3A	4594	4716		FT
14-24-54-13	3A	4583	4706		FT
16-24-54-13	3A	1391	1428		M
02-25-54-13	3B	1392	1432		M
06-25-54-13	3B	1393	1435		M
10-25-54-13	3A	1387	1424		M
12-25-54-13	3B	4572	4709		FT
16-25-54-13	3A	1387	1426		M
08-26-54-13	3B	4594	4727		FT
16-26-54-13	3B	4577	4713		FT
16-27-54-13	3B	1410	1450		M
09-29-54-13	3B	4683	4818		FT
03-32-54-13	3B	1424	1465		M
16-33-54-13	3B	4590	4720		FT
14-34-54-13	3B	4600	4736	4694 - 4754	FT
16-34-54-13	3B	4588	4718		FT
02-35-54-13	3B	1400	1441		M
06-35-54-13	3B	1404	1447		M
07-35-54-13	3A	4563	4683		FT
10-35-54-13	3B	1390	1430		M
12-35-54-13	3B	1399	1442		M
04-36-54-13	3A	1382	1418		M
10-36-54-13	3A	1383	1421		M
11-06-54-14	3A	5162	5274		FT

04-07-54-14	3A	1568	1598		M
11-12-54-14	3A	4911	5030	4965 - 5045	FT
11-13-54-14	3A	4818	4921	4850 - 4947	FT
06-18-54-14	3A	1534	1568		M
10-19-54-14	3A	4951	5062		FT
11-24-54-14*	2A	4781	4894	4863 - 4888	FT
10-28-54-14	3A	4871	4981		FT
11-29-54-14	3A	4889	5000		FT
06-31-54-14	3A	4775	4880		FT
07-34-54-14*	2A	4724	4862		FT
10-35-54-14	3B	4721	4858	4830 - 4885	FT
01-06-55-09	3B	4132	4270		FT
16-05-55-09	3B	3970	4110		FT
04-09-55-09	3B	1176	1219		M
05-09-55-09	3B	3843	3986		FT
10-10-55-09	3B	3861	4010		FT
06-14-55-09	3B	1152	1198		M
08-14-55-09	3B	1152	1198		M
08-15-55-09	3B	1156	1201		M
06-16-55-09	3B	3814	3951		FT
14-19-55-09	3B	1194	1234		M
10-23-55-09	3B	3753	3904		FT
10-32-55-09	3B	3774	3920		FT
10-36-55-09	3B	1102	1148		M
10-08-55-10	3B	4110	4246		FT
06-21-55-10	3B	1281	1322		M
06-26-55-10	3B	4094	4227		FT
07-30-55-10	3B	4228	4361		FT
07-05-55-11	3B	1292	1330		M
14-06-55-11	3B	1296	1335		M
03-08-55-11	3B	1286	1325		M
10-11-55-11	3B	1269	1310		M
07-13-55-11	3B	4243	4367		FT
11-16-55-11	3B	4146	4274		FT
10-18-55-11	3B	4222	4340		FT
13-21-55-11	3B	1312	1350		M
04-22-55-11	3B	4157	4280		FT
06-22-55-11	3B	4233	4361		FT
10-23-55-11	3B	4085	4218		FT
10-24-55-11	3B	4216	4350		FT
07-25-55-11	3B	4167	4300		FT
10-26-55-11	3B	1267	1308		M
13-27-55-11	3B	1323	1362		M
11-30-55-11	3B	1355	1394		M
09-32-55-11	3B	1409	1452		M
04-34-55-11	3B	1325	1365		M
11-02-55-12	3B	4366	4490		FT
11-04-55-12	3B	4458	4580		FT
06-05-55-12	3B	4513	4634		FT
07-06-55-12*	2B	4520	4660		FT
10-07-55-12	3B	4462	4606		FT
10-08-55-12	3B	4423	4570		FT

06-09-55-12	3B	4424	4576	FT
06-10-55-12	3B	4384	4531	FT
07-12-55-12	3B	1302	1345	M
13-13-55-12	3B	1298	1344	M
11-15-55-12	3B	1320	1367	M
10-17-55-12	3B	4409	4554	FT
10-18-55-12	3B	1347	1390	M
06-20-55-12	3B	4389	4540	FT
10-22-55-12	3B	1338	1381	M
06-23-55-12	3B	1321	1365	M
11-24-55-12	3B	1321	1365	M
08-29-55-12	3B	1341	1382	M
07-30-55-12	3B	4376	4513	FT
08-33-55-12	3B	4370	4508	FT
01-35-55-12*	2B	1338	1384	M
09-36-55-12	3B	1391	1434	M
04-01-55-13	3B	1394	1435	M
07-01-55-13	3B	4538	4674	FT
02-02-55-13	3B	4570	4703	FT
04-02-55-13	3B	4585	4720	FT
11-02-55-13*	2B	1397	1442	M
13-02-55-13	3A	4578	4703	FT
15-02-55-13	3B	1393	1435	M
06-03-55-13*	2A	4564	4700	FT
09-03-55-13	3B	4574	4712	FT
11-03-55-13	3B	4550	4680	FT
08-04-55-13	3B	4582	4714	FT
06-08-55-13	3B	4544	4688	FT
01-09-55-13	3B	4539	4674	FT
01-10-55-13	3B	4564	4710	FT
11-10-55-13	3B	4544	4687	FT
12-11-55-13	3B	4536	4680	FT
07-12-55-13	3B	4501	4649	FT
06-13-55-13	3B	4458	4593	FT
12-15-55-13	3B	4489	4617	FT
10-16-55-13	3B	4474	4601	FT
11-20-55-13	3B	4417	4547	FT
10-21-55-13	3B	4449	4580	FT
06-23-55-13	3A	4435	4580	FT
06-24-55-13	3B			
08-26-55-13	3B	1365	1410	M
07-27-55-13	3B	1379	1422	M
12-29-55-13	3B	4415	4550	FT
12-33-55-13	3B	4512	4640	FT
08-34-55-13	3B	1375	1415	M
11-36-55-13	3A	4417	4552	FT
06-05-55-14	3A	4730	4860	FT
06-06-55-14	1A	4925	5033	FT
10-08-55-14*	1A	4870	4976	FT
02-09-55-14*	2A	4859	4984	FT
06-09-55-14*	2A	1475	1511	M
01-10-55-14	3B	1450	1494	M

13-14-55-14	3A	1432	1469		M
11-15-55-14	3A	1446	1487	1478 - 1496	M
10-16-55-14*	2B	1450	1493		M
16-17-55-14*	2A	1466	1506		M
11-19-55-14	3A	4944	5056		FT
15-19-55-14	3A	1491	1524		M
16-19-55-14	3A	1491	1524		M
10-21-55-14	3A	1475	1513		M
13-24-55-14	3B	1445	1482		M
05-26-55-14	3B	1457	1497		M
06-27-55-14	3B	1470	1510		M
16-30-55-14	3A	1486	1523		M
06-16-56-09	3B	3493	3640		FT
06-22-56-09	3B	3390	3540		FT
02-24-56-09	3B	3333	3480		FT
10-24-56-09	3B	3308	3452		FT
02-25-56-09	3B	3282	3435		FT
10-25-56-09	3B	3270	3416		FT
06-28-56-09	3B	1025	1070		M
11-29-56-09	3B	3466	3612		FT
13-31-56-09	3B	1056	1101		M
10-35-56-09	3B	3314	3460		FT
02-36-56-09	3B	3247	3393		FT
06-07-56-10	3B	3919	4051		FT
06-15-56-10	3B	3764	3910		FT
10-18-56-10	3B	3885	4024		FT
08-22-56-10	3B	1114	1157		M
06-29-56-10	3B	3715	3861		FT
06-33-56-10	3B	3639	3781		FT
14-36-56-10	3B	1061	1107		M
07-02-56-11	3B	1294	1335		M
06-03-56-11	3B	1338	1380		M
07-05-56-11	3B	1420	1461		M
07-08-56-11	3B	4543	4678		FT
12-08-56-11	3B	1353	1393		M
11-10-56-11	3B	4360	4495		FT
06-11-56-11	3B	4108	4244		FT
11-12-56-11	3B	3998	4132		FT
06-14-56-11	3B	4040	4174		FT
10-15-56-11	3B	4149	4280		FT
08-19-56-11	3B	1340	1379		M
10-19-56-11	3B	4385	4516		FT
08-20-56-11	3B	1314	1353		M
11-20-56-11	3B	1321	1360		M
11-21-56-11	3B	4167	4300		FT
07-23-56-11	3B	4084	4221		FT
10-29-56-11	3B	4163	4300		FT
06-32-56-11	3B	4150	4298		FT
07-33-56-11	3B	4110	4257		FT
06-03-56-12	3B	4459	4584		FT
07-05-56-12*	2B	4421	4562		FT
11-06-56-12	3B	4430	4550		FT

06-13-56-12	3B	1393	1435	M
06-14-56-12	3B	4477	4628	FT
07-17-56-12	3B	4455	4590	FT
10-29-56-12	3B	4340	4468	FT
04-32-56-12	3B	1293	1332	FT
10-36-56-12	3B	4235	4364	FT
10-04-56-13	3B	4380	4516	FT
02-06-56-13	3B	4370	4499	FT
10-06-56-13*	2B	4311	4455	FT
14-06-56-13	3B	1308	1348	M
02-07-56-13	3B	4350	4477	FT
06-12-56-13	3B	1327	1368	M
10-16-56-13	3B	4287	4410	FT
12-26-56-13	3A	4140	4267	FT
11-32-56-13	3B	4319	4439	FT
11-33-56-13	3B	4178	4300	FT
06-03-56-14	3B	4663	4788	FT
02-05-56-14	3B	1522	1559	M
10-08-56-14	3B	5037	5156	FT
04-13-56-14	3B	4511	4640	FT
02-15-56-14	3B	4561	4684	FT
07-15-56-14	3B	1386	1423	M
16-16-56-14	3B	4558	4687	FT
02-19-56-14	3B	4572	4690	FT
06-23-56-14	3B	4498	4630	FT
16-23-56-14	3B	4520	4650	FT
11-24-56-14	3B	4419	4548	FT
07-34-56-14	3B	4460	4597	FT

APPENDIX 2 -- FACIES SEQUENCES

2.1 General Facies Sequence

The facies sequences preserved in the Carrot Creek -- Cyn-Pem study were subdivided into 3 main types (Chapter 3). Type 1 facies sequences are composed of non-bioturbated sandstone (facies 7 and 7A), Type 2 facies sequences were composed of thick (> 1 m) conglomerate (facies 8), and Type 3 facies sequences were composed of bioturbated mudstones (facies 1 through 5). These sequence were further sub-divided with respect to the depth of erosion on the E5 surface (Chapter 3). In Type 1A sequences there are two sand (facies 7 and 7A) sequences developed separated by bioturbated sandstone (facies 5). In Type 1B sequences the upper sand is removed and E5 rests on the lower sand development. The A and B designation in Types 2 and 3 sequences refers to the "a" and "b" sequences described in Chapter 3. In other words, in Type A sequences the E5 rests in the upper "a" sequence, while in Type B sequences the E5 surface removes the "a" sequence and rests in the lower "b" sequence.

The purpose of this appendix is to illustrate these facies sequence types with examples. For each sequence type six wells were selected and the lithologs are shown below with their corresponding well log. The wells shown were chosen for two reasons:

A. they do not appear anywhere else in the thesis,

B. the cored interval contains the distinguishing criteria of the facies sequence scheme.

Other examples of these facies sequence types may be found on the cross sections shown in Chapter 4. The size of the data base precludes illustrating all of the core examined. All of the lithologs and well logs examined for the study area are stored with Dr. R.G. Walker, Geology Department, McMaster University.

The litholog scales are all in metres. Facies number designation is shown on the right hand side, as well as the position of the E5/T5 surface, the "a" and "b" sequences, and the core depths. The "+" symbol at the top and bottom of some cores indicates that the core continues in this facies for another x m.

The well logs used are generally resistivity logs. Where these were not available, other logs, usually gamma ray, and sometimes sonic logs were subsituted. The positions of the E/T surfaces and the gritty siderite are shown as well as the positions of the "a" and "b" sequences. The cored interval is shown as a solid black bar with the core depths indicated above and below the black bar.

2.2 Conglomerate Facies Sequences

The detailed conglomerate facies sequences are shown in type wells in Chapter 6 and on the cross sections through the gravel pools in Chapter 7. The remaining detail lithologs of the conglomerate sequences are stored with Dr. R.G. Walker, Geology Department, McMaster University.

FACIES SEQUENCE TYPE 1A

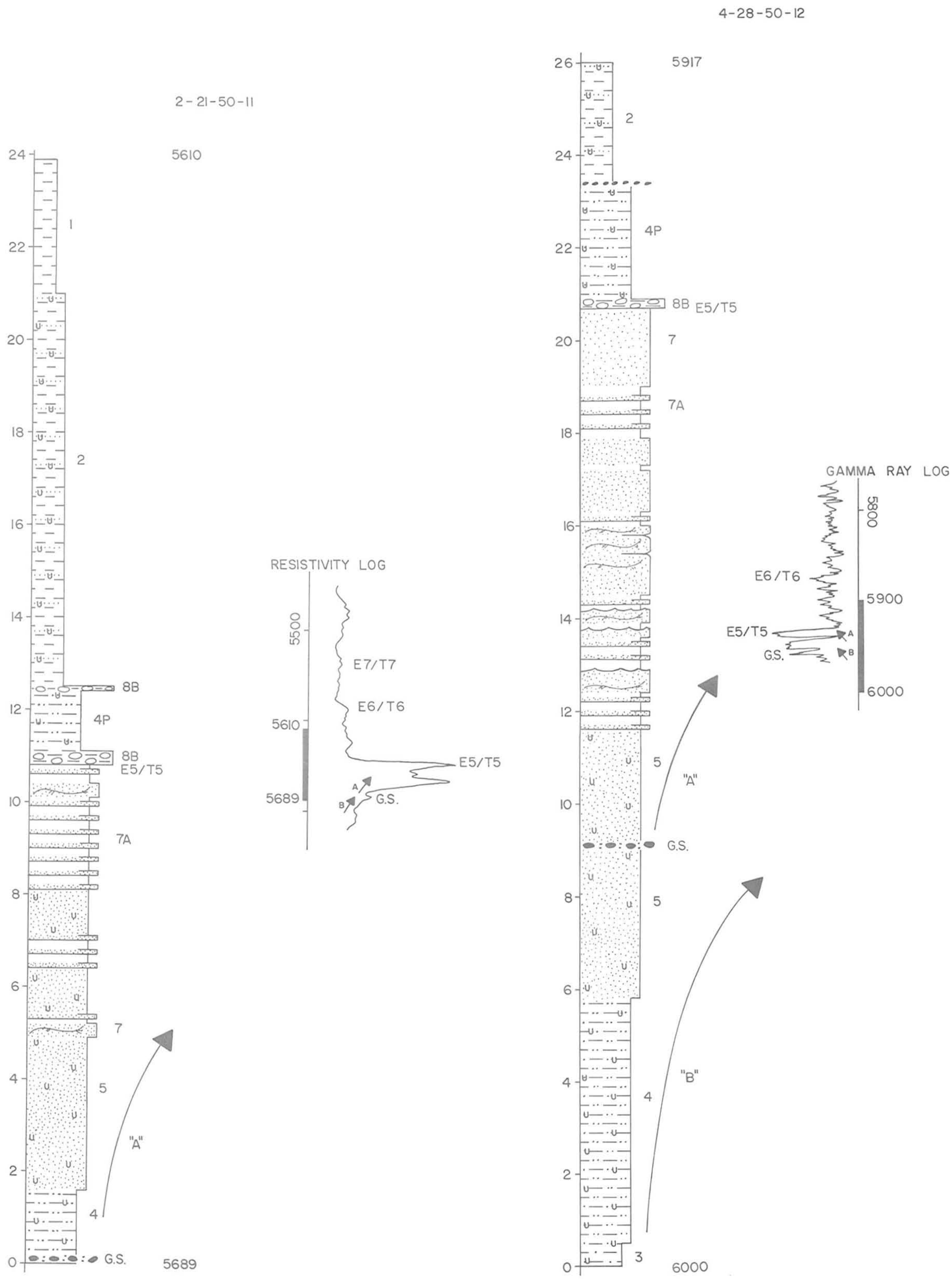
2-21-50-11
5610
5689
1
2
4P
8B
8B
E5/T5
7A
7
5
4
"A"
G.S.
RESISTIVITY LOG
5500
5610
5689
E7/T7
E6/T6
E5/T5
A
B
G.S.
4-28-50-12
5917
6000
2
4P
8B
E5/T5
7
7A
5
"A"
G.S.
5
4
"B"
3
GAMMA RAY LOG
5800
5900
6000
E6/T6
E5/T5
A
B
G.S.

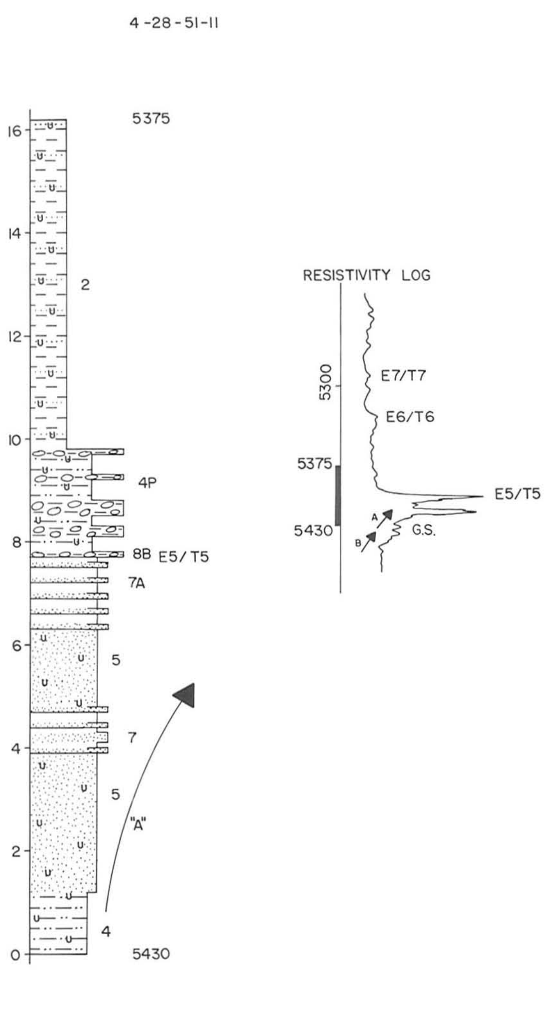
4-28-51-11
5375
5430
2
4P
8B E5/T5
7A
5
7
5
"A"
4
RESISTIVITY LOG
5300
5375
5430
E7/T7
E6/T6
E5/T5
A
B
G.S.

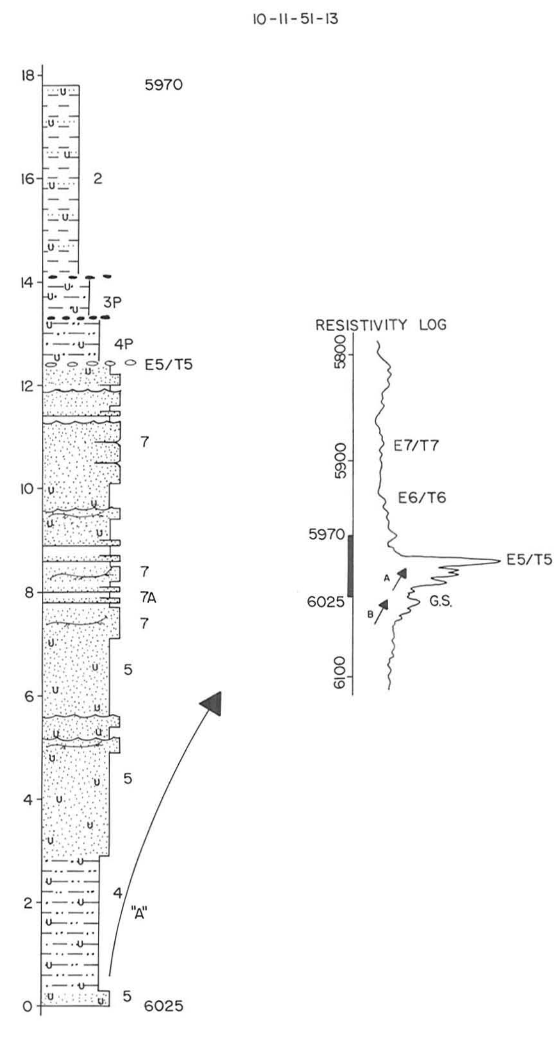
10-11-51-13
5970
6025
2
3P
4P
E5/T5
7
7
7A
7
5
5
4
"A"
5
RESISTIVITY LOG
5800
5900
5970
6025
6100
E7/T7
E6/T6
E5/T5
A
B
G.S.

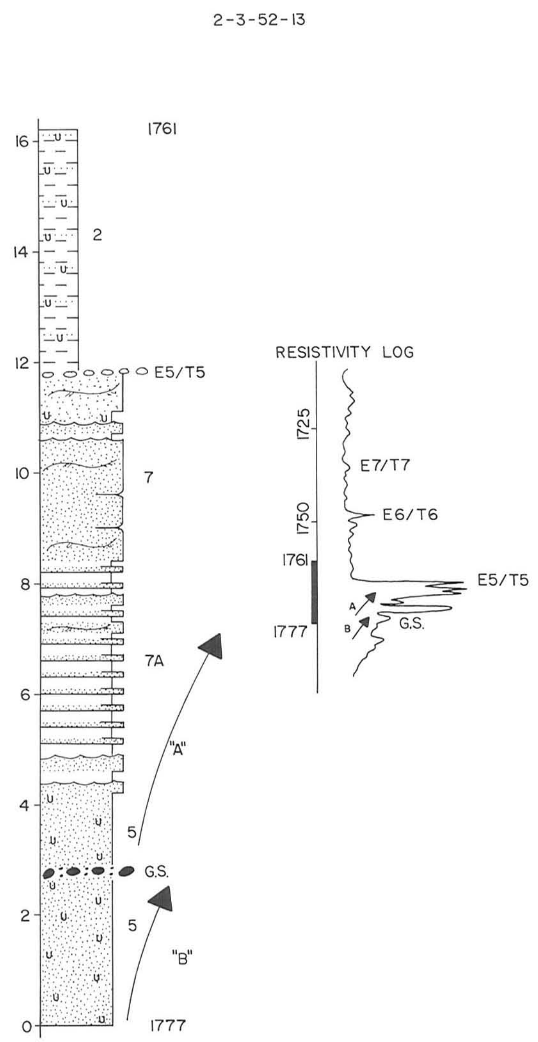
2-3-52-13
1761
2
E5/T5
7
7A
"A"
5
G.S.
5
"B"
1777
RESISTIVITY LOG
1725
E7/T7
1750
E6/T6
1761
E5/T5
A
B
G.S.
1777

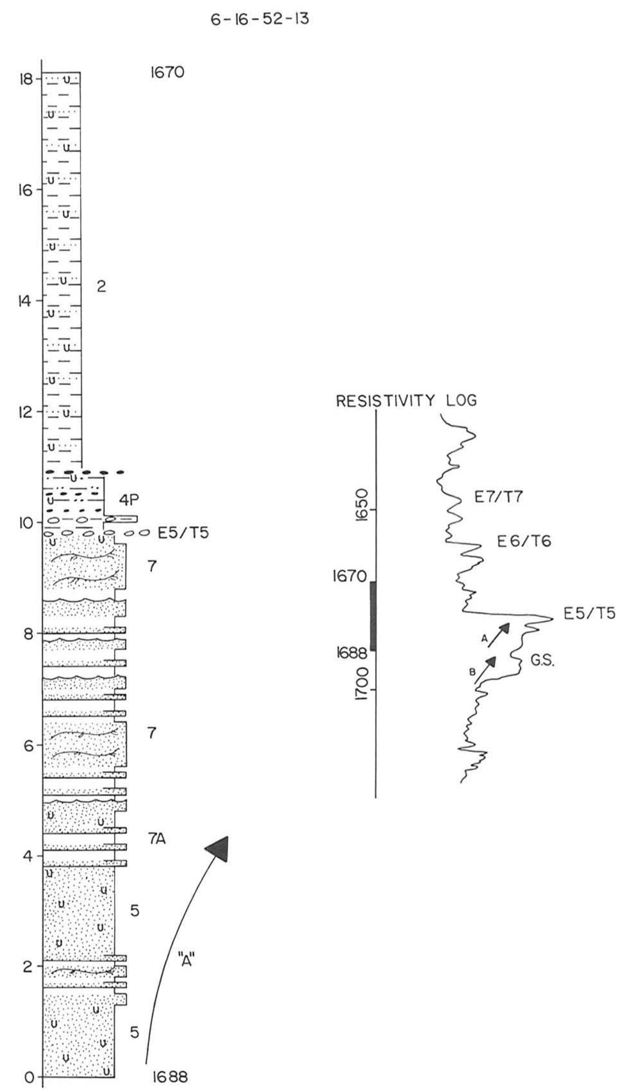
6-16-52-13
1670
2
4P
E5/T5
7
7
7A
5
"A"
5
1688
RESISTIVITY LOG
1650
E7/T7
E6/T6
1670
E5/T5
A
1688
B
G.S.
1700

FACIES SEQUENCE TYPE 1B

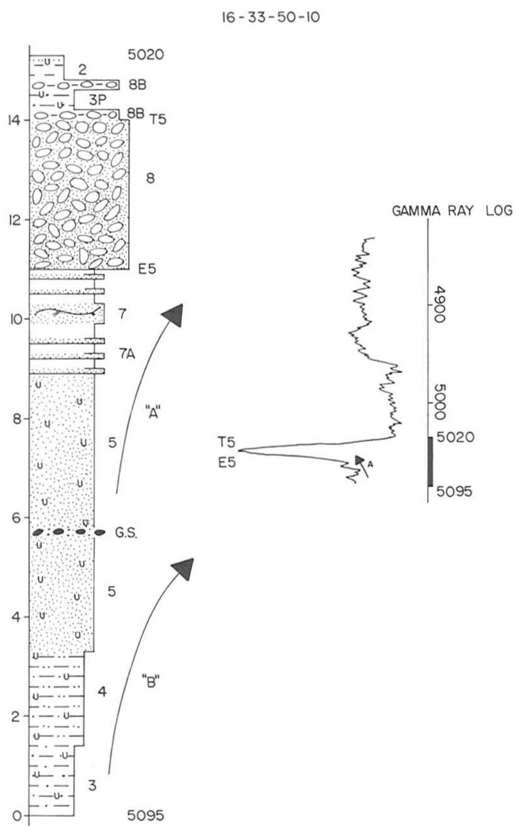
16-33-50-10
5020
2
8B
3P
8B
T5
8
E5
7
7A
"A"
5
G.S.
5
"B"
4
3
5095
0
2
4
6
8
10
12
14
GAMMA RAY LOG
4900
5000
5020
5095
T5
E5
A

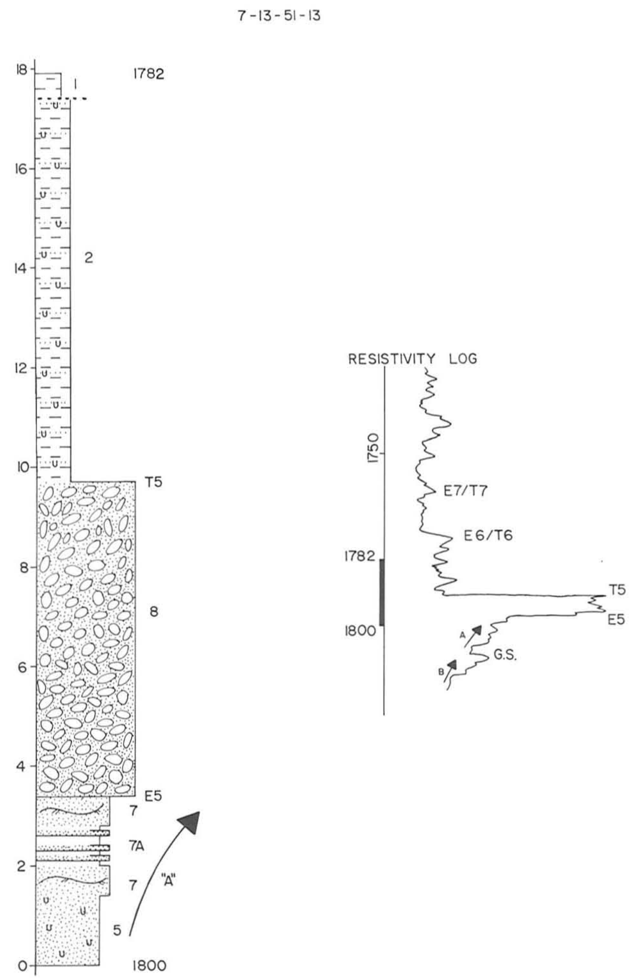
7-13-51-13
1782
1
2
T5
8
E5
7
7A
7
"A"
5
1800
0
2
4
6
8
10
12
14
16
18
RESISTIVITY LOG
1750
E7/T7
E6/T6
1782
1800
T5
E5
A
B
G.S.

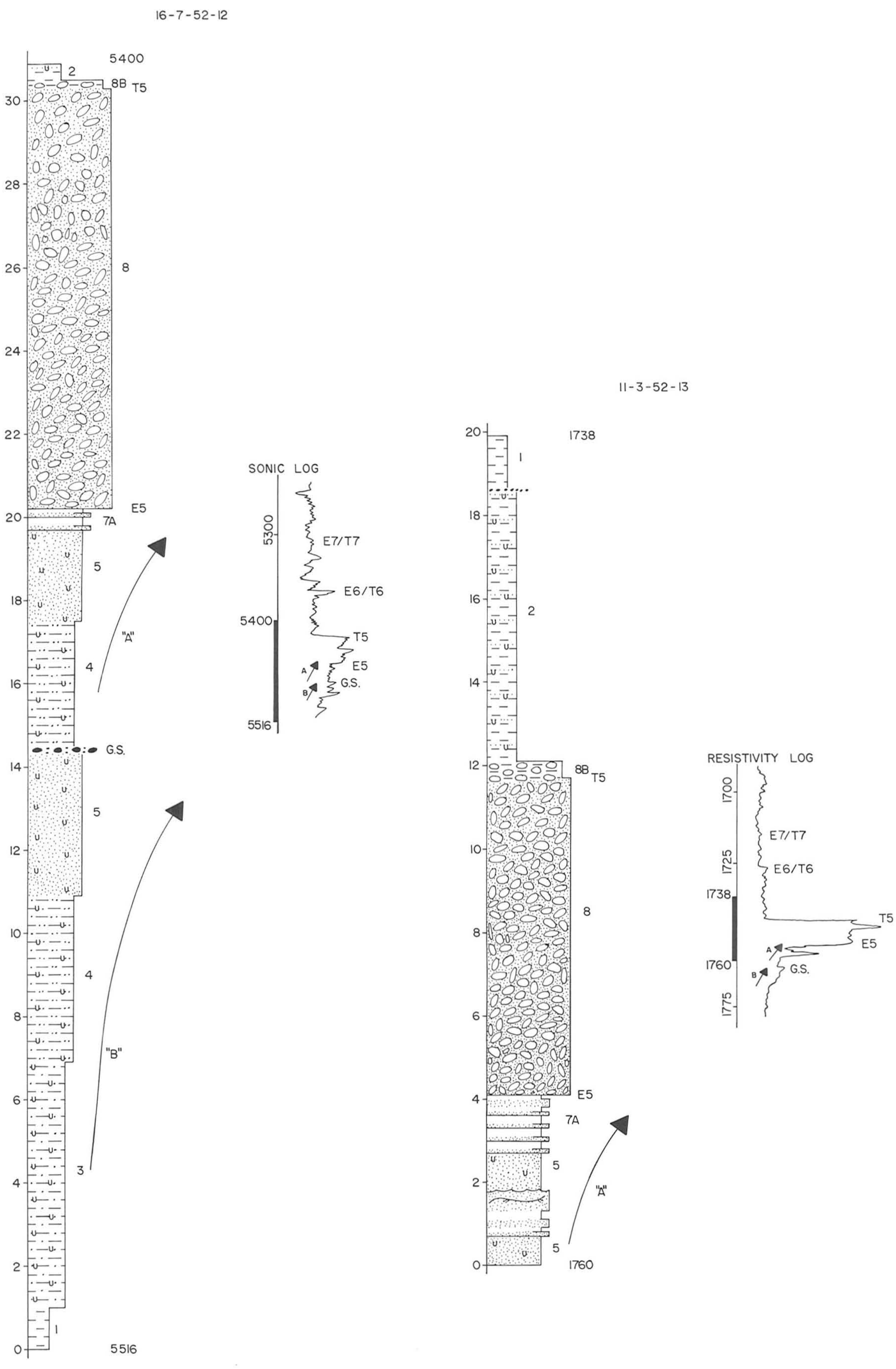
16-7-52-12
5400
2
8B
T5
8
E5
7A
5
"A"
4
G.S.
5
4
"B"
3
1
5516
0
2
4
6
8
10
12
14
16
18
20
22
24
26
28
30
SONIC LOG
5300
E7/T7
E6/T6
5400
T5
E5
A
B
G.S.
5516
11-3-52-13
1738
1
2
8B
T5
8
E5
7A
5
"A"
5
1760
RESISTIVITY LOG
1700
E7/T7
1725
E6/T6
1738
T5
E5
A
1760
B
G.S.
1775

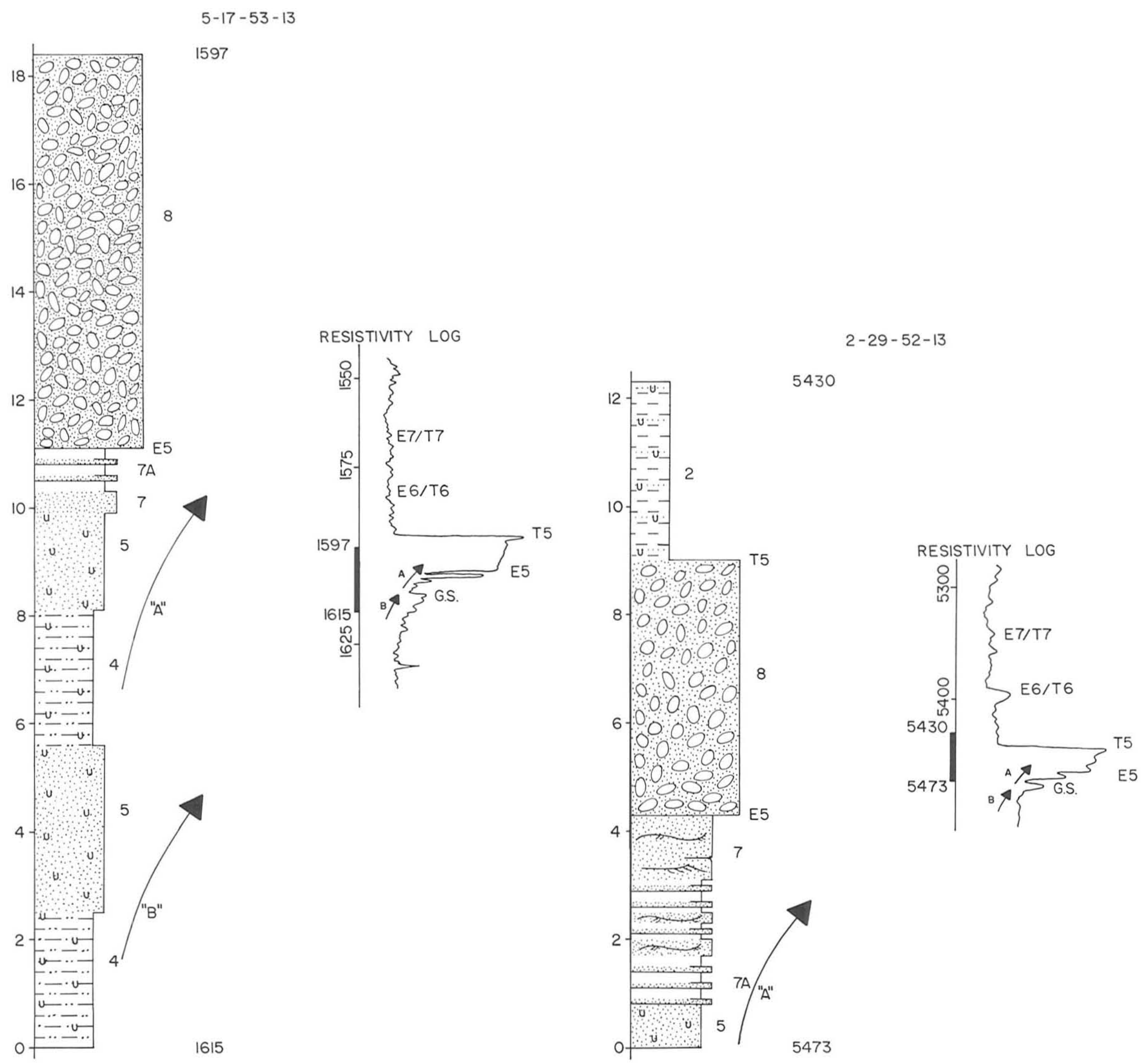

5-17-53-13
1597
1615
8
E5
7A
7
5
4
"A"
"B"
RESISTIVITY LOG
1550
1575
1597
1615
1625
E7/T7
E6/T6
T5
E5
G.S.
A
B
2-29-52-13
5430
5473
2
T5
E5
7A
"A"
RESISTIVITY LOG
5300
5400
5430
5473
E7/T7
E6/T6

FACIES SEQUENCE TYPE 2A

6-4-51-10

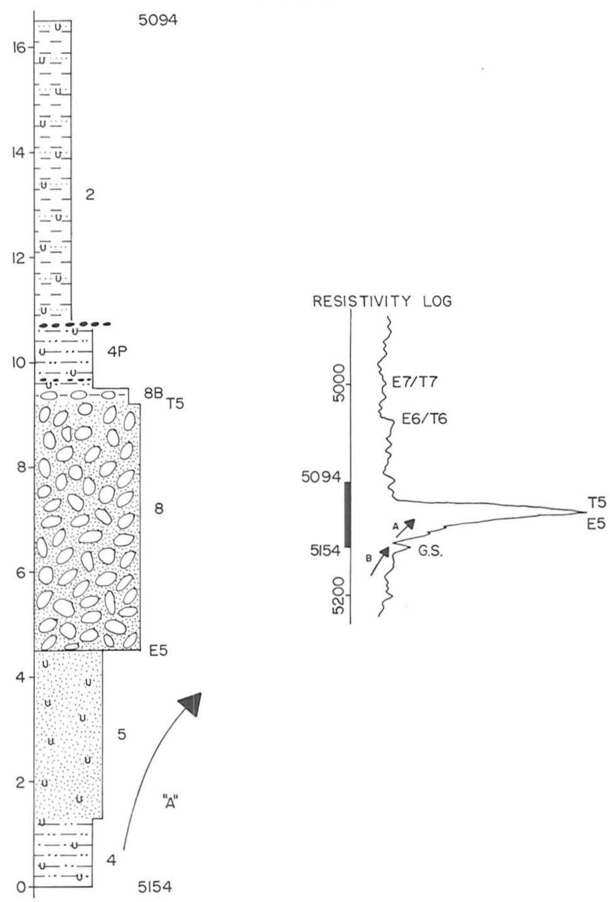

2-15-51-11

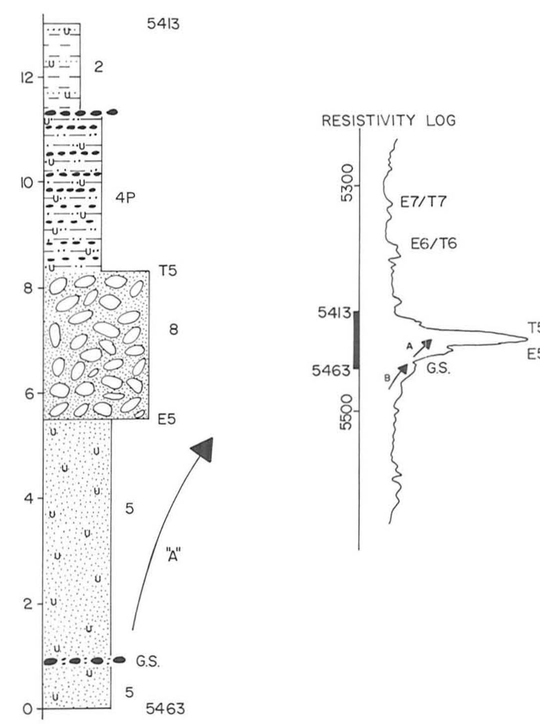

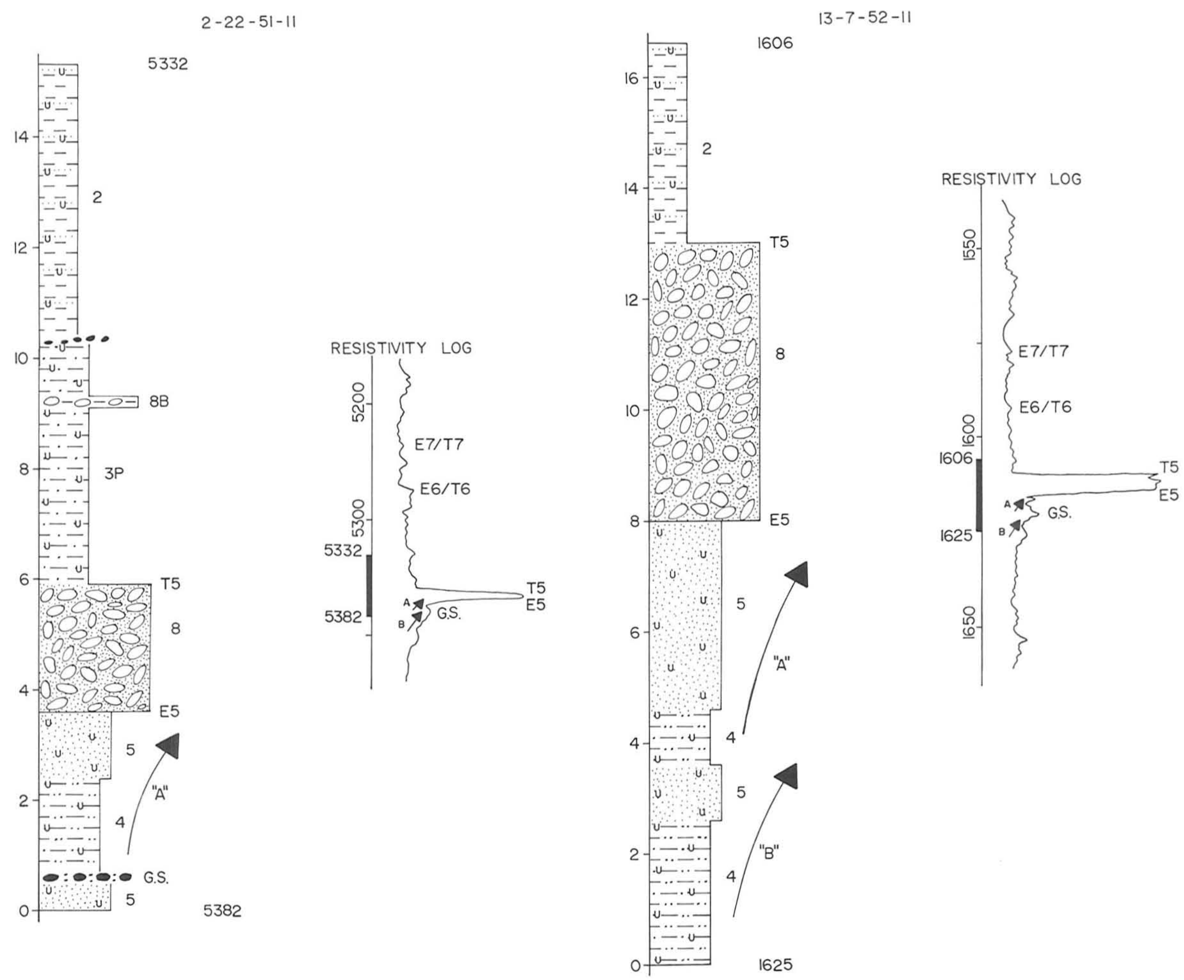
2-22-51-11
5332
5382
2
8B
3P
T5
8
E5
5
"A"
4
G.S.
RESISTIVITY LOG
5200
5300
5332
5382
E7/T7
E6/T6
T5
E5
A
B
13-7-52-11
1606
1625
"B"
RESISTIVITY LOG
1550
1600
1606
1625
1650

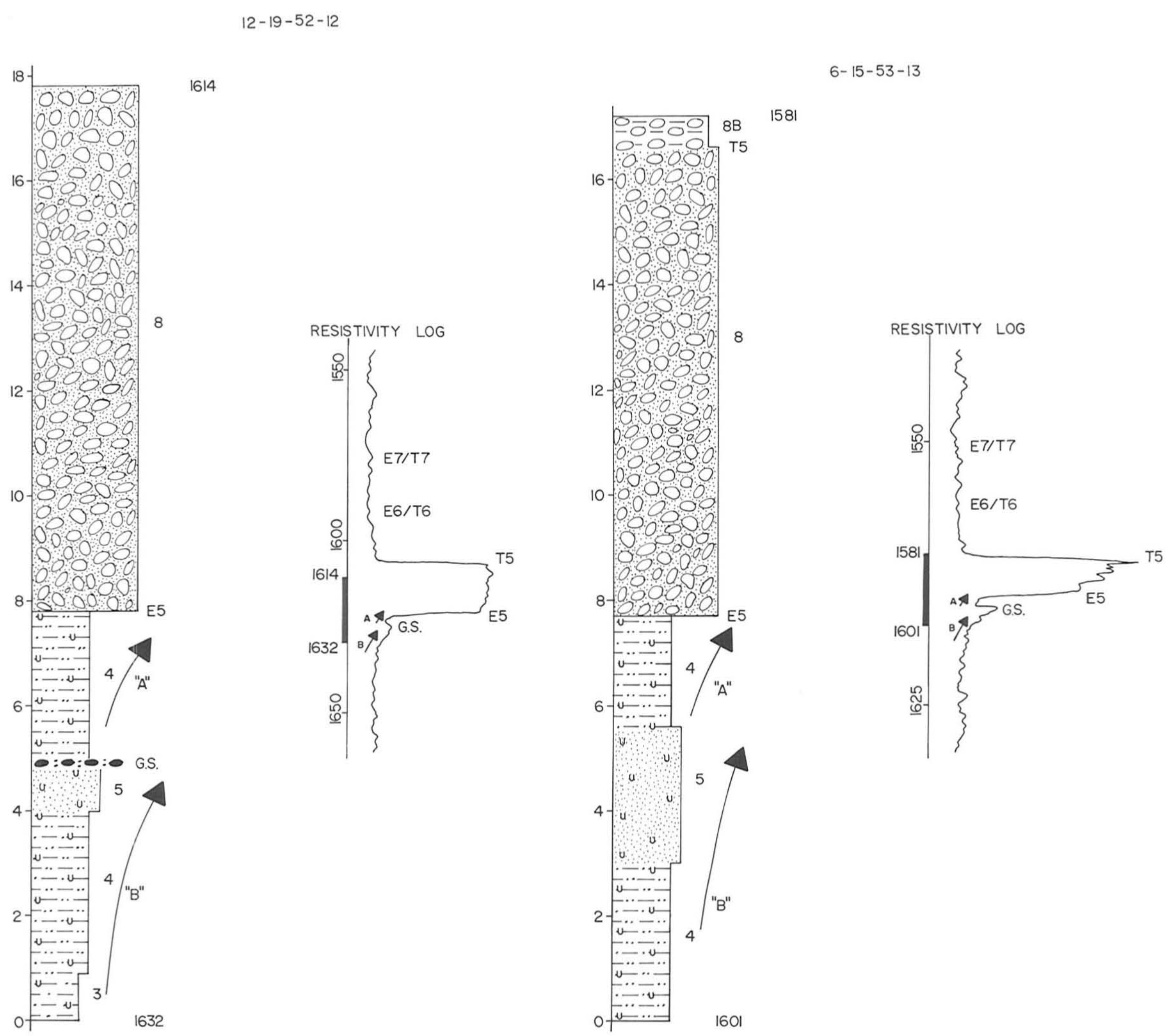

12-19-52-12
1614
8
E5
4
"A"
G.S.
5
4
"B"
3
1632
RESISTIVITY LOG
1550
E7/T7
E6/T6
1600
T5
1614
E5
G.S.
1632
1650
6-15-53-13
8B
1581
T5
8
E5
4
"A"
5
"B"
4
1601
RESISTIVITY LOG
1550
E7/T7
E6/T6
1581
T5
E5
G.S.
1601
1625

FACIES SEQUENCE TYPE 2B

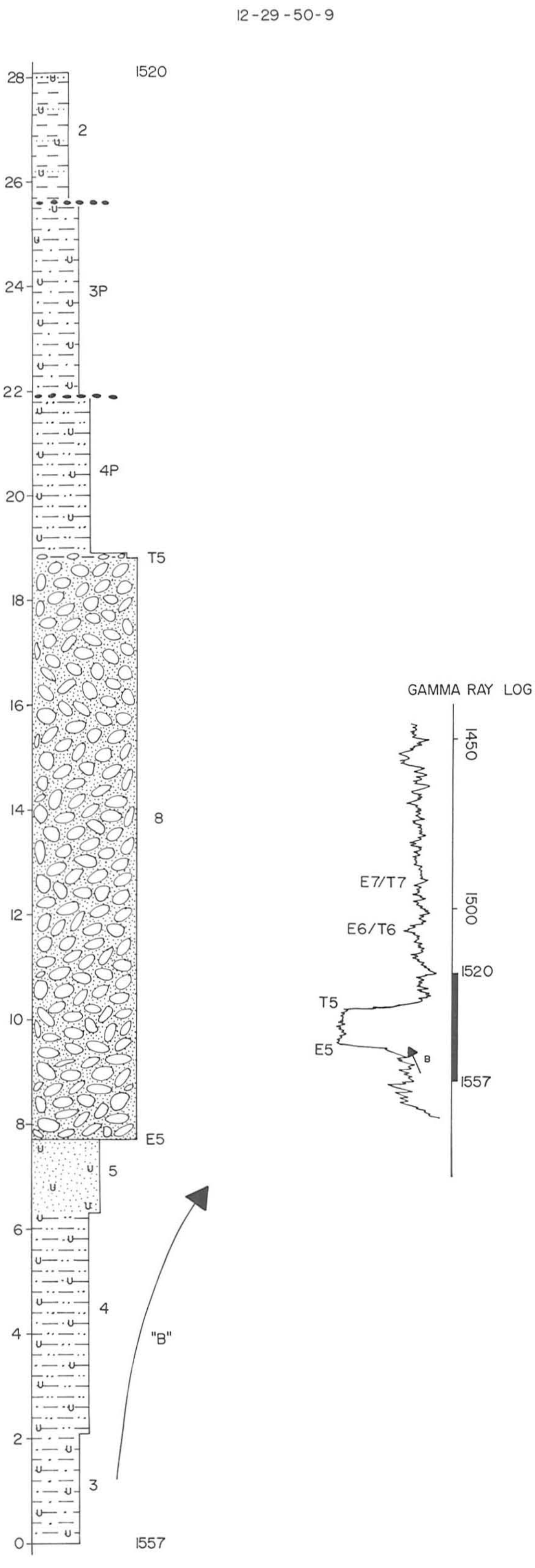

12-29-50-9
1520
2
3P
4P
T5
8
E5
5
4
"B"
3
1557
GAMMA RAY LOG
1450
E7/T7
1500
E6/T6
1520
T5
E5
B
1557

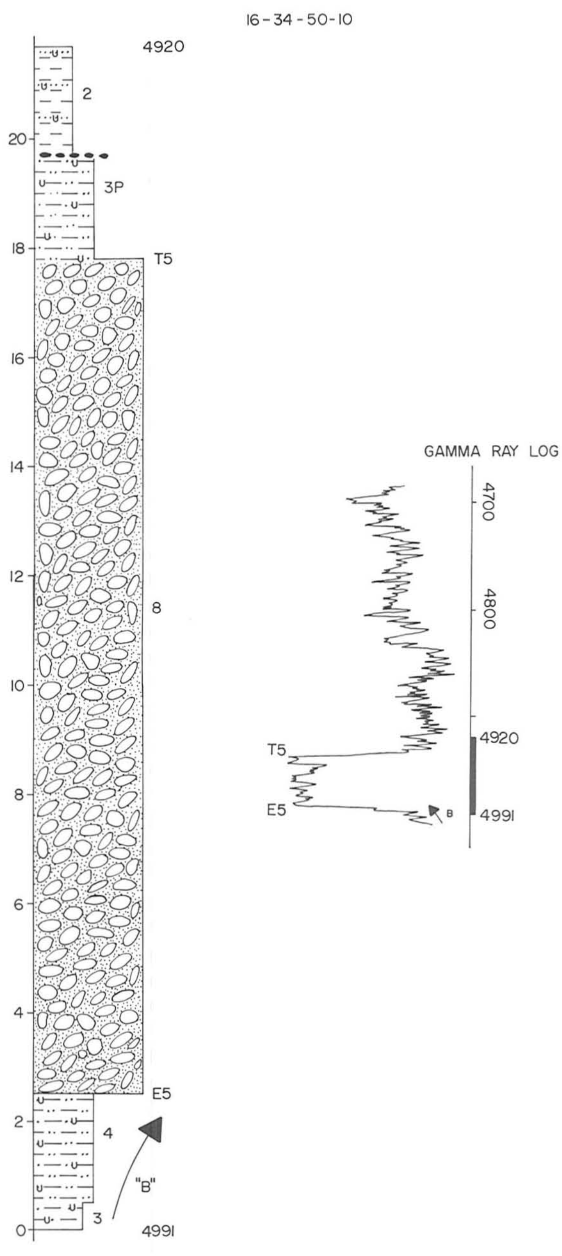

16-34-50-10
4920
2
3P
T5
8
E5
4
"B"
3
4991
GAMMA RAY LOG
4700
4800
4920
T5
E5
B
4991

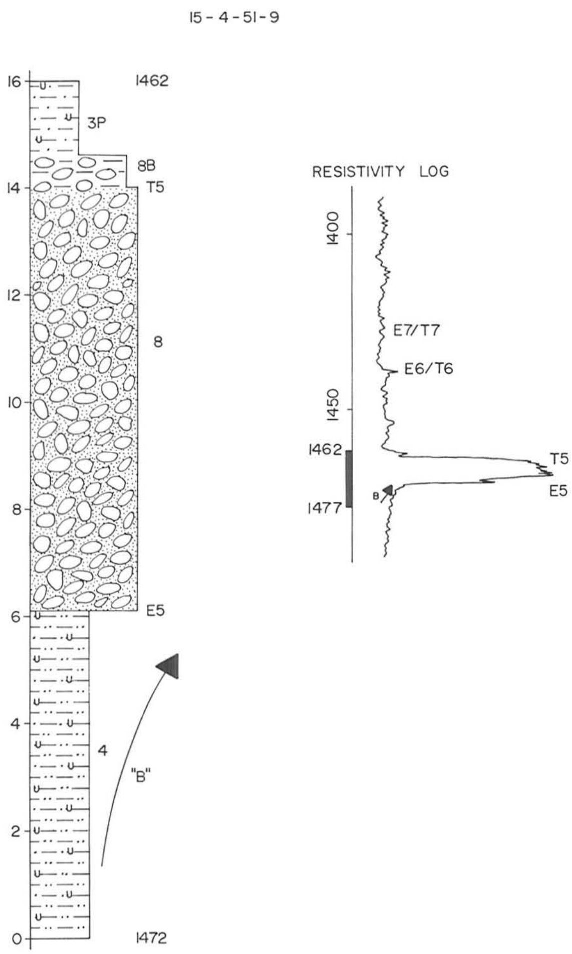
15 - 4 - 51 - 9
1462
3P
8B
T5
8
E5
4
"B"
1472
RESISTIVITY LOG
1400
E7/T7
E6/T6
1450
1462
T5
B
E5
1477
16
14
12
10
8
6
4
2
0

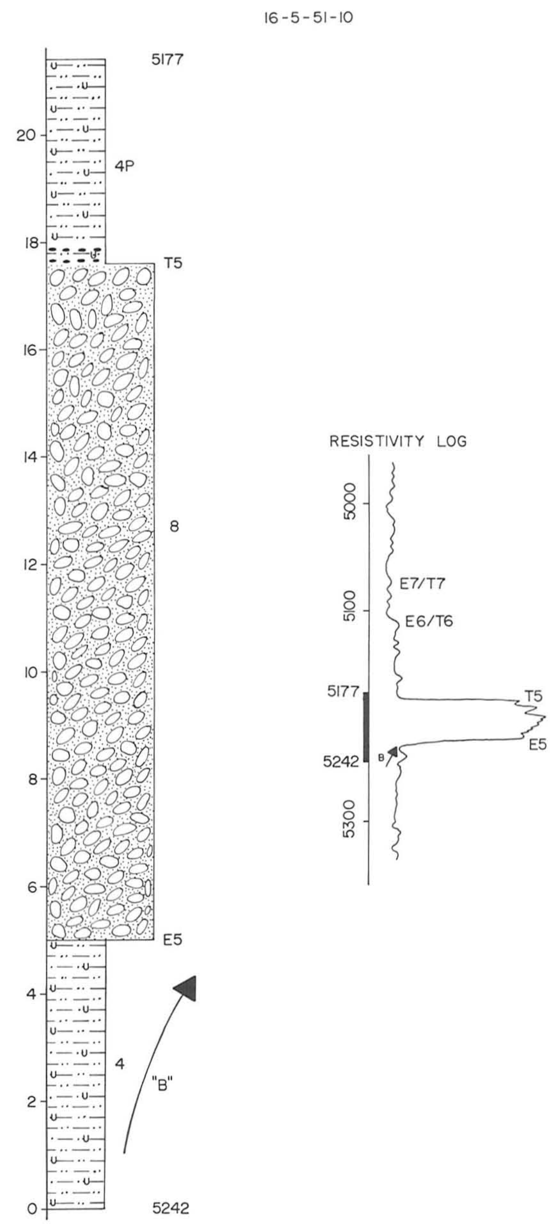
16 - 5 - 51 - 10
5177
4P
T5
8
E5
4
"B"
5242
RESISTIVITY LOG
5000
E7/T7
5100
E6/T6
5177
T5
B
E5
5242
5300
20
18
16
14
12
10
8
6
4
2
0

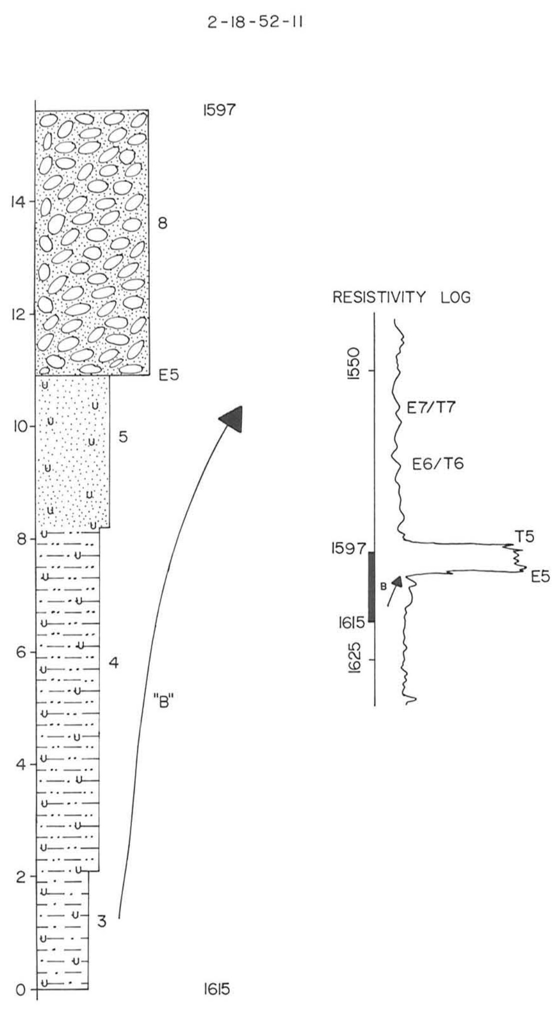
2-18-52-11
1597
1615
14
12
10
8
6
4
2
0
8
E5
5
4
3
"B"
RESISTIVITY LOG
1550
E7/T7
E6/T6
1597
T5
E5
B
1615
1625

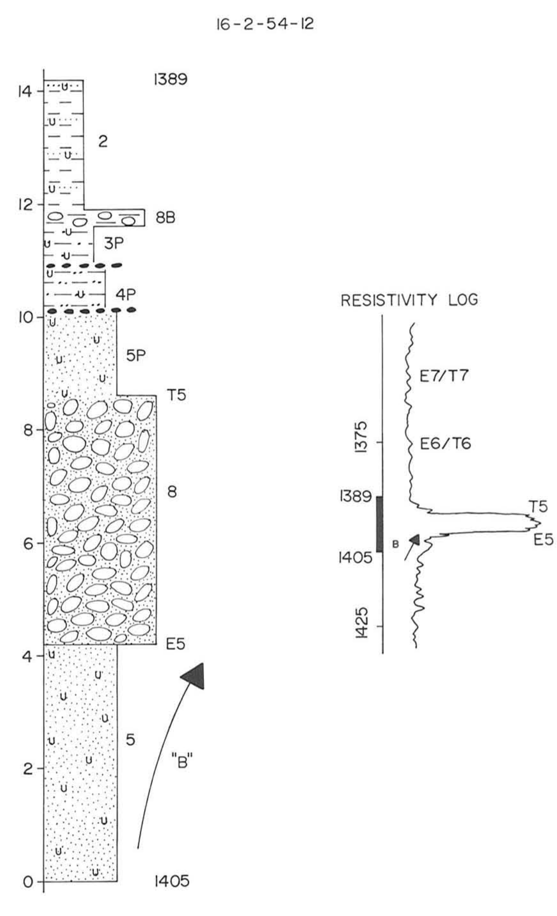
16-2-54-12
1389
1405
14
12
10
8
6
4
2
0
2
8B
3P
4P
5P
T5
8
E5
5
"B"
RESISTIVITY LOG
E7/T7
1375
E6/T6
1389
T5
E5
B
1405
1425

FACIES SEQUENCE TYPE 3A

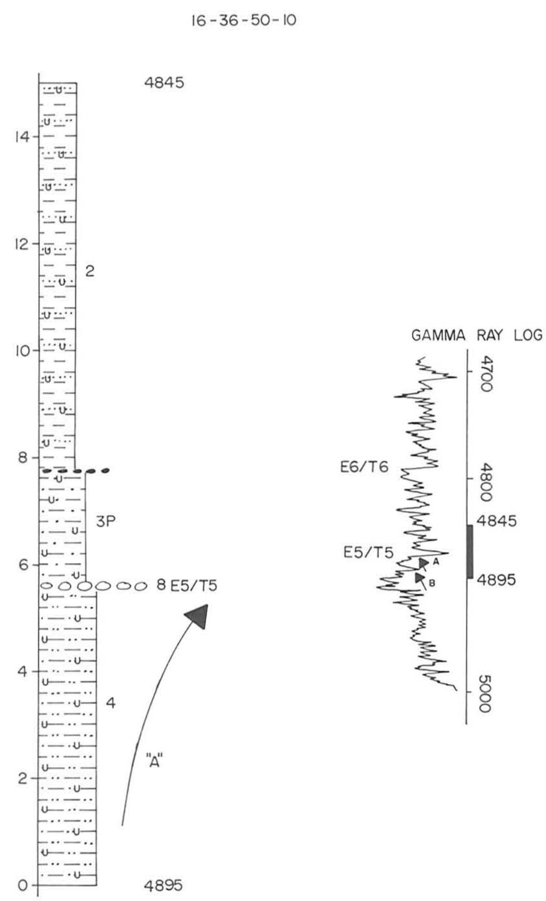
16-36-50-10
4845
4895
2
3P
8 E5/T5
4
"A"
GAMMA RAY LOG
4700
4800
4845
4895
5000
E6/T6
E5/T5
A
B

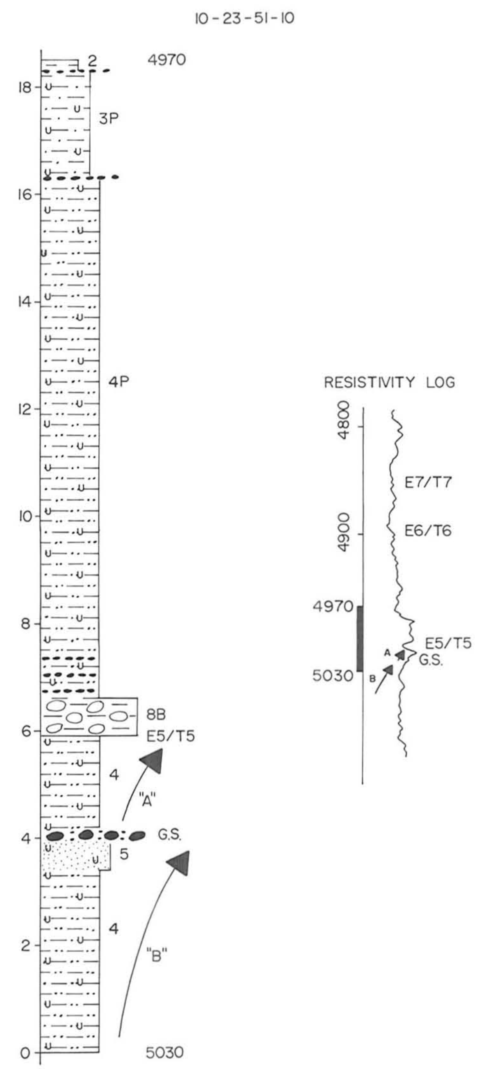
10-23-51-10
4970
5030
2
3P
4P
8B
E5/T5
4
"A"
G.S.
5
4
"B"
RESISTIVITY LOG
4800
4900
4970
5030
E7/T7
E6/T6
E5/T5
G.S.
A
B

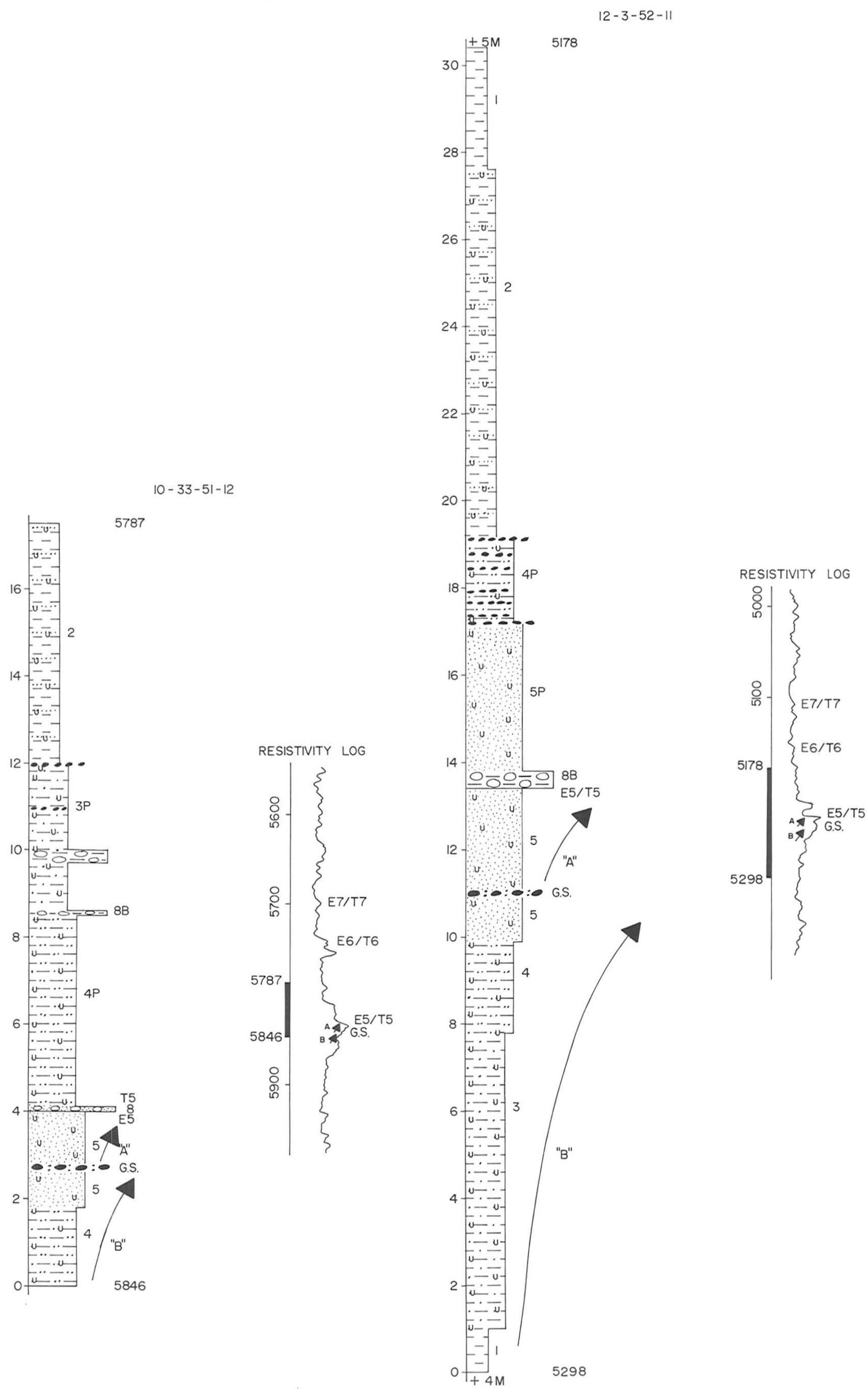

12-3-52-11
+5M
5178
4P
5P
8B
E5/T5
"A"
G.S.
"B"
+4M
5298
RESISTIVITY LOG
5000
5100
E7/T7
E6/T6
5178
E5/T5
G.S.
5298
10-33-51-12
5787
3P
8B
4P
T5
8
E5
"A"
G.S.
"B"
5846
RESISTIVITY LOG
5600
5700
E7/T7
E6/T6
5787
E5/T5
G.S.
5846
5900

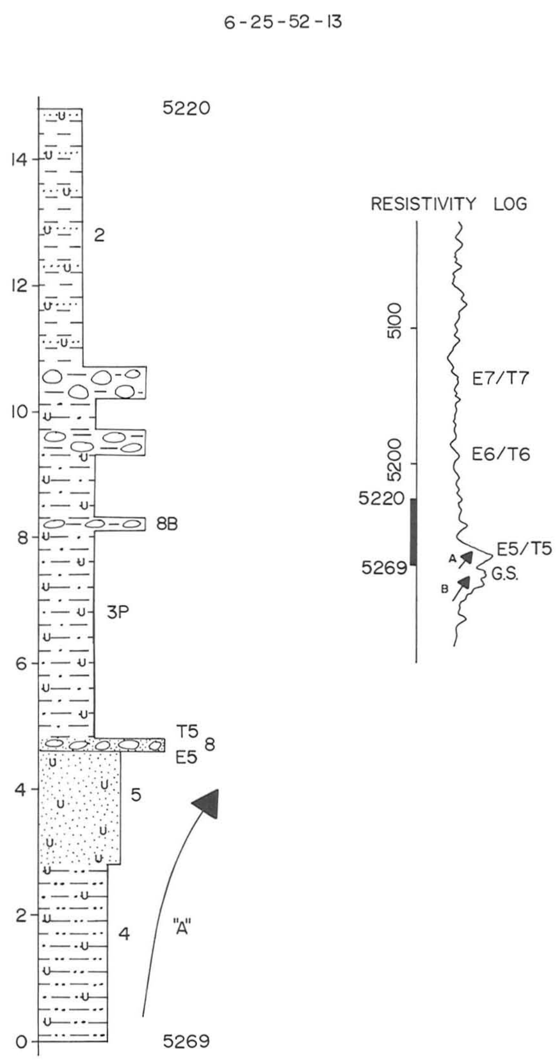
6-25-52-13
5220
5269
2
8B
3P
T5
8
E5
5
4
"A"
RESISTIVITY LOG
5100
5200
5220
5269
E7/T7
E6/T6
E5/T5
A
B
G.S.

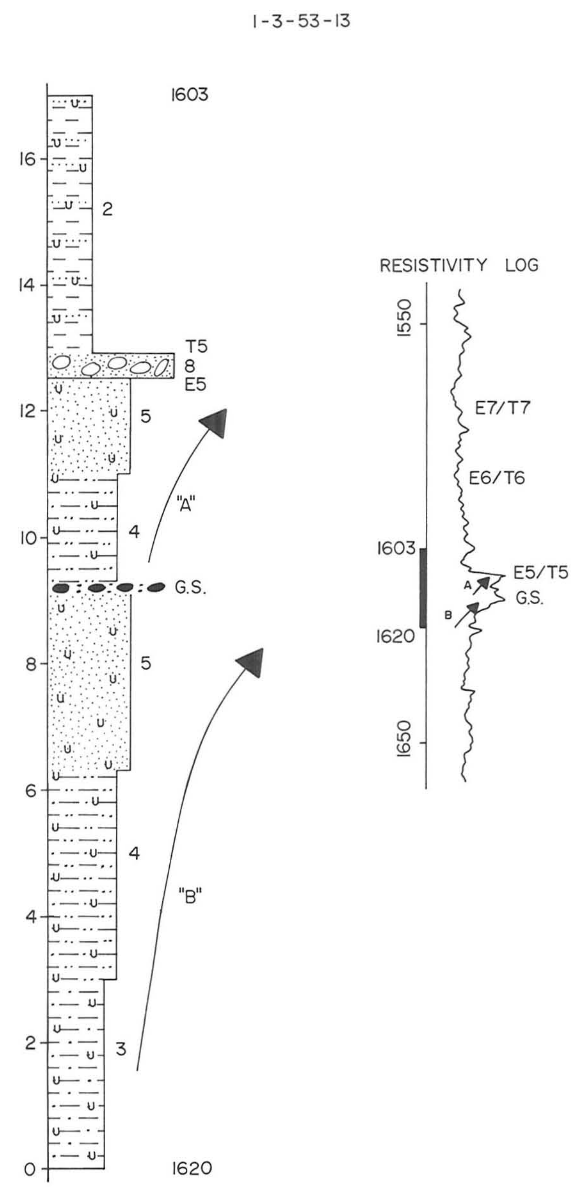
1-3-53-13
1603
1620
2
T5
8
E5
5
4
G.S.
5
4
3
"A"
"B"
RESISTIVITY LOG
1550
1603
1620
1650
E7/T7
E6/T6
E5/T5
A
B
G.S.

FACIES SEQUENCE TYPE 3B

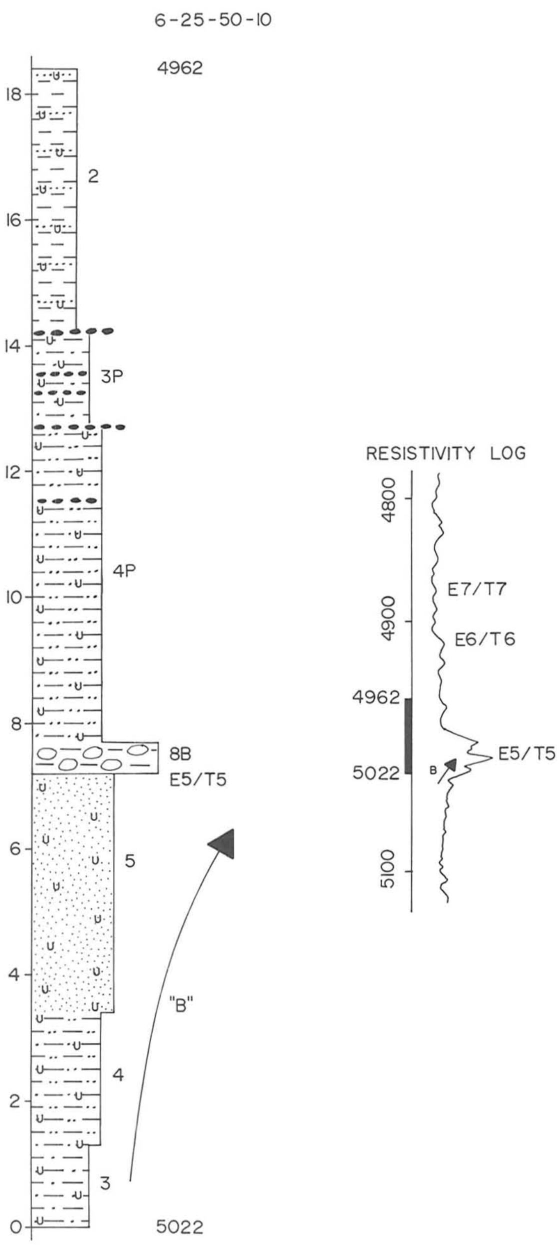
6-25-50-10
4962
5022
2
3P
4P
8B
E5/T5
5
4
3
"B"
RESISTIVITY LOG
4800
4900
4962
5022
5100
E7/T7
E6/T6
E5/T5
B

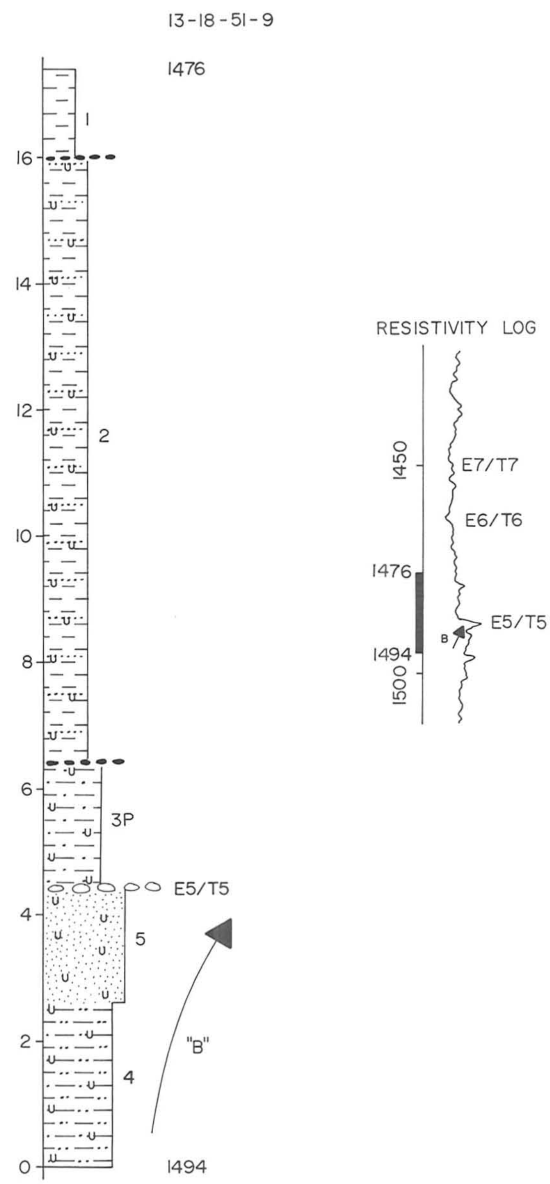
13-18-51-9
1476
1494
1
2
3P
E5/T5
5
4
"B"
RESISTIVITY LOG
1450
1476
1494
1500
E7/T7
E6/T6
E5/T5
B

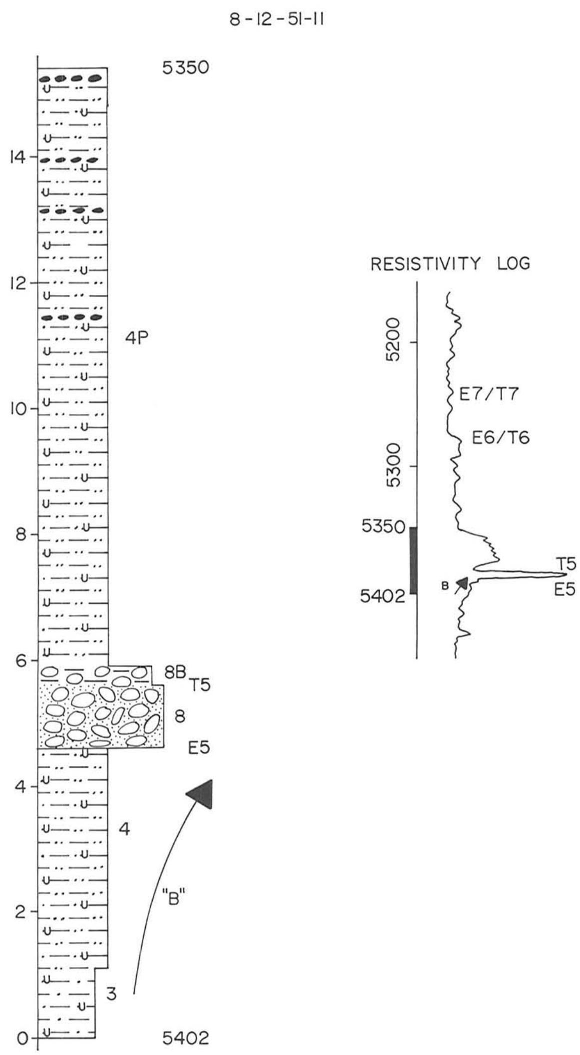
8-12-51-11
5350
5402
14
12
10
8
6
4
2
0
4P
8B
T5
8
E5
4
3
"B"
RESISTIVITY LOG
5200
5300
5350
5402
E7/T7
E6/T6
T5
E5
B

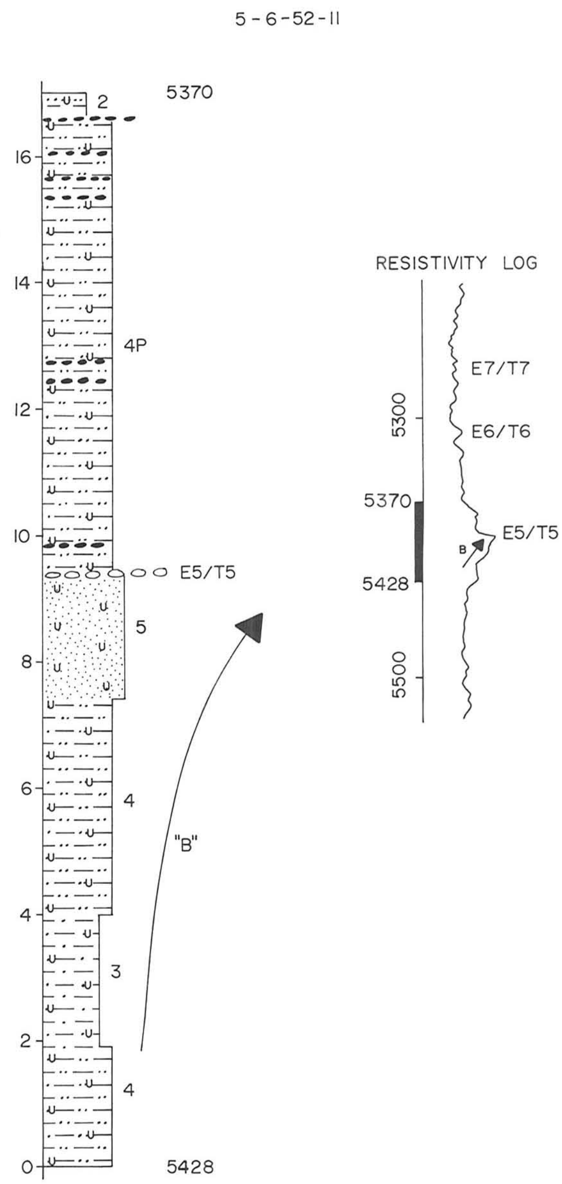
5-6-52-11
5370
5428
16
14
12
10
8
6
4
2
0
2
4P
E5/T5
5
4
3
4
"B"
RESISTIVITY LOG
5300
5370
5428
5500
E7/T7
E6/T6
E5/T5
B

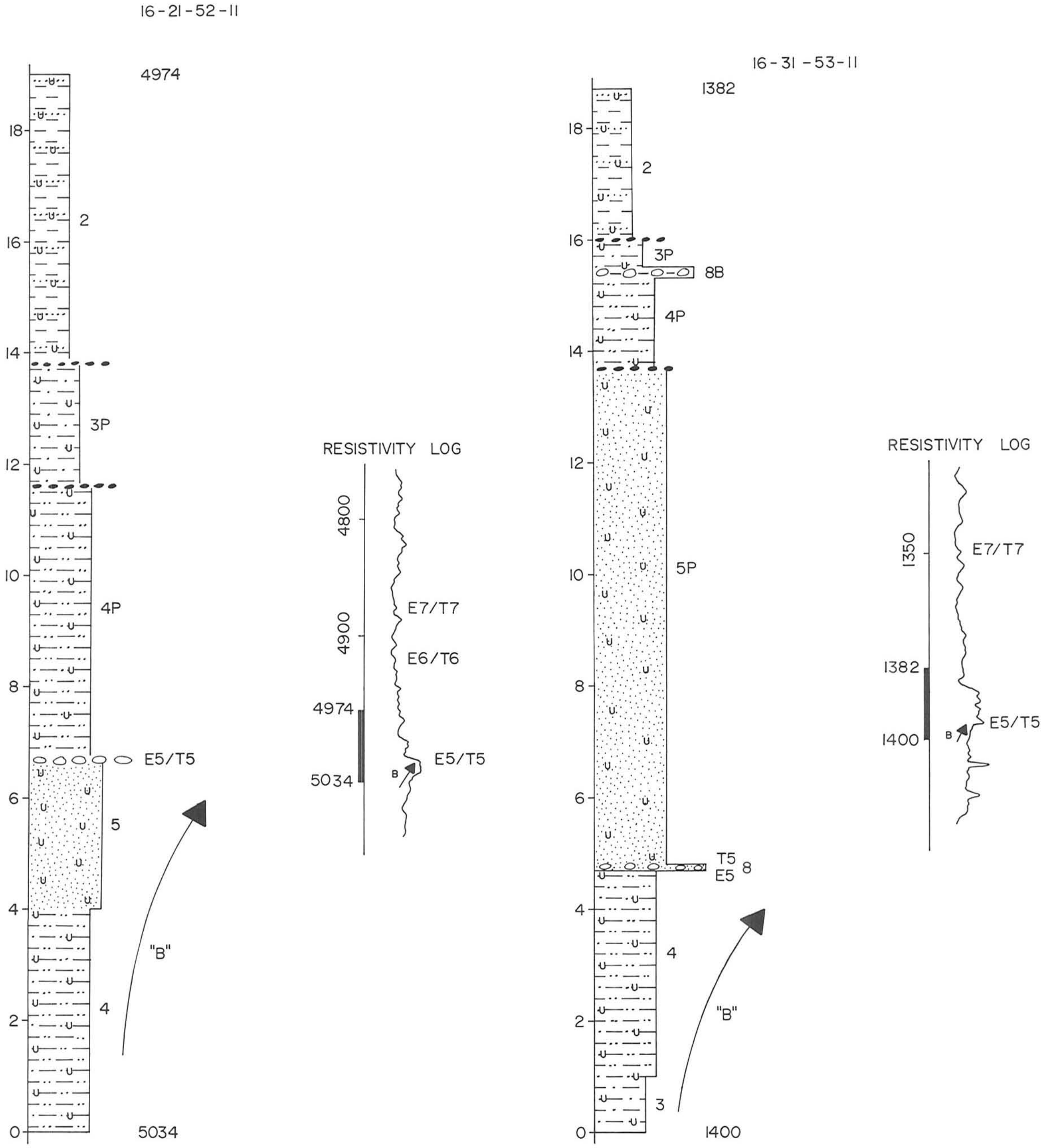

16-21-52-11
4974
5034
2
3P
4P
E5/T5
5
4
"B"
RESISTIVITY LOG
4800
4900
4974
5034
E7/T7
E6/T6
E5/T5
B
16-31-53-11
1382
1400
2
3P
8B
4P
5P
T5
E5
8
4
3
"B"
RESISTIVITY LOG
1350
1382
1400
E7/T7
E5/T5
B

APPENDIX 3 -- ZYCOR

Zycor is the interactive graphics software package used in creating the 3-D mesh diagrams shown in Chapter 4, Figures 4.8 and 4.9. This appendix is a summary of Zycor Technical Note ZTN011 which describes some of the technical details used by the Z-MAP Gridding Module.

Z-MAP is a grid based system, hence all surface data must be converted to a grid. The concept of the grid, with the objective of producing a contour map, is illustrated in Figure A3.1. The top of Figure A3.1 shows a grid overlying the data area. It has 5 horizontal and 7 vertical grid lines, 24 grid cells, and 35 grid nodes. The relationship between the data and the computed grid values is shown in the middle of Figure A3.1. The surface is shaped to fit each of the control points. The bottom of Figure A3.1 shows the contours that were threaded through the grid. The gridding procedure knows how the contours are produced, therefore grid values are computed so the contours will honour the data.

Point Gridding is the term used to describe gridding from irregularly spaced (x,y,z) data, and is performed in three phases. In the first phase the user selects a set of data and enters the control parameters. During the second phase, called pre-gridding, each grid value is computed from the surrounding control points. The post-gridding phase is

Figure A3.1. How a grid is used to contour a surface.

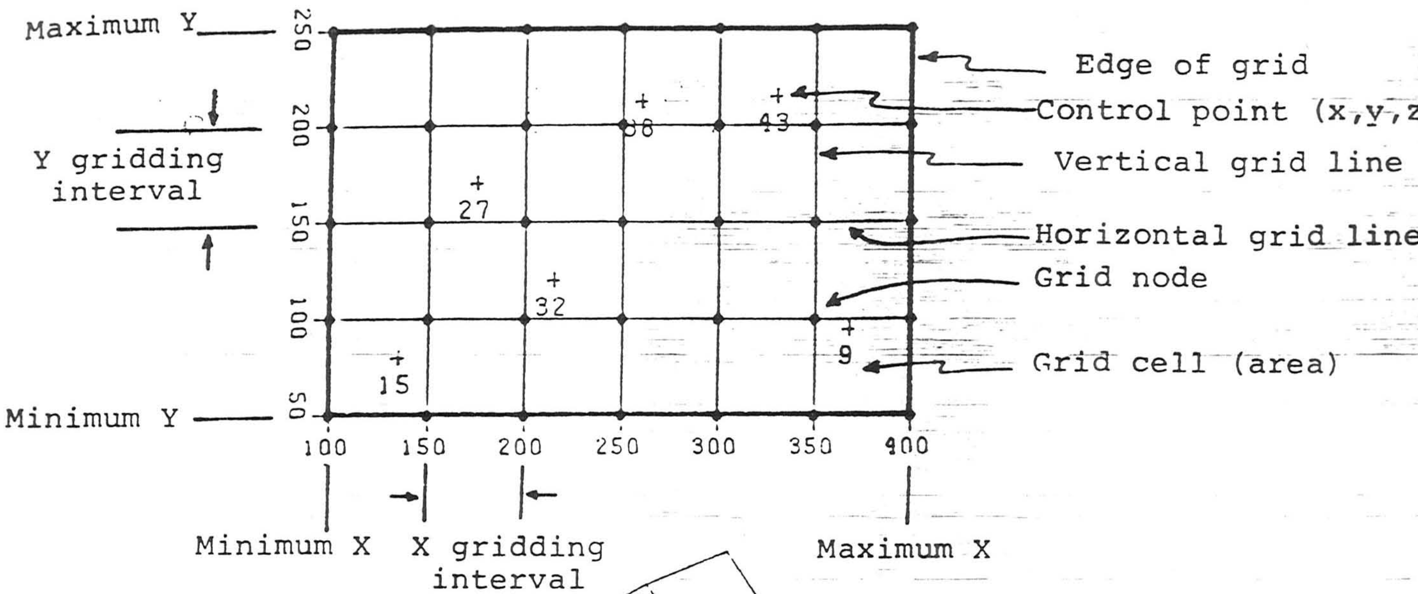

Maximum Y
Minimum Y
Y gridding interval
Minimum X
X gridding interval
Maximum X
Edge of grid
Control point (x,y,z
Vertical grid line
Horizontal grid line
Grid node
Grid cell (area)

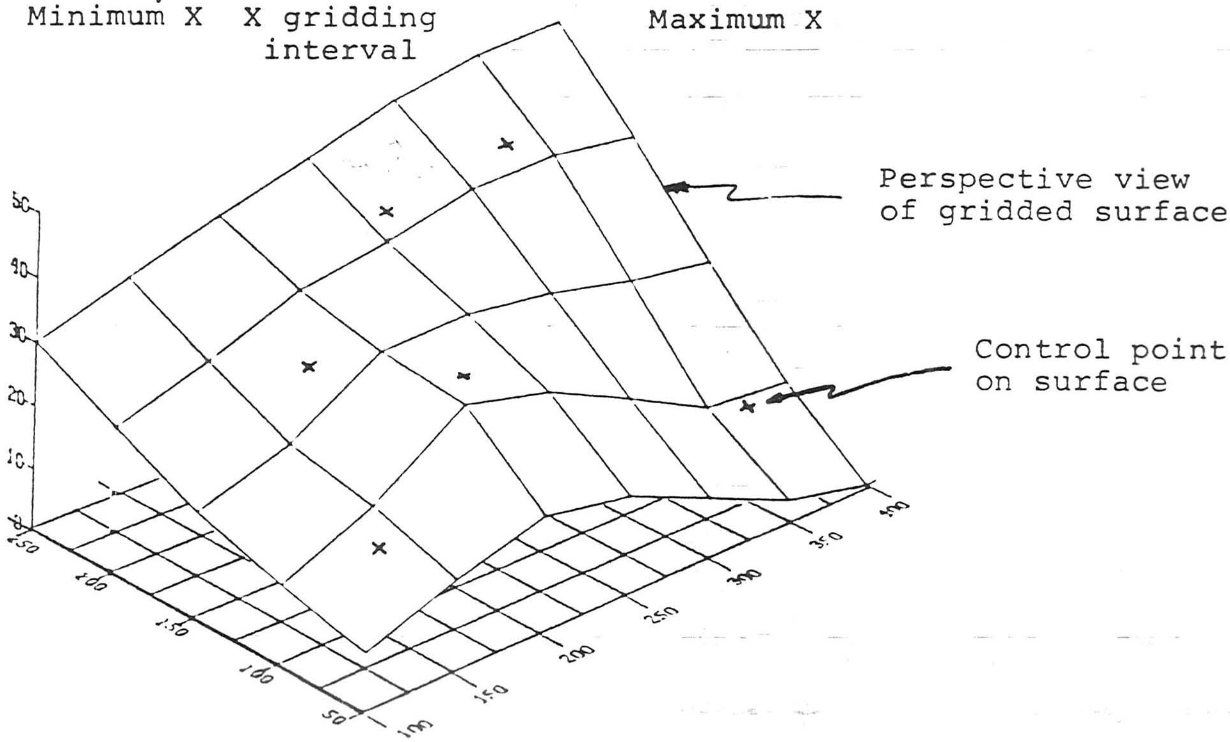

Perspective view of gridded surface
Control point on surface

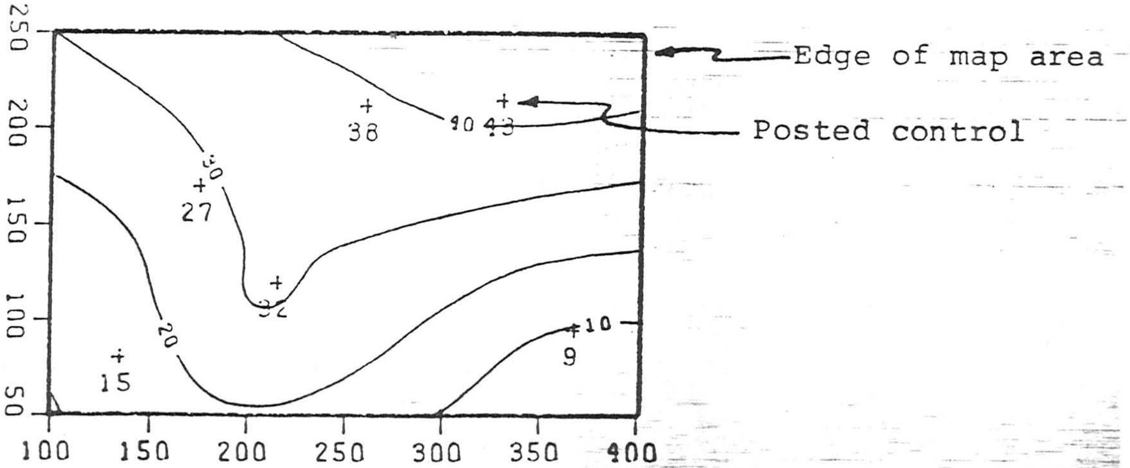

Edge of map area
Posted control

used to improve the aesthetic quality and accuracy of the surface. These phases will be discussed individually below.

1. PARAMETER AND DATA SET-UP

During this phase of the gridding operation, the GRIDDING task communicates with the user to determine which set of data to grid, whether to use faults or control grids, the gridding area and procedures, and appropriate control parameters.

A) Control Point Data Format

Control point data for point gridding are of the general form

$$(x, y, z_1, z_2, \ldots, s_1, s_2, \ldots)$$

where

(x,y) is the horizontal location of the control point,

z_i's are numeric quantities that can be gridded such as elevation, thickness, time, and

s_i's are other types of non-griddable information such as seismic line or shotpoint numbers, well symbol numbers, drillhole identification.

Although these data quantities are ordered in this description, there are no built-in ordering restrictions.

During the set-up phase, it is possible to input and stack-up all controls required to grid up to 20 Z - fields in a single execution of the task. Each Z - field can be gridded exactly like all the others or with a unique set of controls.

B) Description and Specification of Gridding Area

The gridding area is a rectangular area that is bounded by the four control parameters

Minimum Easting (x) coordinate (left edge)

Maximum Easting (x) coordinate (right edge)

Minimum Northing (y) coordinate (bottom edge)

Maximum Northing (y) coordinate (top edge)

This area covers the entire set or a subset of the data that are to be gridded.

These limits are automatically defaulted so they completely enclose the data. The maximum coordinates of the data are rounded up slightly and the minimum coordinates are rounded down to ensure that none of the data are outside the default data area. Only those data points that have valid Z - values are used to compute the default gridding areas if several Z - values in the same set of data are gridded at the same time.

C) Description and Specification of Gridding Intervals

Grid intervals are controlled by the two parameters

Easting (x) gridding interval

Northing (y) gridding interval

These are two of the most important parameters in gridding since they determine how much detail can be retained by the grid values or equivalently, how well the data are honoured. The relationship between gridding intervals, detail, and processing time are as follows: As the gridding intervals decrease, detail increases to a limit and processing time increases.

Detail means the ability to bend or flex to preserve variations in the surface being gridded. Grid detail can only increase up to a limit set by the detail that is inherent in the data. Widely spaced data hold little detail while clustered data can hold more. Similarly, a coarse grid holds less detail than a fine grid. Contours of a coarse grid are necessarily smooth while contours of a fine grid can "snake" around data to illustrate rapid surface changes. It is not possible to induce detail by using a fine grid on widely spaced data. This will simply increase processing time.

The default gridding interval is computed so that on the average, every data point is within its own square cell. This works well for uniformly spaced data. However, if there are clusters of data then there will probably be cells that contain more than one point. This is not necessarily undesirable unless there are major variations in the surface between two or more points inside the same cell. Although all of the points in each cell are used, major variations may tend to average out.

In order to select a more reliable gridding interval, determine the dimensions of the smallest feature that must be preserved by the grid. Then use a gridding interval that is one-half the distance across the feature.

D) Description and Specification of Maximum and Minimum Grid Values

The range of grid values are absolutely constrained to fit between the two control parameters

Minimum allowed computed Z - value

Maximum allowed computed Z - value

Defaults for these values are computed by taking the range of Z - values from the source data, adding one-tenth of the range to the maximum data Z - value to get the upper limit and by subtracting one-tenth of the range from the minimum data Z - value to get the lower limit. This allows for a small amount of smooth extension beyond the data values.

It may be necessary to increase these limits if the data are extrapolated beyond the data perimeter. Extrapolation can continue the trend established by the data and that trend could have reasonable values above or below the data limits. If these limits are not expanded then the trend will be flattened at the limits.

The maximum and minimum limits act as clipping limits in pre-gridding. That is, a computed value beyond a limit is set back to the limit. This can result in sharp transitions from computed Z - values into clipped values that resemble a plateau. In post-gridding, the surface and plateau are smoothly blended together.

2. PRE-GRIDDING PHASE

Pre-gridding is just a step in gridding a set of data. The algorithims are, however, designed so they can be accessed separately and their results saved. Each pre-gridding algorithm contributes its unique character to the grid.

There are three pre-gridding algorithms provided. They are:

WA -- Weighted Averages

LS -- Least Squares

PS -- Projected Slopes

Pre-gridding algorithms are uncoupled. That is, the steps performed to compute a grid value are repeated at each grid node. The results from one set of computations are not used in computing any subsequent grid values. The reason adjacent nodes have similar values is they are computed using largely the same data.

A) Processing Steps and Data Collection Control Parameters

All three pre-gridding algorithms follow basically the same steps to compute grid values. The differ only in the equations used to compute the grid value once the steps are complete. These steps are:

1 At each grid node a circular area of radius REACH[11] is constructed. This is then divided into 8 pie shaped sectors (Fig. A3.2).

2 The closest data (x,y,z) points in each sector

Figure A3.2. The concept of a data collection circle.

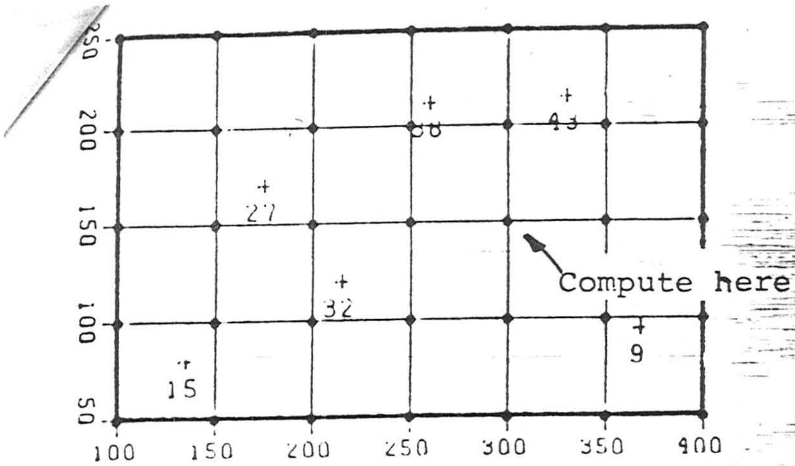

Grid Nodes and Data

A grid value is computed at each grid node using the available data. A circular area is constructed around each node. The node at x=300, y=150 is used as the example.

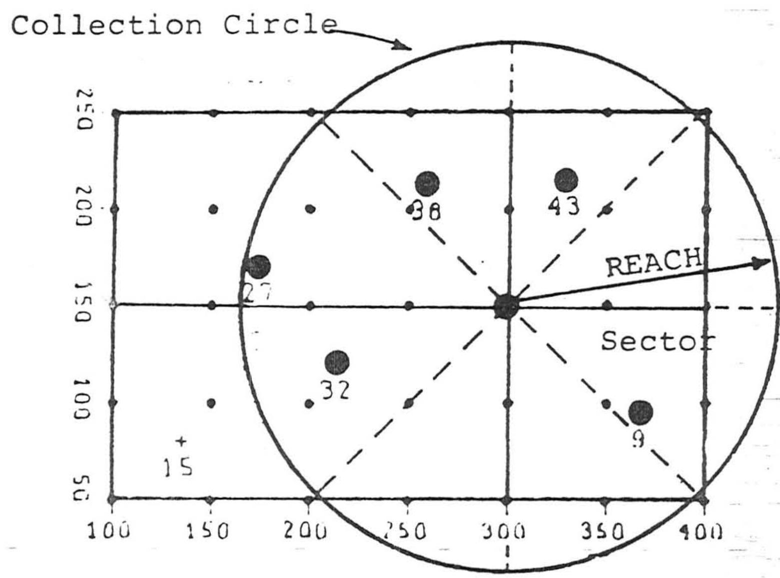

Collection Circle and Data
Used to Compute A Grid Value

The circle with radius REACH is constructed and divided into 8 sectors. The closest points (typically 3) in each sector are identified and used to compute the grid value. Here, the data marked by a black dot are used.

```
     Column Just Produced
            Columns Remaining

 1/   6   +++++    (100,250)
 2/   5   ***++
 3/   4   +**++
 4/   3   +++*+
 5/   2   +++*+    Example Node
 6/   1   +*+*+
 7/   0   +*+++
                   (400,50)
```

The dot matrix produced by gridding tells you what happened at each grid node. This matrix must be rotated 90° counter clockwise for proper alignment.

to the grid node are extracted to compute the grid value. The default is at NPS (Number of Points per Sector) = 3. This means that 24 points will be used if all sectors have 3 or more data points. However, fewer NPS points in each sector does not prevent a grid value from being computed.

3. The distribution of the extracted data around the node is analyzed. There are three tests. If the first test or the second and third tests fail, then the grid node is set to the null value ZNON for the data Z - field.

   a) There must be a minimum number of points per computed grid value (default is 1), otherwise the value is ZNON and step 4 is omitted.

   b) There must be at least one data point in one of the sectors. This is the default setting. If less than the defined number of sectors contain data, then the next test is performed before setting the node to ZNON.

   c) If the distance from the node to the closest data point (x,y,z) is less than distance to extrapolate beyond the data, then the grid value will be computed using the extracted data, otherwise the value is set to ZNON and step 4 is omitted.

4. If the distribution tests pass then the extracted

(x,y,z) data are sent to the WA, LS, or PS algorithm where the grid value is computed. These algorithms will be described later.

5. The value is stored in the grid array at the node location.

6. A symbol code indicating how the above tests came out is put in a dot matrix that is printed during gridding (Fig. A3.2). The symbols and meanings are:

   O - the null value (ZNON) was inserted at this grid node

   / - the grid node was blanked due to faulting

   + - the collected data were used to compute a grid value using the selected algorithm

   * - the collected data were used to compute the grid value, furthermore, one ot the data points was within a fraction of the grid interval from the node

   x - the grid value came from the input control grid

   The matrix is printed across the screen (or page) such that it must be rotated 90° counter-clockwise to properly orient it with the x-y grid nodes.

Steps 1 through 6 are repeated for all grid nodes.

B Important Factors in Selecting Data Collection Control Parameters

The default radius of the circular data collection area around each grid node is one-half the length of the diagonal for the gridding area rectangle. The radius of the data collection circle may vary according to the spacing of the data. In generating the mesh diagrams shown in Chapter 4, the radius of the circular data collection area around each grid node was set to one-quarter the length of the diagonal for the gridding area rectangle.

C The Weighted Averages (WA) Method

The Z - value at each grid node is computed as the weighted average of the Z - values from the (x,y,z) data selected from those around the node. The weight functions used by this method and the following two are described later.

The WA method produces a surface that peaks up or down at the data locations and tends toward the regional average (a flat plane) in the void areas between or beyond the data. It is well suited for gridding noisy or statistical data, particularly when the second weighting function is employed. All grid values will be between the maximum and minimum data values and peaks or valleys occur only at data locations. The WA method should pre-grid for the harmonic flexing post gridding method described later.

D The Least Squares (LS) Method

This was the method used in generating the grid for the 3-D mesh diagrams shown in Chapter 4. At each grid node a simple planar surface is fitted through the selected (x,y,z) data using weighted least squares. The Z - value for the node is then computed as the "height" of the plane at the node's location.

The LS method is recommended for most gridding applications, particularly when coupled with biharmonic or combination flexing. Specifically, well and seismic data should be gridded using LS.

The LS pre-grid surface is fairly smooth from point-to-point. It will continue a linear trend established by the closest data into void areas or beyond the data. It can produce local highs or lows beyond the data range which do not necessarily coincide with data locations. The extent to which the global high or low exceed the data range can be controlled by the maximum and minimum allowed grid values described above.

E The Projected Slope (PS) Method

At each (x,y,z) data point selected from those in the area around the grid node, a planar surface is constructed. This surface is positioned at the Z - value of the data point and given slopes (strike and dip) which are based on field data or computed using other data which surround the data point. By construction, this surface passes precisely through the (x,y,z) data point and it is tangential to the surface being gridded. Each one of these planar surfaces, thus constructed, are projected over to each grid location and their heights are computed. These heights are weighted then averaged to obtain the Z - value for the grid node.

The PS method is recommended only for slowly varying surfaces such as some types of isopachs, as minor errors in the slopes can yield erroneous projected values in void areas or beyond the data. The projected values can easily exceed the data values. When used with post-gridding, it should be followed by biharmonic flexing.

F Weighting or Similarity Functions

Weighting functions are used in the WA, LS, and PS algorithms to compensate for decreasing similarity with distance. A weighting function is a mathematical formula that tries to estimate the extent of similarity as it varies with distance. Two types of weights are available.

The first type of weight is called "sharp" weighting in that it applies very large weights to close data and rapidly decreasing weights to farther data. This is typically used when the grid is supposed to tie to the data.

The second type of weight is called "smooth" weighting since the weght does not change dramatically with increasing distance. The weight at the closest point is unity while points half way between the closest and farthest have a weight of 0.5. The smooth weight tends to produce a smoother pre-grid surface, however, it probably will not fit the data as well.

Both of these weighting or similarity functions are independent of direction. That is, they assume that similarity will decrease with distance at the same rate in all directions. The rate however, does depend on the density of the available data so in one area of a map it might decrease faster than in another area.

3. POST GRIDDING PHASE

Generally post gridding immediately follows the pre-gridding step. The post gridding alogorithms are:

Biharmonic Flexing

Laplacian Flexing

Combination Flexing

Grid Refinement

The first three are used to simultaneously adjust and smooth the grid values to smoothly fit the data. The fourth algorithm is used to cut the gridding interval in half and interpolate all intermediate grid values. This algorithm will not be discussed further here.

A Biharmonic Flexing

The biharmonic flexing algorithm in Z-MAP produces a highly contoured grid to represent the data. That is, every grid value is mathematically coupled to every other grid value and to all the data points. In theory, this coupling yields points on a surface wich resembles a semi-rigid thin plate, that is flexed to fit through every data point and which has no other external forces distorting the sheet. Thus the sheet varies smoothly from one point to another and beyond the perimeter of the data it will smoothly continue the trend imposed by the data.

A large system of equations, one for each grid value, is used to mathematically describe the thin plate and its coupling to the data. These are solved iteratively in order to produce a smooth surface. Biharmonic flexing should be initialized with the LS pre-gridding method.

The biharmonic flexing process starts with the pre-grid estimate and iteratively changes it to more closely resemble the ideal thin plate surface. The process monitors a normalized rate of change in the overall surface smoothness where 1 means substantial improvement and 0 means no improvement. When the rate of change falls below a threshold (default value is 0.25), the process terminates. This usually means that no significant change can be achieved by continuing the process.

Some data types cannot be represented very well by a thin plate. This means that the system of equations which link each grid node to all others and to the data are difficult if not impossible to solve as formulated. Therefore, the process could iterate forever and not arrive at a solution. This is evident when the normalized rate of change in overall smoothness reaches some level above the cutoff threshold and then tends to "bounce up and down" around that level. To prevent the process from running on unchecked, there is a cutoff on the maximum number of iterations (default number is 10).

B Laplacian (Harmonic) Flexing

The Laplacian, also called harmonic, flexing algorithm in Z-MAP is similar in function to the biharmonic flexing algorithm. It is different in that the physical analog resembles a flexible membrane rather than a semi-rigid plate. It produces a surface that tends to be peaked at each data point, varies linearily between data, and flattens out to the average value of the data in voids or beyond the data perimeter. Furthermore, it cannot produce any local highs or lows that do not coincide with data locations or which exceed the data, either inside or outside the data perimeter.

A Laplacian grid is not as smooth as the biharmonic grid. The differences between data locations may not be significant; however, at data locations the biharmonic surface tends to be flatter across the data while a Laplacian surface tends to be pointed. Contours of a biharmonic surface are usually long flowing curves with large arcs and fewer closures. Contours of a Laplacian surface frequently enclose data points.

Laplacian flexing should be initialized by the WA pre-grid method. The grid is then iteratively flexed into membrane shape. The controls are used by Laplacian flexing are the same as those used by biharmonic flexing.

C Combination Flexing

This was the alogorithm used in generating the 3-D mesh diagrams shown in Chapter 4. Biharmonic flexing produces a very smooth surface which passes through the data while Laplacian flexing produces a peaked surface. The biharmonic surface can overshoot the data. The models are combined to produce a surface which is more like a sheet of plastic rather than a semi-rigid plate or a membrane. It does not overshoot as much nor does it exhibit sharp peaking around the data.

This process should be initialized by the LS pre-gridding method. It has the same types of controls described for biharmonic flexing.

The above discussion describes the technical features in Z-MAP Gridding Module used to generate the mesh diagrams shown in Chapter 4. It is presented to give the reader some insight into the method and controls used to generate the 3-D surface, and some idea of the variety of algorithms available in Z-MAP to generate these surfaces.

FOLDOUT I

1

c145

+23d


A
3-14-52-14
13-21-52-13
7-34-52-13
14-35-52-13
10-35-52-13
6-1-53-13
14-12-53-13
12-16-53-12
4-22-53-12
DISMAL RAT
CARROT CREEK
RAVEN RIVER
T5
E5
8B
4P
3P
2
7A
G.S.
"A"
"B"
TERRACE
BEVEL
BUMP
HOLLOW

FOLDOUT 2

B
12-6-50-12
8-26-50-12
8-36-50-12
13-5-51-11
4-16-51-11
10-16-51-11
2-21-51-11
10-21-51-11
2-28-51-11
4-34-51-11
8-3-52-11
9-3-52-11
11-2-52-11
15-11-52-11
11-17-52-10
11-16-52-10
7-10-52-10
5-22-52-10
B
11-24-52-10
DISMAL RAT
CARROT CREEK
RAVEN RIVER
T5
E5
"A"
"B"
G.S.
TERRACE
BEVEL
BUMP
HOLLOW
BUMP
HOLLOW
BUMP
HOLLOW
BUMP
HOLLOW
BUMP
HOLLOW
BASIN PLAIN

FOLDOUT 3

C
6-21-53-14
11-12-54-14
11-13-54-14
11-24-54-14
14-34-54-13
C
15-2-55-13
DISMAL RAT
CARROT CREEK
RAVEN RIVER
T5
E5
8B
4P
3P
8
7
7A
5
G.S.
"A"
4
TERRACE
BEVEL

FOLDOUT 4

D
8-5-50-10
6-11-50-10
6-14-50-10
6-13-50-10
8-19-50-9
10-29-50-9
14-22-50-9
13-34-50-9
2-3-51-9
2-1-51-9
1-11-51-9
D
6-14-51-9
DISMAL RAT
CARROT CREEK
RAVEN RIVER
T5
E5
3P
8B
4P
7A
"A"
"B"
G.S.
5P
TERRACE
BEVEL
HOLLOW
BUMP
HOLLOW
BUMP
HOLLOW
BASIN PLAIN

FOLDOUT 5

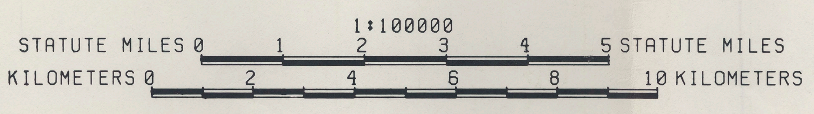

home oil

EROSION SURFACE (E5)
CARROT CREEK STUDY AREA
CONTOUR INTERVAL - 5 M
UTM -117 CLARKE 1866
1 : 100,000

SCALE 1:100000	AUTHOR K. BERGMAN	DATE 2-24-86
FILE NO.		

FOLDOUT 6

CONGLOMERATE ISOPACH MAP (M)
CARROT CREEK STUDY AREA
CONTOUR INTERVAL - 5 M
UTM -117 CLARKE 1866
1 : 100,000

SCALE 1:100000	AUTHOR K. BERGMAN	DATE 2-24 -86
FILE NO.		

C
6-21-53-14
11-12-54-14
11-13-54-14
11-24-54-14
14-34-54-13
C
15-2-55-13
DISMAL RAT
CARROT CREEK
RAVEN RIVER
8B
4P
3P
8
7
7A
5
G.S.
T5
E5
"A"
TERRACE
BEVEL